



U.S. DEPARTMENT OF
ENERGY

PNNL-16891

Prepared for the U.S. Department of Energy
under Contract DE-AC05-76RL01830

Hanford 100-N Area Apatite Emplacement: Laboratory Results of Ca-Citrate-PO₄ Solution Injection and Sr-90 Immobilization in 100-N Sediments

JE Szecsody
CA Burns
RC Moore
JS Fruchter
VR Vermeul

MD Williams
DC Girvin
JP McKinley
MJ Truex
JL Phillips

September 2007



Pacific Northwest
NATIONAL LABORATORY

DISCLAIMER

This report was prepared as an account of work sponsored by an agency of the United States Government. Neither the United States Government nor any agency thereof, nor Battelle Memorial Institute, nor any of their employees, makes **any warranty, express or implied, or assumes any legal liability or responsibility for the accuracy, completeness, or usefulness of any information, apparatus, product, or process disclosed, or represents that its use would not infringe privately owned rights.** Reference herein to any specific commercial product, process, or service by trade name, trademark, manufacturer, or otherwise does not necessarily constitute or imply its endorsement, recommendation, or favoring by the United States Government or any agency thereof, or Battelle Memorial Institute. The views and opinions of authors expressed herein do not necessarily state or reflect those of the United States Government or any agency thereof.

PACIFIC NORTHWEST NATIONAL LABORATORY

operated by

BATTELLE

for the

UNITED STATES DEPARTMENT OF ENERGY

under Contract DE-AC06-76RLO 1830

Printed in the United States of America

Available to DOE and DOE contractors from the
Office of Scientific and Technical Information,
P.O. Box 62, Oak Ridge, TN 37831;
prices available from (615) 576-8401.

Available to the public from the National Technical Information Service,
U.S. Department of Commerce, 5285 Port Royal Rd., Springfield, VA 22161

Hanford 100-N Area Apatite Emplacement: Laboratory Results of Ca-Citrate-PO₄ Solution Injection and Sr-90 Immobilization in 100-N Sediments

J. E. Szecsody
C. A. Burns
R. C. Moore^(a)
J. S. Fruchter
V. R. Vermeul
M. D. Williams
D. C. Girvin
J. P. McKinley
M. J. Truex
J. L. Phillips

September 2007

Prepared for
the U.S. Department of Energy
under Contract DE-AC05-76RL01830

Pacific Northwest National Laboratory
Richland, Washington 99352

(a) Sandia National Laboratories
Albuquerque, New Mexico

Executive Summary

This report summarizes laboratory-scale studies investigating the remediation of Sr-90 by Ca-citrate-PO₄ solution injection/infiltration to support field injection activities in the Hanford 100-N Area. This study is focused on experimentally testing whether this remediation technology can be effective under field-scale conditions to mitigate Sr-90 migration 100-N Area sediments into the Columbia River. Sr-90 is found primarily adsorbed to sediments by ion exchange (99% adsorbed, <1% in groundwater) in the upper portion of the unconfined aquifer and lower vadose zone. Although primarily adsorbed, Sr-90 is still considered a high mobility risk as it is mobilized by seasonal river stage increases and by plumes of higher ionic strength relative to groundwater. This remediation technology relies upon the Ca-citrate-PO₄ solution forming apatite precipitate [Ca₆(PO₄)₁₀(OH)₂], which incorporates some Sr-90 during initial precipitation and additionally slowly incorporates Sr-90 by solid phase substitution for Ca. Sr substitution occurs because Sr-apatite is thermodynamically more stable than Ca-apatite. Once the Sr-90 is in the apatite structure, Sr-90 will decay to Y-90 (29.1 y half-life) then Zr-90 (64.1 h half-life) without the potential for migration into the Columbia River. For this technology to be effective, sufficient apatite needs to be emplaced in sediments to incorporate Sr and Sr-90 for 300 years (~10 half-lives of Sr-90), and the rate of incorporation needs to exceed the natural groundwater flux rate of Sr in the 100-N Area.

A primary objective of this study is to develop an injection sequence to deliver sufficient apatite into subsurface sediments that minimizes initial mobility of Sr-90, which occurs because the injection solution has a higher ionic strength compared to groundwater. This can be accomplished by sequential injections of low, then high concentration injection of Ca-citrate-PO₄ solutions. Assessment of low concentration Ca-citrate-PO₄, citrate-PO₄, and PO₄ solutions show greater Sr and Sr-90 incorporation during initial precipitation and less initial mobilization with solutions with low Ca²⁺ concentration. While all solutions showed nearly the same Sr uptake into apatite (14% to 17% by 2 weeks, 21% to 30% by 5 weeks), the incorporation efficiency (i.e., mmol Sr incorporated per mmol PO₄ injected) was higher for solutions containing citrate. The Sr incorporation rate into apatite during initial precipitation (by 1 month) averaged $4.6 \pm 1.9 \times 10^{-4} \text{ h}^{-1}$ (half-life $1500 \pm 430 \text{ h}$, $8.85 \times 10^{-7} \text{ mg Sr/day/mg apatite}$). The injection solution used in field injections #3 to #18 (10 mM PO₄, 1 mM Ca, 2.5 mM citrate), which is deficient in Ca (a total of 16.7 mM needed to form apatite with 10 mM of PO₄), resulted in the initial Sr and Ca peak (24 h) at 4.7x groundwater. By 30 days, the aqueous Sr concentration was 0.28x groundwater and Ca 0.43x groundwater, as both Sr and Ca are used to form initial apatite precipitates. Reactive transport simulation of the complex ion exchange, biodegradation, and precipitation processes showed that the initial Sr groundwater increase mobilized only 1.5% of the Sr mass in sediments. Citrate biodegradation, a necessary step in Ca-citrate-PO₄ solutions forming apatite, had an average half-life of 50 h (at aquifer sediment/water ratio and temperature), and decreased an order of magnitude with sediment depth as the microbial biomass decreased five orders of magnitude. The rate of citrate biodegradation was relatively invariant with biomass and water saturation (50% to 100%, for vadose zone infiltration) possibly due to the significant injection of microbes in the river water used and subsurface transport of microbes during injections.

Long-term experiments showed the Sr-90 incorporation into apatite was as high as 98% by 15 months. The Sr-90 incorporation rate into solid-phase apatite (i.e., not including more rapid incorporation during initial precipitation) averaged $2.7 \pm 2.6 \times 10^{-5} \text{ h}^{-1}$ (half-life 1080 days, $1.42 \times 10^{-8} \text{ mg Sr/day/mg apatite}$) for sediment/water systems containing 350 pore volumes of Sr-90 laden water. This long-term solid phase Sr-90 incorporation rate was used to calculate the Sr uptake rate in a 30-ft wide (diameter) apatite barrier to compare with the natural groundwater flux rate of Sr. For the field scenario of current injections #3 to #18 (i.e., 10 mM PO₄ injected, or 0.34 mg apatite/g sediment), the Sr uptake rate was $8.8 \times 10^{-6} \text{ mmol Sr/day/cm}^2$. This Sr incorporation rate into apatite was 6.5x greater than the average natural Sr groundwater flux rate ($1.4 \times 10^{-6} \text{ mmol Sr day}^{-1} \text{ cm}^{-2}$, assumes 1 ft/day groundwater flow rate). This indicates Sr would be sequestered in the apatite-laden zone for the *average* Sr groundwater flux rate, but zones of higher groundwater flux (10x to 100x) would exceed the barrier uptake rate for this low apatite loading (0.34 mg apatite/g sediment). In addition, this low apatite loading would also not be able to incorporate Sr and Sr-90 for 300 years. From a mass balance perspective, approximately 3.4 mg apatite per gram of sediment is needed to incorporate Sr and Sr-90 for 300 years (assumes 10% Sr substitution for Ca in apatite). At this higher apatite loading, the Sr uptake rate during initial precipitation ($5 \times 10^{-3} \text{ mmol Sr day}^{-1} \text{ cm}^{-2}$) is 3600x more rapid than the average Sr groundwater flux rate and the Sr uptake rate during solid phase incorporation ($7.8 \times 10^{-5} \text{ mmol Sr day}^{-1} \text{ cm}^{-2}$) is 57x more rapid than the average Sr groundwater flux rate, so the barrier will effectively remove all Sr except in extreme high groundwater flow conditions.

The assumption of whether 10% Sr substitution for Ca in apatite can be achieved was evaluated. Experiments showed measured Sr or Sr-90 fraction substitution for Ca in apatite by 9 months varied from 1% to 16.3%. FTIR scans showed that Sr was indeed substituting into apatite (i.e., crystal structure did not change, other Sr phases were not present). Factors that increased the amount (and rate) of Sr substitution for Ca in apatite included: a) less crystalline/more substituted initial apatite structure, and b) presence of citrate during initial apatite precipitation. Field-scale apatite precipitation in sediments is expected to be less crystalline, so should have greater Sr substitution. There was not a clear trend between higher aqueous Ca²⁺ (such as in groundwater) and Sr substitution. The rate-limiting step in Sr incorporation appears to be solid phase diffusion, based on the low activation energy (11.3 kJ/mol) derived from temperature studies. Measurements of the expected small apatite concentrations in sediment (i.e., 0.3 to 4 mg apatite/g sediment) were successfully made by electron microprobe with elemental detection (lowest detection limits), and by acid dissolution of the sediment and phosphate measurement. Sequential injection experiments were conducted to assess how combinations of Ca-citrate-PO₄ and PO₄ solutions can be used to increase the precipitated apatite mass to incorporate more Sr-90. Sequential treatments (for 1 month) of low- then high Ca-citrate-PO₄ solutions incorporated the greatest Sr-90, and sequential Ca-citrate-PO₄ then PO₄ or PO₄ then Ca-citrate-PO₄ incorporated less Sr-90. These results may be due to the role of microbes in apatite nucleation, with citrate biodegradation increasing microbial biomass. Longer term studies are needed to assess the effectiveness of sequential treatments and the potential impact in sediment permeability.

Contents

Executive Summary	iii
1.0 Introduction	1.1
1.1 Sr-90 Contamination in Subsurface and River Biota	1.2
1.2 100-N Area Remediation History	1.4
1.3 Sr-90 Immobilization with Apatite	1.7
1.4 Subsurface Apatite Placement by Solution Injection	1.8
1.5 Need for Injection/Infiltration Strategy at River Shore	1.9
2.0 Background – Injection of a Ca-Citrate-PO ₄ Solution to Form Apatite In Situ	2.1
2.1 Precipitation of Apatite in Aquifer Sediments with a Ca-Citrate-PO ₄ Solution	2.1
2.2 Characterization of Apatite Precipitate	2.1
2.3 Mass of Apatite Needed for Hanford 100-N Area	2.2
2.4 Sr and Sr-90 Incorporation Rate into Apatite	2.4
2.5 Sr-90 Initial Mobilization and Sequential Injection Strategy	2.5
3.0 Experimental Methods	3.1
3.1 Ca-Citrate-PO ₄ Solutions	3.1
3.2 Batch Experiments with Ca-Citrate-PO ₄ Solutions	3.2
3.3 Apatite and Ca-PO ₄ Solid Phase Characterization	3.4
3.4 1-D Column Experiments with Ca-Citrate-PO ₄ Solutions	3.5
3.5 Major Cation/Anion and Radiochemical Analysis	3.5
4.0 Modeling Methods	4.1
4.1 Modeling Citrate Biodegradation Rate	4.1
4.2 Simulation of Ca-Citrate-PO ₄ Interactions with Sediments during Transport	4.1
4.3 Simulation of Sr-90 Uptake by Apatite with Cation Exchange	4.1
5.0 Results	5.1
5.1 Injection Ca-Citrate-PO ₄ to Form Apatite and Sequester Sr-90	5.1
5.1.1 Sequential Injection Strategy to Minimize Sr-90 Mobilization	5.4
5.1.2 Citrate Biodegradation with Differing Ca-Citrate-PO ₄ Concentration	5.8
5.1.3 Spatial Variation in Citrate Biodegradation in Boreholes	5.12
5.2 Laboratory Support Experiments for Field Injection #1	5.15
5.2.1 Laboratory 1-D Column Transport Experiments	5.15
5.2.2 Stability of Field #1 Tanker Solutions	5.21
5.2.3 Field #1: Electrical Conductivity versus Solution Concentration	5.25
5.2.4 Field #1: Solution Density versus Solution Concentration	5.26

5.2.5	Field #1: Phosphate Measurement and Citrate Interference.....	5.27
5.3	Laboratory Support Experiments for Field Injection #2	5.28
5.3.1	Laboratory 1-D Column Transport Experiments	5.29
5.3.2	Stability of Field #2 Tanker Solutions.....	5.32
5.3.3	Field #2: Electrical Conductivity versus Concentration.....	5.34
5.3.4	Field #2: Phosphate Measurement (Hach 8178) and Citrate Interference....	5.36
5.4	Laboratory Support Experiments for Field Injection #3 to #18.....	5.37
5.4.1	Laboratory 1-D Column Transport Experiments	5.37
5.4.2	Stability of Field #3 to #18 Tanker Solutions	5.39
5.4.3	Field #3 to #18: Electrical Conductivity versus Concentration	5.42
5.4.4	Field #3 to #18: Phosphate Measurement	5.43
5.5	Techniques for Measuring Apatite Precipitate in Sediment.....	5.44
5.6	Ca-Citrate-PO ₄ Injection and the Long-Term Sr-90 Incorporation	5.51
5.6.1	Sr Ion Exchange in Sediment with Groundwater.....	5.51
5.6.2	Sr/Sr-90 Ion Exchange in Sediment with Ca-Citrate-PO ₄ Solutions	5.53
5.6.3	Sr Uptake on Apatite without Sediment	5.56
5.6.4	Sr Uptake by Apatite: Influence of Cations and Temperature.....	5.59
5.6.5	Sr Uptake by Apatite: Solid Phase Characterization.....	5.63
5.6.6	Sr Uptake by Apatite in Groundwater with Sediment.....	5.67
5.7	Alternate Injection Strategy: Injection of PO ₄ Only	5.72
5.7.1	PO ₄ Sorption/Precipitation in Sediments.....	5.72
5.7.2	PO ₄ Injection into Sediments	5.73
5.8	Alternate Injection Strategy: Sequential Injection of PO ₄ and Ca-Citrate-PO ₄	5.76
5.8.1	PO ₄ Addition Then Ca-Citrate-PO ₄	5.76
5.8.2	Ca-Citrate-PO ₄ Addition Then PO ₄	5.77
5.9	Vadose Zone Application: Infiltration of Ca-Citrate-PO ₄	5.79
5.9.1	Citrate Biodegradation and Water Content.....	5.79
5.9.2	Citrate Mineralization and Biomass in Sediments	5.81
5.9.3	1-D Infiltration of Ca-citrate-PO ₄ Solutions.....	5.83
5.9.4	2-D Infiltration Experiments of Ca-Citrate-PO ₄ Solutions.....	5.87
5.9.5	Simulation of Ca-Citrate-PO ₄ or PO ₄ Reactive Transport Experiments	5.94
6.0	Summary	6.1
6.1	Citrate Biodegradation Rate	6.2
6.2	Injection of Ca-Citrate-PO ₄ Solution: Apatite Precipitation and Sr-90 Mobility	6.3
6.3	Apatite Precipitate Characterization: Properties and Mass in Sediment.....	6.4

6.4 Sr-90 Incorporation Mass and Rate Into Apatite	6.5
6.5 Sequential Injection Scenarios.....	6.9
7.0 References	7.1
Appendix – Experimental Data of Injection Solution-Sr -Sediment Reactions	A.1

Figures

1.1 Hanford 100-N Reactor and disposal trench	1.2
1.2 Sr-90 contamination in river sediments and clams	1.2
1.3 Sr-90 contamination in subsurface sediments	1.3
1.4 Crib discharge and Sr-90 levels in well N46.....	1.4
1.5 Cation and anion substitution in apatite	1.8
1.6 Columbia River stage 1994 – 2005.....	1.9
2.1 Characterization of nanocrystalline apatite formed in Hanford sediment by microbially mitigated Ca-citrate degradation in the presence of aqueous phosphorous: TEM, XRD, FTIR, and EDS.....	2.2
3.1 Biodegradation pathway for citrate.....	3.3
3.2 Sr-90 and Y-90 mass and activity for different initial Sr-90 and Y-90 activity: a) and b) 0% Y-90, c) and d) 10% Y-90, e) and f) 50% Y-90, and g) and h) 90% Y-90	3.7
3.3 Sr-90, Y-90, and total activity in a system with no Y-90 initially.....	3.8
5.1 Sr-85 desorption in a 1-D column with Hanford groundwater injection	5.1
5.2 Sr-85 desorption in a 1-D column with Ca-citrate-PO ₄ injection.....	5.2
5.3 Sr-85 desorption in a 1-D column with Hanford groundwater after 89 days contact with a low concentration of Ca-citrate-PO ₄ solution	5.3
5.4 Sr-85 desorption in a 1-D column after the sequential injections: a) low conc. Ca-citrate-PO ₄ (4, 10, 2.4), b) 125 day wait period, and c) high conc. Ca-citrate-PO ₄ (28, 70, 17 mM).....	5.4
5.5 Sr-90 aqueous/solid phase partitioning in batch systems with: a) field Sr-90- contaminated sediment only (no apatite), b) field Sr-90 contaminated sediment and apatite solution addition, c) field and laboratory added Sr-90 with apatite solution addition.....	5.5
5.6 Sr-90 breakthrough in sequential low- and high-concentration Ca-citrate-PO ₄ injections in 1-D columns. Shown are: a) Sr-90 breakthrough curve for 15 pv groundwater injection 32 days after low concentration Ca-citrate-PO ₄ injection, and b) Sr-90 breakthrough curve for 1.5 pv high concentration Ca-citrate-PO ₄ injection	5.8
5.7 Citrate biodegradation pathway	5.8
5.8 Citrate biodegradation by Hanford 100-N sediments verses temperature at: a) 10 mM citrate, b) 50 mM citrate, and c) 100 mM citrate concentration.....	5.9
5.9 Arrhenius plot of citrate biodegradation	5.10
5.10 Citrate mineralization and Ca-citrate-PO ₄ composition.....	5.10

5.11 Apatite precipitation rate and citrate biodegradation: a) precipitation rate in aerobic system (reported as CO ₃); b) precipitation rate in anaerobic system; c) citrate biodegradation in anaerobic system	5.11
5.12 Citrate mineralization versus borehole (composite)	5.12
5.13 Citrate mineralization versus depth in five different boreholes in the 100-N Area.....	5.13
5.14 Citrate mineralization and depth in five boreholes showing a) mineralization half-life, and b) trend of mineralization extent	5.14
5.15 Injection of a Ca-citrate-PO ₄ (4, 10, 2.4 mM) solution in a 20-ft long 1-D column (experiment T43), with a) citrate, PO ₄ , EC, b) Ca, and c) Sr	5.16
5.16 Citrate mineralization and depth in five boreholes showing a) trend of mineral	5.21
5.17 Relationship between: a) Injection #1, solution #1 (Ca-citrate) and electrical conductivity, and b) injection #1, solution #2 (PO ₄) and electrical conductivity	5.25
5.18 Relationship between a 50/50 mix of solution #1 (Ca-citrate) and solution #2 (PO ₄) and electrical conductivity	5.25
5.19 Relationship between a 50/50 mix of solution #1 (Ca-citrate) and solution #2 (PO ₄) and solution density (b), with temperature correction (a)	5.27
5.20 Hach 8114 PO ₄ analysis (molybdovanadate) of UV absorbance at 420 nm: a) without citrate present, b) with citrate present showing significant interference	5.28
5.21 Injection of 4.6 mM Ca, 7.9 mM citrate, 2.5 mM PO ₄ (experiment Y21 in a, c, e), and 2 mM Ca, 5 mM citrate, and 2.2 mM PO ₄ (experiment Y16 in b, d, f).....	5.30
5.22 Ca breakthrough behavior prediction from the ionic strength of the Ca-citrate-PO ₄ composition.....	5.30
5.23 Sr breakthrough behavior prediction from the ionic strength of the Ca-citrate-PO ₄ composition or calcium concentration	5.31
5.24 Electrical conductivity versus concentration measurements for field injection #2: a) solution #1, Ca-citrate, and b) solution #2, PO ₄	5.34
5.25 Electrical conductivity versus Ca-citrate-PO ₄ concentration relationship for field injection #2 solution, assuming a 1:1 mixture of solutions #1 and #2.....	5.35
5.26 Hach 8178 PO ₄ analysis (amino acid) of UV absorbance at 530 nm: a) without citrate present, b) with citrate present showing significant interference.....	5.36
5.27 1-meter long 1-D column experiment (Y87) with the injection of 1 mM Ca, 2.5 mM citrate, and 5 mM PO ₄ with results of: a) PO ₄ breakthrough, b) Ca, Na breakthrough, and c) Sr breakthrough.....	5.38
5.28 1-meter long 1-D column experiment (Y88) with the injection of 1 mM Ca, 2.5 mM citrate, and 10 mM PO ₄ with results of: a) PO ₄ breakthrough, b) Ca, Na breakthrough, and c) Sr breakthrough.....	5.39
5.29 Electrical conductivity versus concentration for solution 1 (a) and solution 2 (b) for field injections #3 to #10).....	5.42
5.30 Electrical conductivity versus concentration for the combined solution #1 and solution #2 for field injections #3 to #10	5.43

5.31 Scanning electron microprobe image of a sediment thin section containing 0.005 mg apatite/g sediment.....	5.45
5.32 Scanning electron microprobe images of sediment samples with differing amounts of added apatite. P elemental scan shown	5.46
5.33 Scanning electron microprobe images of a single apatite crystal	5.47
5.34 Aqueous phosphate measurement after acid dissolution of: a) apatite, b) sediment	5.47
5.35 Aqueous phosphate measurement after acid dissolution of apatite/sediment mixtures: a) 1.65 mg apatite/g sediment (apatite 41% of sediment PO ₄), b) 0.32 mg apatite/g sediment (apatite 8% of sediment PO ₄), and c) 0.05 mg apatite/g sediment (apatite is 1.5% of sediment PO ₄)	5.48
5.36 Aqueous phosphate measurement after acid dissolution of apatite/sediment mixtures with a) 0.5M HCl, and b) 0.1M HCl.....	5.48
5.37 Aqueous phosphate measurement after 15-minute acid dissolution of apatite sediment mixtures using 0.1M or 0.5M HNO ₃	5.49
5.38 Fluorescence scans of precipitated apatite, sediment with no apatite showing low levels of background fluorescence from the sediment	5.49
5.39 Sr-90 sorption: a) in groundwater, b) in mono- or divalent-saturated sediment, and c) time scale for Sr-90 sorption by untreated and apatite-laden 100-N composite sediment.....	5.51
5.40 Sr-85 desorption in a 1-D column with Hanford groundwater injection	5.52
5.41 Sr-85 adsorption in batch experiments (low sediment/water ratio) at differing ionic strength	5.54
5.42 Sr-85 desorption in a 1-D column with Ca-citrate-PO ₄ injection.....	5.55
5.43 Initial rates of Sr sorption by apatite.....	5.56
5.44 Long-term rates of Sr sorption by apatite.....	5.56
5.45 Sr sorption K _d by apatite verses mass of apatite.....	5.57
5.46 Sr ion exchange on apatite in Na- and Ca-saturated systems at differing Sr concentration.....	5.58
5.47 Influence of Ca, groundwater and ionic strength at 82°C on Sr uptake by apatite	5.59
5.48 Sr-90 uptake by hydroxyapatite at 22°C to 82°C in groundwater with model fit of sorption and incorporation rate.....	5.61
5.49 Sr-90 uptake by hydroxyapatite at 22°C to 82°C in deionized water with model fit of sorption and incorporation rate.....	5.61
5.50 Change in Sr-90 incorporate with temperature and calculated activation energy	5.62
5.51 SEM image of citrate precipitated apatite used in Sr incorporation studies at 82°C....	5.65
5.52 Image of apatite grain (a) showing square region for which EDS spectrum was obtained (b) for apatite aged at 82°C for 0.86 months.....	5.65
5.53 SEM image of citrate precipitated apatite used 82°C.....	5.66
5.54 Sr-90 extractions of treated sediments originally containing Sr-90 or with Sr-90 added: a) aqueous + ion exchangeable, and b) solid phase associated	5.67

5.55 Sr uptake from groundwater suspension of 0.34 g/L apatite and 20 g/L sediment at 22°C to 82°C.....	5.68
5.56 Sr uptake from groundwater suspension of 0.34 g/L apatite and 20 g/L sediment at 82°C.....	5.69
5.57 Simulation of Sr-90 mass changes under field conditions of 20% porosity and 0.0038 g apatite/g sediment.....	5.70
5.58 Time scale of PO ₄ removal rate from solution at differing sediment/water ratio (a), at a high PO ₄ concentration (b), and at different Ca/PO ₄ ratios (c).....	5.72
5.59 Adsorption isotherm for Na-PO ₄ at 1 h and 24 h.....	5.73
5.60 Na-PO ₄ injection at different contact times: a) 0.5 mM PO ₄ , 19 minutes residence time, b) 50 mM PO ₄ at 18-minute residence time, c) 50 mM PO ₄ at a 3-h residence time, and d) 50 mM PO ₄ at a 12-h residence time.....	5.73
5.61 Injection of a) 0.63 mM Na-PO ₄ and b) 2.61 mM Na-PO ₄ with PO ₄ , Ca, and Sr behavior shown.....	5.74
5.62 Injection of 10 mM Na-PO ₄ with PO ₄ , Ca, and Sr behavior shown.....	5.75
5.63 Citrate mineralization at different water saturations with: a) 5 mM, b) 25 mM, and c) 125 mM citrate in Ca-citrate-PO ₄ solutions.....	5.79
5.64 Correlation between water saturation and citrate mineralization half-life (a) and extent (b).....	5.80
5.65 Microbial distribution with depth in 100-N wells.....	5.81
5.66 Citrate mineralization and biomass.....	5.82
5.67 Sediment biomass relationship to citrate mineralization rate (a) and mineralization extent (b).....	5.82
5.68 1-D unsaturated column experimental systems used for Ca-citrate-PO ₄ infiltration....	5.84
5.69 1-D unsaturated column experiments varying the infiltration rate with PO ₄ breakthrough mass shown.....	5.85
5.70 1-D unsaturated column experiments varying the infiltration rate with PO ₄ profile in the column after the experiment shown.....	5.85
5.71 1-D unsaturated column experiments of high PO ₄ injection concentration showing a) PO ₄ breakthrough, and b) PO ₄ precipitate profile with depth.....	5.86
5.72 Conceptual profiles for 2-D infiltration into an area with a low hydraulic conductivity zone.....	5.87
5.73 Conceptual profiles for 2-D infiltration into an area with a low hydraulic conductivity zone.....	5.89
5.74 Presimulation of 2-D solution infiltration into a heterogeneous system.....	5.90
5.75 Dye injection into a 2-D system illustrating water infiltration patterns.....	5.90
5.76 Comparison of water content data from 2-D experiment #3 to simulation for vertical transect down the center of the low-K zone.....	5.91
5.77 2-D infiltration experiment showing infiltration of chemicals and eventual formation of apatite precipitate.....	5.92

5.78	2-D infiltration simulation effect of varying the infiltration rate on the apatite precipitate	5.93
5.79	1-D reactive transport simulation of a 1-meter sediment column injection of a PO ₄ solution	5.94
5.80	Simulation of 1-D injection of a Ca-citrate-PO ₄ solution	5.95
6.1	Citrate biodegradation in a) aerobic system and b) anaerobic system	6.2
6.2	1-meter long 1-D column experiment (Y88) with the injection of 1 mM Ca, 2.5 mM citrate, and 10 mM PO ₄ with results of: a) PO ₄ breakthrough, b) Ca, Na breakthrough, and c) Sr breakthrough.....	6.3
6.3	Scanning electron microscope images of a single apatite crystal	6.4
6.4	Aqueous phosphate measurement after 15-minute acid dissolution of apatite sediment mixtures using 0.1M or 0.5M HNO ₃	6.5
6.5	Sr uptake from groundwater suspension of 0.34 g/L apatite and 20 g/L sediment at 82°C with a) solid phase apatite added, and b) Ca-citrate-PO ₄ solution added.....	6.6
6.6	Sr uptake from groundwater suspension of 0.34 g/L apatite and 20 g/L sediment at 82°C	6.7
6.7	Sr uptake from groundwater suspension of 0.34 g/L apatite and 20 g/L sediment at 82°C	6.8

Tables

1.1	ITRD Technology Evaluation 100-NR-2 Operable Unit	1.6
2.1	Apatite mass and change in Sr-90 mobilization	2.3
3.1	Composition of Ca-citrate-PO ₄ solutions utilized for field injections	3.2
5.1	Sequential injection of low- and high-concentration Ca-citrate-PO ₄ into a 1-D column: time course of events and analysis	5.6
5.2	Results of sequential injection of low- and high-concentration Ca-citrate-PO ₄ into a 1-D column, where event is described in Table 5.1	5.7
5.3	Citrate degradation rates at different temperature and concentration	5.9
5.4	Analyzed injection solution concentration for 20-ft 1-D column experiment T43	5.15
5.5	20-ft column physical parameters	5.16
5.6	Breakthrough of injection solution components at 20-ft location	5.17
5.7	Metals breakthrough data at 20-ft location in 1-D column injection of Ca-citrate-PO ₄	5.18
5.8	Major cation mass balance for 20-ft long 1-D column experiment	5.20
5.9	Solution composition for Field Injection #1	5.22
5.10	Mass of chemicals needed for field injection #1	5.22
5.11	Maximum solubility of Ca-citrate-PO ₄ components and long-term stability	5.23
5.12	Concentration of chemicals needed for field injection #2	5.32
5.13	Mass of chemicals needed for field injection #2	5.32
5.14	Solution Stability Criteria for 60,000 gallon injection volume in injection #2	5.33
5.15	Bactericide addition and analytical interference for injection #2 samples	5.34
5.16	Concentration of chemicals needed for field injection #3 to #18	5.40
5.17	Mass of chemicals needed for field injection #3 to #10	5.41
5.18	Solution stability criteria for 140,000 gallon field injection #3 to #10	5.41
5.19	Composition of Ca-citrate-PO ₄ solutions utilized	5.44
5.20	Sr uptake by citrate precipitated apatite in Figure 5.38 after 9.5 months versus aqueous Ca to Sr mole ratio	5.60
5.21	Conditions of Sr sorption-incorporation versus temperature experiments; units in mM	5.60
5.22	Sr uptake mass fraction and rate by apatite versus temperature after 9.6, 8.6 months; GW indicates 100-N groundwater	5.62
5.23	Conditions of Sr sorption-incorporation experiments at 22°C and 82°C	5.63
5.24	Percent distribution of Sr in apatite suspension for Sr-90 series and mole percent of apatite Ca sites occupied by incorporated Sr	5.63

5.25	Percent of total aqueous Sr incorporation into citrate precipitated and Sigma apatites for stable Sr series	5.64
5.26	Sr-90 fraction sorbed in different sediment/apatite/water systems.....	5.70
5.28	Physical characteristics of 1-D unsaturated column experiments	5.84
6.1	Calculated Sr uptake rates in apatite-laden sediment for a 30-ft wide barrier.....	6.9
6.2	Sequential treatments of Sr-90 laden sediment with fraction Sr-90 uptake and efficiency	6.10

1.0 Introduction

A remediation technology focused upon sequestration of Sr-90 in groundwater at the Hanford 100-N Area has been investigated using laboratory-scale experiments and being tested at the field scale. This technology is based on the injection of an aqueous apatite mixture into the aquifer at the 100-N site. In situ apatite formation and subsequent Sr-90 sequestration by this technology occurs by the following steps: 1) injection of Ca-PO₄-citrate solution (with a Ca-citrate solution complex), 2) in situ biodegradation of citrate which slowly releases the Ca required for apatite [Ca₅(PO₄)₃(OH)] precipitation (amorphous, then crystalline), 3) adsorption of Sr-90 to the apatite surface, 4) apatite recrystallization with Sr-90 substitution for Ca (permanent), and 5) radioactive decay of Sr-90 to Y-90 to Zr-90. Although previous studies (Moore et al. 2004) demonstrated that citrate biodegradation/apatite precipitation occurs in several sediments, and U, Tc, Sr, and Pb were sequestered, the purpose of this study was to determine if this technology could precipitate sufficient apatite in 100-N Area sediments and the subsequent Sr-90 removal rate would be rapid enough to immobilize Sr-90 for 300 years. The following sections describe the Sr-90 contamination in the 100-N Area, the mechanism by which Sr and Sr-90 are incorporated into apatite, and the Ca-citrate-PO₄ solution being used to form apatite.

This report represents a comprehensive summary of 100-N Area apatite laboratory-scale studies from 2005 to 2007, which involves both experiments to develop an efficient groundwater injection formulation and the EM-22-funded infiltration strategy. Results of both studies are included as there is significant overlap in underlying processes. Field-scale injection results for the first 18 injections (as of July 2007) and field-scale simulations are described in a separate field-scale report.

1.1 Sr-90 Contamination in Subsurface and River Biota

The Hanford Site is a U.S. Department of Energy (DOE) site located in southeastern Washington State near Richland, Washington. The Hanford 100 Area is located along the Columbia River and includes nine DOE nuclear reactors previously used for plutonium production, one of which is the 100-N Reactor (Figure 1.1). The operation of the 100-N Area nuclear reactor required the disposal of pass-through cooling water from the reactor's primary cooling loop, the spent fuel storage basins, and other reactor-related sources. Two crib and trench liquid waste disposal facilities (LWDFs) were constructed to receive these waste streams, and disposal consisted of percolation into the soil. The first LWDF (1301-N) was constructed in 1963, about 244 meters (800 feet) from the river (Figure 1.1, lower center). Liquid discharges to this facility contained radioactive fission and activation products, including cobalt-60, cesium-137, strontium-90, and tritium. Minor amounts of hazardous wastes such as sodium dichromate, phosphoric acid, lead, and cadmium were also part of the waste stream. When Sr-90 was detected at the shoreline, disposal at the first LWDF was terminated and a second crib and trench (1325-N LWDF) was constructed further inland in 1983. Discharges to 1325-N ceased in 1993. A more complete history of the groundwater contamination at 100-N can be found in the *Hanford 100-N Area Remediation Options Evaluation Summary Report* (TAG 2001).



Figure 1.1. Hanford 100-N Reactor and disposal trench.

Sr-90 transport in subsurface sediments from disposal cribs has reached the Columbia River, as evidenced by Sr-90 in the river, and in the sediments in shallow water (groundwater discharges to the river, red squares, Figure 1.2). In addition, Sr-90 is detected in Asian clams found on the 100-N shoreline (circles, Figure 1.2). The highest sediment and clam Sr-90 concentration is at river tube #5. A proposed 300-ft wide treatment zone of apatite will extend between river tubes 1 to 8.

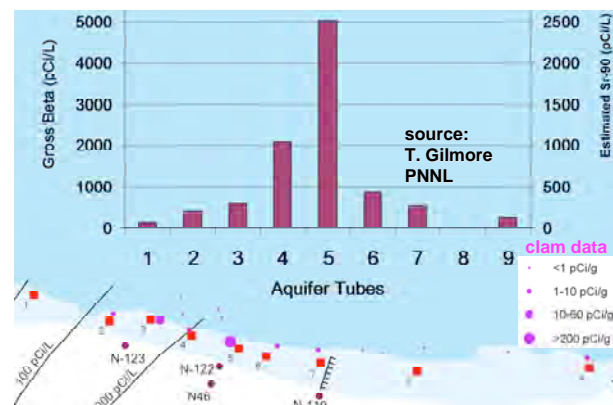


Figure 1.2. Sr-90 contamination in river sediments and clams.

The sediments (gravel with sand/silt) in the 100-N Area consist of a lower Ringold E unit and overlying Hanford formation (15 – 20 ft contact depth), which contain the unconfined aquifer. The Hanford formation is highly transmissive (Ksat 490 – 20,000 ft/day) compared to the underlying Ringold E (20 – 590 ft/day). The Ringold E unit is bounded by the underlying silty Ringold upper mud, approximately 200 ft thick, which acts as an aquitard. Groundwater flows primarily in a north-northwesterly direction most of the year and discharges to the Columbia River. The groundwater gradient varies from 0.0005 to 0.003 ft/ft. Near the LWDF facilities, average groundwater velocities are estimated to be between 0.1 and 2 ft/d, with 1 ft/d average.

Sr-90 contamination in sediments reflects the hydrodynamics in the 100-N Area. Sr-90 has leached from trenches through the variable thickness vadose zone to groundwater and moved toward the Columbia River. Because the river stage changes daily (± 5 ft) and seasonally (± 8 ft for sustained periods), the saturated zone thickness changes and flow reversals do occur (i.e., movement of river water into the aquifer). The result on Sr-90 is a smearing of the plume vertically. Given that the upper Hanford formation has generally 10x greater groundwater flow than the underlying Ringold E Formation, most (but not all) of the Sr-90 contamination is found in the Hanford formation, with roughly a third of the mass in the lower Ringold E (Figure 1.3). The highest concentration found 50 ft inland from the river edge (well N122) is inland from river tube #5 (Figure 1.2), with lower Sr-90 concentrations in wells on both sides of this location. This vertical Sr-90 profile type is previously observed (Serne and LeGore 1996)

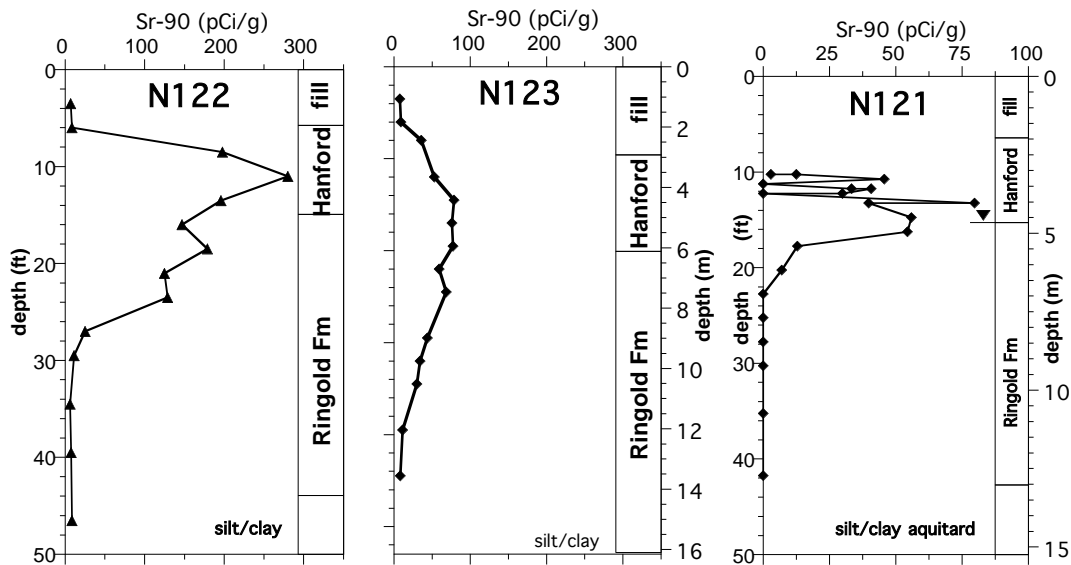


Figure 1.3. Sr-90 contamination in subsurface sediments.

Because of strong Sr-90 adsorption by ion exchange to sediments ($K_d = 25 \text{ cm}^3/\text{g}$ in groundwater, so $R_f \sim 100$; Moore et al. 2006; Routson et al. 1981; Steefel 2004), about 1% of the Sr-90 is in groundwater and 99% on sediments. As such, the pump-and-treat system operated since 1995 has only removed a small amount of Sr-90 from the aquifer, although is effective for removal of mobile contaminants such as tritium. Because of the highly transmissive nature of sediments near the river, the pump-and-treat system removes Sr-90 from inland locations near the disposal trench. Given the high adsorption and short radioactive decay half-life of Sr-90 (29.1 years), only sediments near the river are at risk of entering the river (red/yellow highlighted area, Figure 1.1) before radioactive decay reduces Sr-90 activity to negligible amounts. The pump-and-treat system has not influenced Sr-90 levels in wells near the river (red line, Figure 1.4, well N46 inland of river tube #5 and well N122, Figure 1.3).

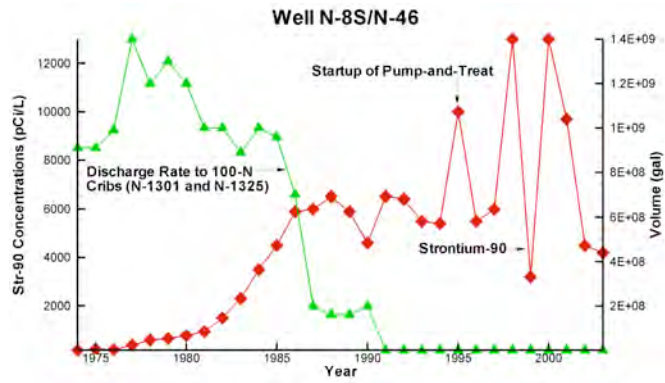


Figure 1.4. Crib discharge (green) and Sr-90 levels in well N46.

1.2 100-N Area Remediation History

The 100-N Area of the Hanford Site was placed on the National Priorities List (NPL) in 1989, the same year the Tri-Party Agreement signed by the DOE, U.S. Environmental Protection Agency (EPA), and the Washington State Department of Ecology (Ecology) established the procedural framework and schedule for the remedial response actions at Hanford. In 1994, the *Limited Field Investigation Report for the 100-NR-2 Operable Unit* (LFI) (DOE-RL 1994) was published and, based on the data presented, a qualitative risk assessment (QRA) was conducted. The QRA indicated that groundwater contaminants in the 100-NR-2 Operable Unit (OU) exceeded human health risk levels, prompting an Expedited Response Action (ERA) to address Sr-90 in groundwater. In 1995, a pump-and-treat system was installed as an interim measure to control the movement of Sr-90 to the Columbia River. A corrective measures study (CMS) (DOE-RL 1997), conducted to support the selection of remedial alternatives to address contamination at the 100-NR-1 and 100-NR-2 OUs, determined that sufficient information was not available to decide a final groundwater remedy. Four alternatives were proposed for consideration as interim remedies (No Action, Institutional Controls, Hydraulic Controls, and Pump-and-Treat), and pump-and-treat was retained as the selected interim remedy because it provides a hydraulic barrier while removing approximately 90% of Sr-90 from extracted groundwater, and does not preclude any potential final remedies.

The remedial action objectives (RAOs) for the 100-NR-2 OU were specified on page 35 of the Interim Action record of decision (ROD):

- Protect the Columbia River from adverse impacts from the 100-NR-2 groundwater so that designated beneficial uses of the Columbia River are maintained. Protect associated potential human and ecological receptors using the river from exposure to radioactive and nonradioactive contaminants present in the unconfined aquifer. Protection will be achieved by limiting exposure pathways, reducing or removing contaminant sources, controlling groundwater movement, or reducing concentrations of contaminants in the unconfined aquifer.
- Protect the unconfined aquifer by implementing remedial actions that reduce concentrations of radioactive and non-radioactive contaminants present in the unconfined aquifer.
- Obtain information to evaluate technologies for Sr-90 removal and evaluate ecological receptor impacts from contaminated groundwater (by October 2005, as amended).
- Prevent destruction of sensitive wildlife habitat. Minimize the disruption of cultural resources and wildlife habitat in general and prevent adverse impacts to cultural resources and threatened or endangered species.

The Interim Action ROD requires that “DOE will investigate groundwater remediation and river protection technologies for Sr-90 contamination and submit information to Ecology within 5 years of this ROD.” “...Pump-and-treat may be considered as an integral part of other alternatives; however, groundwater remediation technologies to be evaluated will focus on innovative technologies to remove Sr-90 from contaminated sediments and groundwater.” (Page 53.) To fulfill the requirements of the Interim Action ROD:

- The pump-and-treat system has operated continuously since 1995. Groundwater monitoring has been conducted as approved by Ecology, and annual reports summarizing the monitoring data and pump-and treat system have been submitted each year since the beginning of operations in 1995.
- Under the Innovative Treatment and Remediation Demonstration (ITRD) Program, the Technical Advisory Group (TAG) for the 100-N Area completed the *Hanford 100-N Area Remediation Options Evaluation Summary Report* in November 2001 (TAG 2001).
- *Strontium-90 at the Hanford Site and its Ecological Implications* (Pacific Northwest National Laboratory [PNNL]) was submitted to DOE in May 2000.
- An ERA is underway in accordance with an approved sampling and analysis plan (DOE-RL 2005). A report is due to Ecology by October 2005.
- A letter report, *Evaluation of Strontium-90 Treatment Technologies for the 100-NR-2 Groundwater Operable Unit*, was submitted to DOE in October 2004 by Fluor/CH2M HILL (Fluor/CH2M HILL 2004). This letter report and related public workshop comments (December 2004), together with the ITRD Report, completes the technology evaluation requirement specified in the Interim Action ROD. This TTP initiates implementation of the previous evaluation efforts.

Installed in 1995, the pump-and-treat system at the 100-N Area uses four extraction wells, a treatment skid, and two injection wells. It is currently operating to retard the movement of contaminated groundwater toward the Columbia River, and in the process is removing small amounts of Sr-90 from the aquifer. As described in the Interim Action ROD, insufficient information existed to recommend a final remedy for Sr-90 in the 100-NR-2 groundwater. Therefore, Ecology, EPA, and DOE proposed to control movement of Sr-90 to the Columbia River as an interim remedial action for river protection. This control was to be provided by the existing pump-and-treat system.

At a pumping rate of 60 gallons per minute (gpm), the pump-and-treat system extracts approximately 0.2-Ci/year, which is about ten times less than the amount removed by radioactive decay of the Sr-90 stored in the aquifer (DOE/RL 2004). As of June 2004, 1.6 Ci of Sr-90 were removed since beginning operations in 1995. Given that there is approximately 80 Ci of Sr-90 in the saturated sediments in the 100-N Area, at this removal rate, the time needed to meet the drinking water standard (8 pCi/L) is approximately 270 years. Although the pump-and-treat system may have met the objective of reducing the flow of groundwater to the river, it has not met the objective of reducing Sr-90 concentrations in aquifer pore fluid at the shoreline or in the stream bank storage zone. Minimizing exposure to eco-receptors in the near-shore aquatic and riparian zone requires a different approach.

In the 2001 ITRD Report, the TAG considered various technologies that would meet the RAOs identified in the Interim Action ROD for protecting the river and the unconfined aquifer, and retained five technologies for further evaluation. TAG's conclusions and recommendations for each technology are presented in Table 1.1.

Table 1.1. ITRD Technology Evaluation 100-NR-2 Operable Unit

Technology	Conclusion	Recommendation
Monitored Natural Attenuation (MNA)	May be appropriate for portion of plume far from the river, but will not limit current discharges of Sr-90 from N Springs.	Should be examined in more detail when establishing Long-Term Stewardship protocols.
Soil Flushing	Likely to be effective in removing Sr-90 in shortest time frame.	Should be examined in more detail with regulators.
Phytoremediation	May be best option for controlling current releases at the river; leaf litter control may be an issue.	Needs more analysis.
Sr-90 stabilization by phosphate injection	Design studies were insufficient to support recommendation of the option.	Re-examine this option after the Tanks Focus Area work is completed.
Barrier technologies (clinoptilolite and sheet pile/cryogenic)	Installation is considered feasible. Bank is stable and erosion potential associated with construction is considered negligible.	Precautions during construction should minimize potential damage.

Based on this evaluation, the ITRD concluded that the DOE should evaluate the following remediation scenarios in more detail:

- Monitored Natural Attenuation (MNA)
- Clinoptilolite Barrier with MNA
- Clinoptilolite Barrier with Phytoremediation on the river side of the barrier
- Sheet Pile/Cryogenic Impermeable Barrier with MNA
- Sheet Pile/Cryogenic Impermeable Barrier with Phytoremediation on the river side of the barrier and Soil Flushing on the inland side

Several important developments occurred prior to and since the completion of the ITRD Report:

- Installation of a sheet pile wall was attempted and found not feasible at this particular site.
- The TAG determined that soil flushing was infeasible, primarily because of the massive volumes of lixiviant required for injection and removal, and the problems inherent in treating and disposing large volumes of radioactive wastewater.
- Renewed interest in Sr-90 stabilization by phosphate injection (chemical injection) is based on reports of successful bench testing at Sandia National Laboratory.

The merits of apatite sequestration and phytoremediation were presented at a workshop in August 2003 by PNNL and Sandia National Laboratory scientists. Because of the potential for these technologies to remove or sequester Sr-90 from the near-river sediments, DOE funded two laboratory studies at PNNL in FY04 to determine their appropriateness for the 100-NR-2 OU:

- Phytoremediation of Sr-90 at the Hanford 100-N Area
- Sr-90 Sequestration by Apatite at the Hanford 100-N Area

1.3 Sr-90 Immobilization with Apatite

Apatite [$\text{Ca}_{10}(\text{PO}_4)_6(\text{OH})_2$] is a natural calcium phosphate mineral occurring primarily in the earth's crust as phosphate rock. It is also a primary component in the teeth and bones of animals. Apatite minerals sequester elements into their molecular structures via isomorphic substitution, whereby elements of similar physical and chemical characteristics replace calcium, phosphate, or hydroxide in the hexagonal crystal structure (Hughes et al. 1989; Spence and Shi 2005). Apatite has been used for remediation of other metals including U (Arey et al. 1999; Fuller et al. 2002, 2003; Jeanjean et al. 1995), lead (Bailliez et al. 2004; Mavropoulos et al. 2002; Ma et al. 1995), Pu (Moore et al. 2005), and Np (Moore et al. 2003). Because of the extensive substitution into the general apatite structure (Figure 1.5), over 350 apatite minerals have been identified (Moelo et al. 2000). Sr incorporation into apatite has also been previously studied (Smiciklas et al. 2005; Rendon-Angeles et al. 2000). Apatite minerals are very stable and practically insoluble in water (Tofe 1998; Wright 1990; Wright et al. 2004). The solubility product of hydroxyapatite is about 10^{-44} , while quartz crystal, which is considered the most stable mineral in the weathering environment, has a solubility product (K_{sp}) of 10^{-4} (Geochem. Software 1994). Strontiapatite, $\text{Sr}_{10}(\text{PO}_4)_6(\text{OH})_2$, which is formed by the complete substitution of Ca by Sr (or Sr-90), has a K_{sp}

of about 10^{-51} , another 10^7 times less soluble than hydroxyapatite (Verbeek et al. 1977). The substitution of strontium for calcium in the crystal structure is thermodynamically favorable, and will proceed provided the two elements coexist. Sr substitution in natural apatites are as high as 11%, although dependent on available Sr (Belousova et al. 2002). Synthetic apatites have been made with up to 40% Sr substitution for Ca (Heslop et al. 2005). The mechanism (solid state ion exchange) of Sr substitution for Ca in the apatite structure has been previously studied at elevated temperature (Rendon-Angeles et al. 2000), but low temperature aqueous rates under Hanford groundwater conditions (i.e., Ca/Sr of 220/1) have not.

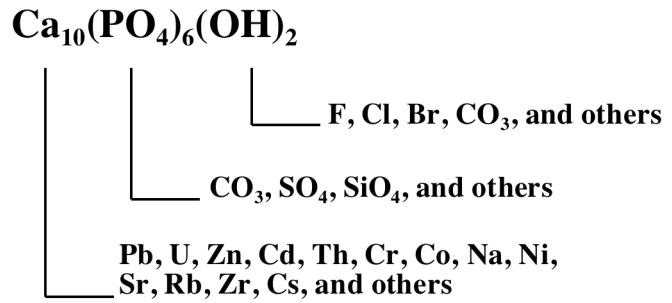


Figure 1.5. Cation and anion substitution in apatite.

1.4 Subsurface Apatite Placement by Solution Injection

The method of emplacing apatite in subsurface sediments at the 100-N Area is to inject an aqueous solution containing a Ca-citrate complex and Na-phosphate. Citrate is needed to keep Ca in solution long enough (days) to inject into the subsurface; a solution containing Ca^{2+} and phosphate only will rapidly form mono- and di-calcium phosphate, but not apatite (Andronescu et al. 2002; Elliot et al. 1973; Papargyris et al. 2002). Relatively slow biodegradation of the Ca-citrate complex (days) allows sufficient time for injection and transport of the reagents to the areas of the aquifer where treatment is required. As Ca-citrate is degraded (Van der Houwen et al. 2001; Misra 1998), the free Ca and phosphate combine to form amorphous apatite. The formation of amorphous apatite occurs within a week and crystalline apatite forms within a few weeks. Citrate biodegradation rates in Hanford 100-N sediments (water-saturated) at temperatures from 10°C to 21°C (aquifer temperature 15°C to 17°C) over the range of citrate concentrations to be used (10 mM to 100 mM) have been determined experimentally and simulated with a first-order model (Bailey and Ollis 1986; Bynhildsen and Rosswall 1997). In addition, the microbial biomass has been characterized with depth and position along the shoreline, and the relationship between biomass and the citrate biodegradation rate determined, as described in the results section. Because Hanford 100-N Area injections typically use river water (~90% to 95%) with concentrated chemicals, microbes in the river water are also injected, which results in a somewhat more uniform citrate biodegradation rate in different aquifer zones.

Emplacement of apatite precipitate by a solution injection has significant advantages over other apatite emplacement technologies for application at the Hanford 100-N Area. The major advantage is minimal disturbance of the subsurface (both vadose and saturated zone), as this technology only requires injection wells (for groundwater remediation) or a surface infiltration gallery (for vadose zone treatment), in contrast with excavation of the river bank for trench-and-fill emplacement of solid phase apatite. Other apatite emplacement technologies were also considered for the 100-N Area (DOE/RL 2005), which included pneumatic injection of solid apatite, vertical hydrofracturing for apatite emplacement both as a permeable reactive barrier and

grout curtain. Although each technology has advantages and disadvantages, the Ca-citrate-PO₄ injection technology was chosen as it appears to provide the most economic emplacement methodology to treat Sr-90 in the near-shore sediments. A weakness of all of these apatite technologies is the Sr-90 is not removed from the sediment until radioactive decay occurs, as the Sr-90 is incorporated into the apatite crystalline structure.

1.5 Need for Injection/Infiltration Strategy at River Shore

The current plan is to inject the Ca-citrate-PO₄ solution separately into the Hanford formation and Ringold E Formation sediments. While there is a high degree of confidence that apatite precipitate will occur, the river hydrodynamics create a significant problem for the seasonal timing of the injection (Figure 1.6). Simulation of injections into the lower (less transmissive) Ringold E Formation at sustained low and high river stage show that the river stage does not move the Ca-citrate-PO₄ injection plume a significant distance before apatite is expected to precipitate, so the time of year for injection into the Ringold E Formation is best at lower river stages (late fall) to get some apatite movement toward the river, but the timing isn't critical.

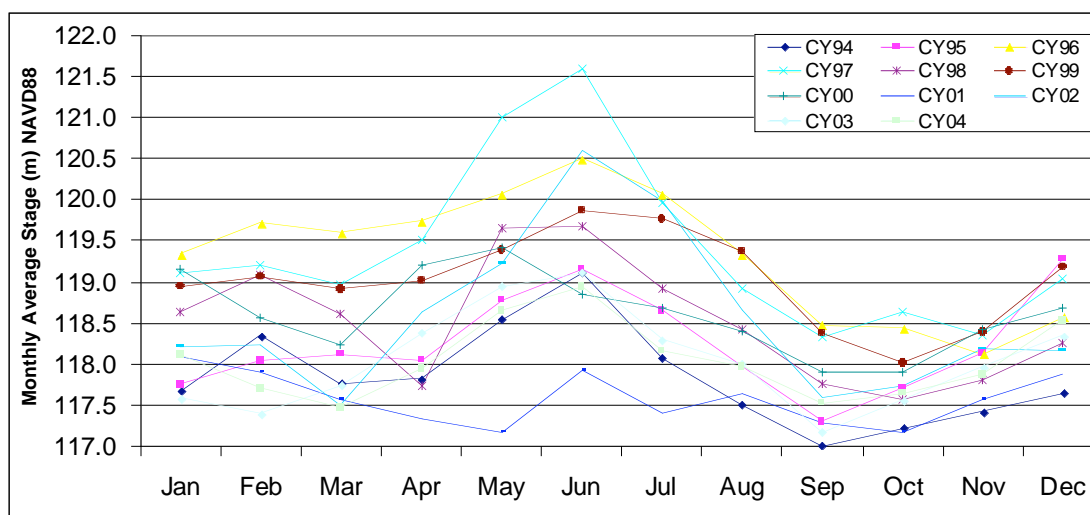


Figure 1.6. Columbia River stage 1994 – 2005 (Edrington 2005).

In contrast, apatite-forming solution injection into the upper Hanford formation needs to be done during high river stage so that the formation is water saturated (i.e., late spring, Figure 1.5). In addition, because movement of the solution is desired toward the river, the most desirable injection river stage would be a high river stage (saturating the formation) followed by a moderate river stage, to get slow flow toward the river. Injection during low river stage would result in rapid movement of the injection solution into the river (days) before precipitation would occur. Therefore, river hydrodynamics have a potentially significant influence on the effectiveness of the emplacement of the solution by injection. There are only short periods throughout the year where the river stage conditions are optimal for injection. The effectiveness of the low- and high-river stage injections (~18 injections completed by July 2007) are described in the follow-on study to this report which is focused mainly upon laboratory-scale results of forming apatite and sequestering Sr-90.

Infiltration of the Ca-citrate-PO₄ solution (EM-22 funded study) could be accomplished at a different river stage than injection, so an infiltration strategy extends the amount of time that apatite could be emplaced. Infiltration into the Hanford formation sediments would be optimal at periods of low river stage (leaving a greater thickness of unsaturated porous media), so could occur during summer/fall, or the second low stage of early spring. The formation of apatite during infiltration during these periods is less influenced by transmissivity in the formation and river stage, and more dependent on the rate of infiltration. Another potential benefit to infiltration is that cost of implementation may be much less than injection, as wells (a significant cost) do not need to be installed, although there is some cost associated with the infiltration method (i.e., trenches, drip emitters, etc).

2.0 Background – Injection of a Ca-Citrate-PO₄ Solution to Form Apatite In Situ

2.1 Precipitation of Apatite in Aquifer Sediments with a Ca-Citrate-PO₄ Solution

The method of emplacing apatite in subsurface sediments at the 100-N Area is to inject an aqueous solution containing a Ca-citrate complex and Na-phosphate. Citrate is needed to keep Ca in solution long enough (days) to inject into the subsurface; a solution containing Ca²⁺ and phosphate only will rapidly form mono- and di-calcium phosphate, but not apatite (Andronescu et al. 2002; Elliot et al. 1973; Papargyris et al. 2002). Relatively slow biodegradation of the Ca-citrate complex (days) allows sufficient time for injection and transport of the reagents to the areas of the aquifer where treatment is required. As Ca-citrate is degraded (Van der Houwen et al. 2001; Misra 1998), the free Ca and phosphate combine to form amorphous apatite. The formation of amorphous apatite occurs within a week and crystalline apatite forms within a few weeks. Citrate biodegradation rates in Hanford 100-N sediments (water-saturated) at temperatures from 10°C to 21°C (aquifer temperature 15°C to 17°C) over the range of citrate concentrations to be used (10 mM to 100 mM) have been determined experimentally and simulated with a first-order model (Bailey and Ollis 1986; Bynhildsen and Rosswall 1997). In addition, the microbial biomass has been characterized with depth and position along the shoreline, and the relationship between biomass and the citrate biodegradation rate determined, as described in the results section.

2.2 Characterization of Apatite Precipitate

Previous studies have used multiple characterization techniques employed (Figure 1.6) to assess the crystal chemistry of the apatite formed by the microbial digestion of Ca-citrate in sediments. These techniques (and others) were used in this study to assess both the apatite purity formed, but additionally the amount of organic carbon in the apatite (due to the presence of microbial biomass), inorganic carbon, and the mass of apatite in sediment (generally present at low concentrations). Previous studies showed that high-resolution transmission electron microscopy (HRTEM) and X-ray powder diffraction (XRD) were used to assess apatite crystallinity and to document the transformation from an amorphous calcium phosphate to nanocrystalline apatite. Energy dispersive (EDS) and Fourier transform-infrared (FT-IR) spectroscopy were used to analyze the chemical constituents. Blade-like crystals in an amorphous matrix are approximately 0.1 μm in size (Figure 2.1a, upper left). This was consistent with the observed broad overlapping peaks in the XRD pattern at 2 microns of approximately 32°, a typical characteristic of poorly crystallized apatite (Figure 2.1b, upper right; Waychunas 1989; Nancollas and Mohan 1970; Hughes and Rakovan 2002). The remaining peaks in the XRD correspond to components of the sediment. Fourier transform infrared (FTIR) spectra are given for pure hydroxyapatite (top spectrum) produced by precipitation and heat treatment at 700°C and calcium phosphate precipitates in the Hanford 100-N sediment after one month (bottom spectrum). The lower resolution of the PO₄⁻ bands confirms the lower crystallinity of the sample, as observed by both

HRTEM and XRD. The bands at 1455 cm^{-1} and 879 cm^{-1} indicate the presence of carbonate in the apatite structure. The TEM-EDS spectrum identifies calcium and phosphate as the major components with a stoichiometric apatite ratio of approximately 5:3.

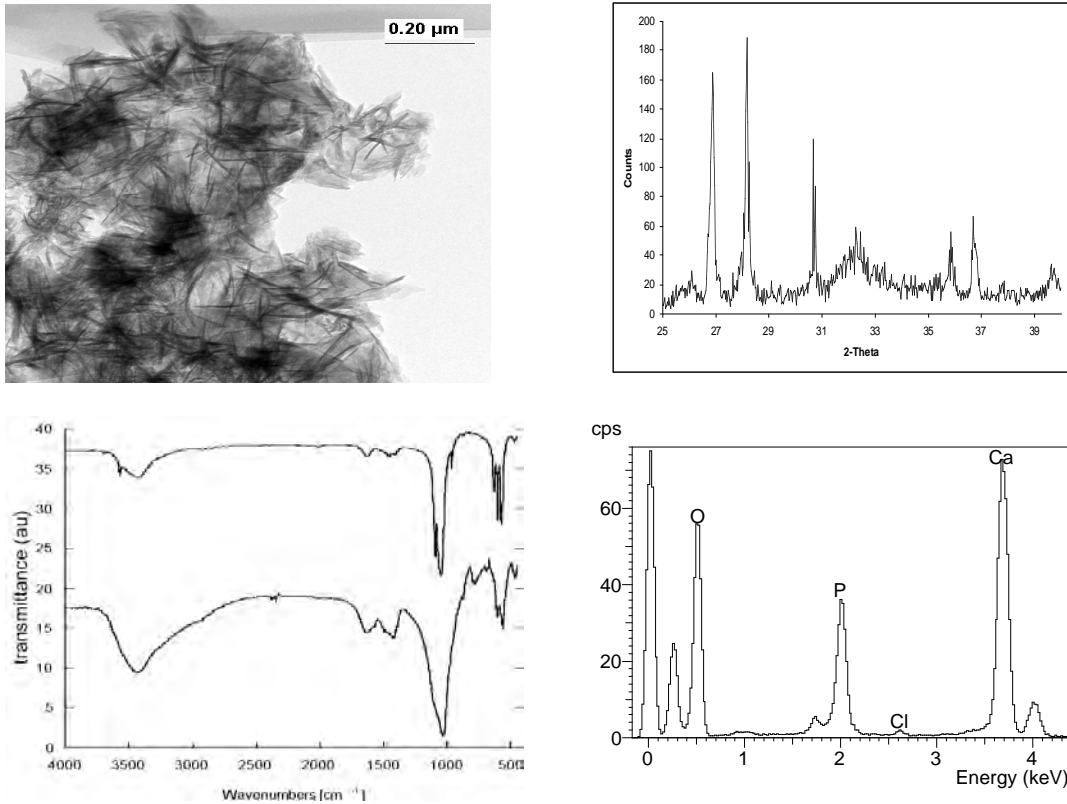


Figure 2.1. Characterization of nanocrystalline apatite formed in Hanford sediment by microbially mitigated Ca-citrate degradation in the presence of aqueous phosphorous: a) TEM, b) XRD, c) FTIR, and d) EDS

2.3 Mass of Apatite Needed for Hanford 100-N Area

Two factors control the amount of apatite needed to sequester Sr-90 in the Hanford 100-N Area. First, from a mass balance point of view, a specific amount of apatite is needed that will remove all Sr and Sr-90 from groundwater over the next 300 years (i.e., 10 half lives of Sr-90 decay, half-life 29.1 years). This calculation is dependent on the crystal substitution of Sr for Ca in apatite. If 10% substitution is assumed, then 1.7 mg of apatite is sufficient to sequester Sr and Sr-90 from the estimated 3300 pore volumes of water that will flow through an apatite-laden zone. This calculation assumes an average groundwater flow rate of 0.3 m/day and a 10-m thick apatite-laden barrier. The 1.7-mg apatite/g of sediment does occupy some pore space in the aquifer, which has an average field porosity of 20%. Given a crystal lattice dimensions of 9.3A by 6.89 A (i.e., assume a cylinder of dimensions $7.5\text{E-}21\text{ cm}^3/\text{atom}$), the 1.7-mg apatite/g sediment would occupy 13.6% of the 20% pore space, so there should be some decrease in permeability.

The second factor that would control the amount of apatite needed to sequester Sr-90 is the rate of incorporation. This permeable reactive barrier concept of apatite solids in the aquifer works if the flux rate of Sr and Sr-90 is slower than the removal rate of Sr and Sr-90 by apatite. If the groundwater flow rate is too high, even highly sorbing Sr and Sr-90 could advect through the apatite-laden zone more quickly than it is removed. The way to circumvent this issue is to have additional apatite in the groundwater system (upgradient) to essentially remove Sr-90 at an increased rate. Based on the experience in the 100-D Area where partially reduced sediment is slowly removing chromate (and nitrate), seasonal fluctuations in the river level lead to specific times of year when flow in the aquifer exceeds the chromate removal rate of the reduced sediment. Therefore, numerous experiments have been conducted in this study to clearly define the rate at which Sr and Sr-90 is incorporated into the crystal structure of apatite.

Because Sr and Sr-90 interact with apatite by two processes (sorption by ion exchange and incorporation into sediment), the effect of addition of a small amount of apatite to sediment and the subsequent change in both sorption and incorporation can be calculated (Table 2.1). These calculations assume no Sr/Sr-90 is incorporated into apatite during the initial precipitation (experiments show 25% to 40% is incorporated).

Table 2.1. Apatite mass and change in Sr-90 mobilization

System	Injected PO₄ (mM)	g apatite/ g sediment	Predicted^(a) Sr-90 (pCi/L) w/sorption only	Predicted^(a) Sr-90 (pCi/L) w/incorporation
groundwater	0.0	0.0	1000	1000
field inj. #1, #2	2.4	9E-5	999	165
field inj. #3-10	10	3.8E-4	974	44
Max. single inj.	24	9E-4	928	18
300 yr capacity	90	3.4E-3	767	4
(a) assumptions: 1000 pCi/L initially in groundwater, Sr/sediment $K_d = 25 \text{ cm}^3/\text{g}$, Sr/apatite = $1370 \text{ cm}^3/\text{g}$, 10% Sr substitution for Ca in apatite.				

What these calculations show is that even though the Sr sorption to apatite is very high ($K_d = 1370 \text{ cm}^3/\text{g}$), because the mass of apatite is so small (as precipitate in pore space of sediment), the resulting sorption of Sr and Sr-90 onto apatite/sediment is small. The net effect is that right after apatite is placed in sediment (i.e., weeks), there will be little observed decreased in the Sr-90. Over the time scale of months, however, Sr and Sr-90 are slowly removed, and the amount of incorporation (10% crystal substitution of Sr for Ca in apatite is assumed in these calculations) is fairly significant. Even the 2.4-mM of PO₄ injected in field injections #1 and #2 should eventually result in a 8x decrease in the Sr-90 concentration (after 6 to 12 months). This small amount of apatite will be exhausted after a few years, so additional apatite is needed. A sequential low concentration injection followed by a 6- to 12-month wait period, then one or more high concentration injections are proposed, as described in Section 2.5. The purpose of these injections is to emplace sufficient apatite for 300 years of capacity, but minimize the initial desorption of Sr-90 in the injection zone.

2.4 Sr and Sr-90 Incorporation Rate into Apatite

Because Sr^{2+} and Sr-90 behave essentially the same as Ca^{2+} , some Sr and Sr-90 is incorporated in apatite during the initial precipitation. Thermodynamically strontiapatite [$\text{Sr}_{10}(\text{PO}_4)_6(\text{OH})_2$, $K_{\text{sp}} = 10^{-51}$] is favored relative to hydroxyapatite [$\text{Ca}_{10}(\text{PO}_4)_6(\text{OH})_2$, $K_{\text{sp}} = 10^{-44}$]. However, the more rapid the apatite precipitation is, the Ca/Sr ratio in the crystalline structure will simply reflect the Ca/Sr ratio in the solution. Therefore, while it is relatively easy to make 40% Sr-substituted apatite from a solution containing 40% Sr, Hanford groundwater Ca/Sr ratio is 220:1. Results in this report show that the amount of Sr substitution into apatite during the initial precipitation is far greater than 0.4% (1/220), and is generally in the 30% to 40% range, so reflects the influence of thermodynamics on the slow precipitation.

Once solid phase apatite is precipitated, Sr and Sr-90 will additionally be incorporated into the apatite structure by solid phase dissolution/recrystallization, as described below. The initial step in this process is Sr and Sr-90 sorption to the apatite surface. Results in this study show this sorption is quite strong ($K_d = 1370 \pm 439 \text{ L/Kg}$) or 55 times stronger affinity than to sediment ($K_d = 24.8 \pm 0.4 \text{ L/Kg}$). The rate of metal incorporation into the apatite crystal lattice can be relatively slow, on the order of days to years (LeGeros et al. 1979; Vukovic et al. 1998; Moore 2003, 2005). While there have been a number of studies of this Sr-substitution rate into apatite (Hill et al. 2004; Lazic and Vukovic 1991; Raicevic et al. 1996; Heslop et al. 2005; Koutsoukos and Nancollas 1981), geochemical conditions differ from the application in groundwater at the Hanford 100-N Area. However, in the presence of soluble phosphates, apatite acts as a seed crystal for the precipitation of metal phosphates (Vukovic et al. 1998). Homogeneous nucleation (precipitation directly from solution) will generally not occur except at very high metal concentrations, for example, greater than 10 parts per million (ppm). However, at low concentrations of the substituting cation (such as calcium) and in the presence of small amounts of phosphate and a seed crystal of apatite, heterogeneous nucleation occurs on the surface of the apatite seed crystal (Lower et al. 1998). The apatite itself serves as a small, but sufficient source of phosphate to solution, and thus perpetuates the precipitation reaction. Over time, the precipitated metals are sequestered into the apatite crystal matrix. The mechanism (solid state ion exchange) of Sr substitution for Ca in the apatite structure has been previously studied at elevated temperature (Rendon-Angeles et al. 2000), but low temperature aqueous rates under Hanford groundwater conditions (i.e., Ca/Sr of 220/1) have not.

The amount of Sr-90 incorporation into solid phase apatite has been characterized in previous studies by a variety of methods. The most reliable types of studies that prove the phenomena use pure apatite in a solution containing a specific Sr concentration, and the apatite solid phase is analyzed for percent Sr substitution by: a) dissolution and aqueous Sr or Sr-90 analysis, or b) electron microprobe with EDS or elemental detection of Sr. Analysis of the remaining Sr and Sr-90 aqueous concentration in a apatite/water system is insufficient to determine if Sr/Sr-90 has been incorporated into apatite. However, if the Sr/Sr-90 aqueous concentration, and ion exchangeable Sr concentrations are analyzed, then the remaining Sr/Sr-90 must be incorporated into the apatite structure.

Therefore, sequential extractions of selected chemical extraction were used to remove ion exchangeable Sr-90, organic-bound Sr-90, carbonate-bound Sr-90, and remaining (residual)

Sr-90. Both Sr and Sr-90 were analyzed in extractions to determine if the Sr was retained differently from the Sr-90. It was expected that Sr was geologically incorporated into many different sediment minerals (Belousova et al. 2002), so should be more difficult to remove compared with Sr-90, which was recently added to the systems. The ion-exchangeable extraction consisted of the addition of 0.5M KNO_3 to the sediment sample for 16 h (Amrhein and Suarez 1990). The organic-bound extraction conducted after the ion-exchangeable extraction consisted of 0.5M NaOH for 16 h (Sposito et al. 1982). The carbonate-bound extraction conducted after the organic-bound extraction consisted of the addition of 0.05M Na_3EDTA for 6 h (Sposito et al. 1983a, 1983b; Steefel 2004). The residual extraction conducted after the carbonate-bound extraction consisted of the addition of 4M HNO_3 at 80°C for 16 h (Sposito et al. 1983a, 1983b). Apatite dissolution rates are highest at low pH (Chairat et al. 2004), so this extraction is expected to remove Sr-90 that is incorporated into the apatite.

2.5 Sr-90 Initial Mobilization and Sequential Injection Strategy

Because ~90% of the Sr and Sr-90 in the Hanford 100-N Area groundwater sediments is held by ion exchange, any solution that is injected into the aquifer (or infiltrating into the vadose zone) that has a higher ionic strength relative to groundwater (11.5 mM) and/or proportionally higher percentage of divalent cations will cause Sr and Sr-90 to desorb from sediments. At 100-N Area pH (~7.8), Sr K_d value is ~15 L/Kg, or an approximate retardation factor of 125 (i.e., ~99% of the Sr and Sr-90 mass is sorbed). As described in the results section of this report, injection of a low concentration of the Ca-citrate- PO_4 (4, 10, 2.4) solution results in a ~10 times increase in Sr and Sr-90 aqueous concentration. Injection of a much higher concentration Ca-citrate- PO_4 (40, 100, 24) solution results in >50 times increase in Sr and Sr-90 aqueous concentration. Injection of a Ca-citrate- PO_4 solution at the field scale will mobilize some Sr and Sr-90 in the injection zone (~3% of the sorbed Sr-90 mass for a low Ca-citrate- PO_4 concentration injection), and less Sr-90 for the zone that the spent solution migrates through. As described in an earlier section, a total mass of ~1.7 mg apatite per gram of sediment is needed (assuming 10% Sr substitution for Ca in apatite) to sequester Sr-90 for 300 years (i.e., ~10 half lives of the Sr-90 decay with a half-life of 29.1 years). This mass of apatite is equivalent to injections totaling 90 mM PO_4 .

In order to emplace the total amount of phosphate needed to achieve sufficient Sr-90 sequestration capacity and minimize Sr-90 mobilization during the injections, a sequential injection strategy can be used. Injection of a low concentration of the Ca-citrate- PO_4 (1, 2.5, 10, see Table 3.1) solution will cause a small increase in the Sr and Sr-90 during the weeks of emplacement (~5x increase in aqueous concentration). Over the time scale of 6 to 12 months, most of the Sr-90 in the injection zone will be incorporated into the apatite structure. Note that this relatively low concentration injection has some capacity to incorporate Sr-90, but insufficient capacity to sequester Sr-90 that is upgradient of this apatite-laden zone that is slowly migrating toward the river over the next 300 years. After the time interval to sequester the local Sr-90 in the injection zone, then one or more higher concentration Ca-citrate- PO_4 (1, 25, 100, for example) can be injected with minimal Sr-90 mobilization. These sequential experiments have been successfully conducted in the laboratory, so should work at the field scale for a system with a downgradient injection zone (where apatite is emplaced) with most of the Sr-90 mass upgradient of the apatite-laden zone. One zone that would be difficult to manage at the field scale is the aquifer zone downgradient of the injection zone (i.e., between the injection wells and the river). If the low

concentration Ca-citrate-PO₄ injections are designed such that the solution is leaching out into the river, then apatite precipitate should occur all the way to the river bank sediments, and there will be initial ~5x increase in aqueous Sr-90 and a subsequent decrease (over months) in aqueous Sr-90. However, if the low concentration injections do not reach the river edge, there will be Sr-90 mass in the near-river sediment held only by ion exchange (i.e., zone where the solution did not reach). Later high concentration injections will mobilize this Sr-90, resulting in high concentration Sr-90 peak concentrations in groundwater for a short period of time while the injected/spent solution slowly leaches out into the river. This may be mitigated to some extent by the presence of Coyote willows along the river bank (i.e., the active bioremediation), which if emplaced for the first few years during the apatite injections could limit Sr-90 transport into the river.

3.0 Experimental Methods

3.1 Ca-Citrate-PO₄ Solutions

This technology uses a Ca-citrate-PO₄ solution that does not precipitate until the citrate is biodegraded. The composition of this solution has changed over time, reflecting: a) increasing utilization of available Ca²⁺ from groundwater (and on ion exchange sites) rather than injecting all the Ca²⁺ needed, and b) minimizing Sr and Sr-90 ion exchange release from sediment upon injection. Initially, the solution composition did not reflect utilization of Ca²⁺ from groundwater or ion exchange sites, so the solution injected for field injection #1 (Table 3.1) utilized a higher concentration of calcium chloride [$CaCl_2 \cdot 2H_2O$] and trisodium citrate [$HOC(COONa)(CH_2COONa)_2 \cdot 2H_2O$] compared to later injections. When combined, the solution at this low concentration is stable for days, depending on whether microbes are present in the makeup water (i.e., citrate biodegrades).

Solution for Field Pilot Test #1. The field injections of 60,000 gallons to 140,000 gallons (each) delivered the solution to each well using concentrated mixtures of calcium chloride and trisodium citrate (called solution 1, in one tanker truck) and a second solution of the phosphates and nitrate (called solution 2, in a second tanker truck), and river water. The maximum concentration that can be used also depends on the makeup of the water. In a laboratory setting with deionized water, a 80-mM Ca, 200-mM citrate, and 50-mM PO₄ solution is stable for ~12 hours at room temperature. Stability of the solutions utilized at the field scale was tested in the laboratory, and solution 1 (56 mM Ca, 140 mM citrate) and solution 2 (28 mM phosphates and 14 mM nitrate) mixed up in deionized water were stable at 4°C for 7 days (Table 3.1). The mixture of phosphates defines the final pH of 7.5. The solutions were refrigerated to minimize microbial growth. The mixing of solution 1, solution 2, and river water is done at the well head continuously during injection. This solution has an ionic strength of 99.5 mM, which is 8.6 times that of groundwater.

Solution for Field Pilot Test #2. Based on laboratory experiments described in this report, the solution composition was modified to include half of the calcium chloride and half of the sodium citrate, given the significant amount of calcium available exchanging of sediments. In addition, it was determined that less N was needed (and as ammonium rather than nitrate) for biodegradation, so diammonium phosphate was used instead of multiple sodium phosphates and separate ammonium nitrate. This Ca-citrate-PO₄ (2, 5, 2.4) solution has an ionic strength of 60.7 mM, so resulted in less Sr and Sr-90 ion exchange during injection, compared with the solution used in field injection #1.

Solution for Field Injections #3 to #18. Further laboratory experiments described in this report showed that apatite precipitation would occur with even less calcium chloride and sodium citrate injection. Because ultimately significantly more PO₄ mass was needed for the ultimate capacity of 300 years to sequester Sr-90 than the 2.4 mM PO₄ (see background section), the solutions used in field injections #3 to #18 had 10 mM PO₄, or four times that of field injections #1 and #2. Laboratory experiments showed that the initial Sr and Sr-90 ion exchange would be about the same as field pilot test #2. An additional change was to decrease the amount of ammonium, due to the ion exchange affinity. While the major divalent cations (Ca²⁺, Mg²⁺, Sr²⁺) had roughly the

same ion exchange affinities, the monovalent cations differed. Na^+ had half the affinity of Ca^{2+} , but both K^+ and NH_4^+ had significantly higher affinities relative to Na^+ . Therefore, there is less ion exchange if Na^+ is utilized instead of NH_4^+ .

Table 3.1. Composition of Ca-citrate- PO_4 solutions utilized for field injections.

Name (conc in mmol/L)	Composition ^(a)	pH	Max. solubility ^(b)	Ionic str. (mM)	Field Use
Ca-citrate- PO_4 (4, 10, 2.4)	Solution 1: 4.0 mM calcium chloride 10 mM trisodium citrate Solution 2: 2.0 mM disodium phosphate 0.4 mM sodium phosphate 1.0 mM ammonium nitrate	7.5 ± 0.1	56 mM 140 mM 28 mM 14 mM	99.5	Field injection #1
Ca-citrate- PO_4 (2, 5, 2.4)	Solution 1: 2.0 mM calcium chloride 5.0 mM trisodium citrate Solution 2: 2.4 mM diammonium phosphate 1.0 mM sodium bromide	8.0 ± 0.1	40 mM 100 mM 480 mM 200 mM	60.7	Field injection #2
Ca-citrate- PO_4 (1, 2.5, 10)	Solution 1: 1.0 mM calcium chloride 2.5 mM trisodium citrate Solution 2: 8.1 mM disodium phosphate 1.4 mM sodium phosphate 0.5 mM diammonium phosphate 1.0 mM sodium bromide	7.8 ± 0.1	48 mM 120 mM 526 mM 91 mM 32 mM 65 mM	84.5	Field injections #3 to 18 (2/07 to 4.07)
100-N groundwater	1.3 mM Ca, 0.2 mM K, 0.54 mM Mg, 1.1 mM Na, 0.60 mM Cl 0.69 mM SO_4 2.72 mM HCO_3	7.7-8.3		11.5	
(a) Concentrations listed are for the final mix of solutions 1 + 2.					
(b) Tested solubility in complete solution.					

3.2 Batch Experiments with Ca-Citrate- PO_4 Solutions

The process of apatite precipitation using Ca-citrate- PO_4 solutions involves contacting the solution with sediment so that: a) microbes in the sediment biodegrade the citrate by a fermentation process, b) the slow release of Ca from the citrate complex results in slow precipitation of apatite. Citric acid is utilized by many organic systems as part of the TCA (Krebs) photosynthetic process (Figure 3.1), where the citrate (a C6 organic acid) is converted to C6, C5, and C4 organic acids producing CO_2 and H^+ , then cycled from oxaloacetic acid (C4) to citric acid (Bailey and Ollis 1986). Citrate can also be further degraded to acetic acid (C2), formaldehyde, formic acid (C1) and CO_2 . For the purpose of this study, citrate is used to complex Ca, so only the decrease in citrate concentration (by biodegradation) is of significance, as the lower molecular weight organic acids only form weak complexes with Ca. Citrate ferments to form acetate and formate as has been observed in unamended sediments from the Hanford Site and in these same sediments amended with a known citrate-fermenting microorganism (results section).

A lag time of about 3 days prior to fermentation was observed in the unamended sediments likely due to low initial populations of microorganisms. While acetate and formate are the primary fermentation products, the amended sediments showed small amounts of lactate and propionate produced in addition to the acetate and formate. In these experiments, citrate fermentation followed the reaction stoichiometry shown in Eq. (3.1).



Biomass in the pre-test unamended sediment sample was 1.51×10^5 cells/g-soil and an average of 2.25×10^8 cells/g-soil after the 16-day incubation period. Using a generic cell formula of $\text{C}_5\text{H}_7\text{O}_2\text{N}$, the molecular weight of cells is 113 mg/mmmole. These anaerobic citrate biodegradation experiments show that 73% of the carbon from citrate can be accounted for in formate and acetate, and it is likely that the other 25% is carbon dioxide, as shown in Eq. (3.1).

Initial Ca-citrate- PO_4 experiments were conducted in batch systems, and various aqueous species concentrations were measured (i.e., citrate, degradation products, PO_4 , Ca, etc). This type of data is predominantly used to determine the rate of citrate biodegradation, which is approximately equal to the rate of apatite precipitate formation (although apatite precipitate is not measured in this type of experiment). These experiments typically consisted of 10 to 100 mL of water mixed with 1 to 60 g of 100-N sediment, and the reaction pathway followed for 1 to 2 weeks by periodic sampling of the aqueous solution.

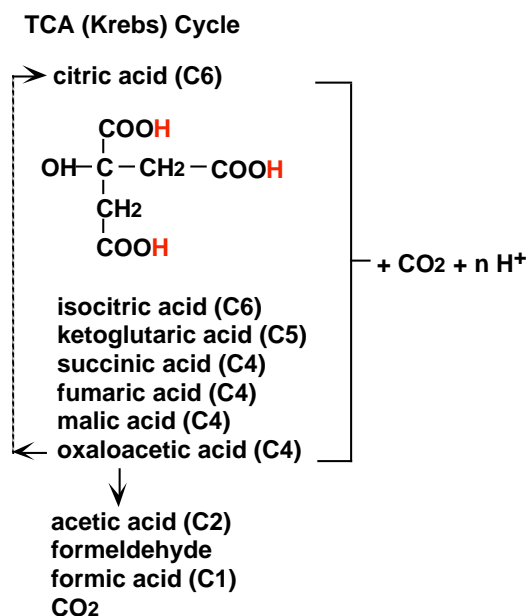


Figure 3.1. Biodegradation pathway for citrate.

Solution stability experiments involved mixing up high concentrations of solutions (Table 3.1), and quantifying the composition of the precipitate. In most cases, Ca-citrate precipitated out of solution (as measured by FTIR), as the solution was slightly over saturated. Laboratory solutions made up with deionized water and aseptically filtered with a 0.1- μm filter to remove most microbes remained stable the longest. However, other solution stability experiments were conducted with groundwater and river water, as these occur during field-scale injections. The Hanford 100-N groundwater contains $\sim 10^5$ cfu/mL and the river water contains $\sim 10^7$ cfu/mL, so Ca-citrate- PO_4 solutions in most cases degraded within 24-48 h, with measured loss of citrate and PO_4 (due to precipitation). For this reason (i.e., citrate degradation if the solution contains microbes), the concentrated chemicals are mixed with river water and injected into the well within minutes (i.e., continuously over the 8 h to 60 h injection periods).

Additional Ca-citrate- PO_4 batch experiments are conducted to measure the composition of the apatite precipitation. In the batch experiments described above where the solution is fully mixed

with the sediment, the amount of precipitation is relatively small and difficult to measure both the quantity of precipitate and its composition. For example, a 2.4-mM PO_4 solution will result in 0.05 mg of apatite per gram of sediment (i.e., 0.005%), which is too small for x-ray diffraction (0.5% or possibly as low as 0.1%). One approach used was to precipitate apatite from higher concentration solutions. A solution containing 28 mM PO_4 (maximum solubility of the Ca-citrate- PO_4 solution) would result in 0.56 mg apatite per gram of sediment (0.056%), assuming 100% of the aqueous PO_4 precipitates. Because only the microbes from the sediment are needed (if Ca from ion exchange sites are not being utilized), an approach used to additionally concentrate the amount of apatite produced was to use a small amount of sediment (2 to 5 g) in a woven Teflon bag in 5 liters of a high concentration apatite solution. This isolates the sediment from the precipitate, which can be dried and characterized. Due to the extremely low soil to solution ratio in these experiments, the citrate biodegradation rate was considerably slower (weeks).

3.3 Apatite and Ca- PO_4 Solid Phase Characterization

Apatite characterization methods used included: a) x-ray diffraction, b) electron microprobe analysis with EDS detector (purity of apatite formed), c) electron microprobe analysis with elemental detector (for Sr substitution in apatite), d) apatite dissolution in 0.5 M or 4 M nitric acid and aqueous PO_4 analysis (i.e., aqueous PO_4 extraction), e) surface area measurement by BET, f) inorganic carbon analysis (to determine if carbonate is present in the apatite, g) organic carbon analysis (to determine if microbial biomass is incorporated into the apatite), and h) fluorimetry for specific substituted apatites.

Aqueous PO_4 extraction experiments consisted of mixing 0.5 to 5.0 g of sediment (with or without precipitated apatite) with 5 mL of 0.5 M or 4 M HNO_3 and PO_4 analysis of samples taken at time intervals ranging from minutes to days. It was determined that the 100-N sediment (without added apatite precipitate) contains approximately 2.3 mg PO_4/g of sediment. Electron microprobe analysis does show some P in quartz-associated mineral grains, so these may be primary mineral phases. It was also noted that phosphoric acid was used in the 100-N trenches, so there may be some PO_4 associated with the waste. A 2.4-mM PO_4 solution would result in 0.05 mg apatite/g sediment or 0.028 mg PO_4/g of sediment. Because this represents only 1.2% of the PO_4 initially in the sediment, it is unlikely that it can be accurately measured. A 15-mM PO_4 solution would result in 0.315 mg apatite/g or 0.18 mg PO_4/g (7.8% of the PO_4 initially in the sediment). Finally, a total of 90 mM PO_4 solution would result in 1.65 mg apatite/g of sediment or 0.94 mg PO_4/g sediment (41% of the PO_4 initially in the sediment). This higher concentration can possibly be identified by this aqueous PO_4 extraction. Experiments conducted with the pure precipitated apatite showed that it dissolved in the 0.5 M HNO_3 by 10 minutes, whereas the PO_4 from the sediment took 1 to 4 h to dissolve. Therefore, utilizing low acid concentrations and short extraction time increases the apatite precipitation identification.

Thin sections of sediment and sediment/apatite mixtures were prepared for the electron microprobe by mixing specific concentrations of apatite with sediment, then encasing the dried composite in epoxy and making a 10-micron-thick section. Microprobe analysis could identify extremely small concentrations of apatite. Typically a 2-mm by 2-mm section of the thin section was scanned with a 15- μm beam, 15 μm scan step, 120 x 120 grid (14,400 points) with

1000 mseconds scan per point, for a total scan time of 30 h per sample. With that relatively long scan time at each point, P could be detected at a concentration of 10 ppm within the 15 μm beam using elemental detectors. In addition to scanning for P, Mg, and Ca were also measured.

3.4 1-D Column Experiments with Ca-Citrate-PO₄ Solutions

1-D column experiments were conducted with 100-N sediment in which various Ca-citrate-PO₄ solutions were injected, with effluent measurements made of Ca, citrate, PO₄, Na, Sr, Sr-90, and other cations/anions commonly found in Hanford groundwater. These 1-D column experiments are idealized representations of the type of reactions that would occur at the field scale. Various types of different columns were used in an effort to achieve field-realistic parameters. Field injections in a well represent radial injection through 10 to 20 ft of sediment (i.e., decreasing velocity) over 16 h to 60 h. 1-D column experiments have linear flow fields (i.e., constant flow throughout the 1-D column), so residence times in the column (i.e., the time a conservative tracer is in contact with sediment in the column) of 5 to 10 h represented what should occur in the field inner ~12 feet of radial injection (with a ~10 h residence time). While the field typically contained sandy gravels, gravel was sieved from the laboratory sediment and the <4-mm size fraction used. Since the fines represented 59.24% by weight (i.e., 41% was >4 mm, 100-N 2004 composite), a weight equivalent of 41% coarse accusand (#20) was added to the sediment to make up the mass of inert (assumed) gravel. The purpose of this sand addition was so that ion exchange and sorption properties measured would be approximately equal to what should occur at the field scale without calculation.

3.5 Major Cation/Anion and Radiochemical Analysis

Liquid scintillation counting was used for Sr-90, Sr-85, Ca-45, Na-22, and C-14 analysis. ICP was used for measurement of cations and ion chromatography for selected anions (citrate, phosphate, carbonate). In addition, a colorimetric method was used for phosphate analysis for selected samples. For most radionuclides, counting was relatively straightforward, with a 0.1-mL to 1.0-mL sample mixed with scintillation fluid, and counting dependent on the activity of the sample (typically 10 minutes to 180 minutes per sample). Scintillation counting was performed using a Packard 2550 liquid scintillation counter with newly upgraded counting software. Quench for each sample was compared to a quench curve for each isotope. Typical background was 18 to 22 counts per minute/mL, and a typical experiment had 10,000 to 20,000 counts per minute/mL of the radionuclide added. Field sediments with field-contaminated Sr-90 contained lower counts.

Counting the activity of Sr-90 was slightly more complicated because Sr-90 decays to Y-90 (29.1 y half-life) and Y-90 decays far more rapidly to Zr-90 (64.1 h half-life). The result is that there is far more (4054x) decay activity measured from the Y-90 decay than Sr-90 decay. Quantifying the Sr-90 concentration requires waiting (~30 days or ~10 half lives of the Y-90 64.1 h) after which point half of the activity measured is from Sr-90 and half from Y-90 decay. Simulations of Sr-90 and Y-90 radioactive decay with different starting proportions were conducted to examine the secular equilibrium wait time.

At secular equilibrium where half of the activity is from Sr-90 and half from Y-90, 99.97% of the mass is Sr-90 and 0.0252% is Y-90. Solutions (with no solids) should be at secular equilibrium, so can be counted immediately. In contrast, an experiment containing a Sr-90 solution and a solid phase (sediment, apatite) may not be at secular equilibrium initially due to preferential sorption of Y over Sr (which should take minutes to hours). Therefore, aqueous samples taken from an experiment should also be at secular equilibrium (especially experiments sampled after 30 days). However, a solid phase extraction (i.e., for example dissolving apatite with acid to extract the Sr-90) will likely not be at secular equilibrium. For all cases that contained >0.025% Y-90 initially, total activity decreases over time (~30 days; Figure 3.2). For one case containing no Y-90 initially (and cases containing <0.025% Y-90), total activity increases over time. Therefore, counting before 30 days, then at 30 days (with counts increasing or decreasing) is indicative of the solid phase extraction conducted preferentially removing more or less Y-90 relative to Sr-90. Secular equilibrium is reached within 30 days for most cases (percent Y-90 from 0% to 10%, equilibrium is 0.0252%, Figure 3.2 a-d) likely to occur. A longer (1.5 to 2 months) period of time to reach secular equilibrium is needed for extreme cases containing >10% Y-90 (Figure 3.2 e-h).

Radiochemical analysis of Sr-90 experiments in this study have typically found counts increasing over 30 to 40 days, which implies the sample was extracted deficient in Y-90 (<0.024%). However, for the most extreme case of 0% Y-90 initially, secular equilibrium is reached within 14 days (Figure 3.2b and Figure 3.3). Additional count increases observed for 30 to 40 days is suggestive of an experimental artifact. This issue is currently being investigated.

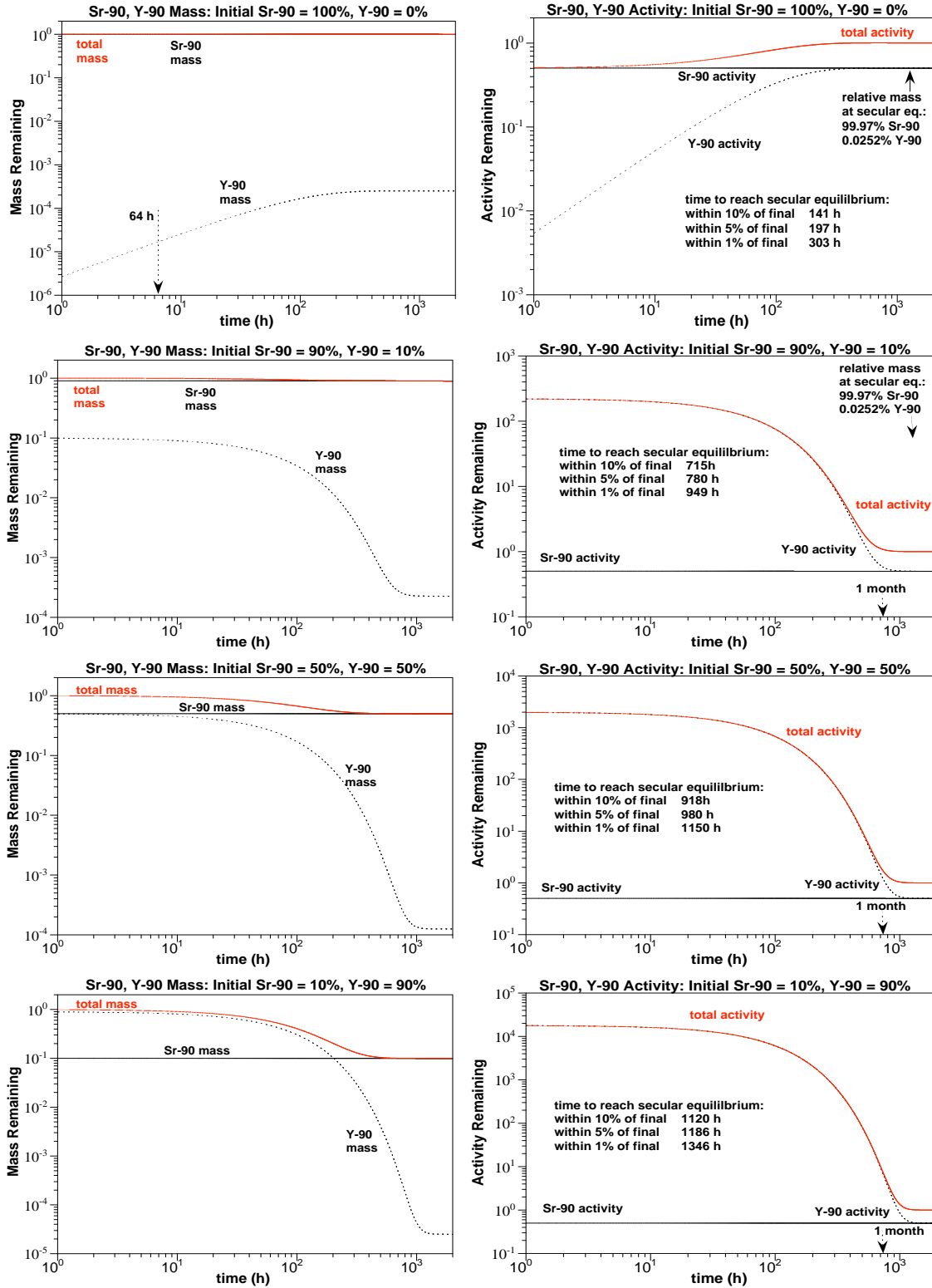


Figure 3.2. Sr-90 and Y-90 mass and activity for different initial Sr-90 and Y-90 activity: a) and b) 0% Y-90, c) and d) 10% Y-90, e) and f) 50% Y-90, and g) and h) 90% Y-90.

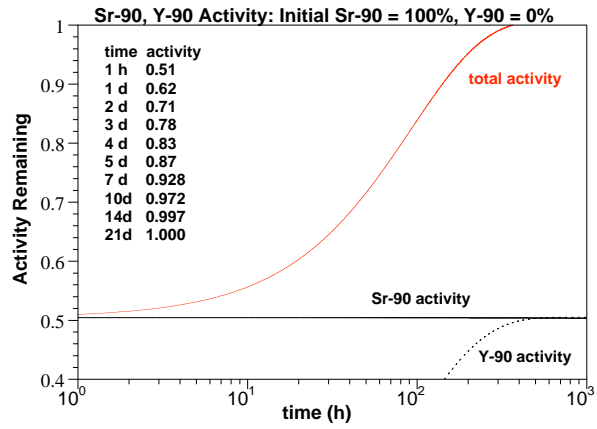


Figure 3.3. Sr-90, Y-90, and total activity in a system with no Y-90 initially.

4.0 Modeling Methods

4.1 Modeling Citrate Biodegradation Rate

Citric acid is utilized by many organic systems as part of the TCA (Krebs) photosynthetic process, where the citrate (a C₆ organic acid) is converted to C₆, C₅, and C₄ organic acids producing CO₂ and H⁺, then cycled from oxaloacetic acid (C₄) to citric acid (Bailey and Ollis 1986). Citrate can also be further degraded to acetic acid (C₂), formaldehyde, formic acid (C₁) and CO₂. For the purpose of this study, citrate is used to complex Ca, so only the decrease in citrate concentration (by biodegradation) is of significance, as the lower molecular weight organic acids only form weak complexes with Ca. Two different modeling approaches were considered to quantify citrate biodegradation, a first-order model and Monod model. A first-order model is an empirical approach that describes citrate removal with a single reaction rate coefficient. A Monod model is also an empirical approach that describes citrate removal externally to microbial organisms with a similar mathematical form of enzyme degradation of a compound (Michaelis-Menton kinetics). Monod kinetics is utilized when the observed data clearly shows a considerable slowing of reaction rate at low concentration that cannot be accounted for using the simpler first-order kinetic model. A Monod kinetic model would describe the data equally as well with small half-saturation constants, but would describe the data more poorly with higher concentration half-saturation constants, which would slow citrate biodegradation at low concentration, the opposite effect of that observed. The changes in citrate biodegradation rate at different temperature was then used to calculate the activation energy at different citrate concentration (10, 50, 100 mM). Very low activation energy (<10 kJ/mol) would indicate the reaction may be diffusion controlled, whereas a high activation energy would generally indicate biochemical reaction control on the rate.

4.2 Simulation of Ca-Citrate-PO₄ Interactions with Sediments during Transport

A reactive transport code (STOMP, White and Oostrom 2004) was used to simulate laboratory-scale experiments of Ca-citrate-PO₄ reactions with sediment. The purpose of this EM-22 project-funded task (M. Rockhold) was to eventually be able to simulate field-scale injections and infiltration scenarios. The reactions account for the observed increase in aqueous Sr-90 in groundwater during the Ca-citrate-PO₄ (generally due to cation exchange reactions) during the first few hours of injection, and subsequent citrate biodegradation, apatite formation, and only Sr removal by precipitation with apatite. The reactions included: a) Sr, Ca, Mg, Na, K, NH₄ ion exchange, b) metal-OH, -CO₃, -PO₄, and -citrate aqueous speciation, c) citrate biodegradation, and d) solids apatite, CaCO₃, and SrCO₃, which was 42 reactions with 51 species. Selected simulations are included in this report.

4.3 Simulation of Sr-90 Uptake by Apatite with Cation Exchange

A smaller set of reactions was used in a reactive transport code (RAFT) to simulate the influence of long-term presence of apatite in sediment on the Sr-90 mobility (i.e., months to 100s of years). Because the citrate reactions described above are relatively short term (i.e., hours to months),

they were not included in these simulations. Simulations with this model (EM-22 funded task) will approximate the long-term migration of Sr (and Sr-90) through the apatite-laden zone (i.e., as a permeable reactive barrier), with Sr ion exchange onto sediment, Sr ion exchange onto apatite, and Sr incorporation into apatite. A smaller set of cations were used for these simulations that included calcium, strontium, and sodium.

5.0 Results

This remediation technology using an aqueous Ca-citrate-PO₄ mixture to permanently immobilize Sr-90 in groundwater at the Hanford 100-N Area. Sr-90 sequestration with this technology occurs by the following steps: 1) injection of Ca-PO₄-citrate solution (with a Ca-citrate solution complex), 2) in situ biodegradation of citrate resulting in apatite [Ca₆(PO₄)₁₀(OH)₂] precipitation (amorphous, then crystalline), 3) adsorption of Sr-90 to the apatite surface, 4) apatite recrystallization with Sr-90 substitution for Ca (permanent), and 5) radioactive decay of Sr-90 to Y-90 to Zr-90. Because cations (Sr, Sr-90) are retained on the sediment by ion exchange, an increase in the ionic strength of the solution relative to groundwater (and combination of mono- and di-valent cations) causes some Sr and Sr-90 desorption (i.e., mobilization) within hours, which will remain until the spent solution is advected downgradient. In order to minimize this Sr-90 mobilization, yet inject enough Ca-citrate-PO₄ to precipitate sufficient apatite to sequester Sr-90 for 300 years, a sequential injection strategy was developed in which a low Ca-citrate-PO₄ concentration is initially injected, followed by months to a year wait period, then one or more high Ca-citrate-PO₄ concentration injections are made. The low concentration solution causes minimal (<10x Sr-90 groundwater increase) Sr-90 increase, and provides sufficient apatite to sequester Sr-90 in the injection zone (i.e., diameter of 30 to 50 ft). Once Sr-90 is immobilized in this zone, higher Ca-citrate-PO₄ solution concentrations can be injected with minimal Sr-90 mobilization. These higher concentration injection(s) build up the apatite precipitate capacity to sequester the majority of the Sr-90 that will slowly migrate into this precipitate zone from upgradient (inland) locations. Laboratory experiments demonstrating the sequential injection strategy are described in Section 5.1, whereas Sr-90 mobilization with the initial Ca-citrate-PO₄ solution are described in Sections 5.2, 5.3, and 5.4. The Ca-citrate-PO₄ solution composition changed over time in order to minimize Sr-90 mobilization, yet still inject enough PO₄ to precipitate sufficient apatite to sequester the Sr-90 in the injection zone.

5.1 Injection Ca-Citrate-PO₄ to Form Apatite and Sequester Sr-90

Small 1-D column experiments were conducted to measure the amount of Sr-90 mobilized by injection of a Ca-citrate-PO₄ solution relative to Hanford groundwater. Batch studies show that Sr (and Sr-90) $K_d = 25.96 \pm 0.89 \text{ cm}^3/\text{g}$ (see Section 5.6.1) in Hanford groundwater (<4 mm size fraction of 100-N composite sediment). For a baseline of Sr behavior in sediments, two 1-D columns in which Sr-85 was added to the sediment and allowed to equilibrate for several days, injection of Hanford groundwater resulted in a K_d of 11.8 and 9.1 cm³/g (i.e., $R_f = 61$ and 47.6, respectively, Figure 5.1).

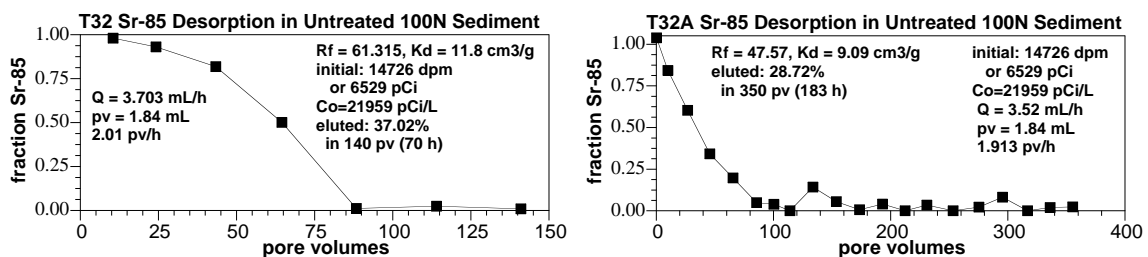


Figure 5.1. Sr-85 desorption in a 1-D column with Hanford groundwater injection.

In these experiments, a total of 140 and 350 pore volumes of Hanford groundwater were flushed through the columns. Over that amount of flushing, 37% and 29% of the Sr-85 was eluted. These results are applicable to the field, as the “flushing” with groundwater is simply exchanging the Sr-85/Sr on the sediment surface sites with Sr in groundwater. In general, the system is at equilibrium at all times, as there is no change in the mixture of cations (Ca, Na, K, Sr) and anions (CO₃, Cl, SO₄), and we assume the sediment was initially in equilibrium with groundwater.

In comparison, injection of a Ca-citrate-PO₄ solution caused initial peaking desorption of Sr-85 (Figure 5.2), but ultimately less Sr-85 was eluted (so some was sequestered due to the incorporation in precipitating apatite). The initial high concentration Sr-85 peak was dependent on the Ca-citrate-PO₄ composition and concentration, which is better described in Sections 5.2 to 5.4. There are limitations in these small experiments with the sample collection size being somewhat large relative to the size of the peak, so some of the peak shape is lost. The general nature of the breakthrough curve shape, however, is shown, with a higher concentration Sr-85 initial peak with a higher concentration injection of Ca-citrate-PO₄.

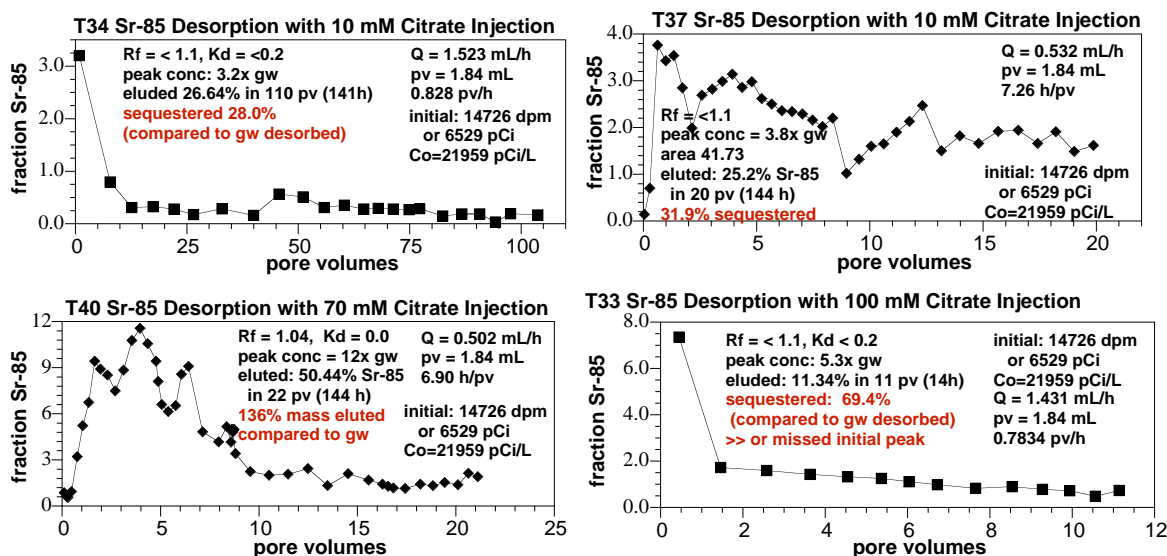


Figure 5.2. Sr-85 desorption in a 1-D column with Ca-citrate-PO₄ injection.

If a low concentration Ca-citrate-PO₄ (4, 10, 2.4 mM, details in Table 3.1) is injected, the Sr-85 peaked at a minimum of 3x to 4x groundwater concentration (Figure 5.2a,b), although later experiments in which finer sampling of this initial peak are taken (both in laboratory- and field-scale experiments), this Sr or Ca or Sr-90 peak is actually about 10x groundwater concentration. The ionic strength of this solution is 99.5 mM, compared to 11.5 for Hanford groundwater (predominantly Ca, Mg-CO₃), so the ionic strength increase of 8.6x roughly approximates the divalent cation desorption. Interestingly, both of these low concentration experiments ultimately sequestered some Sr-85 (i.e., eluted less than when groundwater was injected through the column, Figure 5.1). In both experiments, 28% to 32% less Sr-85 was eluted from the column, which was presumed caused by the Sr-85 being incorporated into apatite as it was precipitating.

If a high concentration Ca-citrate-PO₄ solution (28, 70, 17 mM) was injected into the Sr-85-laden sediment, higher initial Sr-85 desorption peak was observed. In these small columns with sample size limitations, the initial peak observed was 7.5x to 12x increase in groundwater concentration, although the actual peak height should be considerably larger (100x is estimated). In one of these experiments, 69% of the Sr-85 was sequestered (i.e., retained in the column, relative to a groundwater injection), and in the other column, all of the Sr-85 injected was eluted (i.e., less retention relative to groundwater injection). In general, conclusions that can be drawn from these small experiments are limited, and processes hypothesized were investigated in detail in other experiments. These experiments did show that Sr-85 (and Sr and Sr-90) would desorb at greater concentrations proportional to the concentration of the Ca-citrate-PO₄ injected. In addition, some Sr-85 was retained by sediments, which was presumed to be caused by the precipitation of apatite with some incorporation of the Sr-85.

The influence of a 89-day wait period after a low Ca-citrate-PO₄ concentration (4, 10, 2.4 mM) solution was injected is shown in Figure 5.3. Compared to groundwater injection with no treatment (Figure 5.1), 53% less Sr-85 desorbed, which is presumed incorporated into apatite. Compared to the 1-D experiment in which the Ca-citrate-PO₄ solution is immediately desorbed (Figures 5.2 a, b), there is a significantly lower initial peak after the 89 day reaction period (Figure 5.3), and additional Sr-85 sequestration (i.e., 53% sequestered with the 89 day wait, as opposed to 28% to 32% sequestered for desorption within days). It should also be noted that the noise in the data, especially at low concentration in long-term experiments, is significant. This is caused by the limitation of using Sr-85, which has a relatively short half-life (64.84 days), so all data needs to be corrected for decay. Counts near background are, therefore, amplified, which creates greater noise in the long-term experiments.

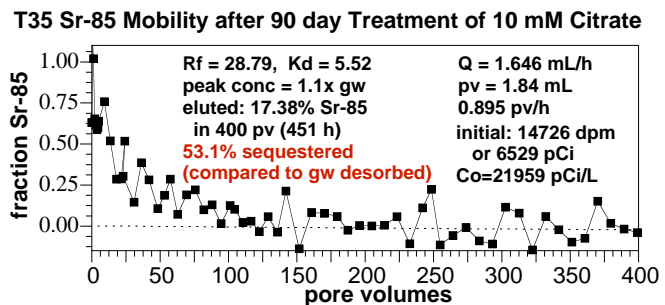


Figure 5.3. Sr-85 desorption in a 1-D column with Hanford groundwater after 89 days contact with a low concentration of Ca-citrate-PO₄ solution.

5.1.1 Sequential Injection Strategy to Minimize Sr-90 Mobilization

As described earlier, an injection strategy of injecting a low concentration of the Ca-citrate-PO₄ solution followed by months to a year wait period, then one or more high concentration injections was developed to minimize the initial Sr-90 desorption peak that would occur in the field if a high Ca-citrate-PO₄ concentration solution were injected. In one sequential injection study, a low concentration Ca-citrate-PO₄ solution (4, 10, 2.4 mM) was initially injected into the column, then the solution was allowed to stand for 125 days (3000 h), then a high concentration Ca-citrate-PO₄ solution (28, 70, 17 mM) was injected (Figure 5.4).

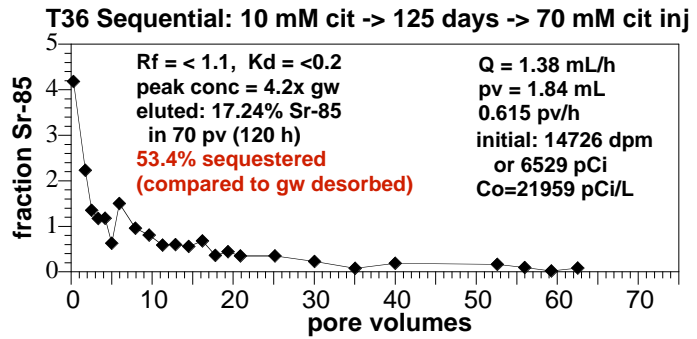


Figure 5.4. Sr-85 desorption in a 1-D column after the sequential injections: a) low conc. Ca-citrate-PO₄ (4, 10, 2.4), b) 125 day wait period, and c) high conc. Ca-citrate-PO₄ (28, 70, 17 mM).

Results (Figure 5.4) show that 53.4% of the Sr-85 was sequestered over the 125-day wait period, so there was no additional Sr-85 desorption caused by the high Ca-citrate-PO₄ solution injection compared to a parallel experiment in which groundwater was injected after a 89-day wait (Figure 5.3). These results are the same because the Sr-85 in both cases is in contact with the same low Ca-citrate-PO₄ solution for 89 to 125 days – the only difference between the experiments is the solution used after the wait period to elude it. While the experiment is a success (i.e., the Sr-85 immobilized is not readily removed by ion exchange with a high ionic strength solution), there is still some Sr-85 mobilized after a 125-day wait period.

In a long-term set of batch experiments, the rate of Sr-90 incorporation into apatite was investigated. Some results are presented in this section, and additional experiments (at differing temperature, ionic strength, Ca/Sr ratio) are in other results sections (5.5, Long-Term Effects). To measure the amount of Sr-90 incorporation into apatite-laden sediment, solid-phase (i.e., sediment + apatite) were periodically taken and sequential extractions performed, as described in the experimental section. These sequential extractions are aqueous (i.e., measure the Sr-90 in the aqueous phase), ion exchangeable (i.e., measure Sr-90 eluded with 0.5M KNO₃), carbonate extraction (i.e., measure Sr-90 eluded with 0.05M Na-EDTA), and finally residual (i.e., measure Sr-90 eluded with 4M HNO₃). Basically these are sequentially stronger solutions.

In untreated sediment (i.e., no apatite added), at the sediment/water ratio of this batch experiment, 5.6% of the Sr-90 was aqueous (Figure 5.5a). In addition, the ion exchangeable fraction was 85%, giving the total “mobile” (= aqueous + ion exchangeable) fraction of 90%, which remained constant over time, since there was no apatite addition. In contrast, the addition of the Ca-citrate-PO₄ solution (4, 10, 2.4 mM) caused several changes in Sr-90 proportions over time, as shown in Figure 5.5b. Between 100 and 300 h, the aqueous + ion exchangeable Sr-90 (mobile) fraction decreased from 90% to 43% (red squares, Figure 5.5b), which is consistent with previous experiments reported, in which a fraction of the Sr-90 (not all) is incorporated into apatite as it precipitates in 100s of hours. The sequential extractions of the solid phase (carbonate and residual together = solid-associated) show that the remaining Sr-90 fraction (41%) cannot be mobilized with a high ionic strength solution as it is incorporated into apatite.

Further proof is shown in Section 5.5, Results, in which the Sr-90 incorporation rate into pure apatite (no sediment) is quantified, and is the same as shown here. By 11,000 h, nearly all (99.94%) of the Sr-90 is associated with the solid phase (i.e., incorporated into apatite). The first-order half-life for this incorporation process is 180 days (black dashed line, Figure 5.5c). It should be noted that once the apatite is formed (100s of hours), the rate of Sr-90 incorporation into apatite is dependent on the solution composition to some extent (see Section 5.5, Results). In this experiment shown here, the spent Ca-citrate-PO₄ solution remained in contact with the sediment/apatite for the entire experiment, which results in somewhat less Sr-90 sorption than if groundwater were in contact with the sediment/apatite. In experiments described in Section 5.6, results show that the Sr-90 incorporation half-life (normalized to 15°C groundwater temperature) is 72 days, if the Sr-90 is in contact with groundwater. It is hypothesized that this more rapid 72-day half-life is more representative of what would occur in the field, as the spent Ca-citrate-PO₄ solution will advect downgradient within a month or two in the 100-N Area.

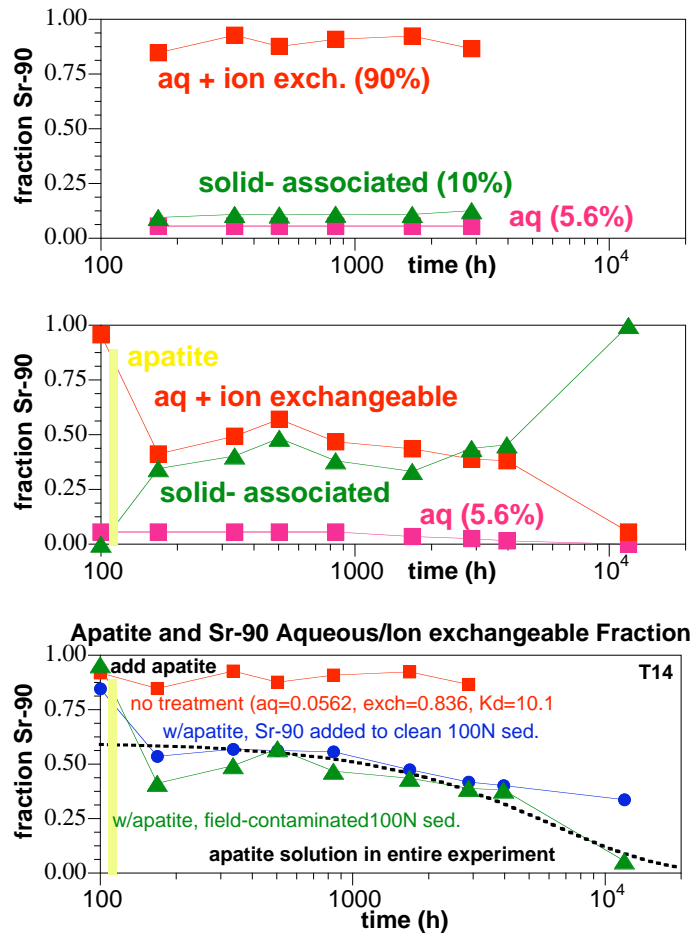


Figure 5.5. Sr-90 aqueous/solid phase partitioning in batch systems with: a) field Sr-90-contaminated sediment only (no apatite), b) field Sr-90 contaminated sediment and apatite solution addition, c) field and laboratory added Sr-90 with apatite solution addition.

Another set of 1-D column experiments was conducted to further investigate the changes in Sr-90 (aqueous, ion exchangeable, residual on surface) that occur during sequential low, then high concentration Ca-citrate-PO₄ injections. To meet the objectives of analyzing the sediment for the ion exchangeable and residual fraction of the Sr-90, the experiment consisted of (3) small 1-D columns (10-cm length x 0.765-cm diameter) in series, where columns were sacrificed at different points in time during the sequential injections. The series of events is described in Table 5.1.

Table 5.1. Sequential injection of low- and high-concentration Ca-citrate-PO₄ into a 1-D column: time course of events and analysis.

Time Course of Events and Analysis	data
1. Sr-90 Equilibrated With Sediment in 1-D Columns	total Sr-90 mass
<ul style="list-style-type: none"> • Sr-90 mixed with sediment, 3.5 days (ion exchange) • packed into (3) columns 10 cm length x 0.765 cm diameter 	total Sr-90 mass in (3) columns
2. Inject Low Conc. Ca-citrate-PO ₄ (4, 10, 2.4 mM) for 1.5 pv	Sr-90 mass eluded in low conc. inj.
<ul style="list-style-type: none"> • no btc, effluent Sr-90 recorded • reaction time to precipitate: 32 day wait at 82C 	
3. Inject groundwater, 1.5 pore volumes, Sr-90 breakthrough curve	Sr-90 mass eluded in gw injection
<ul style="list-style-type: none"> • one column taken apart, sequential extractions on sediment to characterize Sr-90 incorporation • reaction time to incorporate Sr-90 in apatite: 90 days at 82C 	Sr-90 ion exch. + incorp.
4. Inject High Conc. Ca-citrate-PO ₄ (28, 70, 17 mM), Sr-90 breakthrough curve	Sr-90 mass eluded in high conc. inj.
<ul style="list-style-type: none"> • reaction time to precipitate: 32 day wait at 22C 	
5. Inject groundwater, 1.5 pore volumes, Sr-90 breakthrough curve	Sr-90 mass eluded in gw injection
<ul style="list-style-type: none"> • one column taken apart, sequential extractions on sediment • reaction time to incorporate Sr-90 in apatite: 90 days at 82C 	Sr-90 ion exch. + incorp.
6. Final column taken apart to determine Sr-90 incorporated	Sr-90 ion exch. + incorp.

Sr-90 data obtained from this sequence of experiments shows how Sr-90 mass changes from being predominantly held on the surface by ion exchange (with a small amount in aqueous solution) to being predominantly incorporated in apatite mass, with a small amount on the surface held by ion exchange and a small amount in aqueous solution (i.e., similar to the batch results shown in Figure 5.5b). The two types of Sr-90 data obtained are from breakthrough curves (i.e., Sr-90 mass eluded at different points in the sequence from groundwater or Ca-citrate-PO₄ solution injection) and sequential extractions of the sediment to obtain ion exchangeable Sr-90 (i.e., 0.5M KNO₃ extracted) and residual Sr-90 (i.e., 4 M HNO₃ at 80°C extracted). Results (Table 5.2) are reported in μCi of Sr-90 mass balance for each event. If only aqueous samples were analyzed (i.e., effluent breakthrough curve, then only the “eluded” and “aqueous in column” columns are filled in, whereas additional data is only obtained when solid phase sequential extractions are conducted when the columns are taken apart (3 times during the sequential experiment).

Table 5.2. Results of sequential injection of low- and high-concentration Ca-citrate-PO₄ into a 1-D column, where event is described in Table 5.1.

Event	Sr-90 mass balance (uCi)					total in column	eluded
	aqueous in column	ion exch.	immobile residual	mobile aq+ ion ex.			
1. Sr-90/ sediment	0.2441					0.2441	
equilibrium	0.0017	0.2424				0.2441	
	0.0013	0.1895				0.1908	0.0532
2. Inject low conc. 32 day wait						0.1801	0.0107
3. inject gw						0.1778	0.00231
	1.02E-04	0.1261	0.0516	0.1261		0.1778	
90 day wait							
4. inject high conc. 30 day wait						0.1527	0.0251
						*	*
5. inject gw	*	*	*	*		*	
90 day wait							
6. final col.	*	*	*	*		*	

* in progress

Results of this sequential injection study show Sr-90 mass balance at different points in the sequence (Table 5.2) and Sr-90 breakthrough curves showing concentration (Figure 5.6). There was 0.1908 μ Ci of Sr-90 adsorbed to sediment in the (3) columns for 3.5 days (third line, Table 5.2), of which 99.3% was adsorbed to the sediment. A total of 5.6% of the Sr-90 in the column was eluded during the low Ca-citrate-PO₄ (4, 10, 2.4 mM) injection, and a total of 1.3% additional Sr-90 mass was eluded with a 15 pore volume groundwater flush 32 days after the low concentration Ca-citrate-PO₄ injection (Figure 5.6a). The final Sr-90 groundwater concentration (at 15 pv, Figure 5.6a) is 32.78 dpm/mL. The peak Sr-90 concentration during the first pore volume of this groundwater flush was 9.4x greater (at <0.1 pv), due to the ionic strength of the spent Ca-citrate-PO₄ solution. At this point in time, one of the three columns was taken apart and sediment extractions conducted to determine the proportion of the Sr-90 mass in different phases. Of the total of 0.1778 μ Ci Sr-90 mass in the three columns, 0.06% was aqueous (down from 0.7% before treatment), 71% was ion exchangeable (down from 99.3% before treatment), and 32% was incorporated into the apatite (up from 0.0% before treatment). While this is promising, this shows that 32 days is not enough time to incorporate enough Sr-90 before subsequent injections. A period of 90 days was used after this groundwater injection to allow some additional Sr-90 to be incorporated into the apatite. During the subsequent high concentration Ca-citrate-PO₄ injection (Figure 5.6b), 14.1% of the Sr-90 mass was eluded, with a concentration 421x the low groundwater Sr-90 concentration. This high concentration Ca-citrate-PO₄ injection is near the maximum solubility of the constituents (28, 70, 17 mM). A 120-day reaction period is then planned before the second of three columns is taken apart and Sr-90 mass balance determined by sequential extractions (in progress). The final 90-day wait period is still in progress, so additional incorporation that occurs is not known at this time.

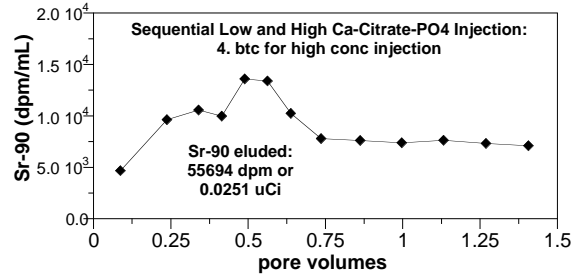
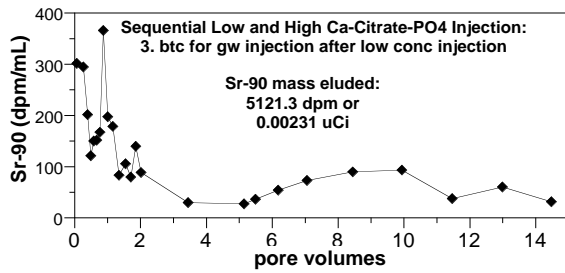


Figure 5.6. Sr-90 breakthrough in sequential low- and high-concentration Ca-citrate-PO₄ injections in 1-D columns. Shown are: a) Sr-90 breakthrough curve for 15 pv groundwater injection 32 days after low concentration Ca-citrate-PO₄ injection, and b) Sr-90 breakthrough curve for 1.5 pv high concentration Ca-citrate-PO₄ injection.

5.1.2 Citrate Biodegradation with Differing Ca-Citrate-PO₄ Concentration

Injection of the Ca-citrate-PO₄ solution (Table 3.1 for detailed solution composition) results in the formation of apatite by several mechanisms: a) slow release of Ca from the Ca-citrate complex, resulting in apatite formation, not mono- or di-calcium phosphate, and b) inhibitory effect of the presence of the citrate on apatite formation, also resulting in the slow formation of apatite. In order to predict the rate of apatite precipitation, an understanding of the factors that control the citrate biodegradation rate need to be known. In this section, results of experiments quantifying the citrate degradation/mineralization rates as a function of Ca-citrate-PO₄ concentration and temperature are shown. In the following section, citrate degradation/mineralization rates were determined in sediments from the 12 different injection boreholes of the 100-N Area. In Section 5.7.1, Results, additional citrate biodegradation rate experiments are shown as a function of water content (EM-22 funded), and in Section 5.7.2, results of citrate mineralization studies varying the microbial biomass are shown (also EM-22 funded).

Citric acid is utilized by many organic systems as part of the TCA (Krebs) photosynthetic process, where the citrate (a C₆ organic acid, Figure 5.7) is converted to C₆, C₅, and C₄ organic acids producing CO₂ and H⁺, then cycled from oxaloacetic acid (C₄) to citric acid (Bailey and Ollis 1986). Citrate can also be further degraded to acetic acid (C₂), formaldehyde, formic acid (C₁), and CO₂. For the purpose of this study, citrate is used to complex Ca, so only the decrease in citrate concentration (by biodegradation) is of significance, as the lower molecular weight organic acids only form weak complexes with Ca.

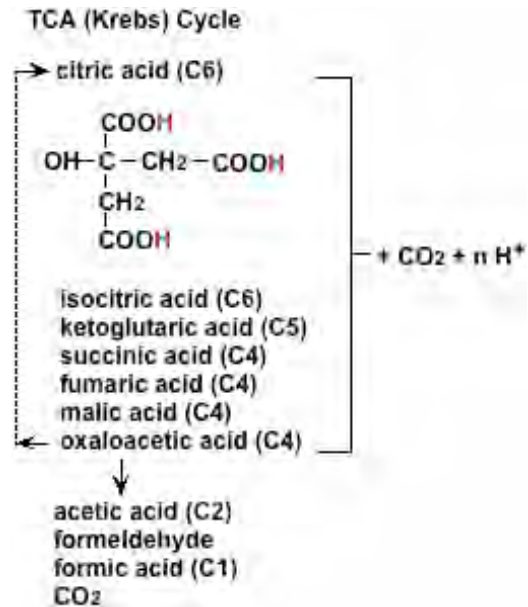


Figure 5.7. Citrate biodegradation pathway.

Two different modeling approaches at PNNL were considered to quantify citrate biodegradation, a first-order model (Figure 5.8) and Monod model. A first-order model is an empirical approach that describes citrate removal with a single reaction rate coefficient. A Monod model is also an empirical approach that describes citrate removal externally to microbial organisms with a similar mathematical form of enzyme degradation (Michaelis-Menton kinetics). Monod kinetics is utilized when the observed data clearly shows a considerable slowing of reaction rate at low concentration that cannot be accounted for using the simpler first-order kinetic model.

Citrate biodegradation experiments show a slower rate at colder temperature and at higher citrate concentration (Figure 5.8, Table 5.3). At 10 mM citrate concentration, citrate was not detectable by 200 h (21°C) to 300 h (10°C, Figure 5.8a). At 50 mM citrate concentration, citrate was nondetect by 250 h (21°C) to 450 h (10°C, Figure 5.8b). At 100 mM citrate concentration, a small amount of citrate remained at 300 h (21°C) to 600 h (10°C, Figure 5.8c). At each concentration, duplicate experiments showed similar results.

A first-order model (lines, Figure 5.8) showed good fits, and indicated that in some cases, citrate biodegradation may be somewhat more rapid at lower concentration than a first order approximation. For example, the 100 mM citrate data at 10°C (Figure 5.8c) showed a good first order fit to 500 h, but then citrate degraded more rapidly. This effect is observed for all citrate concentrations at 10°C, but not at 21°C. A Monod kinetic model would describe the data equally as well with small half-saturation constants, but would describe the data more poorly with higher concentration half-saturation constants, which would slow citrate biodegradation at low concentration, the opposite effect of that observed. Therefore, a pseudo first-order model was used to quantify the rate data (Table 5.3).

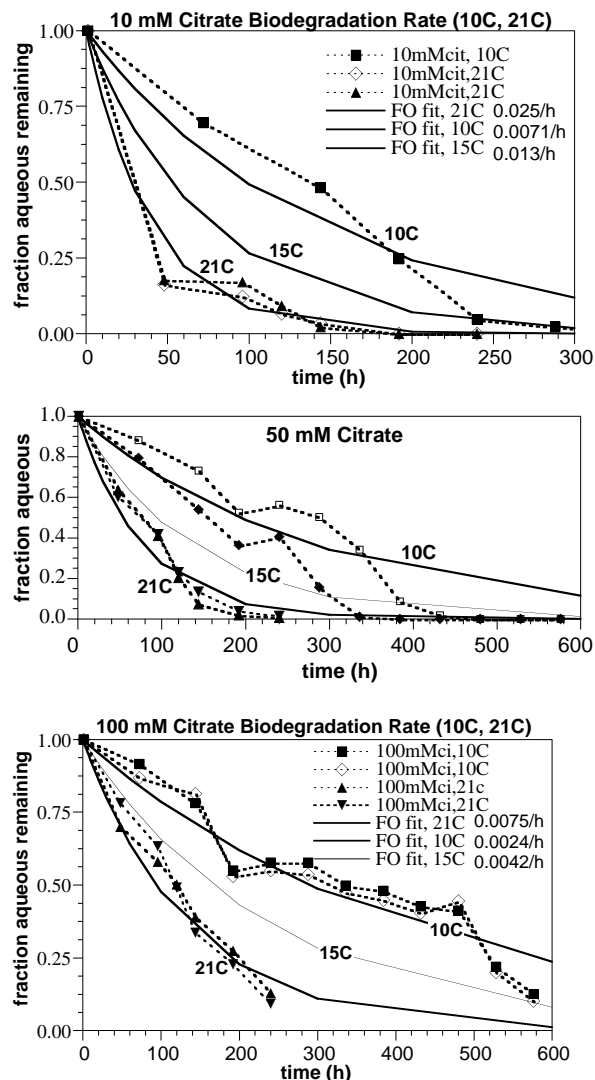


Figure 5.8. Citrate biodegradation by Hanford 100-N sediments versus temperature at: a) 10 mM citrate, b) 50 mM citrate, and c) 100 mM citrate concentration. Experiments conducted at SNL.

Table 5.3. Citrate degradation rates at different temperature and concentration.

Citrate (mM)	Rate (1/h) 10°C	Rate (1/h) 15°C	Rate (1/h) 21°C
10	0.0071	0.013	0.025
50	0.0074	0.0036	0.013
100	0.0024	0.0042	0.0075

Rates determined from these experiments (Table 5.3) show that the citrate biodegradation rate increases with temperature (2.7x from 10°C to 25°C) and decreases with increasing citrate concentration (3.0x from 10 mM to 100 mM; Figure 5.8). The initial injections at 10 mM citrate and 15°C have an estimated half-life of 50 h.

The citrate biodegradation rate was 3.0x slower (10°C data) to 3.3x slower (21°C data) as the citrate concentration increased from 10 mM to 100 mM. The citrate biodegradation rate averaged 3.3x slower as the temperature decreased from 21°C to 10°C. The activation energy estimated from the reaction rate change with temperature is 35 kJ/mol (10 mM citrate), 16 kJ/mol (50 mM citrate), and 32 kJ/mol (100 mM citrate). These activation energies indicate the rate is controlled by the biochemical reaction and not diffusion, which is expected (Figure 5.9).

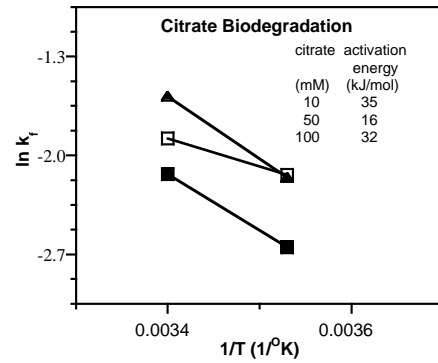


Figure 5.9. Arrhenius plot of citrate biodegradation

Aerobic vs. Anaerobic Degradation. In batch and 1-D column systems, Sandia National Laboratory (SNL) and PNNL showed that citrate biodegradation to CO₂ occurred within 75 to 100 h in aerobic systems (Figure 5.10a), and to formate and acetate within 100 to 200 h in anaerobic systems (Figures 5.10b and 5.10c). In the 100-N Ringold portion of the aquifer, most of the citrate biodegradation will occur anaerobically, given the relative concentrations of citrate to oxygen. In the Hanford formation, the uppermost portion of the aquifer, degradation will most likely be aerobic, but this would be dependent on the infiltration rate and the resulting water saturation. High infiltration rates would have higher water saturations, so citrate biodegradation would be anaerobic.

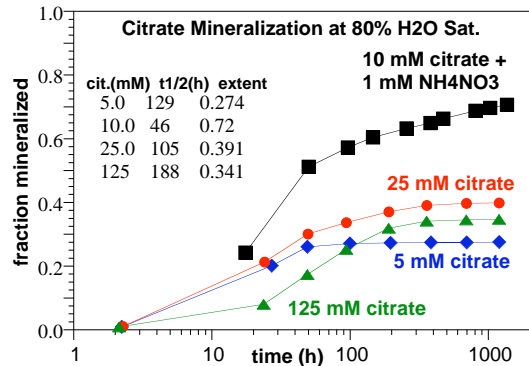


Figure 5.10. Citrate mineralization and Ca-citrate-PO₄ composition.

Mineralization of ^{14}C -labeled citrate (5-2-2.4 mM mix) was examined over a range of initial citrate concentrations (5, 10, 25 and 125 mM) in the composite 100-N sediment at 20°C to 22°C . The ^{14}C activity per ml of water was identical in all experiments. Overall, there was a trend of slower citrate mineralization with increasing citrate concentration – consistent with the previous trends shown (Figure 5.11). With the same Ca-citrate- PO_4 solution composition, the citrate mineralization rate was about twice as slow for 125 mM as 5 mM citrate concentration. Note that nearly all of these experiments with similar composition had nearly the same mineralization extent 30% to 40%. If the amount of N was increased significantly, then the citrate mineralization rate increased dramatically and extent increased (10 mM citrate data, Figure 5.11). Therefore, it is possible to control the citrate mineralization rate by limiting the nitrogen (i.e., difference between the 5 mM citrate with low N and 10 mM citrate with high N). Additional experiments with these different solutions were conducted at different water saturations (described in Section 5.7).

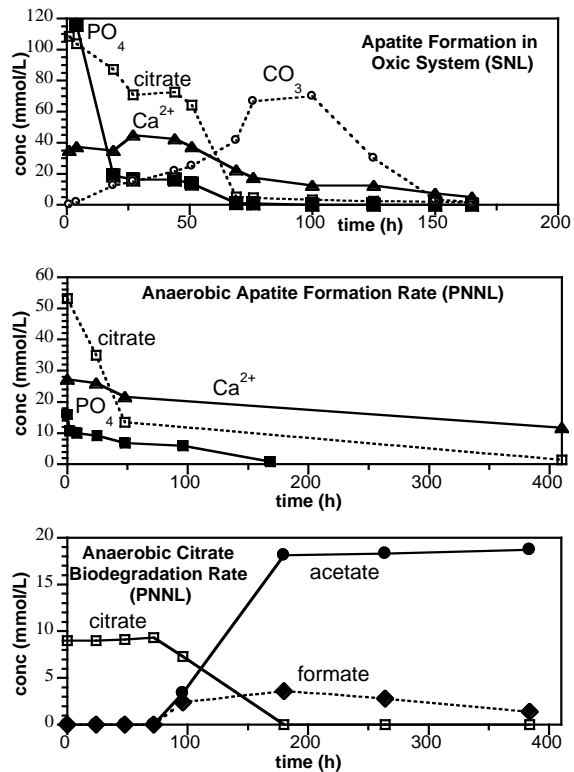


Figure 5.11. Apatite precipitation rate and citrate biodegradation: a) precipitation rate in aerobic system (reported as CO_3); b) precipitation rate in anaerobic system; c) citrate biodegradation in anaerobic system.

5.1.3 Spatial Variation in Citrate Biodegradation in Boreholes

The spatial variation citrate biodegradation/mineralization at the 100-N site was investigated as a function of depth and location in sediments from monitoring and injection wells along the Columbia River shoreline at the 100-N remediation site. The main control of citrate biodegradation and mineralization (keeping the solution composition constant) is the microbial biomass. Sediment microbial biomass was specifically investigated (Section 5.7.1), and generally showed decreasing biomass with depth. As described in Section 5.7.1, there is a general trend of increasing citrate mineralization with increasing biomass. However, with a 5 order of magnitude increase in biomass, the citrate mineralization rate only increased an order of magnitude. It should be noted that the Ca-citrate-PO₄ solution used in these laboratory experiments are mixed exactly as field injections are, with 5% concentrated chemicals (by volume) and 95% river water. The river water contains a significant microbial population (March 2007 measurement 10⁷ cfu/mL), which will augment subsurface biomass. There are several factors that control the transport of microbes that are injected (or infiltrated) including the velocity, ionic strength of the solution, and solution composition. The influence of these factors on the transport of microbes has not been investigated. However, results reported below represent citrate mineralization rates that should occur when the specified Ca-citrate-PO₄ solution (mixed in river water) is infiltrated into the Hanford sediment.

In this section, citrate mineralization in Hanford 100-N sediment depth composites (typically 6 to 15 ft) of the Hanford formation at field water saturation were investigated. The field water content of these sediments was ~15% (by weight), or about 40% saturation. As described in Section 5.7.1, the citrate mineralization rate increased with water content from these very low water contents to 60-70% saturation. Between 70% and 100% water saturation, there was no difference in the citrate mineralization rate. For the experiments in this section, sufficient water was added to the sediment to be water saturated (Figure 5.12). These experiments were then spiked with ¹⁴C-labeled citrate (4 mM), 2 mM Ca, and 2.4 mM PO₄ (i.e., solution used in field injection #2). In all cases, citrate was mineralized to some extent (16% to 21% in 200 h), with one case of 11% mineralization extent. The mineralization rate did not vary significantly between borehole composites, with the half-life averaging 250 ± 114 h (range 133 h to 472 h). These results indicate that Ca-citrate-PO₄ injections in all boreholes should likely result in roughly the same citrate biodegradation rate, with no significant trends over lateral distance along the injection barrier.

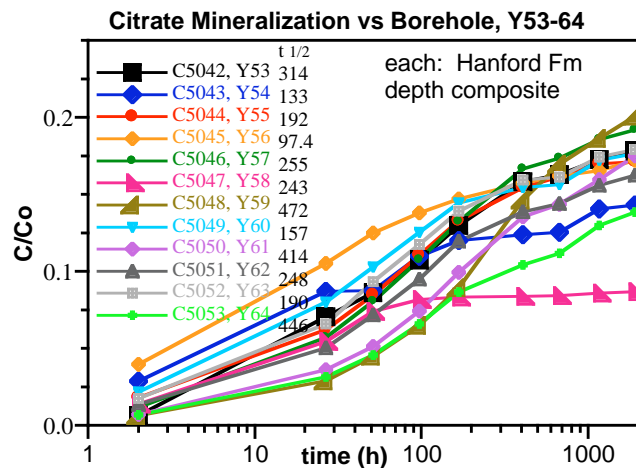


Figure 5.12. Citrate mineralization versus borehole (composite).

Depth discrete samples were taken in some of the boreholes in the 100-N Area, so citrate mineralization studies were conducted in five different boreholes at differing depth (Figure 5.13). Given that the water table is generally (i.e., most of the year) at ~20 ft depth), shallower samples are typically not water-saturated. For brief periods in the spring, the water table can rise a few feet. For these experiments, water-saturated conditions were used in all samples.

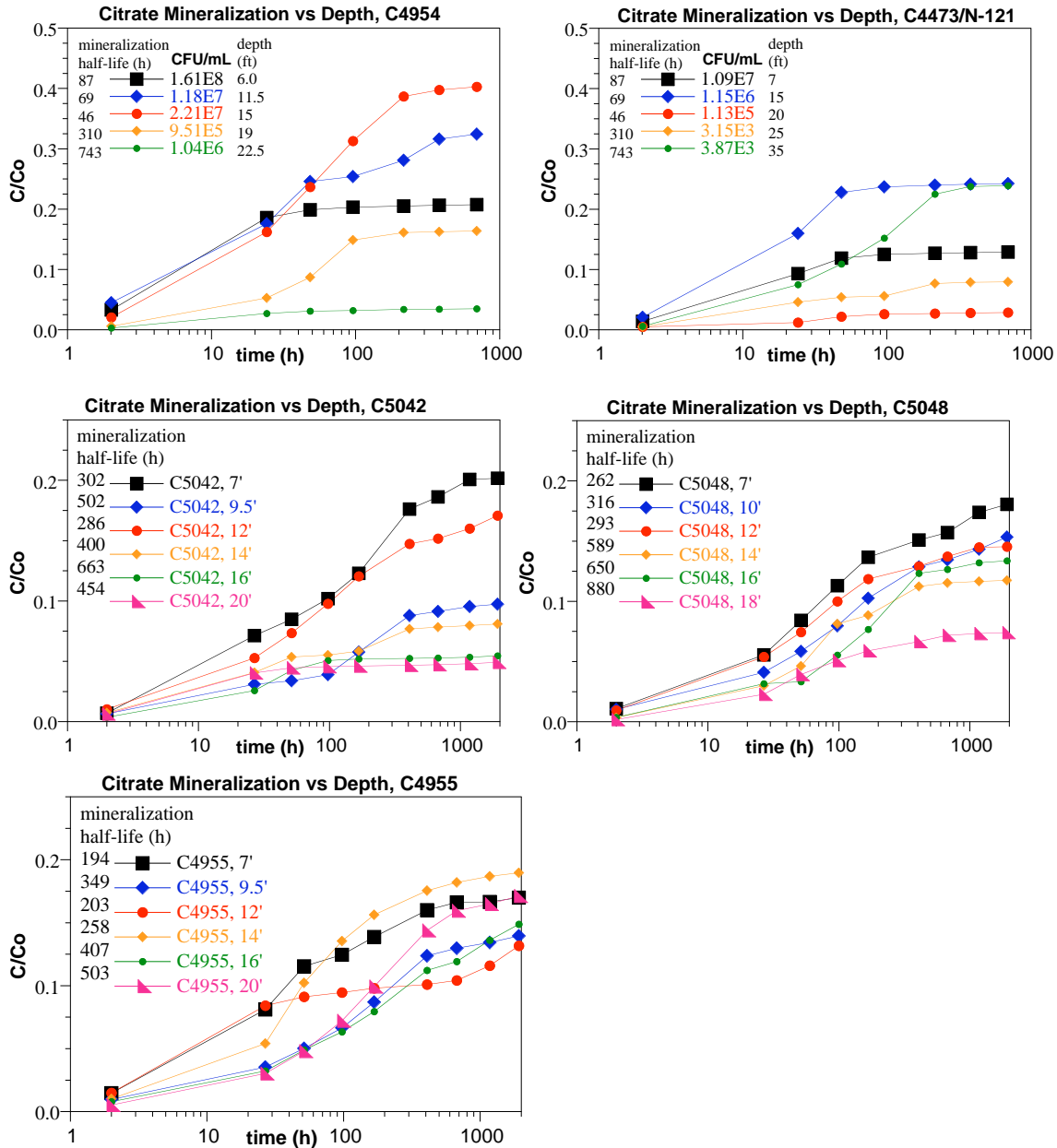


Figure 5.13. Citrate mineralization versus depth in five different boreholes in the 100-N Area.

Application to Ca-citrate-PO₄ injections is, therefore, direct (i.e., same water saturation conditions), although generally >15 ft depth is all that can be accessed by injection even at high water levels. Treatment of shallower depths may be more efficiently treated by infiltration from the surface or from some shallow depth (i.e., trenches to below the road fill). These experiments were then spiked with ¹⁴C-labeled citrate (4 mM), 2 mM Ca, and 2.4 mM PO₄ (i.e., solution used in field injection #2). As fully described in Section 5.7, the main variable that controls the citrate mineralization rate is the microbial biomass. In Section 5.7, results are shown of the microbial biomass variability with depth and citrate mineralization rate variation with microbial biomass. Because microbial biomass decreases with depth, experiments conducted in this section are expected to show decreasing citrate mineralization rate with increasing depth.

Results of the citrate mineralization studies in five boreholes with depth (Figure 5.13) show a rather imperfect correlation between mineralization rate decreasing with depth. Because the true independent variable is microbial biomass, deeper samples in different boreholes may have different biomass. For example, the 20-ft depth for C5042, 18-ft depth for C5048, and 20-ft depth for C4473 had relatively slow mineralization rates and extent, but in contrast, the 20-ft depth for C4955 had the highest mineralization rate in that borehole. Plotting the depth versus mineralization half-life and mineralization extent in each borehole (Figure 5.14) shows the general trend of decreasing rate (increasing mineralization half-life) with depth, but there is no correlation of mineralization extent. Similar to the conclusion reached in Section 5.7 on the correlation between microbial biomass and mineralization rate; if some microbes are present in the sediment, citrate degradation will occur at a generally predictable rate. Significantly less presence of microbes (i.e., greater depth) results in only slightly slower citrate degradation rate.

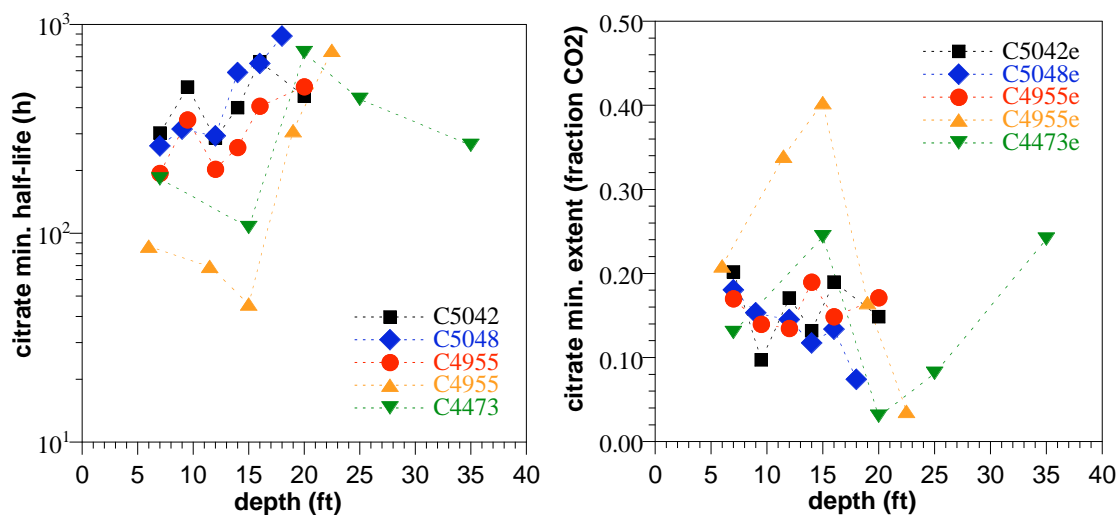


Figure 5.14. Citrate mineralization and depth in five boreholes showing a) mineralization half-life, and b) trend of mineralization extent.

One more factor additionally contributes to the mineralization rate being roughly the same with depth for field-scale injections. A significant biomass population is injected at the field scale because river water is being used for makeup water. Field injections #1 through #10 use approximately 90% river water with 10% (by volume) concentrated chemicals mixed up in

deionized water in tanker trucks. The microbial biomass in the river water likely varies with season and location. River water samples taken in March 2007 show 10^7 cfu/mL. In comparison, microbial biomass measurements taken in sediment cores at depth range in value from 10^8 cfu/g to 10^3 cfu/g (Section 5.7), with greater values in shallow depths, and >20 ft depth (typical groundwater) at 10^3 to 10^5 cfu/g. Given the field porosity of 20% and bulk density of 1.95 g/cm^3 , the field soil/water ratio is 9.75 g/mL , so injected water in pores in the sediment would be equivalent to $1\text{E}6$ cfu/g.

5.2 Laboratory Support Experiments for Field Injection #1

Laboratory 1-D flow experiments were specifically conducted to predict behavior that would be observed at the field scale for the first field injection of a Ca-citrate- PO_4 solution. Numerous small-scale (i.e., 10 to 20 cm length) 1-D flow experiments had already been conducted, but the initial “snow plow” effect of ion exchange upon breakthrough was difficult to accurately sample with these very small columns, so 100-cm (3.2-ft) and 20-ft long columns were used to more accurately represent a 20- to 30-ft radius field injection (described in Section 5.2.1). In addition, field support experiments were conducted to: a) quantify the stability of the Ca-citrate and Na- PO_4 tanker trucks at high concentration and low temperature (Section 5.2.2), b) quantify the relationship between electrical conductivity and solution of the two separate tanker trucks and the mix (Section 5.2.3), c) quantify the relationship between solution density and solution concentration (Section 5.2.4), and d) quantify the amount of interference of citrate on field PO_4 measurement (Hach 8114).

5.2.1 Laboratory 1-D Column Transport Experiments

A 1-D column experiment of 20-ft length was conducted to quantify geochemical changes that would occur in Hanford sediments with a low concentration Ca-citrate- PO_4 (4, 10, 2.4 mM, see Table 3.1 for complete description) injection. More specifically, the purpose of this experiment was to a) collect K_d data for citrate, Ca, and phosphate, and b) collect ICP metals data for a citrate injection. The <4 mm size fraction of the Hanford formation was used (<4 mm was 59.4% of the total), but 20/30 sand was added for the other 41% (by weight), so assuming the sand is just as inert as the cobbles, the K_d values from this experiment should be the same as should occur in the field. The injection solution was 10 mM citrate, 4 mM Ca and 2.4 mM PO_4 mixed up in Hanford 100-N Area groundwater (Table 2.1), although later experiments used closer to the composition in the field: 5% deionized water and 95% river water. This batch of groundwater was somewhat lower ionic strength, with an analyzed 17.71 mg/L Ca (0.44 mM). The analyzed injection solution concentrations were nearly the calculated concentrations. There may be some adjustment for the Ca values, as the calibration curve may change. Analyzed concentrations of the injected solution (Table 5.4) showed slightly lower Ca than expected.

Table 5.4. Analyzed injection solution concentration for 20-ft 1-D column experiment T43.

Ion	mg/L	mM
Ca	146.9	3.67
PO_4	228.1	2.401
citrate	2320.	10.31

The column(s) consisted of four columns of clear polyvinyl chloride (PVC) with dimensions 1.5-cm inside diameter (ID) by 152 cm length (5.0 ft), with a volume of 269.3 cm³. Based on the column volume, wet and dry sediment weights, the following parameters were calculated (Table 5.5).

Table 5.5. 20-ft column physical parameters.

location	total volume (cm ³)	pore volume (cm ³)	sediment (g)	porosity (cm ³ /cm ³)	dry bulk den. (g/cm ³)
0 – 5 ft	269.3	85.95	521.61	0.3192	1.937
0 – 10 ft	538.6	169.67	1023.7	0.3150	1.901
0 – 20 ft	1077.2	326.37	2121.3	0.3030	1.969

The experiment was set up to collect samples at 5 ft, 10 ft, and 20 ft. The column flow rate was set to achieve 1.0 pore volume in ~10 h (20-ft location), to be roughly equivalent to a 10-h injection. Flow was continued for 25 h injecting the solution. This is a linear column with constant flow rate and not radial flow (decreasing velocity with distance from injection well), so the shape of the breakthrough will be somewhat different for radial injection. There were some experimental artifacts: a) slow flow for the first 4 hours, and b) 0 to 5 ft column section clogged at 10.5 h, so was removed. These artifacts affect the 5-ft and 10-ft data, but not the 20-ft data.

Injection Solution Breakthrough. The apatite solution breakthrough (Figure 5.15, normalized to injection concentrations, actual concentrations shown in appendix) shows essentially no lag for Ca (R_f = 0.921) and citrate (R_f = 0.969), but retardation for PO₄ (R_f = 2.41, K_d = 0.217 cm³/g). These values should be the same as at field scale, as the <4 mm sediment was additionally filled in with 41% sand (equivalent of >4 mm). The electrical conductivity (EC) is not conservative (R_f = 2.59; Table 5.6), and shows initial rapid breakthrough for half of the EC (roughly equivalent to Ca-citrate breakthrough), and a slow tailing to 4 pore volumes (roughly equivalent to the PO₄ breakthrough).

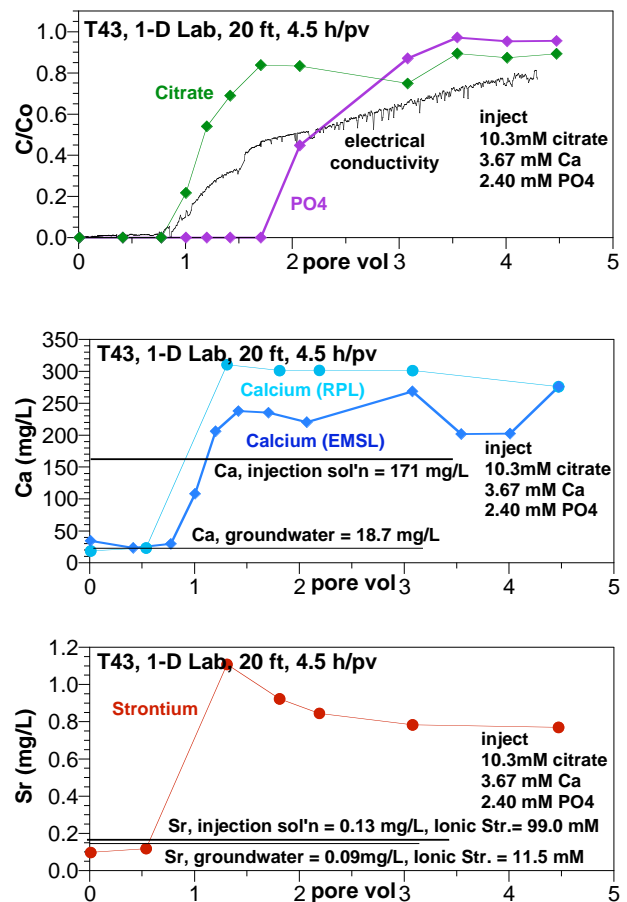


Figure 5.15. Injection of a Ca-citrate-PO₄ (4, 10, 2.4 mM) solution in a 20-ft long 1-D column (experiment T43), with a) citrate, PO₄, EC, b) Ca, and c) Sr.

While calcium breakthrough appears unretarded (Figure 5.15), the breakthrough concentration was 11x to 13x higher than groundwater and about 2x greater than the injection concentration. This is likely correct, as some calcium is desorbing from the sediment due to ion exchange caused by the apatite solution being a higher ionic strength than groundwater. Strontium, which should behave similarly to calcium, shows nearly the same behavior, with an initial peak concentration of 10x groundwater (at 1.0 pore volumes, tapering off to 8x groundwater concentrations). These characteristic “snow plow” or initial peaking breakthrough occurs with injection of a higher ionic strength solution into a system with lower ionic strength (with a similar mix of mono and divalent cations). Because of the experimental artifacts, breakthrough curves for 5 ft and 10 ft are suspect and not considered as accurate (in the appendix). They roughly show similar results as the 20-ft location (lag with PO₄, no lag for Ca and citrate).

Table 5.6. Breakthrough of injection solution components at 20-ft location (experiment T43).

parameter	Rf	Kd (cm³/g)	peak (vs gw)
electrical conductivity	2.59	0.244	no peak
Ca	0.921	0.0	11x-13x gw
citrate	0.969	0.0	no peak
PO ₄	2.41	0.217	no peak
Sr	~1.0	0.0	10x-11x gw

Metals Elution from Solution Injection. Trace metals were analyzed at the 20-ft location over the 25-h (4.5 pore volume) injection of the Ca-citrate-phosphate solution (Table 5.7). A table of the results is in the appendix. Samples analyzed included the following:

- seven samples of column breakthrough
- groundwater and groundwater/citrate injection solution
- three different types of metals extractions from sediments (1:1 water:sed., ion exchangeable (0.5M KNO₃), acid extraction (EPA 3051))
- analysis of metals in acids, and ICP instrument blank

Calcium breakthrough is observed in the ICP data that is the same as the separate Ca analysis (Figure 5.15), with initial low Ca concentration in groundwater (18.7 mg/L or 0.44 mM) achieving the injection solution concentration at about 1 pore volume (171 mg/L or 4.26 mg/L). There was some difference in the injection solution analyzed for Ca between the two different laboratories (4.26 mM and 3.67 mM), both by ICP. Ion exchangeable Ca was 260 mg/L (6.48 mM). The phosphate breakthrough curve could also be observed in the ICP data (P, second page) with complete breakthrough by 3 pore volumes. Sodium breakthrough also showed lag to a few pore volumes.

Table 5.7. Metals breakthrough data at 20-ft location in 1-D column injection of Ca-citrate-PO₄ (4, 10, 2.4 mM, experiment T43).

Analyte: ID	Pore volumes	Al µg/L	As µg/L	B µg/L	Ba µg/L	Be µg/L	Bi µg/L	Ca µg/L	Cd µg/L	Co µg/L
200	0.01	(4.98E+02)	<2.50E+04	(2.41E+02)	(1.65E+01)	(8.37E+00)	(1.81E+02)	1.86E+04	<2.50E+02	(4.39E+00)
209	0.54	(5.32E+02)	<2.50E+04	(2.01E+02)	(7.09E+00)	(7.55E+00)	<2.50E+03	2.34E+04	<2.50E+02	(3.00E+00)
216	1.31	1.40E+04	<2.50E+04	(5.37E+02)	(4.90E+02)	(2.87E+01)	(8.90E+01)	3.11E+05	(1.17E+01)	(3.54E+00)
221	1.81	1.29E+04	(3.60E+01)	(3.25E+02)	(3.46E+02)	(1.12E+01)	<2.50E+03	3.01E+05	<2.50E+02	(3.62E+00)
225	2.19	7.18E+03	<2.50E+04	(2.91E+02)	(3.75E+02)	(1.13E+01)	(1.30E+02)	3.02E+05	<2.50E+02	(3.64E+00)
227	3.08	(4.76E+03)	<2.50E+04	(9.31E+01)	(4.42E+02)	(2.96E+00)	(1.02E+01)	3.01E+05	<2.50E+02	(2.21E+00)
230	4.47	(4.29E+03)	(9.57E+01)	(1.25E+02)	(4.28E+02)	(7.43E+00)	<2.50E+03	2.76E+05	<2.50E+02	(1.00E+00)
	citrate solution	(1.02E+03)	<5.00E+04	(2.14E+02)	(1.00E+01)	(1.72E+01)	<5.00E+03	1.71E+05	<5.00E+02	<5.00E+00
	groundwater	(3.15E+01)	<2.00E+03	(8.03E+00)	(2.17E+01)	(5.90E-01)	<2.00E+02	1.87E+04	<2.00E+01	(1.17E+00)
231	water/sed. 1:1	(5.14E+02)	<2.50E+04	(2.52E+02)	<2.50E+03	(9.41E+00)	<2.50E+03	1.43E+04	<2.50E+02	(1.79E+00)
232	0.5 M KNO3	(3.99E+02)	(3.36E+01)	(8.38E+01)	7.14E+03	(6.60E+00)	<2.50E+03	2.60E+05	<2.50E+02	(7.91E+00)
233	4 M scid extraction	1.73E+05	<2.50E+05	3.70E+06	(2.87E+03)	<2.50E+03	<2.50E+04	(3.62E+04)	(2.73E+02)	(2.34E+00)
234	acid blank	(5.99E+03)	<2.50E+05	3.50E+06	<2.50E+04	(9.25E+01)	<2.50E+04	(2.97E+03)	<2.50E+03	(1.06E+00)
	instrument EQL	<1.00E+02	<5.00E+02	<1.00E+02	<5.00E+01	<5.00E+00	<5.00E+01	<1.00E+02	<5.00E+00	<5.00E+00

Analyte: ID	Pore volumes	Cr µg/L	Cu µg/L	Fe µg/L	K µg/L	Li µg/L	Mg µg/L	Mn µg/L	Mo µg/L	Ni µg/L
200	0.01	<6.25E+02	(1.63E+02)	(2.55E+01)	(2.45E+04)	(1.50E+02)	4.26E+03	(1.95E+02)	(6.37E+01)	(5.91E+00)
209	0.54	<6.25E+02	(1.46E+02)	(9.83E+00)	(7.40E+03)	(1.14E+02)	5.43E+03	(2.45E+02)	(1.88E+02)	(7.52E+00)
216	1.31	<6.25E+02	(1.92E+02)	2.70E+03	(1.60E+04)	(2.11E+02)	5.93E+04	1.21E+04	(1.96E+02)	(1.80E+00)
221	1.81	<6.25E+02	(1.34E+02)	2.32E+03	(1.99E+04)	(1.96E+02)	5.90E+04	8.47E+03	(1.55E+02)	(1.05E+00)
225	2.19	<6.25E+02	(1.50E+02)	2.13E+03	(9.82E+03)	(2.71E+02)	6.08E+04	5.04E+03	(1.63E+02)	(7.95E+00)
227	3.08	<6.25E+02	(1.14E+02)	2.51E+03	(9.02E+03)	(1.36E+02)	4.03E+04	3.03E+03	(1.94E+02)	(3.80E+00)
230	4.47	<6.25E+02	(1.65E+02)	2.53E+03	(9.99E+03)	(2.19E+02)	2.14E+04	2.37E+03	(1.05E+02)	(5.91E+00)
	citrate solution	<1.25E+03	(1.92E+02)	(1.54E+02)	(3.08E+04)	(2.05E+02)	(4.29E+03)	(6.18E+00)	(2.86E+02)	(8.52E+00)
	groundwater	<5.00E+01	(1.16E+01)	(3.63E+00)	(8.17E+02)	(9.49E+00)	4.30E+03	(1.82E-01)	(1.85E+01)	(8.51E+00)
231	water/sed. 1:1	<6.25E+02	(1.32E+02)	(4.47E+01)	(4.37E+03)	(1.75E+02)	3.36E+03	(1.72E+02)	(1.20E+02)	(5.26E+00)
232	0.5 M KNO3	<6.25E+02	(8.79E+01)	(3.29E+01)	1.55E+07	(1.76E+02)	4.37E+04	3.44E+03	(2.17E+02)	(5.18E+00)
233	4 M scid extraction	(9.38E+02)	(1.37E+03)	5.82E+05	(3.38E+05)	(1.02E+03)	(7.08E+03)	1.58E+04	(7.70E+02)	(1.17E+00)
234	acid blank	<6.25E+03	(1.20E+03)	(2.94E+02)	(1.95E+04)	(1.82E+03)	(9.78E+01)	<2.50E+03	(6.51E+02)	(1.82E+00)
	instrument EQL	<1.25E+01	<5.00E+01	<1.00E+01	<1.25E+03	<5.00E+01	<5.00E+01	<5.00E+00	<1.00E+01	<2.50E+00

Analyte: ID	Pore volumes	P µg/L	Pb µg/L	Se µg/L	Sr µg/L	Tl µg/L	V µg/L	Zn µg/L	Na µg/L	Si µg/L
200	0.01	(4.10E+02)	<1.25E+03	(1.89E+02)	(9.76E+01)	<2.50E+03	<1.25E+03	(1.51E+01)	1.62E+04	(3.83E+03)
209	0.54	(2.30E+02)	(1.16E+02)	(2.83E+02)	(1.19E+02)	(1.90E+02)	(6.57E+01)	<1.25E+03	1.39E+04	(3.91E+03)
216	1.31	(5.60E+02)	(2.27E+00)	(1.06E+03)	(1.11E+03)	(5.09E+01)	<1.25E+03	(2.47E+00)	1.28E+05	(7.96E+03)
221	1.81	8.78E+03	<1.25E+03	(3.57E+02)	(9.23E+02)	<2.50E+03	<1.25E+03	<1.25E+03	2.74E+05	(1.13E+04)
225	2.19	4.09E+04	(1.88E+01)	(1.38E+03)	(8.45E+02)	<2.50E+03	(1.29E+00)	<1.25E+03	4.17E+05	(1.16E+04)
227	3.08	6.99E+04	<1.25E+03	(1.51E+03)	(7.83E+02)	(9.14E+00)	(2.52E+00)	<1.25E+03	5.74E+05	(7.92E+03)
230	4.47	6.89E+04	<1.25E+03	(8.69E+02)	(7.70E+02)	<2.50E+03	<1.25E+03	<1.25E+03	6.66E+05	(5.45E+03)
	citrate solution	7.12E+04	<2.50E+03	(1.32E+03)	(1.27E+02)	(2.26E+01)	(1.38E+02)	<2.50E+03	7.00E+05	<1.00E+04
	groundwater	(3.63E+01)	<1.00E+02	(4.52E+01)	(8.55E+01)	(1.44E+01)	(1.03E+00)	(4.28E+00)	1.96E+03	(1.64E+03)
231	water/sed. 1:1	(1.78E+02)	<1.25E+03	(2.40E+01)	(6.76E+01)	<2.50E+03	(4.04E+01)	<1.25E+03	1.03E+04	(1.14E+03)
232	0.5 M KNO3	(5.08E+02)	<1.25E+03	(1.29E+03)	(1.64E+03)	<2.50E+03	(4.45E+01)	<1.25E+03	1.55E+04	<5.00E+03
233	4 M scid extraction	(1.63E+04)	(2.19E+02)	<5.00E+04	(2.24E+03)	(3.27E+03)	(1.46E+03)	(1.37E+03)	9.03E+04	1.12E+07
234	acid blank	(1.28E+03)	(8.26E+02)	(5.00E+03)	<2.50E+04	<2.50E+04	(9.13E+02)	<1.25E+04	(1.30E+04)	(1.53E+03)
	instrument EQL	<6.25E+01	<2.50E+01	<1.00E+02	<5.00E+01	<5.00E+01	<2.50E+01	<2.50E+01	<1.00E+02	<1.00E+04

Analyte: ID	Pore volumes	S µg/L	Ti µg/L	Zr µg/L	Ag µg/L	Re µg/L	Sb µg/L
200	0.01	5.44E+03	(1.65E+00)	<2.50E+02	<5.00E+03	<5.00E+02	<2.50E+05
209	0.54	8.15E+03	<2.50E+02	<2.50E+02	<5.00E+03	(2.85E+01)	<2.50E+05
216	1.31	3.81E+03	<2.50E+02	(2.22E+01)	<5.00E+03	(5.67E+01)	<2.50E+05
221	1.81	4.03E+03	<2.50E+02	(3.51E+00)	<5.00E+03	(1.00E+01)	<2.50E+05
225	2.19	1.78E+03	<2.50E+02	(4.59E+00)	<5.00E+03	<5.00E+02	<2.50E+05
227	3.08	1.68E+03	<2.50E+02	<2.50E+02	<5.00E+03	(3.76E+00)	<2.50E+05
230	4.47	2.10E+03	<2.50E+02	<2.50E+02	<5.00E+03	(1.50E+01)	<2.50E+05
	citrate solution	(5.21E+03)	<5.00E+02	<5.00E+02	<1.00E+04	(8.32E+01)	<5.00E+05
	groundwater	3.28E+03	<2.00E+01	<2.00E+01	<4.00E+02	<4.00E+01	<2.00E+04
231	water/sed. 1:1	4.64E+03	(2.64E-01)	<2.50E+02	<5.00E+03	(7.52E+01)	<2.50E+05
232	0.5 M KNO3	3.82E+03	<2.50E+02	<2.50E+02	<5.00E+03	<5.00E+02	<2.50E+05
233	4 M scid extraction	(6.75E+03)	9.50E+04	(1.37E+03)	<5.00E+04	<5.00E+03	<2.50E+06
234	acid blank	(1.12E+04)	(1.73E+02)	(1.19E+03)	<5.00E+04	(1.46E+02)	<2.50E+06
	instrument EQL	<2.00E+02	<5.00E+00	<5.00E+00	<1.00E+02	<1.00E+01	<5.00E+03

EQL = Estimated Quantification Limit (results above CCV std) S = detector saturated (results above CCV std)

(###) = value analyzed below instrument EQL

R = radial mode

"<" = Instrument returned a zero or negative value. Result reported as "< sample EQL"

Samples not bracketed by CCV standards w/in ±10%

Many trace metals were present in the injection solution, so “metals leaching off sediment” is defined by increasing concentration of a metal not present in the injection solution. These trace metals that may have leached off the sediment included: Ba, Fe, Mg, Mn, and Sr. Trace metals that showed no change included: Be, K, S. Trace metals that were present in the injection solution that showed *an increase* (i.e., not leaching off the sediment): Al, As, Ca, Co, Fe, K, Li, P, Se, V, Zn, and Na. Trace metals in the injection solution that showed *no change* included: B, Cd, Cr, Cu, Li, Mo, Ni, Pb, Tl, V, Si, Ti, Zr, Ag, Re, and Sb. The 4 M HNO₃ acid extraction showed that there is considerably more Ba, Fe, Mn, and Sr that did not leach off the sediment due to the citrate injection.

Cation Exchange from the Surface Soils and Ca desorption due to citrate solution injection. The cation exchange capacity of the Hanford formation sediment and major cations were quantified on the <4 mm size fraction (Table 5.8). In order to compare this data to the field or experiment T43 results (with sand/sediment mix), the fraction <4 mm (0.594) is used to correct the data.

Table 5.8. Major cation mass balance for 20-ft long 1-D column experiment (experiment T43).

Cations on 100-N Hanford Fm (<4 mm) by ion exchange in equilibrium with groundwater					
fraction	fraction	fraction	fraction	fraction	<4 mm=0.594
K	Mg	Sr	Na	Ca	ave CEC
0.042	0.168	0.024	0.027	0.772	3.43E-05
mmol/g	mmol/g	mmol/g	mmol/g	mmol/g	eq/g
1.45E-03	2.88E-03	4.11E-04	9.36E-04	1.28E-02	
if all surface cations were in solution (Pb = 1.969 g/cm ³ , porosity = 0.303, T43, with < 4 mm)					
mmol/cm ³	mmol/cm ³	mmol/cm ³	mmol/cm ³	mmol/cm ³	
5.59E-03	1.11E-02	1.59E-03	3.61E-03	4.96E-02	
groundwater (from T43)					
(mmol/cm ³)	(mmol/cm ³)	(mmol/cm ³)	(mmol/cm ³)	(mmol/cm ³)	
2.09E-05	1.77E-04	2.28E-06	8.52E-05	4.66E-04	
10 mM citrate injection solution (T43 analysis)					
(mmol/cm ³)	(mmol/cm ³)	(mmol/cm ³)	(mmol/cm ³)	(mmol/cm ³)	
7.88E-04	1.77E-04	3.67E-03	3.04E-02	3.67E-03	
Ca breakthrough curve (20 ft, 3.0 pv): 6.72E-3 mmol/cm ³ 1.83 times the citrate injection concentration if 1.00x from the citrate (assume), then 3.05E-3 from sediment (or 6.2% of the Ca desorbed from the sediment)					

For this low citrate concentration injection (10 mM), calcium did not show the characteristic ion exchange “peaking” breakthrough curve, although it is clear that some calcium and magnesium was removed from the surface by ion exchange. By rough estimate, about 6.2% of the Ca in the effluent is from the surface. Essentially by not doing cation exchange correctly, in groundwater the Ca behaves exactly the same as Sr (and should), with a pseudo-R_f = 106 and K_d = 16.2. In the 10 mM citrate solution, the Ca R_f decreases to 16.3 (K_d = 2.35 cm³/g), which means 6.2% of the Ca desorbed from the surface during the experiment to produce the 6.7 mM Ca at 3.0 pore

volumes while injecting 3.67 mM Ca. These retardation factor (Rf) values were determined from solution and surface concentrations shown in Table 5.6.

A second large 1-D column experiment was conducted with the injection of the same Ca-citrate-PO₄ solution to confirm the results (experiment Y14), as there were some flow anomalies in experiment T43. Results (Figure 5.16) show nearly identical behavior in this 100-cm long (3.2-ft) column to the 20-ft long column (Figure 5.15). Both Ca and Sr breakthrough was nearly unretarded (at 1.0 pore volume) with peaking behavior of 10-11x groundwater concentrations (i.e., so Sr-90 is expected, on average, to peak at 10x groundwater concentration in the field injection #1). Citrate breakthrough was unretarded (Rf = 1.0) with no peak, and PO₄ breakthrough was retarded, with the PO₄ retardation factor varying with injection velocity. As described more fully in Section 5.7.6, phosphate sorbs to sediment within minutes, but one or more phosphate phases begin to precipitate within hours and continue to precipitate for 100s of hours. Injection of a PO₄-containing solution would, therefore, show both retardation and mass loss, although the retardation (i.e., reversible) should be mainly caused by sorption, as mass loss alone would not cause any retardation. The phosphate retardation observed in experiment Y14 (Rf = 2.1, residence time in column 3.3 h) was slightly smaller than observed in experiment T43 (20-ft column, Rf = 4.5, residence time 4.5 h), as there was less reaction time to sorb the PO₄.

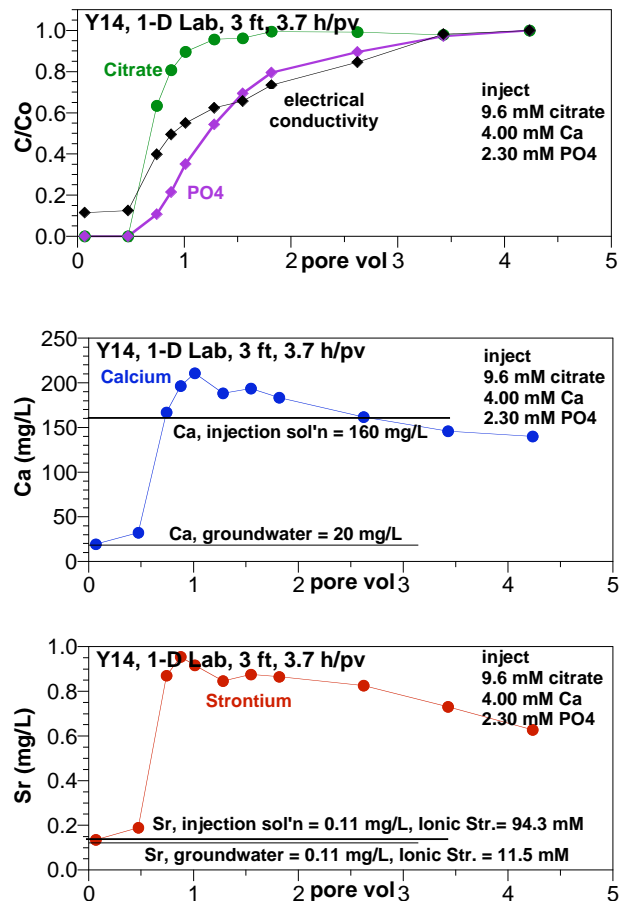


Figure 5.16. Citrate mineralization and depth in five boreholes showing a) trend of mineral.

Additional 1-meter column experiments were conducted after injection #1 in which Ca-citrate concentration was decreased relative to PO₄ (Section 5.3.1).

5.2.2 Stability of Field #1 Tanker Solutions

The stability of the two solutions used at the field-scale injection #1 were investigated at high concentration and low temperature to determine the limits for the tanker trucks. Following is the recipe for the low concentration apatite injection solutions (Tables 5.9 and 5.10).

Table 5.9. Solution composition for Field Injection #1.

- 10 mM trisodium citrate [$\text{HOC}(\text{COONa})(\text{CH}_2\text{COONa})_2 \cdot 2\text{H}_2\text{O}$] fw 294.1 g/mol
 - granular is more soluble than powdered
 - reagent grade (quality) for the citrate: USP/FCC
(lower grades contain up to 5 ppm heavy metals)
- 2.0 mM disodium phosphate [Na_2HPO_4], fw 141.96 g/mol
 - reagent grade (quality): certified ACS grade
(lower grades can contain extra NaOH, which is only a small problem, changes pH and ionic strength)
- 0.4 mM sodium phosphate [NaH_2PO_4], fw 119.98 g/mol
 - reagent grade (quality): certified ACS grade
(lower grades can contain 8 ppm arsenic and 10 ppm heavy metals)
- 1.0 mM ammonium nitrate [NH_4NO_3], fw 80.04 g/mol
 - granular
 - reagent grade (quality): certified ACS
- 4.0 mM calcium chloride, [$\text{CaCl}_2 \cdot 2\text{H}_2\text{O}$], fw 147.02 g/mol
 - reagent grade (quality): certified ACS
(lower grades can contain 20 ppm lead)

A pH specification of 7.5 ± 0.1 for the [Na_2HPO_4]/ [NaH_2PO_4]/ [NH_4NO_3] solution was included in the procurement requirements. At these molar concentrations, a 30,000 gal injection volume would consist of the following dry chemical weights:

Table 5.10. Mass of chemicals needed for field injection #1.

- Mix #1 (Solution #1)
 - 734.7 lbs of trisodium citrate
 - 146.9 lbs of calcium chloride
- Mix #2 (Solution #2)
 - 70.9 lbs of disodium phosphate
 - 12.0 lbs of sodium phosphate
 - 20.0 lbs of ammonium nitrate

Because we are relying on microbial degradation of the citrate for apatite formation to occur, make up water for these solutions should not contain residual chlorine or any other form of bactericide.

CaCl_2 / trisodium citrate was found to be unstable at a concentration mix of 80/200 mM at pH 7.5 in DI water. A precipitate, most probably calcium citrate, forms within hours of preparing the solution at room temperature. The corresponding phosphate/nitrate solution (50/20 mM) is also not stable in solution. Decreasing the concentrations of the mix to 64/160 mM resulted in an increase in stability with a precipitate forming after approximately 10 days when stored in the refrigerator (4°C , Table 5.11). Initially it was thought that this solution ratio was stable and it was used to make up the required Ca/citrate and phosphate/nitrate solutions in Hanford groundwater. The Ca/Citrate solution produced a precipitate within 6 hours at room temperature and the corresponding phosphate/nitrate solution required at this ratio also produced a very small

amount of precipitate after 48 hours at room temperature. Further reducing the citrate solution concentration to 56/140 mM in Hanford groundwater produced a solution that was stable at room temperature for up to 6 days after which time a very small amount of precipitate forms which may not be a problem for our application, the corresponding phosphate/nitrate solution shows no signs of precipitation after 14 days at room temperature.

Table 5.11. Maximum solubility of Ca-citrate-PO₄ components and long-term stability.

Ca/Citrate (mM)	PO ₄ /NO ₃ (mM)	ground water used	stability time	tested at 22C	tested at 4C
80/200	50/20	yes	<12 hrs	yes	
80/200	50/20	no	<12 hrs	yes	
64/160	40/16	no	<10 days		yes
64/160		yes	<6 hrs	yes	
	40/16	yes	<48 hrs	yes	
56/140		yes	3-10 days		yes
56/140		yes	<7 days	yes	
	28/14	yes	>17 days	yes	
28/70		no	>17 days		yes

All solution were pH adjusted to pH=7.5

Based on these data, maximum solution concentration should be kept below 140 mM citrate to prevent precipitation. For the FY06 low concentration injections, the concentrations can be kept below this value by having the vendor deliver each 30,000 gal injection volume as a single load. Thus, the minimum delivery volume should be specified as 3000 gallons for the Ca/Citrate solution and 2500 gallons for the PO₄/NO₃ solution. These volume requirements should be easily met by a standard tanker truck with pup (trailer) configuration.

Another concern is that the citrate solution biodegrades, so if any microbes get into the solution they will multiply in days and eventually result in a significant consumption of citrate. Cold temperature (4°C) will minimize microbial growth, but citrate is less soluble and reaction rates slower at cold temperature so chilling the solution is not necessarily desirable (but acceptable if required). We are conducting experiments to assess citrate degradation, but don't expect a significant impact unless poor handling/shipping practices are used by the vendor. The procurement should specify that the tankers be cleaned (and depending on what we find during our current experiment, the citrate tank sterilized [hopefully this won't be required]) and that shipments be delivered within 4 hours of completing the process of dissolving and mixing the two separate components of the apatite solution (Ca/Citrate and PO₄/NO₃).

Preparation of Solution 1: citrate solution. Given that the solubility of mixed salts at high ionic strength are difficult to predict, a laboratory solubility/stability study was carried out. The maximum amount of calcium citrate that can be readily substituted into solution 1 is 10 mM. The order of additions for this solution is critical and should be carried out accordingly: trisodium citrate should be dissolved in DI first followed by trisodium citrate, at this point most of the water should be added leaving just enough to accurately add the remaining CaCl₂. The citrate

mix needs to be heated to approximately 35°C and mixed well to completely dissolve (sonicate). Finally add the CaCl₂ and make up to the mark once the solution has cooled. Once in solution the calcium citrate is stable for more than two months. The amount of calcium citrate needs to be decreased in the presence of groundwater due to the amount of Ca present in groundwater. A solution of the above formula has proven to be stable for more than 7 days at room temperature. The stability test is continuing at this time. The stability of this citrate solution is comparable to citrate solutions without calcium citrate. This solution could be preserved if it was sterile filtered once it was mixed and stored in a sterile storage container, the citrate concentration would remain stable since no bacteria would be present to start the biodegradation process.

Preparation of Solution 2: Phosphate solution. The final pH of the final mixed solution can be controlled by appropriately mixing different phosphate salts together. Here the ammonium phosphate and disodium phosphate are used at different molar ratios to obtain a pH of 7.5 and to minimize the ionic strength of the final solution mix. Disodium phosphate does have a tendency to clump when added in large amounts and should be mixed thoroughly and may require sonication at the field scale. Both ammonium phosphate and ammonium nitrate are highly soluble and pose no dissolution problems. This solution is stable for over a week and has a pH of 7.54. The amount of ammonium nitrate could be decreased even further once a study of the nitrogen requirements of the bacteria of interest has been more thoroughly carried out.

5.2.3 Field #1: Electrical Conductivity versus Solution Concentration

During the field injections, real-time data is needed in order to insure that the injections are actually resulting in the Ca-citrate-PO₄ solution is flowing into the aquifer. In addition, while there are volumetric flow meters on the tanker #1 and tanker #2 feed and the combined feed, these flow meters were somewhat unreliable, so relationships between solution composition and electrical conductivity were also used as a backup of adjusting the injection concentrations. For monitoring of the solution flowing in the aquifer, electrical conductivity provides only a rough estimate of some portion of the injection solution arrival, as shown in Figures 5.17 and 5.18. Initial breakthrough of Ca and citrate and lagged breakthrough of PO₄ results in the EC breakthrough being bimodal, with initial partial breakthrough likely dominated by the Ca and citrate, and the second breakthrough portion being dominated by the PO₄ breakthrough.

The relationship between the trisodium citrate/calcium chloride (i.e., solution #1) composition and electrical conductivity is exact. A laboratory (YSI or Yellow Springs Instrument) electrical conductivity meter and the field electrical conductivity meter were used for these measurements (<1% difference between meters). This Ca-citrate solution showed some solubility issues at >120 mM concentration, which is observed on the relationship with electrical conductivity (Figure 5.17a). Attempts were made three times to mix these high concentration solutions, and the observed lower electrical conductivity than predicted is likely caused by not all of the citrate being solubilized.

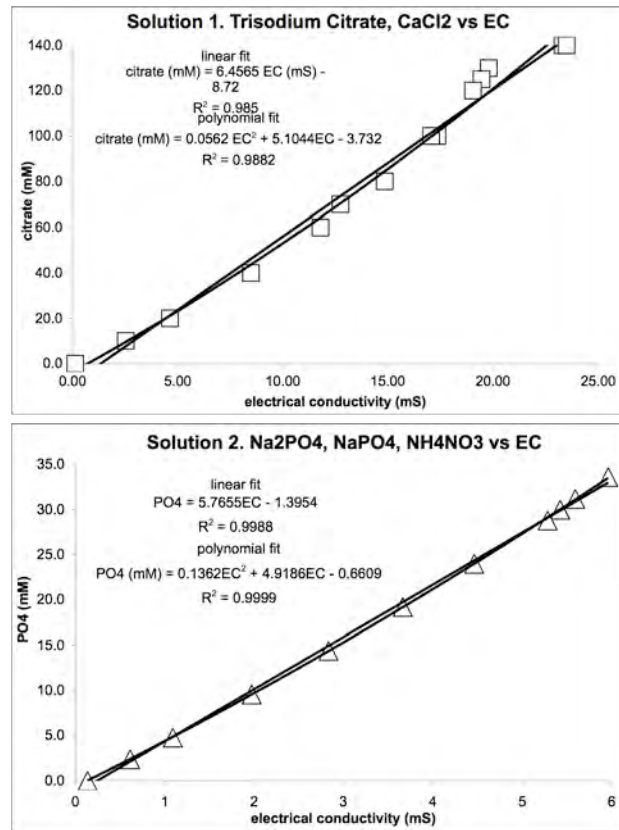


Figure 5.17. Relationship between: a) Injection #1, solution #1 (Ca-citrate) and electrical conductivity, and b) injection #1, solution #2 (PO₄) and electrical conductivity.

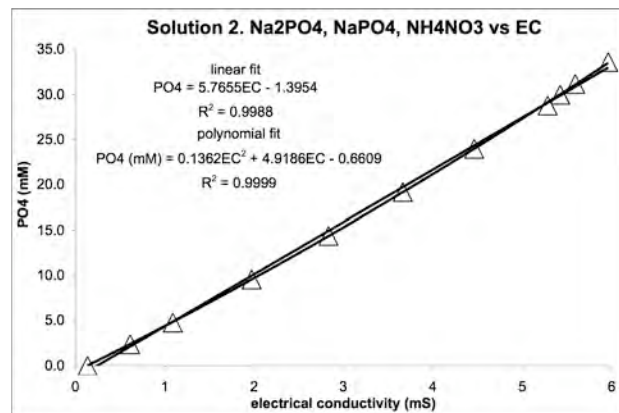


Figure 5.18. Relationship between a 50/50 mix of solution #1 (Ca-citrate) and solution #2 (PO₄) and electrical conductivity.

The relationship between the phosphate solution (solution #2) and electrical conductivity is also exact (Figure 5.17b). There were no solubility issues with this high concentration solution.

The relationship between the combination of solution #1 and solution #2 and electrical conductivity is not unique, meaning any combination of the two solutions will produce an electrical conductivity. What is presented in Figure 5.18 is an exact 50/50 mix of solution #1 and solution #2. What is needed to determine the exact solution composition is one more measurement – phosphate, as described below. The relationship between the mixed solution and electrical conductivity shows a fairly linear trend, especially in the range being injected at field scale (i.e., 10 mM citrate).

The procedure developed to determine the composition of field injection #1 is the following:

1. measure PO_4 by Hach kit (mM, see Section 5.2.5)
2. calculate what the EC should be from $\text{EC}_{\text{calculated}} = [\text{PO}_4(\text{mM}) + 0.7553]/1.084$ and calculate what the citrate concentration should be = $[\text{PO}_4(\text{mM}) * 4.167]$
3. measure the EC of the mixed solution (called $\text{EC}_{\text{measured}}$)
4. calculate $\text{deltaEC} = \text{EC}_{\text{measured}} - \text{EC}_{\text{calculated}}$ (+ value = additional citrate in mix, - value = less citrate in mix)
5. calculate how much citrate is off
 $\text{deltaCitrate}(\text{mM}) = 4.159(\text{deltaEC}) - 3.136$
(note that the + or – for deltaEC needs to be included in the following:
final citrate citrate (mM) = calculated citrate + deltaCitrate (mM)

For field injection #1, a Hach method 8114 (molybdovanadate) was used, which was later determined to be inaccurate due to the presence of citrate (i.e., citrate interferes with the measurement). For field injection #2, a Hach method 8178 (amino acid) was used, which does not have citrate interference issues.

5.2.4 Field #1: Solution Density versus Solution Concentration

In addition to measuring the electrical conductivity to estimate solution concentration, an alternate method of measuring the solution density was also investigated. Measuring the solution density for a solution in the tanker truck would simply involve weighing the solution in a graduated cylinder, and measuring the temperature of the solution. The temperature is used to correct for density changes with temperature.

While there was a good relationship between the solution density and the solution composition (Figure 5.19), the changes in density were too small to be able to accurately adjust the solution composition. The relationship between solution concentration and electrical conductivity were much more sensitive (Section 5.2.3), and used at the field scale. It should also be noted that this density/mix concentration relationship was developed for the mixed solution [i.e., solution 1 (Ca-citrate) and solution 2 (PO₄)], so is only accurate with a 50/50 mixture of solution 1 and solution 2. As with the electrical conductivity/concentration relationship, an additional field PO₄ measurement is needed to determine if the mixed solution had the correct concentration of components.

Solution density versus concentration relationships were not developed for individual solutions 1 and 2, but would be approximately double the concentrations indicated in Figure 5.19b, so would still not be very sensitive a measurement technique compared to electrical conductivity.

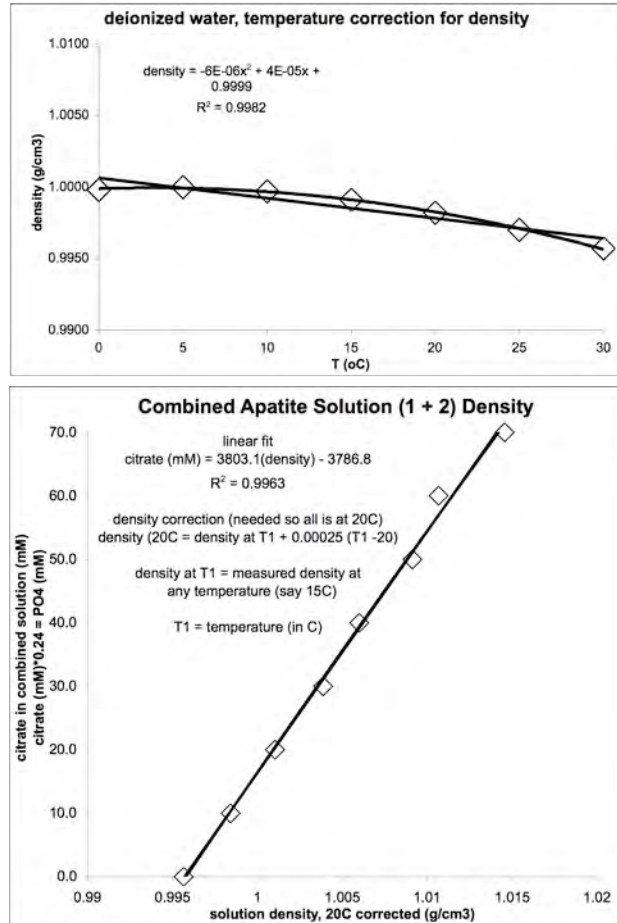


Figure 5.19. Relationship between a 50/50 mix of solution #1 (Ca-citrate) and solution #2 (PO₄) and solution density (b), with temperature correction (a).

5.2.5 Field #1: Phosphate Measurement (Hach 8114) and Citrate Interference

For field injection #1, a technique to rapidly measure phosphate in the field was needed in conjunction with the electrical conductivity versus total solution concentration relationship (Section 5.2.3) to determine the concentrations of Ca-citrate and phosphate being injected. The Reactive phosphorous (also called Orthophosphate or Molybdovanadate) method from Hach Industries is a relatively rapid method for measuring phosphate (0 to 45 mg/L or 0.45 mmol/L). Because the phosphate injection concentration is higher (2.4 mmol/L) a 5:1 dilution (maximum) is needed with samples. According to the Hach method 8114, citrate up to 1000 mg/L (5.3 mmol/L) does not interfere with the orthophosphate measurement. Therefore, the injection solution with 10 mmol/L citrate would likely cause some problems. If the citrate concentration remained relatively constant (i.e., samples of the injection stream), the PO₄ measurements would be accurate even with citrate present. However, if the citrate concentration varied significantly (i.e., samples from monitoring wells over time in which citrate was partially to fully degraded), then the PO₄ method would not be accurate. In addition, citrate degradation products (smaller

molecular weight organic acids, Figure 5.7) may also interfere with the PO₄ measurement method. While most of these organic acids are not specifically listed, formate is.

Calibration of PO₄ concentration versus absorbance (at 420 nm) by the Hach 8114 (molybdovanadate) method with no citrate present (Figure 5.20a) shows a linear relationship, as expected. With differing concentrations of citrate present (Figure 5.20b), the reported PO₄ concentration varied. According to the Hach 8114 method, the standard reaction time for the molybdovanadate is 3 minutes, and with this reaction time (diamonds, Figure 5.20b), there was significant interference of the presence of citrate at all concentrations (even 2 mM, well below Hach's listed interference limit of 5 mM). The interference can be alleviated to some extent by greater reaction time as shown by the 30 minute and 1 h reaction times (Figure 5.20b) with a flatter slope at low citrate concentrations. Additional time (15 h, data not shown) was similar to 1 h data. The PO₄ accuracy for a 3-minute measurement was 90% (with 4 mM citrate) and 72% (with 10 mM citrate), whereas the PO₄ accuracy for a 1-hour measurement was 97% (4 mM citrate) and 87% (with 10 mM citrate). In the field, the interference of the citrate in this Hach 8114 method for PO₄ measurement was considered too great, and a different Hach method (8178, Section 5.3.5) was used in subsequent field tests, which did not have interference.

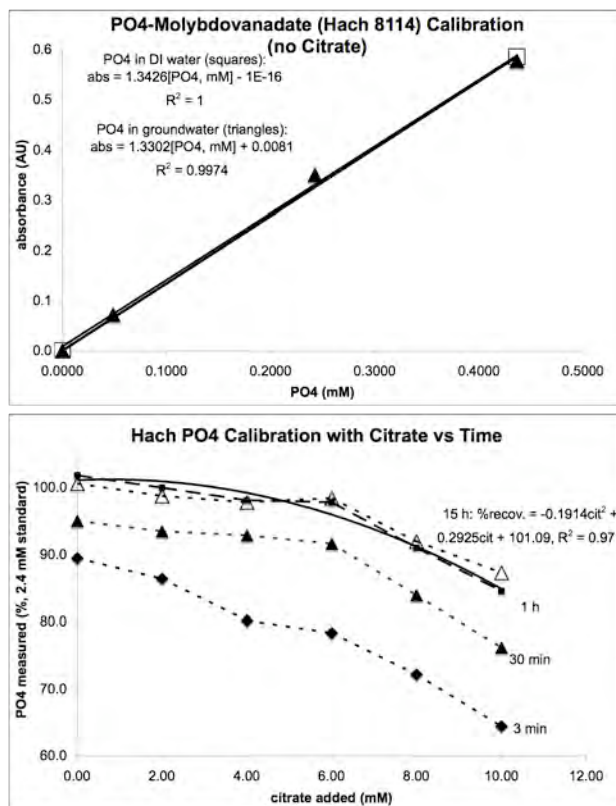


Figure 5.20. Hach 8114 PO₄ analysis (molybdovanadate) of UV absorbance at 420 nm: a) without citrate present, b) with citrate present showing significant interference.

5.3 Laboratory Support Experiments for Field Injection #2

The original Ca-citrate-PO₄ formulation provides for the exact proportions of chemicals needed to precipitate apatite [Ca₁₀(PO₄)₆(OH)₂], with a Ca/PO₄ molar ratio of 10/6 and a Ca/citrate ratio of 4/10, based on geochemical simulations in which 10 mM of citrate is needed to complex 4 mM of Ca. If the Ca is not complexed, it will immediately form a precipitate with PO₄ (likely a mono- or di-Ca-PO₄). As described in detail in the background section, the presence of citrate has an additional role of inhibiting the immediate formation of Ca-PO₄ precipitates. Both the slow degradation of citrate (as an inhibitor) and increasing presence of microbes result in the slow formation of apatite (not mono- or di-Ca-PO₄). In 1-D laboratory experiments (Section 5.2.1, Figures 5.15 and 5.16) and field experiment #1, the resulting Ca solution concentration was ~80% greater than the injection solution, as a result of ion exchange (i.e., the

high Na concentration injected displaced some Ca off sediment ion exchange sites). Optimizing this Ca-citrate-PO₄ solution mixture is a balance of injecting a sufficiently concentrated solution to form enough apatite to sequester Sr and Sr-90, but keep the ionic strength low enough to not desorb too much Sr-90. Results of the 1-D laboratory experiments (Figures 5.15 and 5.16) showed Ca and Sr desorption was 10-11x groundwater concentration, so the Sr-90 was predicted to increase 10x. This did provide a good estimate of the mean concentration increase for field injection #1, in which the average Sr-90 groundwater increase was 10.5x over baseline concentration. Due to heterogeneities entrapping more Sr-90 in some locations (likely low-K units and in the capillary fringe zone), the variability of the Sr-90 increase in field injection #1 was significant (range of Sr-90 increase was 0 to 25x). Therefore, in order to decrease the Sr-90 increase (i.e., have less Ca, Sr, and Sr-90 exchange off sediment surfaces), yet still inject sufficient PO₄, it was decided to alter the Ca-citrate-PO₄ injection formulation to inject less Ca-citrate. Because additional Ca was present in groundwater due to the higher ionic strength solution injection, less Ca-citrate was needed to be injected.

5.3.1 Laboratory 1-D Column Transport Experiments

Five additional 1-meter column experiments were conducted varying the Ca-citrate concentration (keeping the PO₄ concentration constant at 2.4 mM) to measure the peaking Ca and Sr behavior. The citrate concentration was varied between 5 mM and 10 mM. Complete breakthrough data is shown in the appendix (experiments Y14 to Y17, Y21 to Y24). Results of two experiments with 4.6 mM Ca and 7.9 mM citrate (experiment Y21, Figure 5.21) and 2 mM Ca and 5 mM citrate (experiment Y16, also Figure 5.21) show the obvious effect of ion exchange; injection of a lower ionic strength solution results in less Ca and Sr desorption from the sediment. With 2.4 mM of PO₄ injected, a total of 4 mM (or 160 mg/L) Ca in solution is needed to stoichiometrically form apatite. Injection of the 4.6 mM Ca solution (experiment Y21, Figure 5.21) resulted in too much Ca in solution (240 mg/L or 6 mM), whereas injection of 2 mM Ca (experiment Y16, Figure 5.21) resulted in too little Ca in solution (110 mg/L or 2.75 mM). Additional experiments are in the appendix.

Additional information was obtained from this breakthrough data, with the Ca and Sr peak concentration of 5-7x for the 2 mM Ca injection (ionic strength 62 mM), and 7-9x for the 4.6 mM Ca injection (ionic strength 79 mM). The lab in PO₄ breakthrough was relatively invariant with solution concentration (Rf 2.0 to 2.7).

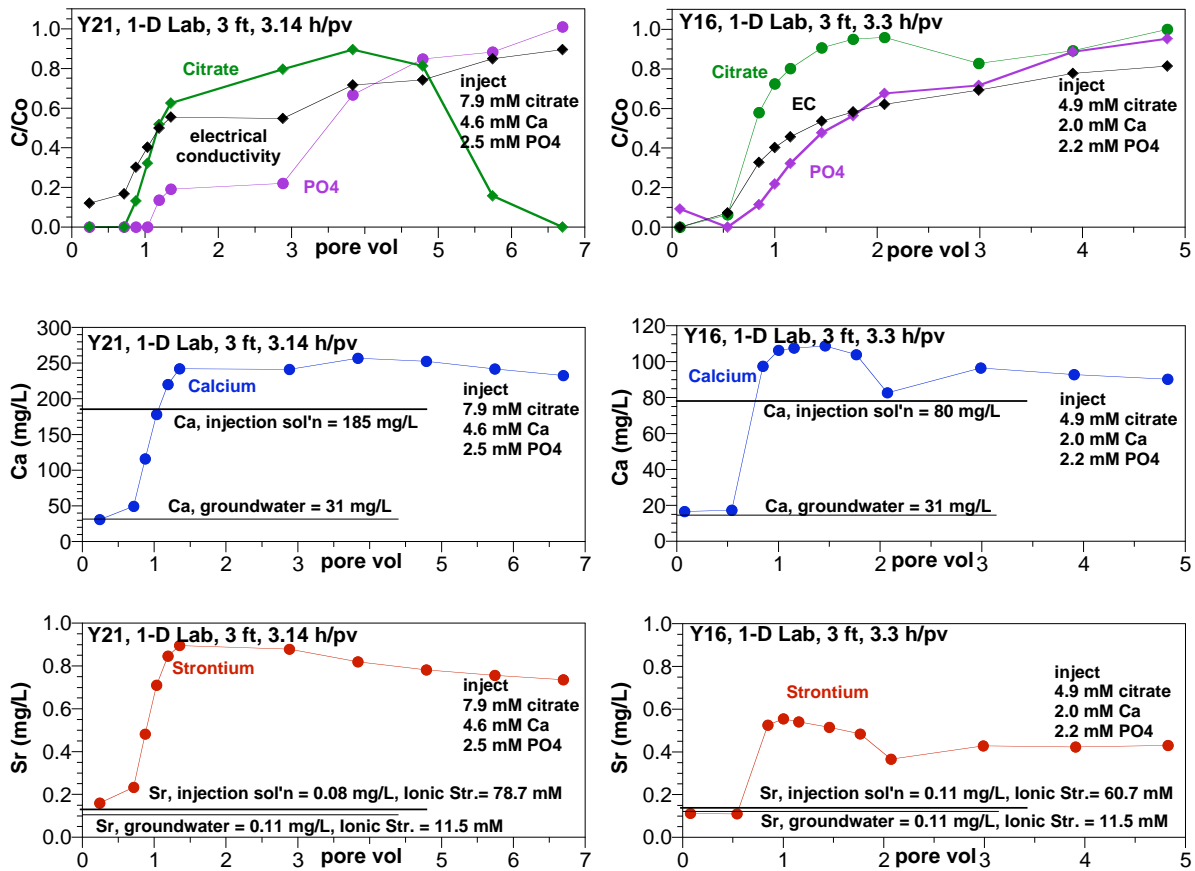


Figure 5.21. Injection of 4.6 mM Ca, 7.9 mM citrate, 2.5 mM PO₄ (experiment Y21 in a, c, e), and 2 mM Ca, 5 mM citrate, and 2.2 mM PO₄ (experiment Y16 in b, d, f).

The peaking Ca and Sr behavior (Figure 5.21, 5-22 and previous higher concentration injections Figures 5.15 and 5.16) shows expected ion exchange behavior where injection of a higher ionic strength solution desorbs more Ca and Sr (and Sr-90) from the sediment ion exchange sites. Both the peak Sr or Ca concentration and final concentration can be predicted from the solution composition, as shown in Figure 5.22 and Figure 5.23. These relationships between ionic strength of the solution and peak or equilibrium Ca or Sr concentration are only valid if the same type of solution composition is used. In this series of experiments, the phosphate concentration remained relatively constant at 2.4 mM, and the Ca and citrate

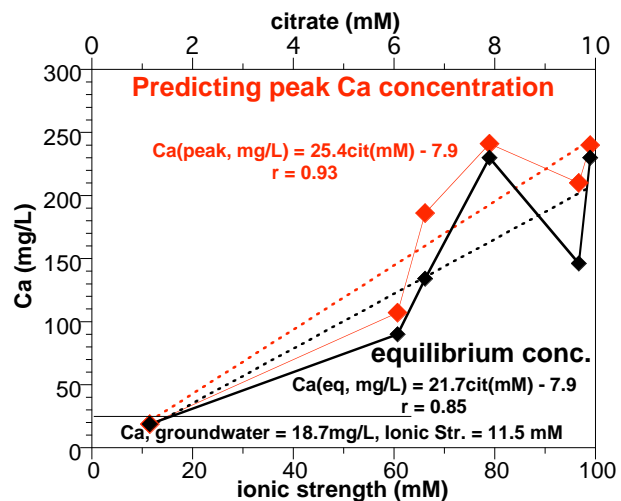


Figure 5.22. Ca breakthrough behavior prediction from the ionic strength of the Ca-citrate-PO₄ composition.

concentration was altered, which is valid for field injection #2, in which 2.0 mM Ca, 5 mM citrate, and 2.4 mM PO₄ was injected (see Table 3.1 for complete composition of field injection #2, and Section 5.3.2). For these field injections #3 to #10, different proportions of components were used (i.e., mainly less Ca-citrate and greater PO₄). The final Sr concentration prediction (Figure 5.23b) between Ca and Sr shows a 1:1 relationship (i.e., Sr behavior is the same as Ca behavior), with the exception of site saturation (CEC sites are 77% Ca saturated, whereas sites are only 2.4% Sr saturated).

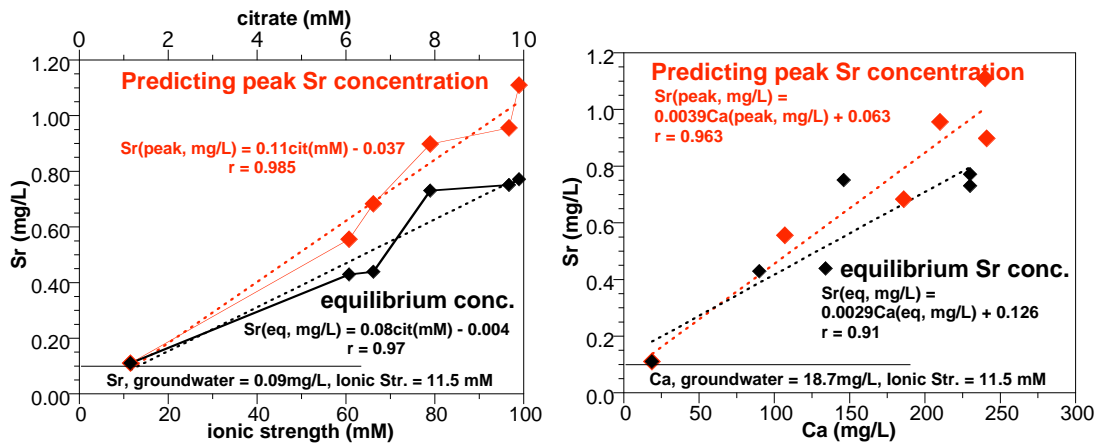


Figure 5.23. Sr breakthrough behavior prediction from the ionic strength of the Ca-citrate-PO₄ composition or calcium concentration.

A more comprehensive approach for predicting ion exchange behavior is being investigated in the EM-22 funded apatite infiltration project in which simulation of all of the ion exchange (and other reactions) are included. In conjunction with these column experimental data, then prediction of peaking behavior and mass balance of Sr-90 on surfaces and in solution can be made. The modeling progress to date is described in Section 5.7.8.

5.3.2 Stability of Field #2 Tanker Solutions

Following is the recipe for the low concentration apatite injection solution for the second pilot-scale field test (Tables 5.12 and 5.13):

Table 5.12. Concentration of chemicals needed for field injection #2.

5.0 mM trisodium citrate [$\text{HOC}(\text{COONa})(\text{CH}_2\text{COONa})_2 \cdot 2\text{H}_2\text{O}$] fw 294.1 g/mol

- granular is more soluble than powdered
- reagent grade (quality) for the citrate: USP/FCC
(lower grades contain up to 5 ppm heavy metals)

2.0 mM calcium chloride, [$\text{CaCl}_2 \cdot 2\text{H}_2\text{O}$], fw 147.02 g/mol

- reagent grade (quality): certified ACS
(lower grades can contain 20 ppm lead)

2.4 mM diammonium phosphate [$(\text{NH}_4)_2 \text{HPO}_4$] fw 132.1 g/mol

- (also called ammonium phosphate dibasic)
- pH 8.0 ± 0.1
- reagent grade (> 98%)

1.0 mM sodium bromide (tracer, 80 mg/L Br⁻ or 103 mg/L NaBr, fw 103 g/mol)

At these molar concentrations, a 60,000 gal injection volume would consist of the following dry chemical weights:

Table 5.13. Mass of chemicals needed for field injection #2.

Mix #1: (Ca/citrate)

735 lbs of trisodium citrate
147 lbs of calcium chloride

Mix #2: (PO_4/Br)

158 lbs of diammonium phosphate
51 lbs of sodium bromide

Because we are relying on microbial degradation of the citrate for apatite formation to occur, make up water for these solutions should not contain residual chlorine or any other form of bactericide.

Solution Stability Concerns. Solubility limits for each of the apatite solution components, based on laboratory evaluation and relevant solubility limits reported in the literature, are provided in Table 5.14. Maximum delivery concentrations will be maintained below these limits to avoid chemical precipitation during transport (suggested maximums listed table). Mix 2 volumes will need to be larger to stay with the operational range of the injection and process monitoring equipment. Based on preliminary discussions with the vendor, the preferred approach would be to use a three chambered tanker trailer and ship both Mix #1 and Mix #2 as a 2,500-gal solution.

Table 5.14. Solution Stability Criteria for 60,000 gallon injection volume in injection #2.

Apatite Solution Components	Max Conc. (mM)	Suggested maximum conc. (mM)	Dry Chemical Weights (lbs)	Min Tanker Volume (gal)
trisodium citrate	140	100	735	2143
calcium chloride	56	40	147	2143
diammonium phosphate	960	480	158	150
sodium bromide	400	200	51	150

Another stability concern is the potential for biodegradation of the citrate solution during transport. Solution #1 (trisodium citrate and calcium chloride) should be mixed up by completely dissolving the trisodium citrate first, then adding the calcium chloride. Potential mitigation approaches include, but are not limited to, steam cleaning or some other sterilization approach of dissolving/mixing equipment, using distilled make-up water, filter sterilization (0.2 micron) of make-up water, UV sterilization of make-up water, and chilling the solution for transport. The approach should follow industry standards for citrate solution transport that assures the citrate solution will not be appreciably degraded during transport or during the 48 to 54 hrs it takes to inject the solution.

Samples containing typical monitoring well injected (or degraded) components were used to determine what preservative for the organic acids would be used. Results from citrate analysis for field injection #1 showed significant degradation for samples analyzed weeks after the experiment, as opposed to laboratory experiment examples were not preserved, but refrigerated and all analyzed within 48 h of taking the sample. This short turn around time is generally not possible for field experiments in which 100s of samples are taken. Field (and laboratory) samples taken for citrate/formate analysis are also filtered (0.22 μm), but additional measures are needed to prevent microbial degradation of the organic acids. Bactericides gluteraldehyde, sodium azide, and 2-bromoethanesulfonic acid were spiked in a test calibration stuck containing citrate, formate (citrate degradation product), bromide, and phosphate (Table 5.15). Results showed that the gluteraldehyde interfered significantly with phosphate analysis (not a problem, as separate samples with preservative for the citrate sample), but prevented formate analysis (problem). The 2-bromoethanesulfonic acid also interfered with formate analysis. The sodium azide, however, did not interfere with citrate or formate analysis. Another preservative method that has been used in other microbial studies was to freeze samples in the field (with liquid nitrogen) to prevent any microbial degradation of the organic acids, then thawing out samples right before analysis.

Table 5.15. Bactericide addition and analytical interference for injection #2 samples.

Solution Type	Formate ug/ml	Bromide ug/ml	Phosphate ug/ml	Citrate ug/ml
Calibration Stock-1 (CS-1)	101	87.6	138	116
CS-1 + 100 ul of 25% gluteraldehyde	ND	70.2	929	109
Recovery (%)	NA	80.2	671	93.6
Calibration Stock-2 (CS-2)	105	87.2	139	123
CS-2 + 100 ul of 0.1% sodium azide	102	ND	136	114
Recovery (%)	96.8	NA	97.8	92.7
Calibration Stock-3 (CS-3)	104	89.4	141	120
CS-3 + 0.0063g 2-bromoethanesulfonic acid	184	ND	137	120
Recovery (%)	177	NA	97.3	100

ND indicates that an interference prevented the measurement of the analyte
NA indicates not applicable

5.3.3 Field #2: Electrical Conductivity versus Concentration

The relationship between solution concentration and electrical conductivity for the separate tanker trucks (i.e., separate solutions #1 and #2) and the combined injection solution was revised to reflect the revised Ca-citrate-PO₄ composition. The composition of solution #1 (Ca-citrate) was unchanged from injection #1, so the concentration versus electrical conductivity (Figure 5.24a) was the same (not remeasured). Solution #2 was changed significantly with the injection of only ammonium phosphate and NaBr instead of a mixture of Na and NH₄ phosphates (Figure 5.24b).

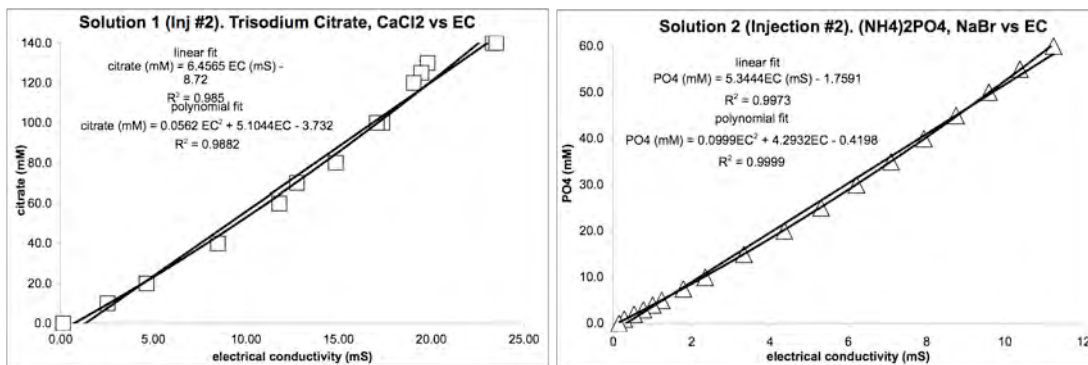


Figure 5.24. Electrical conductivity versus concentration measurements for field injection #2: a) solution #1, Ca-citrate, and b) solution #2, PO₄.

The combined Ca-citrate-PO₄ solution for injection #2 electrical conductivity at different concentration (Figure 5.25) assumes a 1:1 mixture of solutions #1 and #2, so as with injection #1, measurement of electrical conductivity alone of the combined solution does not mean the proportions of the chemical are correct. Additional PO₄ measurement is needed. Due to the problems with Hach method 8114 (interference with citrate), a different PO₄ measurement method (older method Hach 8178, amino acid) was used, as described in the following section.

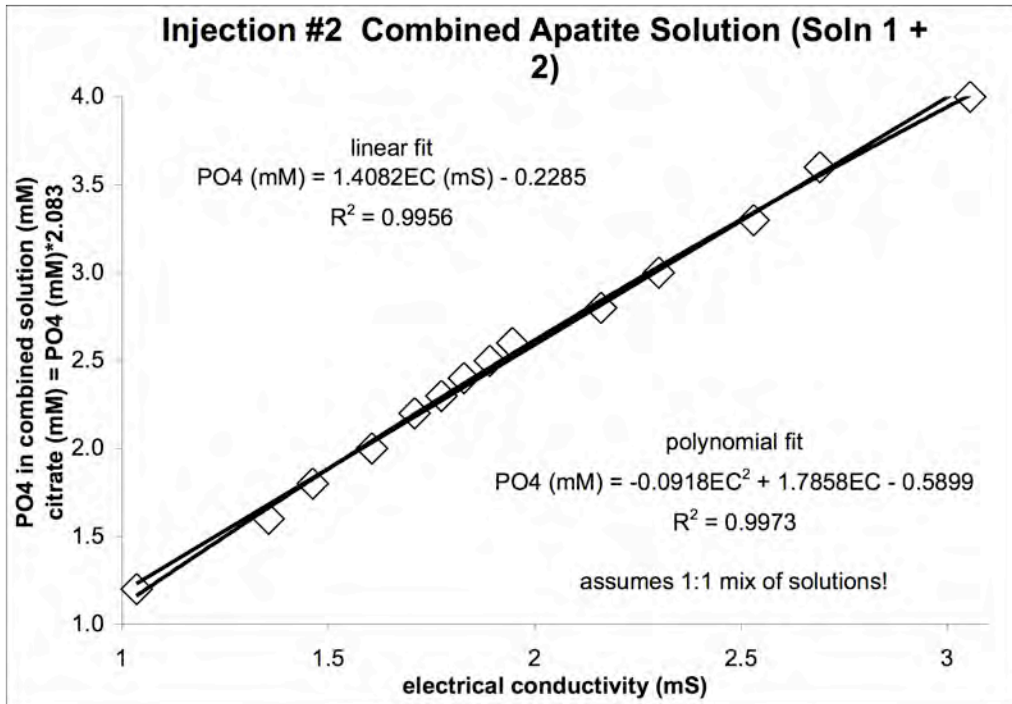


Figure 5.25. Electrical conductivity versus Ca-citrate-PO₄ concentration relationship for field injection #2 solution, assuming a 1:1 mixture of solutions #1 and #2.

The procedure developed to determine the composition of field #2 injection is the following (different calculation compared with field injection #1):

1. measure PO₄ by Hach 8178 (mM, see Section 5.3.4)
2. calculate what the EC should be from $EC_{calculated} = [PO_4(mM) + 0.2285]/1.41$ and calculate what the citrate concentration should be $calculatedCitrate(mM) = [PO_4(mM)*2.083]$
3. measure the EC of the mixed solution (called EC_{measured})
4. calculate $\Delta EC = EC_{measured} - EC_{calculated}$ (+ value = additional citrate in mix, - value = less citrate in mix)
5. calculate how much citrate is off
 $\Delta Citrate(mM) = 2.938(\Delta EC) - 0.476$
 (note that the + or - for ΔEC needs to be included in the following:
 final citrate citrate (mM) = calculated citrate + $\Delta Citrate$ (mM))

5.3.4 Field #2: Phosphate Measurement (Hach 8178) and Citrate Interference

A second method for measuring phosphate (Hach 8178) was investigated because of the interference of citrate with the Hach 8114 method used in field injection #1 caused some problems (see Section 5.2.5). This Hach 8178 method (also called Orthophosphate or Amino Acid Method) uses a different set of reagents and has to react for 10 minutes (instead of 3 minutes for Hach 8114). The range of this Hach 8178 is slightly smaller (0 to 30 mg/L) than the previous method, but the presence of citrate at the concentrations of interest do not interfere with the phosphate analysis.

At the PO_4 injection concentration of interest (2.4 mM for field #1 and field #2), the presence of anything less than 20 mM citrate does not interfere with the analyzed PO_4 concentration (Figure 5.26), which is well within the 5-mM citrate concentration for injection #2 and 10-mM citrate concentration for injection #1. At much greater citrate concentrations, the presence of citrate results in less apparent measurement of PO_4 , possibly due to the amino acids complexing with citrate. If additional (2x) amino acid reagents are added to a solution of 2.4 mM PO_4 and 80 mM citrate, then the PO_4 measurement is 97%, indicating there was insufficient reagents without adding excess (i.e., which is presumed to be caused by complexation with the citrate).

For field injections #3 to #10, the Ca-citrate- PO_4 mixture (1 mM, 2.5 mM, 10 mM) would be accurately measured with this Hach 8178 method. The solution would need to be diluted to be in the range of this method, so the resulting citrate concentration would be proportionally lower than in field injection #1 and #2.

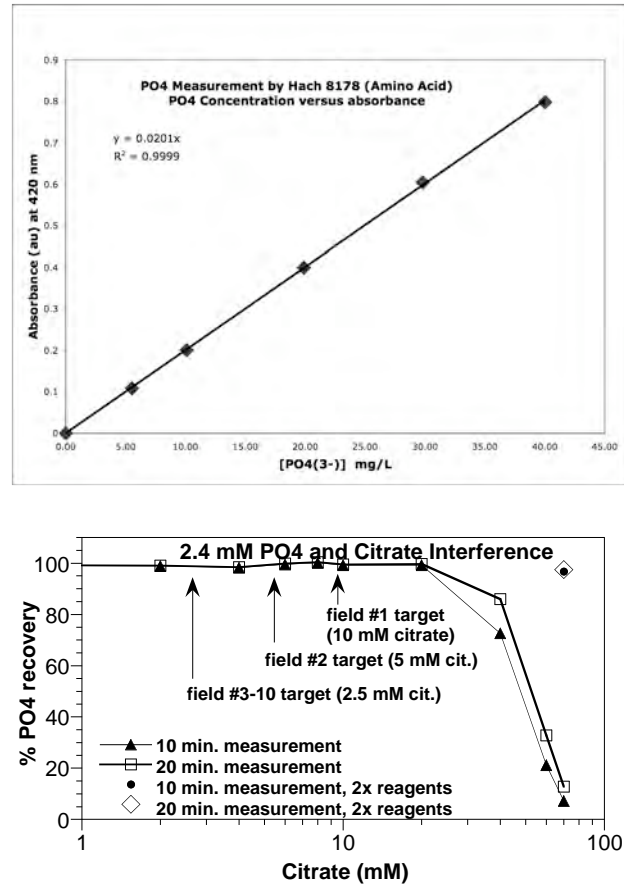


Figure 5.26. Hach 8178 PO_4 analysis (amino acid) of UV absorbance at 530 nm: a) without citrate present, b) with citrate present showing significant interference.

5.4 Laboratory Support Experiments for Field Injection #3 to #18

Field injection #1 had an initial Sr-90 increase of 10.5x (range 0 to 25x), the average of which was predicted from Sr and Ca peaking breakthrough in laboratory experiments (10x to 11x increase relative to groundwater). Field injection #2 had an initial Sr-90 increase of 3.3x (range 0 to 6.2x), which was slightly smaller than predicted from laboratory experiments (4.5x to 6x). Calculations of the mass of apatite needed to lower the Sr-90 concentration (Table 2.1) show that additional PO₄ needs to be injected, so the objective of laboratory experiments before field injection #3 was to alter the injection formulation to maintain <6x increase in Sr-90 concentration, but inject a greater mass of PO₄. Two different approaches were considered: a) increasing the PO₄ and decreasing the Ca-citrate (following Section 5.4.1), and b) injecting PO₄ only (described in Section 5.6.2).

5.4.1 Laboratory 1-D Column Transport Experiments

Two long-term 1-D column experiments (1-meter length) were conducted to assess the injection of greater relative mass of PO₄ and less mass of Ca and citrate. In previous experiments, the objective of the column experiment was to quantify the initial peak concentration of Ca and Sr (to predict Sr-90 peak in the field), and quantify the relative breakthrough location of PO₄, Ca, Sr, citrate, and electrical conductivity. Phosphate breakthrough lags relative to other components, so additional solution needs to be injected at the field scale to achieve some PO₄ mass to a 20-ft radius. To meet those objectives, injection of ~5 pore volumes of the Ca-citrate-PO₄ solution over the time scale of 24 h was sufficient. Additional objectives for the 1-D column experiments in this study are: a) assess the change in Sr and Ca groundwater concentration for 30 days after the injection, and b) assess PO₄ precipitate mass by conducting mass balance on the PO₄ breakthrough curve. To meet these additional objectives, the 1-D column experiments became slightly more complicated, with injectate and flow rate approximating what occurs in the field: a) injection of ~5 pore volumes of the Ca-citrate-PO₄ solution for 24 h relatively rapidly (5.5 h/pore volume), then b) slow injection of groundwater for 30 days (approximating groundwater flow into the treatment zone after the injection is over, 300 h to 600 h/pore volume). To obtain better mass balance on the phosphate, additional groundwater was injected at a rapid (5.5 h/pore volume) for an additional 6 pore volumes after the 30 days of slow groundwater flow (this does not approximate any field conditions), is only conducted to obtain phosphate breakthrough curve mass balance.

Two long-term 1-D column experiments (1-meter length) were conducted at differing Ca-citrate concentrations to assess cation (Ca, Sr, Sr-90) initial mobility, cation and anion retardation (mainly PO₄), and PO₄ mass balance. In the first experiment, 1 mM Ca, 2.5 mM citrate, and 5 mM PO₄ was injected (experiment Y87), and in the second experiment 1 mM Ca, 2.5 mM citrate, and 10 mM PO₄ was injected (experiment Y88). In the first experiment, breakthrough of Ca, Sr, and Na were essentially unretarded (Figure 5.27 b, c), with Sr peak (24 h) at 4.2x groundwater and Ca peak (24 h) at 3.7x groundwater. The Na peak was 11x groundwater. Because the injection formula was designed as a divalent cation-poor solution, as apatite/ other PO₄ precipitation occurred, divalent cations present (i.e., both injected and removed from sediment surfaces by ion exchange, Ca, Sr, Sr-90, Mg) would be removed. After 30 days, the aqueous Sr concentration was 0.63x of groundwater and Ca 0.73x groundwater. The phosphate injection breakthrough curve showed partial breakthrough (peak at 60% of injected concentration) with a retardation factor of 1.3. Overall PO₄ mass balance after 32 days showed that 43% of the injected PO₄ precipitated.

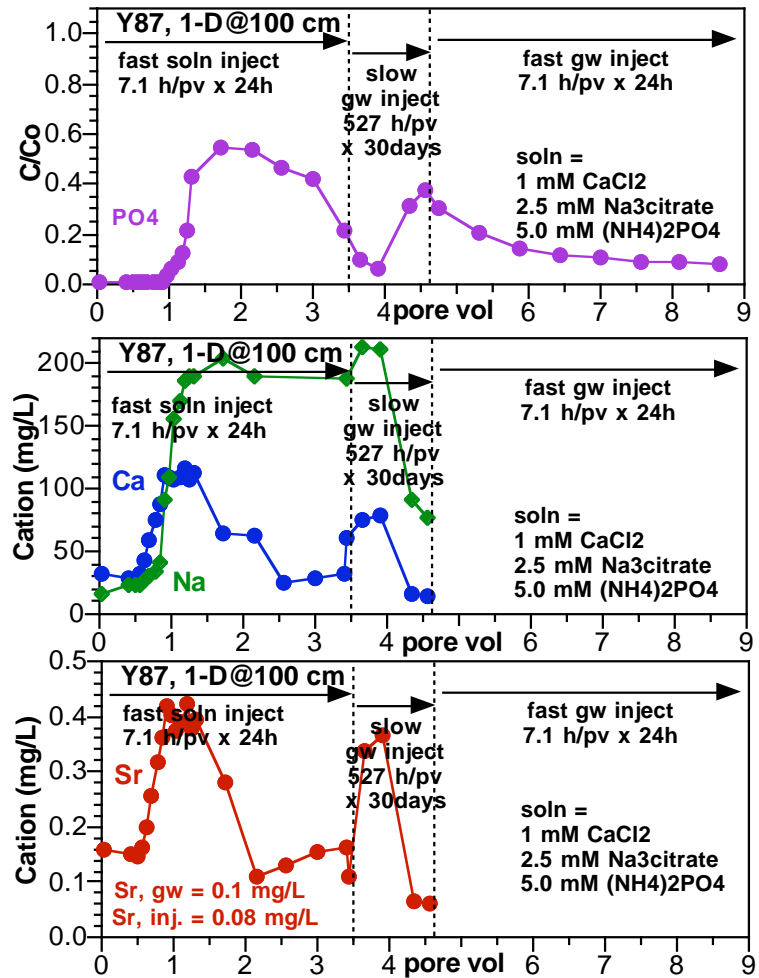


Figure 5.27. 1-meter long 1-D column experiment (Y87) with the injection of 1 mM Ca, 2.5 mM citrate, and 5 mM PO₄ with results of: a) PO₄ breakthrough, b) Ca, Na breakthrough, and c) Sr breakthrough.

The nature of the precipitate in this experiment investigated. While it is clearly established that a Ca-citrate-PO₄ solution with exact proportion forms apatite (confirmed by x-ray diffraction, EDS analysis on electron microprobe, FTIR scan, and fluorescence scan on many different samples precipitated at PNNL and SNL), mono- and di-calcium phosphate will rapidly precipitate from a solution of inorganic PO₄ and Ca (no citrate present). Because the amount of precipitate is relatively small, at present, only the electron microprobe with EDS detector could be used to determine the crystal structure of the Ca-PO₄ precipitates. This experiment will likely precipitate a combination of apatite and mono- and di-Ca-PO₄, which, over time, will recrystallize as

apatite. Natural sediment systems follow a crystallization sequence of monocalcium phosphate, dicalcium phosphate dihydrate, octacalcium phosphate, and finally hydroxyapatite (Lindsay et al. 1989; Syers and Curtin 1989).

In the second 1-meter long experiment (Y88, Figure 5.28), a total of 10 mM PO₄ was injected with 1 mM Ca and 2.5 mM citrate, so the injection solution was significantly deficient in Ca (a total of 16.7 mM needed to form apatite with 10 mM of PO₄). Solution injection in this experiment resulted in the Sr peak (24 h) at 4.7x groundwater and Ca peak (24 h) at 4.5x groundwater. By 30 days, the aqueous Sr concentration was 0.28x groundwater and Ca 0.43x groundwater. Phosphate breakthrough (Figure 5.28a) reached 76% of injection concentration with a retardation factor of 1.7. The total PO₄ mass balance at 32 days showed that 29% of the PO₄ injected precipitated in the column (0.61 g of 2.66 g injected), which was actually greater than the previous experiment (0.56 g of 1.29 g injected). The percentage precipitate is somewhat artificial; an artifact of the limited volume of the column. At the field scale, essentially all of the injected PO₄ would precipitate. This column (from experiment Y88) is currently being stored to allow further Sr sequestration by the apatite, and will be injected with a high Ca-citrate-PO₄ concentration solution at a future date. Experiment Y88 was simulated with a reactive transport code (Section 5.7.8).

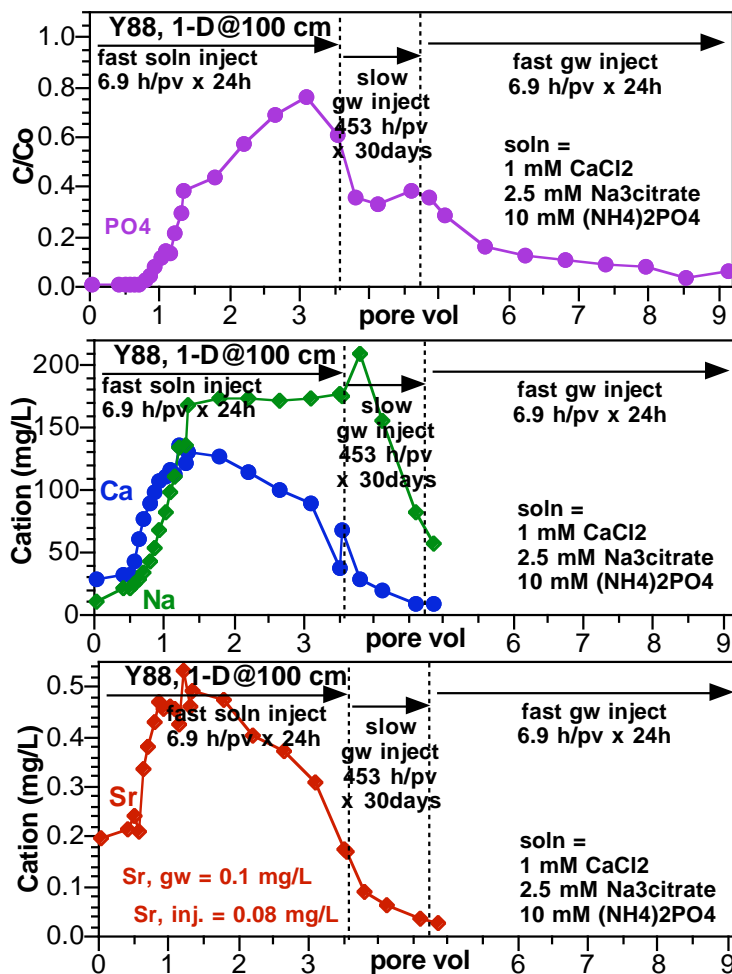


Figure 5.28. 1-meter long 1-D column experiment (Y88) with the injection of 1 mM Ca, 2.5 mM citrate, and 10 mM PO₄ with results of: a) PO₄ breakthrough, b) Ca, Na breakthrough, and c) Sr breakthrough.

5.4.2 Stability of Field #3 to #18 Tanker Solutions

The solution used for field injections #3 to #18 consisted of 1 mM Ca, 2.5 mM citrate and 10 mM PO₄. Column experiments in the previous section used ammonium phosphate (100%), but field injections used a combination of primarily (9.5 mM) Na-phosphates with a small amount (0.5 mM) of ammonium phosphate. The reason for this change in the monovalent cation

associated with the phosphate is the ion exchange affinity for ammonium being significantly stronger than sodium (a result learned from simulation of ion exchange reactions, as described in Section 5.7.8). The result is injection of predominantly Na will cause less Ca and Sr mobility compared with injecting the same concentration of NH_4 . Some NH_4 (0.5 mM) was still injected to provide an N source for microbes.

Solution Composition. Following is the recipe for the low concentration apatite injection solution for the 8 injections targeting the Ringold Formation (Table 5.16):

Table 5.16. Concentration of chemicals needed for field injection #3 to #18.

2.5 mM trisodium citrate [$\text{HO}(\text{COONa})(\text{CH}_2\text{COONa})_2 \cdot 2\text{H}_2\text{O}$] FW 294.1 g/mol

- also called sodium citrate dihydrate, ACS registry **6132-04-3**
- granular is more soluble than powdered
- reagent grade (quality) or equivalent for the citrate: USP/FCC (lower grades contain up to 5 ppm heavy metals)

1.0 mM calcium chloride, [CaCl_2], FW 110.98 g/mol

- reagent grade (quality) or equivalent: certified ACS, ACS registry **10043-52-4** (lower grades can contain 20 ppm lead)

8.1 mM disodium hydrogenphosphate [Na_2HPO_4], FW 141.96 g/mol

- also called disodium phosphate, anhydrous
- reagent grade (quality) or equivalent: certified ACS, ACS registry **7558-79-4** (lower grades can contain extra NaOH, which is only a small problem, changes pH and ionic strength)

1.4 mM sodium dihydrogenphosphate [NaH_2PO_4], FW 119.98 g/mol

- also called monosodium phosphate, anhydrous
- reagent grade or equivalent: certified ACS grade, ACS registry **7558-80-7** (lower grades can contain 8 ppm arsenic and 10 ppm heavy metals)

0.5 mM diammonium hydrogenphosphate [$(\text{NH}_4)_2\text{HPO}_4$], FW 132.1 g/mol

- also called diammonium phosphate
- granular is more soluble than powdered
- reagent grade (quality) or equivalent: certified ACS, ACS registry **7783-28-0**

1.0 mM sodium bromide [NaBr], FW 102.90 g/mol

- reagent grade (quality) or equivalent: certified ACS, ACS registry **7647-15-6**

At these molar concentrations, a 140,000 gal injection volume would consist of the following dry chemical weights (Table 5.17):

Table 5.17. Mass of chemicals needed for field injection #3 to #10.

Mix #1: Ca/citrate in deionized water

- 857 lbs of trisodium citrate dihydrate
- 129 lbs of calcium chloride, anhydrous

Mix #2: PO₄/Br in deionized water

- 1341 lbs of disodium phosphate, anhydrous
- 196 lbs of monosodium phosphate, anhydrous
- 77 lbs of diammonium phosphate
- 120 lbs of sodium bromide

Solution Stability Concerns. Because we are relying on microbial degradation of the citrate for apatite formation to occur, make up water for these solutions should not contain residual chlorine or any other form of bactericide. Solubility limits for each of the apatite solution components, based on laboratory evaluation and relevant solubility limits reported in the literature, are provided in Table 5.18. Maximum delivery concentrations (and associated minimum tanker volume) shall be maintained within these limits to avoid chemical precipitation during transport.

Mix #1 (trisodium citrate and calcium chloride) should be mixed up by completely dissolving the trisodium citrate first, then adding the calcium chloride. When making up Mix #2, disodium hydrogenphosphate, (FW 141.96) is soluble in 8 parts of water and hence should be added first in, at a minimum, 8 times the volume of water to mass of chemical used. Next diammonium hydrogenphosphate should be added (solubility 1g/1.7 mL water) followed by sodium bromide (1g/1.1 mL water) and finally sodium dihydrogenphosphate, which is freely soluble. The criteria provided in Table 5.18 will result in a solution that is stable at both room temperature and 5°C for >3 days (this solution is thermodynamically stable and should not form a precipitate).

Table 5.18. Solution stability criteria for 140,000 gallon field injection #3 to #10.

Apatite Solution Components	Max Conc. (mM)	Dry Chemical Weights (lbs)	Min Tanker Volume (gal)
trisodium citrate dihydrate	120	857	2920
calcium chloride, anhydrous	48	129	2920
diammonium phosphate	32	77	2150
sodium bromide	65	120	2150
disodium phosphate, anhydrous	526	1341	2150
monosodium phosphate, anhydrous	91	196	2150

Another stability concern is the potential for biodegradation of the citrate solution during transport. Potential mitigation approaches include, but are not limited to, steam cleaning or some other sterilization approach of dissolving/mixing equipment, using distilled make-up water, filter sterilization (0.2 micron) of make-up water, UV sterilization of make-up water, and chilling the solution for transport. The approach should follow industry standards for citrate solution transport that assures the citrate solution will not be appreciably degraded during transport or during the 48 to 60 hrs it takes to inject the solution.

5.4.3 Field #3 to #18: Electrical Conductivity versus Concentration

The relationship between solution concentration and electrical conductivity for solution #1 (Ca-citrate) is the same as in previous injections #1 and #2 (Figure 5.29a; i.e., the composition of this solution has not changed). In contrast, the relationship between the phosphate solution and electrical conductivity is different from previous injections (Figure 5.29b).

The relationship between the mixed apatite solution (i.e., combined solution #1 and solution #2) was refined in this case to be the same as occurs at the field scale. About 90% river water was used as makeup water to mix with solution #1 (made with deionized water) and solution #2 (made with deionized water). Over a wide concentration range, the relationship was linear (Figure 5.30a). Additional electrical conductivity standards were made for the region at the expected field injection concentrations (Figure 5.30b). The desired electrical conductivity of the mix is 2.29 mS.

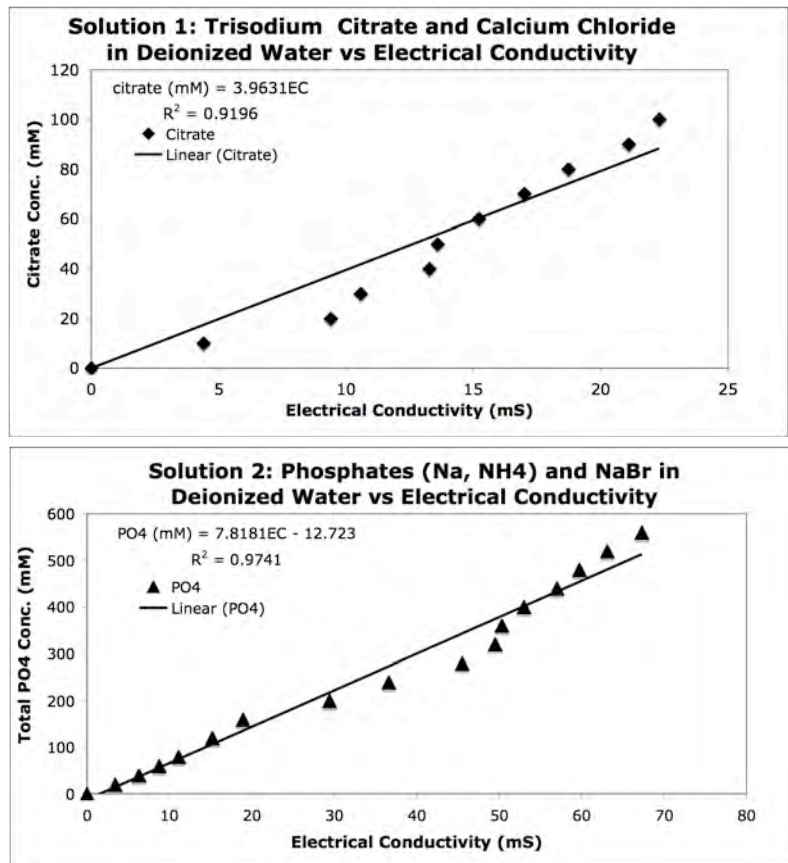


Figure 5.29. Electrical conductivity versus concentration for solution 1 (a) and solution 2 (b) for field injections #3 to #10).

Due to turbulence that occurs in the mixing skid at the field scale, it was necessary to determine how long a time period was required after chemicals were mixed that the electrical conductivity would stabilize. At the skid, solution #1, solution #2, and river water are mixed, and immediately sampled, so there is little time for the sample to stabilize. A laboratory experiment demonstrating this mixing (Figure 5.30c) showed that it can take 3 to 4 minutes for the solution electrical conductivity to equilibrate. What is likely occurring is that solution complexes [(Ca, Na, Mg-citrate) and (Ca, Na, Mg)-phosphate] require some time to reach equilibrium. The net result is while a sample can be taken seconds after the citrate and phosphate solutions are mixed, a few minutes are needed before an accurate electrical conductivity measurement can be made.

5.4.4 Field #3 to #18: Phosphate Measurement (Hach 8178)

No additional modification of field phosphate measurements were made after field injection #2, so for field injections #3 to #18, when field phosphate was measured, the Hach 8078 kit was used, as described in Section 5.3.4.

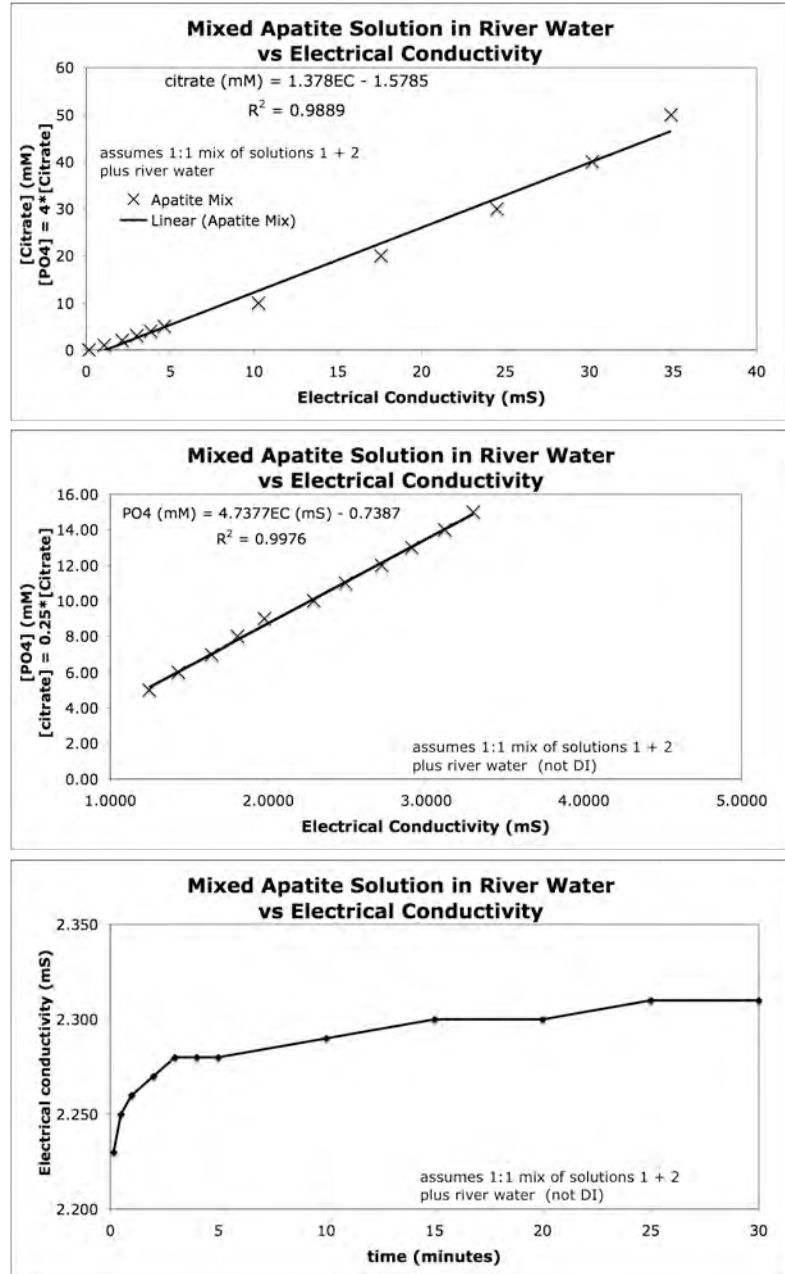


Figure 5.30. Electrical conductivity versus concentration for the combined solution #1 and solution #2 for field injections #3 to #10. Shown in (a) is a wide concentration range and (b) narrow concentration of the field injections (10 mM citrate, with desired EC = 2.29 mS).

5.5 Techniques for Measuring Apatite Precipitate in Sediment

As described in the background section 2.2, multiple techniques have been used to identify the mass of apatite precipitate that results from Ca-citrate-PO₄ injections. At the low concentrations in the first 18 injections (i.e., 2.4 mM to 10 mM PO₄ injected), the concentration of apatite that is expected to precipitate is quite small; about 10⁻⁴ g apatite/g sediment (2.4 mM PO₄ injections #1 and #2) and 4 x 10⁻⁴ g apatite/g sediment (10 mM PO₄ injections #3 to #18; see Table 2.1). Techniques have been used and are being developed on this project include: a) x-ray diffraction, b) scanning electron microscope with EDS and elemental detectors, c) acid dissolution of the sediment and phosphate measurement (i.e., aqueous PO₄ extraction), and d) fluorescence of substituted apatites. Results of these techniques are described below. Additional characterization techniques were used on the apatite precipitate to determine specific properties that included: a) BET surface area, b) FTIR scan to determine apatite crystallinity and change in crystallinity upon Sr substitution, and c) organic and inorganic carbon analysis. Some of these techniques overlap in application to determine the amount of Sr substitution in the apatite, which is described in Section 5.6.

The use of x-ray diffraction to identify the small concentrations of apatite in sediment has not been used due to the very low concentrations. X-ray diffraction is typically limited to 0.5% or above for proper identification. X-ray diffraction has been used to identify that a pure phase precipitate has the crystal structure of apatite (i.e., Figure 2.1b). The scanning electron microscope has successfully been used to identify low concentrations of apatite in sediment. The process involves taking a small sediment sample (0.5 g), encasing it in epoxy, then creating a thin section of the sediment sample, which shows both surface precipitates and crystal structure of the sediment minerals. A total of 12 thin sections were made with a range of apatite concentrations in the sediment (Table 5.19).

Table 5.19. Composition of Ca-citrate-PO₄ solutions utilized.

name	sediment (g)	apatite (g)
Y25	2.0	0.0 (none, background)
Y26	2.0	0.000033 g
Y27	2.0	0.00010 g
*this is equivalent to the 10 mM citrate injection		
Y28	2.0	0.00033 g
Y29	2.0	0.00063 g
**this is equivalent to a 70 mM citrate injection		
Y30	2.0	0.0010 g
Y31	2.0	0.0033 g
Y32	2.0	0.0

The scanning electron microprobe (SEM) can identify elements at an extremely small point (~10 micron beam width, adjustable), so to identify small amounts of apatite in sediment grains, an automated scanning routine was used. Using a beam width of 15 microns and scan time of 100 milliseconds per point, a 60 x 60 grid was scanned on each sample (i.e., 3600 points, 900 microns x 900 microns), which took approximately 12 hours. The SEM used had multiple high resolution element detectors, which were set on the elements Ca, P, Si, and Fe. The silica is used to correct for the sediment area (to exclude the area on the slide composed of epoxy). One example (Figure 5.31) shows the electron backscatter (brighter color for more dense material; epoxy is black) shows that sediment grains compose about 60% of the surface area of the slide. The Ca image (Figure 5.31b, warmer color indicates higher concentration) shows many minerals that contain calcium, whereas the P image (Figure 5.31c) shows very few mineral phases containing P. Note that some mineral phases do contain P, so the combination of P plus Ca (Figure 5.31d, in yellow) can indicate the possible presence of added apatite, but additional scans of those specific points are needed to confirm the spot is indeed added apatite.

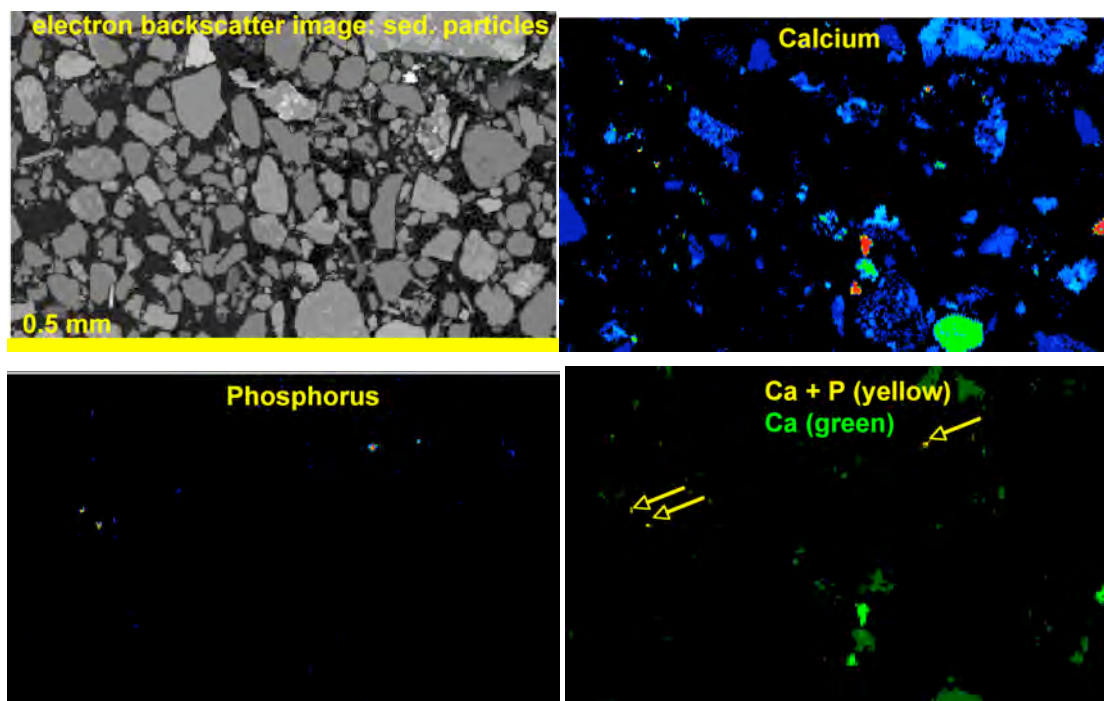


Figure 5.31. Scanning electron microprobe image of a sediment thin section containing 0.005 mg apatite/g sediment. Images are: a) electron backscatter illustrating sediment grains (grey) in the black epoxy background, b) calcium density, c) P density, and d) addition of Ca + P.

Images of the P density of three separate samples (Figure 5.32) show an increasing number of spots of phosphorus, which is likely the added apatite. Multiple spots were then revisited and scanned for a longer period of time to identify whether the spot was a sediment mineral containing P or the added apatite. For example, the large white spot in the upper left corner of the 0.16 mg apatite/g sediment image is a sediment mineral that contains P.

To illustrate the identification process, a single small P spot from one image (Figure 5.33a) was focused on at high magnification (Figure 5.33b). This electron backscatter image shows that this crystal is highly likely added apatite, as sediment grains are generally far larger. An EDS detector scan of this grain (Figure 5.33c) with peaks clearly shows that the crystal structure is apatite (pure apatite phase EDS scan in Figure 2.1d, for comparison).

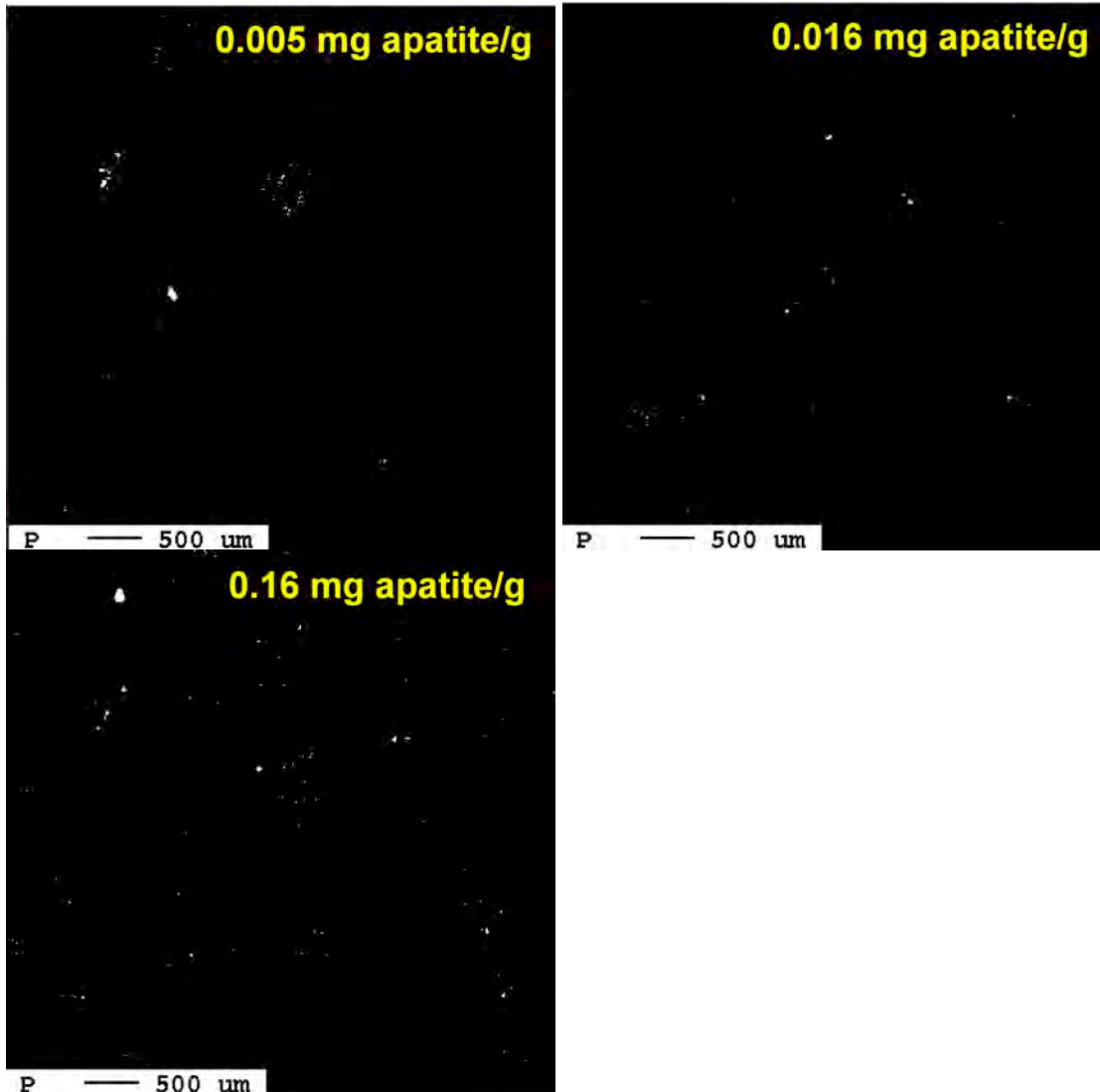


Figure 5.32. Scanning electron microprobe images of sediment samples with differing amounts of added apatite. P elemental scan shown.

While the use of the electron microprobe shows that very small concentrations of apatite can be quantitatively identified, the true cost of the process is significant, as is the time to process the samples. As such, other, simpler techniques were investigated, as a rapid and reliable method of identifying small concentrations of apatite is needed for the field-scale application.

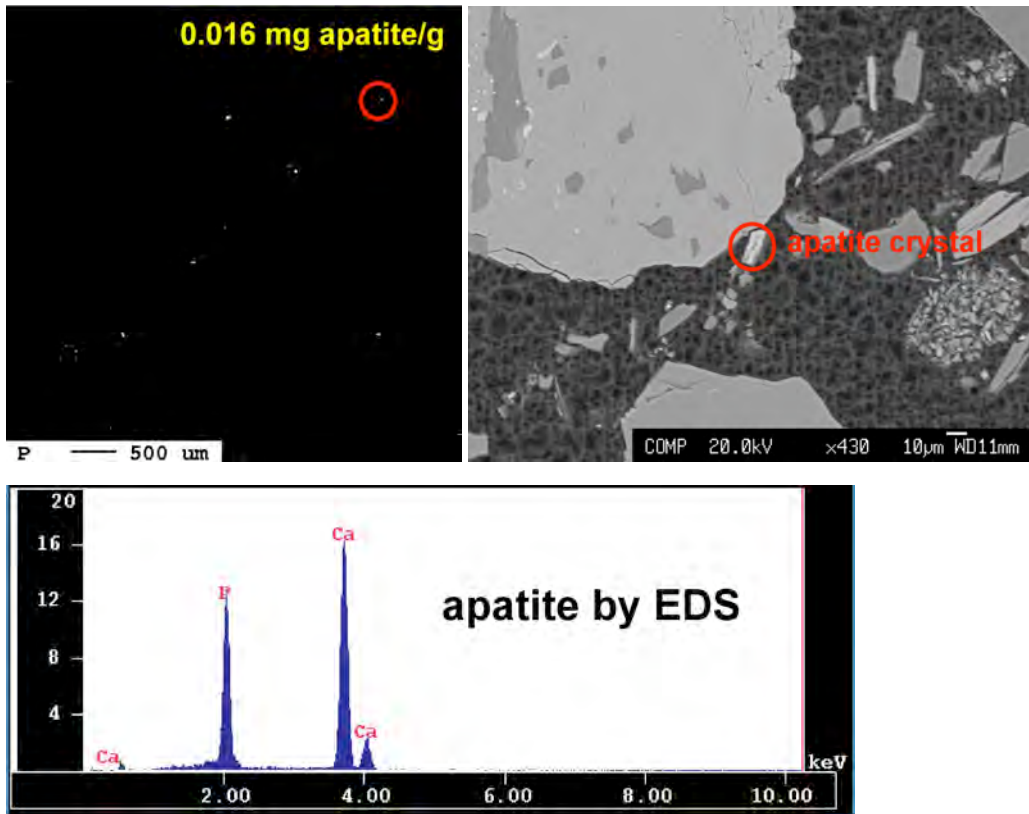


Figure 5.33. Scanning electron microscope images of a single apatite crystal.

One alternative method was aqueous measurement of phosphate, after the apatite was dissolved in acidic solution. This technique was experimented with to determine whether it can be used to measure low concentrations of apatite in the sediment. Acid dissolution of the sediment/apatite mixture will result in PO_4 from both sediment minerals and the added apatite. Because the added apatite are relatively small (sub micron) crystals, a weak acid for a limited amount of time may dissolve all the added apatite but dissolve less of the sediment mineral phase PO_4 . Initial experiments with 0.5M and 5.0 M HNO_3 (Figure 5.34) showed that even by 15 minutes, aqueous PO_4 had reached equilibrium. For the acid dissolution of the pure apatite (no sediment, Figure 5.34a), the amount recovered was equal to the predicted amount for both the 0.5M and 5M HNO_3 , so the lower acid concentration was sufficient. For the acid dissolution of the sediment (no apatite, Figure 5.34b), equilibrium took an hour for the 0.5M HNO_3 , but both acid concentrations resulted in $\sim 2 \text{ mg PO}_4/\text{g}$ of sediment (i.e., background PO_4).

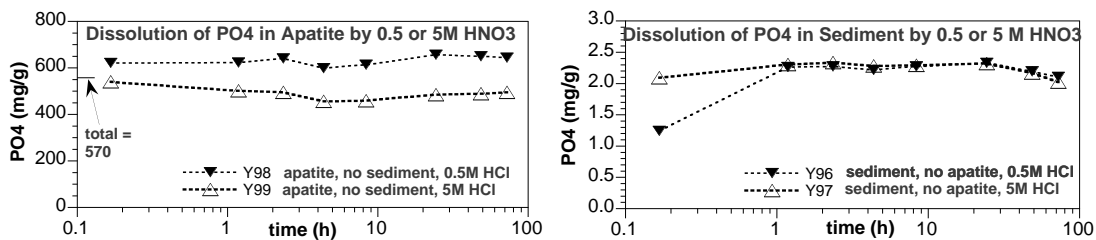


Figure 5.34. Aqueous phosphate measurement after acid dissolution of: a) apatite, b) sediment.

Initial experiments then differing concentrations of apatite added to sediment to determine how low a concentration of added apatite could be measured with this background (sediment) PO_4 . Three different apatite additions were made (1.65 mg/g sediment, 0.32 mg/g, and 0.05 mg/g). Assuming all the PO_4 from the apatite dissolved, the aqueous PO_4 (above the background PO_4 from the sediment) should increase 41%, 8%, and 1.5%, respectively. Therefore, given the variability in the background PO_4 from the sediment, the highest apatite concentration should be measured, but possibly one or both of the lower concentrations. Results (Figure 5.35) showed a significant variability in the background PO_4 (50%), which were later found to be experimental artifacts caused by whether the sediment was dried or not. Dissolution by both 0.5M and 5M HNO_3 was similar, and the time scale of <1 h was sufficient for subsequent experiments.

A second series of phosphate dissolution experiments was conducted in which 0.1M and 0.5M HNO_3 was used for only three time periods: 15 minutes, 1 h, and 24 h. In these experiments, four different apatite concentration additions were made, and the sediment only was additional analyzed. These experiments (Figure 5.36) showed a direct relationship between the measured aqueous PO_4 and the addition of apatite. This relationship held for the 0.5M HNO_3 for 15 minutes, 1 h, and 24 h. For the 0.1M HNO_3 , the amount of measured aqueous PO_4 decreased over time, probably due to the sediment buffering the pH (to be more neutral pH), so some PO_4 was then precipitating. In conclusion, both the 0.5M and 0.1M HNO_3 treatments for 15 minutes could be used to dissolve the added apatite (Figure 5.37a), where the slopes were the same (i.e.,

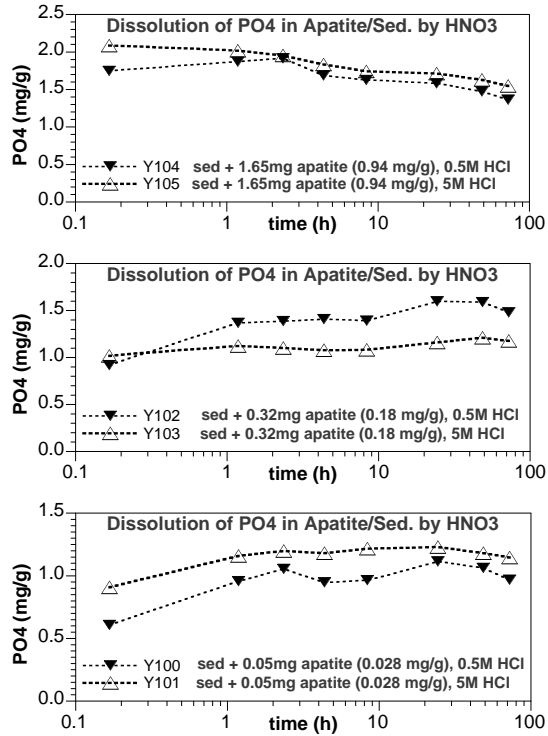


Figure 5.35. Aqueous phosphate measurement after acid dissolution of apatite/sediment mixtures: a) 1.65 mg apatite/g sediment (apatite 41% of sediment PO_4), b) 0.32 mg apatite/g sediment (apatite 8% of sediment PO_4), and c) 0.05 mg apatite/g sediment (apatite is 1.5% of sediment PO_4).

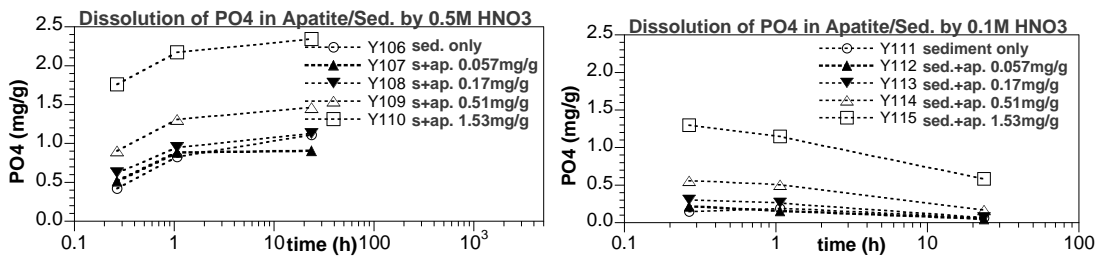


Figure 5.36. Aqueous phosphate measurement after acid dissolution of apatite/sediment mixtures with a) 0.5M HCl, and b) 0.1M HCl.

because of the same amount of addition). The intercepts (i.e., baseline PO₄ from sediment minerals dissolving) differed, with the weaker acid dissolving less of the apatite minerals, as expected, so produced a lower baseline. This apatite addition to sediment was repeated (Figure 5.37b) with similar results, namely apatite additions can be measure down to about 0.1 to 0.2 mg apatite/g of sediment. Therefore, field injections #1 and #2, which resulted in a calculated 0.1 mg apatite/g of sediment are likely not detectable, but field injections #3 to #18 (calculated 0.4 mg apatite/g sediment, Table 2.1) are likely detectable. Additional work is needed on this method, with larger samples to even out heterogeneities in the sediment, and multiple points of analysis (i.e., triplicate samples) to insure statistically accurate phosphate values.

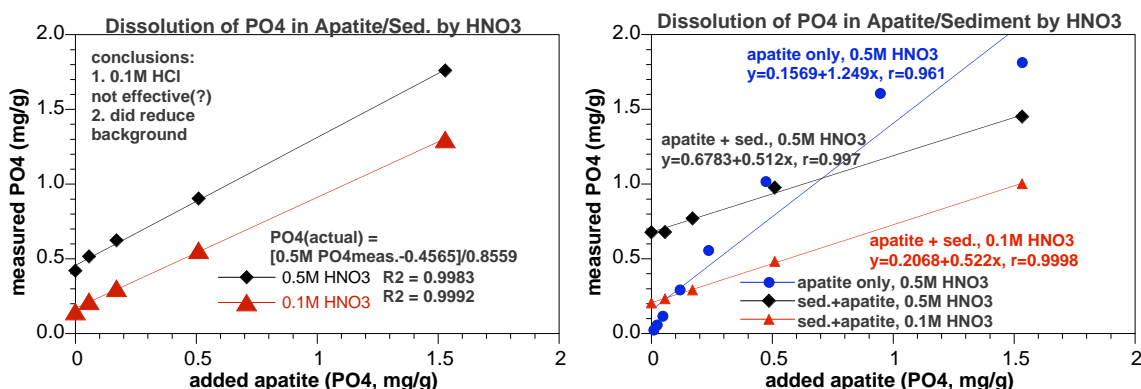


Figure 5.37. Aqueous phosphate measurement after 15-minute acid dissolution of apatite sediment mixtures using 0.1M or 0.5M HNO₃.

A third method of measuring added apatite in sediment investigated was the use of fluorescence scans. While pure hydroxyapatite does not fluoresce, apatites with F or carbonate substitution do fluoresce. Apatite precipitated in groundwater (Figure 5.38, black line) does fluoresce, and the sediment sample (no apatite added, green line) does not. This method is still in development, and how low a concentration of substituted apatite cannot be measured as yet.

A surface area measurement of the Ca-citrate-PO₄ precipitated apatite (61.5 m²/g) was somewhat greater than the Sigma apatite (52 m²/g). The inorganic carbon content of the precipitated apatite was measured at 0.02%, so in spite of high carbonate concentrations in groundwater, there appears to be little carbonate substitution into the apatite under the conditions (i.e., pH ~7.8, field injections ranged from 7.5 to 8.0). In the laboratory precipitate at very high microbial biomass concentrations (10⁹ cfu/mL), there was some incorporation of organic carbon into the apatite (i.e., 0.78% organic carbon). It is expected that field injections will not have as high a biomass concentration (certainly for the injections so far the citrate concentration was far less than

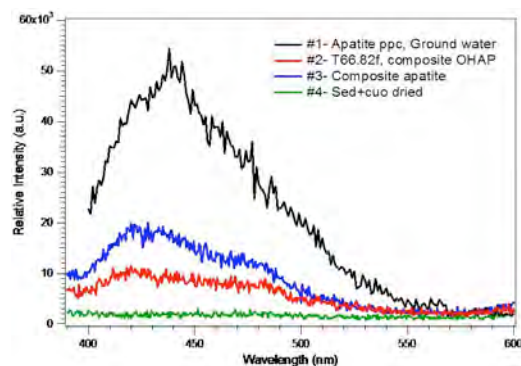


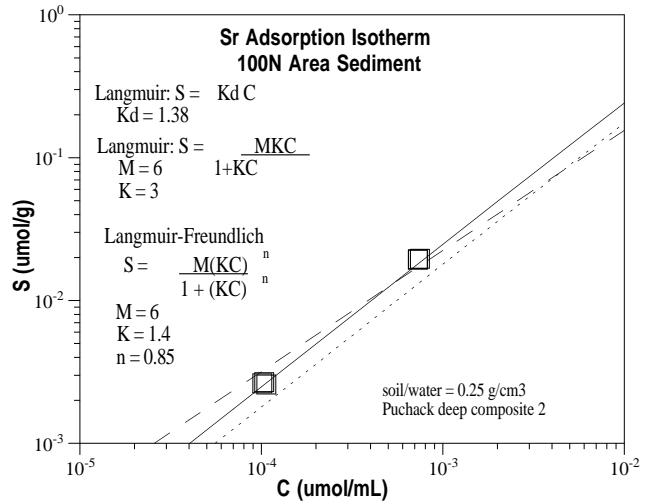
Figure 5.38. Fluorescence scans of precipitated apatite (black, blue, red), sediment with no apatite (green) showing low levels of background fluorescence from the sediment.

used in the laboratory experiments). Additional characterization of the precipitated apatite and the Sr substitution in apatite is described in Section 5.6.5. FTIR scans of the precipitated apatite showed that that over time as Sr is substituting into the apatite for Ca, the structure is still hydroxyapatite, and not secondary phases (SrPO_4 or $\text{Sr}(\text{OH})_2$).

5.6 Ca-Citrate-PO₄ Injection and the Long-Term Sr-90 Incorporation

5.6.1 Sr Ion Exchange in Sediment with Groundwater

Batch experiments were conducted to measure the Sr-90 sorption rate in untreated and Ca-citrate-PO₄ solution-treated 100-N sediments and Sr-90 sorption at differing concentration (Figure 5.39). In some experiments, Sr-85 is used (easier to count, but short half-life, so not for long-term experiment), and in other experiments Sr-90 was used (30-day wait period before it can be accurately counted, see Section 3.1.5). The starting sediment in both cases was a composite from the 10- to 42-ft depth at well N-121. The treated sediment contained approximately 0.5 g of apatite after being contacted with a Ca-citrate-PO₄ mixture (25, 50, 17.5 μM) for 3 days. This one treated sediment is referred to below as the apatite-laden sediment. To achieve a soil/water ratio near that in saturated porous media in both the untreated and apatite-laden sediments, 70 ml of Hanford groundwater containing 0.2 mg Sr/L was added to 116 g sediment. Each of these experiments was initiated by the addition of Sr-90 to achieve 45,000 pCi/L. The ionic strength in the treated sediment was approximately 0.1 M, diluted from the original Ca, PO₄, citrate treatment mixture, while that of the untreated sediment was that of the groundwater (0.011M). At specified time intervals, 0.5 mL of water was removed, filtered with a 0.45-micron PTFE filter (13-mm diameter), and placed in a scintillation vial with scintillation fluid. These samples were counted after 30 days after Sr-90/Yt-90 secular equilibrium was achieved and the Sr-90 activity was half of the total activity.



Sr-85 Sorption Isotherm on 100N Sediment

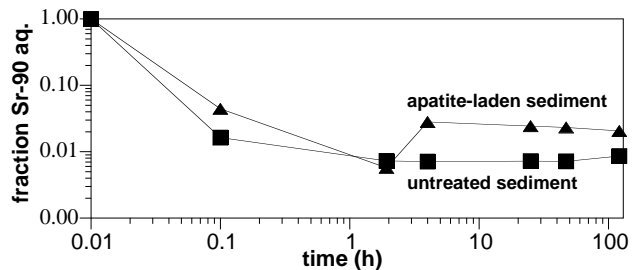
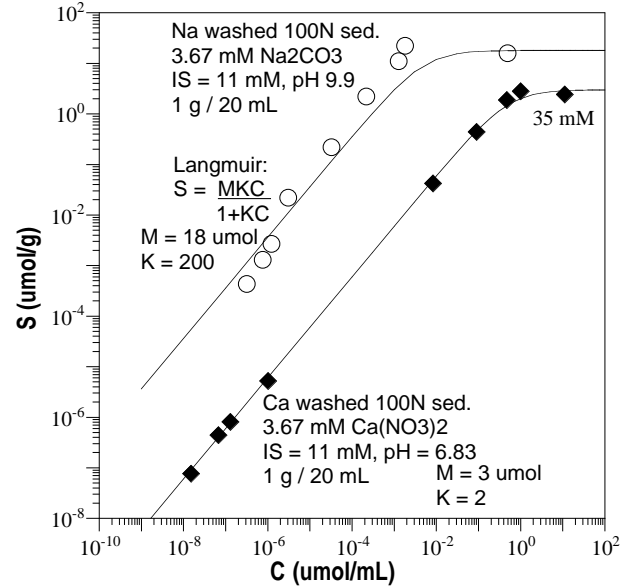


Figure 5.39. Sr-90 sorption: a) in groundwater, b) in mono- or divalent-saturated sediment, and c) time scale for Sr-90 sorption by untreated and apatite-laden 100-N composite sediment.

Sr-90 added to aqueous suspensions of untreated and treated 100-N sediments was rapidly sorbed (Figure 5.39c). The untreated sediment reached sorption equilibrium (Figure 5.39c, squares) within 2 h, giving a Sr K_d value of $24.7 \text{ cm}^3/\text{g}$. For the apatite-laden sediment that contained precipitated apatite, there was initial rapid uptake of Sr-90 (<1 h) that was likely sorption. In this case, the solution Sr-90 continued to decrease even after 120 h, likely due to some uptake by the apatite. Thus, we can conclude that for both the untreated and apatite treated sediment sorption is quite rapid.

The mechanism for Sr retention by sediment is ion exchange, as demonstrated in isotherm (and other) experiments. The 24-h Sr-90 sorption in groundwater (Figure 5.29a) also showed a Sr K_d value of $24.7 \text{ cm}^3/\text{g}$. In Ca-saturated sediment (black diamonds, Figure 5.29b), Sr-85 sorption over a wide range of concentration showed Langmuir behavior, indicating retention by primarily one type of site. If the slope at low Sr concentration was not equal to 1, this can indicate more than one type of surface site. Because the system is Ca-saturated (ionic strength 11 mM), both Ca and Sr compete for the same sites. In a Na-saturated sediment, 24-h Sr sorption isotherm (open circles, Figure 5.29b) showed similar Langmuir behavior, but with ~600x greater retention of Sr due to it more easily displacing Na from ion exchange sites. In typical groundwater, the molar ratio of Ca/Sr is 220x to 400x, so this 600x greater retention simply reflects the divalent Sr displacing the monovalent Na on surface sites.

Small 1-D column experiments were conducted to measure the amount of Sr-90 mobilized by injection of a Ca-citrate- PO_4 solution relative to Hanford groundwater. Previous batch studies show that Sr (and Sr-90) $K_d = 25 \text{ cm}^3/\text{g}$ in Hanford groundwater (<4 mm size fraction of 100-N composite sediment). For a baseline of Sr behavior in sediments, two 1-D columns in which Sr-85 was added to the sediment and allowed to equilibrate for several days, injection of Hanford groundwater resulted in a K_d of 11.8 and $9.1 \text{ cm}^3/\text{g}$ (i.e., $R_f = 61$ and 47.6 , respectively, Figure 5.40), or slightly lower than shown in the previous batch studies (Figure 5.39).

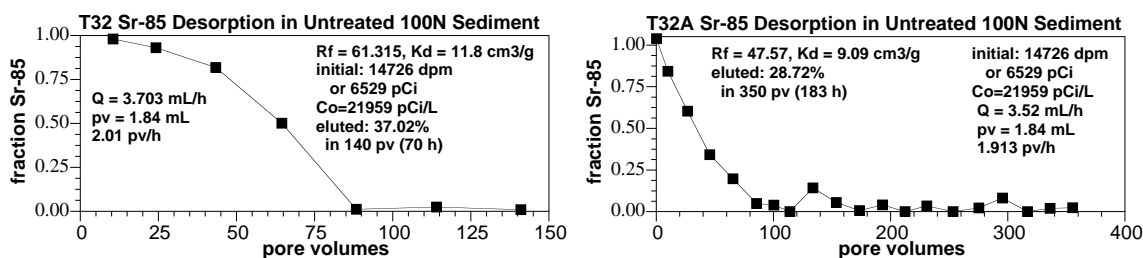


Figure 5.40. Sr-85 desorption in a 1-D column with Hanford groundwater injection.

In these experiments, a total of 140 and 350 pore volumes of Hanford groundwater were flushed through the columns. Over that amount of flushing, 37% and 29% of the Sr-85 was eluded. These results are applicable to the field, as the “flushing” with groundwater is simply exchanging the Sr-85/Sr on the sediment surface sites with Sr in groundwater. In general, the system is at equilibrium at all times, as there is no change in the mixture of cations (Ca, Na, K, Sr) and anions (CO_3 , Cl, SO_4), and we assume the sediment was initially in equilibrium with groundwater.

Sr sorption to apatite-laden sediment was less than the untreated sediment, primarily due to the higher ionic strength of the injection solution. For the apatite-laden sediment, the apparent K_d at 120 h was $7.6 \text{ cm}^3/\text{g}$, which was smaller than the untreated sediment due to the higher solution ionic strength (described in detail in the following section). This was not unexpected because Sr-90 retention in Hanford 100-N sediments was primarily due to ion exchange (Serne and LeGore 1995). In a study of the influence of major ions on Sr retention by Hanford sediments, Routson et al. (1981) reported a Sr K_d of $49 \text{ cm}^3/\text{g}$ (0.001M NaNO_3) and K_d of $16 \text{ cm}^3/\text{g}$ (0.1M NaNO_3), so there was a 3x decrease in the K_d value by increasing the ionic strength with Na^+ (which was the predominant cation in the treated sediment after dilution with Hanford groundwater). In general, Sr^{2+} retention by ion exchange is controlled to a large extent by divalent cation (primarily Ca^{2+} and Mg^{2+}) concentration, as shown by a similar change in Ca^{2+} ionic strength (0.001 to 0.1) which resulted in a 38x decrease in the Sr K_d value from $25 \text{ cm}^3/\text{g}$ (in groundwater) to $2.0 \text{ cm}^3/\text{g}$ (Ca-citrate- PO_4 at 40 mM, 100 mM, and 24 mM). Evidence to support our contention that sorption is predominately ion exchange is provided solid phase extraction of these sediments in Sections 5.5.3 and 5.5.5.

5.6.2 Sr/Sr-90 Ion Exchange in Sediment with Ca-Citrate- PO_4 Solutions

Sr adsorption in natural groundwater and in differing ionic strength solutions showed expected ion exchange behavior. The purpose of these experiments is to measure the adsorption of strontium in natural Hanford groundwater and be able to predict how this adsorption may change with the injection of the apatite solution (Ca, Na, PO_4 , citrate). Batch experiments were conducted with the 100-D composite sediment from borehole C4473 (depths 10 ft to 42 ft) with various Sr concentrations. Sr-85 was used as the isotopic tracer. The natural Sr adsorption was measured at two different Sr concentrations. The influence of ionic strength was tested with three different solutions: a) Na_2SO_4 solutions, b) fresh apatite solution, and c) “spent” apatite solution. In each case, Sr adsorption was measured with the electrical conductivity so there would be a K_d prediction ability based on the ionic strength of the apatite solution. While these batch studies show general trends of ion exchange behavior, at the low sediment/water ratio used (1 g/15 mL), they are not representative of the exact behavior that would be observed in the field at a much higher sediment/water ratio (i.e., 1 g/0.2 mL). The reason for this difference is the influence of the mass of ions on the surface dominates the field system (at the high sediment/water ratio), whereas the mass of ions in solution dominates the lab system. For example, Sr-90 ion exchange in groundwater ($K_d = 25 \text{ cm}^3/\text{g}$) indicates the field system should have 0.3% to 0.6% of the Sr-90 in solution (99.7% on the surface), and in contrast, the laboratory system had 37% of the Sr-90 in solution (62% sorbed). With this large difference in mass, these batch studies simply cannot reflect the large ion changes in ion concentration that would occur (described in following sections in column studies).

Three batch vials at two differing Sr concentrations (no apatite solution, groundwater ionic strength) showed that the Sr K_d value in groundwater is 25.96 ± 0.89 . Sr adsorption in sodium sulfate solutions was subsequently investigated. Five different concentrations of sodium sulfate were mixed in Hanford 100-N groundwater to compare with the apatite solutions to determine if sodium concentration by itself was a good predictor of Sr adsorption. The Sr K_d decreased with increasing ionic strength (Figure 5.41), as predicted, and were comparable to previously published results. The Hanford 200 area sediment in NaNO_3 solutions (Routson et al. 1981) had

a Sr K_d value of 49 cm^3/g (0.001 M NaNO_3), 42 cm^3/g (0.015 M NaNO_3), and 16 cm^3/g (0.1 M NaNO_3), so most of the K_d decrease occurred at ionic strength greater than 0.01 mol/L.

Sr adsorption in mixtures of fresh Ca-citrate- PO_4 solutions (2 mM to 100 mM citrate) and groundwater were compared with “spent” apatite solution and the sodium sulfate solution. These results show a much more dramatic decrease in Sr K_d compared with the sodium sulfate, possibly due to aqueous Sr complexation with citrate (Figure 5.41). These K_d values would, however, be representative of Sr adsorption that would be expected in the first few weeks after an apatite injection. The K_d value decreased from 26 to 2.0 cm^3/g (13x) as the ionic strength increased from 0.005 mol/L to 0.1 mol/L. In comparison, the same increase in NaNO_3 ionic strength (Routson et al. 1981) showed a 4.1x decrease in Sr adsorption.

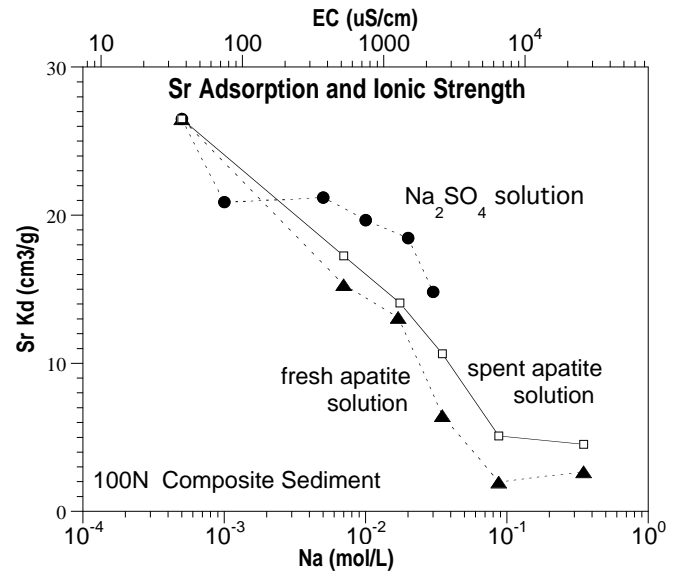


Figure 5.41. Sr-85 adsorption in batch experiments (low sediment/water ratio) at differing ionic strength.

Sr adsorption in mixtures of a 5-week old apatite solution and groundwater showed less influence on the Sr adsorption than the fresh apatite solution (Figure 5.41). The K_d value decreased from 26 to 5.1 cm^3/g (5.1x) as the ionic strength increased from 0.005 mol/L to 0.1 mol/L, which was similar to the change noted with NaNO_3 solutions (Routson et al. 1981). These experiments are more representative of the solution that will be encountered downgradient of an apatite injection.

The injection of an apatite solution will decrease adsorption of freshly adsorbed Sr from 26 cm^3/g (in groundwater) to 4.5 cm^3/g (spent apatite solution) or 2.7 (fresh apatite solution) for higher concentration Ca-citrate- PO_4 solutions. As groundwater dilutes the plume, there is less influence on the Sr adsorption. While these early batch experiments showed some desorption of Sr-85 in the higher concentration Ca-citrate- PO_4 solutions, later large-scale laboratory experiments and field studies showed considerably greater desorption. The reason these batch studies are not representative of field results is the very low sediment/water ratio used in batch experiments (with Sr-85 sorbed on the sediment) leading to significant dilution in these batch studies. At the field scale (and larger laboratory 1-D columns) with high sediment water ratios, there is significantly greater mass of Sr-90 on the sediment relative to the amount of water being injected.

The Sr ion exchange behavior (change in aqueous/solid partitioning) is also observed during 1-D column studies. Injection of a Ca-citrate- PO_4 solution caused initial peaking desorption of Sr-85 (Figure 5.42), but ultimately less Sr-85 was eluted (so some was sequestered due to the incorporation in precipitating apatite). The initial high concentration Sr-85 peak was dependent

on the Ca-citrate-PO₄ composition and concentration, which is fully described in Sections 5.2 to 5.4. There are limitations in these small experiments with the sample collection size being somewhat large relative to the size of the peak, so some of the peak shape is lost. The general nature of the breakthrough curve shape, however, is shown, with a higher concentration Sr-85 initial peak with a higher concentration injection of Ca-citrate-PO₄.

If a low concentration Ca-citrate-PO₄ (4, 10, 2.4 mM, details in Table 3.1) is injected, the Sr-85 peaked at a minimum of 3x to 4x groundwater concentration (Figure 5.42a), although later experiments in which finer sampling of this initial peak are taken (both in laboratory- and field-scale experiments), this Sr or Ca or Sr-90 peak is actually about 10x groundwater concentration. The ionic strength of this solution is 99.5 mM, compared to 11.5 for Hanford groundwater (predominantly Ca, Mg-CO₃), so the ionic strength increase of 8.6x roughly approximates the divalent cation desorption. Interestingly, both of these low concentration experiments ultimately sequestered some Sr-85 (i.e., eluted less than when groundwater was injected through the column, Figure 5.42). In both experiments, 28% to 32% less Sr-85 was eluted from the column, which was presumed caused by the Sr-85 being incorporated into apatite as it was precipitating.

If a high concentration Ca-citrate-PO₄ solution (28, 70, 17 mM) was injected into the Sr-85-laden sediment, higher initial Sr-85 desorption peak was observed. In these small columns with sample size limitations, the initial peak observed was 7.5x to 12x increase in groundwater concentration, although the actual peak height should be considerably larger (100x is estimated). In one of these experiments, 69% of the Sr-85 was sequestered (i.e., retained in the column, relative to a groundwater injection), and in the other column, all of the Sr-85 injected was eluted (i.e., less retention relative to groundwater injection). In general, conclusions that can be drawn from these small experiments are limited, and processes hypothesized were investigated in detail in other experiments. These experiments did show that Sr-85 (and Sr and Sr-90) would desorb at greater concentrations proportional to the concentration of the Ca-citrate-PO₄ injected. In addition, some Sr-85 was retained by sediments, which was presumed to be caused by the precipitation of apatite with some incorporation of the Sr-85.

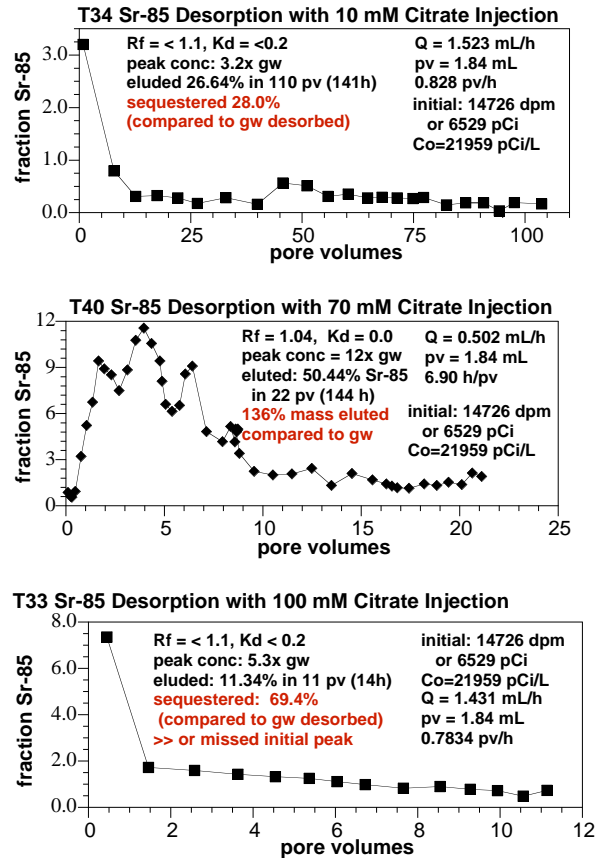


Figure 5.42. Sr-85 desorption in a 1-D column with Ca-citrate-PO₄ injection.

5.6.3 Sr Uptake on Apatite without Sediment

The sorption of Sr by crystalline citrate precipitated apatite was investigated in batch experiments to determine 1) the rate of removal of Sr naturally occurring in 100-N groundwater, and 2) how this Sr was initially bound to the apatite within the first four days of contact. Both of these objectives are important in determining the effectiveness of and modeling of Sr remediation strategies. The 100-N groundwater used contained 0.225 mg/L of Sr (2.3 μM) to which a Sr-85 tracer was added. The loss of Sr-85 from solution was measured in a series of 10 ml apatite groundwater suspensions at pH 7 and room temperature. The solid to solution ratio (r_{sw}) in these individual suspensions varied from 0.27 to 30 g/L (x100). This covers the range of estimated apatite mass required for the Sr barrier described in Section 2.3 (Table 2.1). After addition of the groundwater containing Sr and Sr-85 the individual suspensions were repetitively sampled for 100 h.

In all suspensions two distinct rate steps were obvious for the sorption process. The initial sorption of Sr was quite rapid occurring with sorption half-lives ranging from 1.3 to 5.8 minutes for the high to low solid/solution ratio, respectively (Figures 5.43 and 5.44). First order fits of the data are shown by solid lines and yielded rates of 32.2, 12.2 and 7.2 h^{-1} and intrinsic of 1.1, 5.9 and 20.6 (h g L^{-1}) for the 30, 2.1 and 0.27 g/L suspensions, respectively. Following the initial rapid sorption step, sorption continued out to 100 h (Figure 5.43b) at which point experiments were terminated. First order fits for the times >2 h (solid curves) provided rates of 0.085, 0.085 and 0.045 h^{-1} for the same three suspensions. The initial rapid removal of Sr from solution is most likely due to reaction of Sr with easily accessible exchange sites on the apatite surface, with the slower step resulting from intra particle diffusion to less accessible sites.

The fraction of Sr removed from solution is clearly dependent on the r_{sw} of the suspension with approximately 33 and 95.5 % of the Sr sorbed for the 0.27

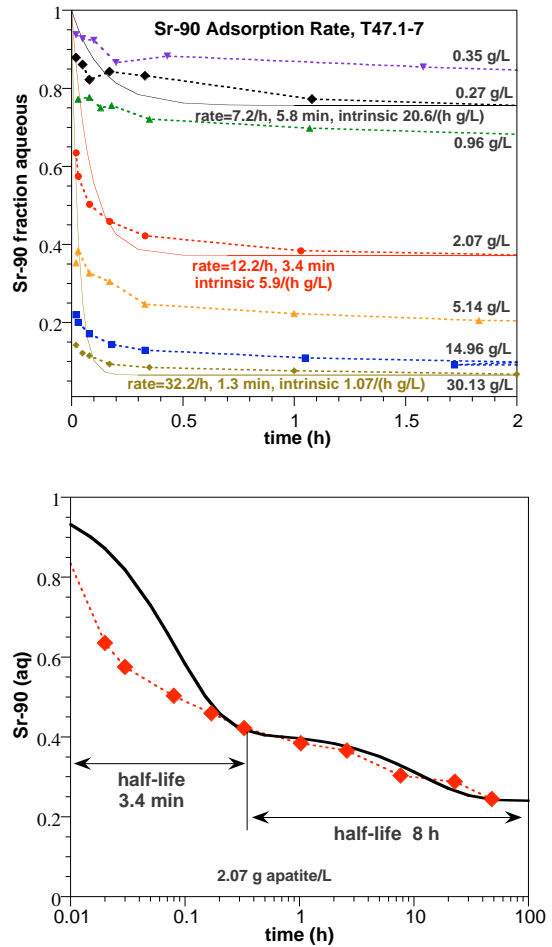


Figure 5.43. Initial rates of Sr sorption by apatite.

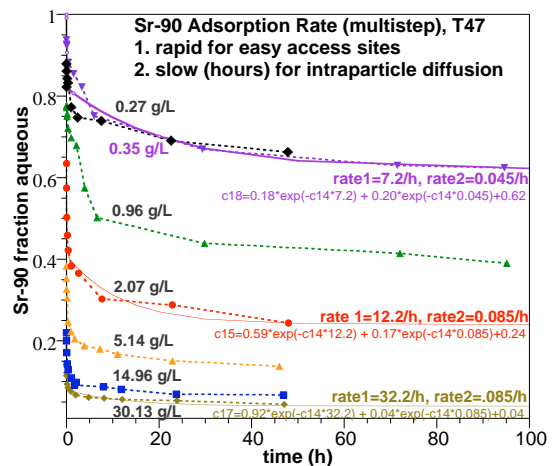


Figure 5.44. Long-term rates of Sr sorption by apatite.

and 30.1 g/L apatite suspensions. The K_d s calculated from this data after 100 h of contact show a near linear inverse dependence on the solid/solution ratio (Figure 5.45), and an average $K_d = 1370 \pm 429 \text{ cm}^3/\text{g}$. This shows that the adsorption affinity of Sr for the apatite surface is 55x stronger than the sediment (i.e., $\text{Sr } K_d(\text{apatite}) = 1370$, $K_d(\text{sed.}) = 25$). It is likely that the trend observed reflects a lack of sorption equilibrium for the higher apatite concentrations (i.e., diffusion into pores is taking longer), or reflects a small change in pH.

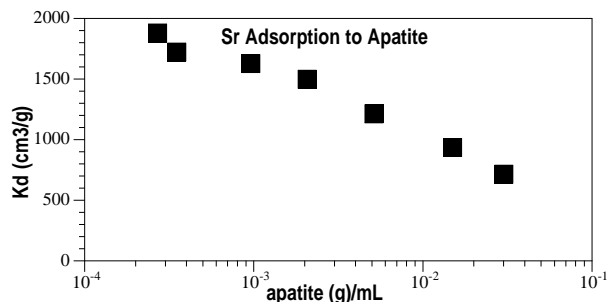


Figure 5.45. Sr sorption K_d by apatite versus mass of apatite.

Using the observed density and pore volume of 100-N sediments, the apatite soil to water ratios used in these experiments can be converted into g apatite/g sediment. That is, 30.1 and 0.27 g/L are equivalent to 3.1×10^{-3} and 2.7×10^{-5} g apatite/g sediment, respectively. This covers the range of apatite mass/g sediment targeted for field injections # 1 through #10 and 300-yr capacity barrier for Sr removal described above in Table 2.1. Based on the assumptions made in Table 2.1 this range of r_{sw} covers the quantity of apatite anticipated in field injections #1 through #10, with the maximum r_{sw} equivalent to that required for the 300-yr capacity barrier. The small variation in K_d with changes in r_{sw} , or g apatite/g sediment, suggests that the inevitable spatial variations in the precipitation of apatite in the field will not significantly effect the sorption of Sr by apatite. As a result, the K_d s and the rates of sorption derived from these experiments should provide a reasonable basis for field simulations.

A parallel experiment to those shown in Figure 5.45 was conducted using a suspension containing 0.37 g apatite/L to determine if Sr-90 removed from solution in these experiments was bound to the apatite surface by ion exchange and whether after 100 hr Sr-90 incorporation into the apatite structure (recrystallization) could be detected. After a 100-h contact time, the suspension was centrifuged and following decanting of the supernatant, the wet apatite pellet was extracted with 0.5 M KNO_3 for 100 h. A correction was made for the aqueous Sr-90 remaining in the pore water of the wet apatite pellet. The fraction sorbed was consistent with the 0.35 g/L suspension shown in Figure 5.45 and all of the sorbed fraction was recovered by the KNO_3 extraction, within the 4 % error of the extraction and correction for solution Sr-90 in the wet apatite. This indicates first, that Sr is bound to the apatite surface by ion exchange and second that after 100 h incorporation of Sr into the apatite structure at room temperature was not detectable, or if incorporation did occur it was less than 4%.

The Sr sorption on apatite (24 h) as a function of Sr concentration was also investigated. The pH (pzc) of the apatite is approximately 7.6, so Sr sorption at lower pH (pH 7.12 was investigated, Figure 5.46) should have much lower sorption (i.e., sites neutral to slightly positively charged) than Sr sorption at higher pH (pH 9.44 shown in Figure 5.46). Sr sorption at different concentration was fairly linear, reflecting a single type of sorption site, as expected. The adsorption maxima, unfortunately, was not well characterized, and is 30 mmol/g or higher. Comparison of Sr sorption on pure apatite at pH 7.1 (Figure 5.46, triangles) to sediment at pH 7.1 (Figure 5.39b)

indicates the Sr affinity for the apatite surface is 100x greater than for the sediment (i.e., $M \times K = K_d$, for low concentrations not near the maxima). This is similar to the 55x from different experiments (Figures 5.39a and 5.45). The relative adsorption maxima values on apatite (30 mmol/g) and sediment (18 $\mu\text{mol/g}$) show at 1660x greater number of sites for the apatite. Relative sorption was also calculated for expected field apatite concentrations. For field injections #3 to #18, it is expected that there would be 0.00038 g of apatite per gram of sediment (Table 2.1), assuming 100% of the phosphate injected forms apatite precipitate. At this low concentration, Sr adsorption mass balance is 99.2% sorbed, with 97.23% sorbed on sediment and 2.0% sorbed on apatite. At the final maximum apatite concentration of 0.0038 g apatite per gram of sediment (Table 2.1, 300-yr design capacity), 99.34% of the Sr-90 is adsorbed, but with 82.4% sorbed on sediment and 16.9% sorbed on apatite.

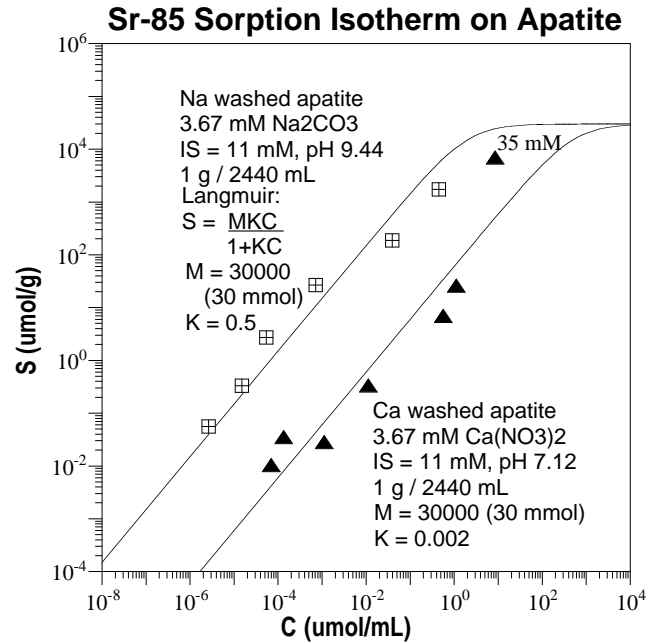


Figure 5.46. Sr ion exchange on apatite in Na- and Ca-saturated systems at differing Sr concentration.

Sorption of Sr-90 on sediment and apatite performs several functions. First, sorption simply decreases the Sr-90 flux toward the river, whether or not apatite is present. As described earlier (Table 2.1), the influence of adding apatite will not be apparent in the short time frame as the fraction of Sr-90 in solution changes very little. Sorption on the apatite, however, is also necessary for incorporation into the apatite structure. If there were absolutely no Sr-90 sorption on apatite, there would likely be no Sr incorporation into the structure. It was hypothesized that the incorporation rate is dependent on the amount of Sr sorption on apatite. However, simulation of these ion exchange and Sr incorporation processes shows that the Sr incorporation rate does not change with less Sr sorption to apatite. The reason appears to be that the ion exchange is 5 to 6 orders of magnitude more rapid compared to incorporation, so as long as there is some Sr sorption on apatite, the incorporation reaction will proceed.

5.6.4 Sr Uptake by Apatite: Influence of Cations and Temperature

The sorption and subsequent incorporation of aqueous Sr by apatite is known to depend on solution composition and in particular on the mole ratio of aqueous Ca to Sr ($Ca_{aq}:Sr_{aq}$) (Raicevic et al. 1996; Heslop et al. 2005). For this reason the influence of aqueous Ca and solution composition on the uptake of Sr by citrate precipitated apatite has been investigated. A series of batch experiments have been conducted using either distilled water or groundwater suspensions of apatite which differed in their $Ca_{aq}:Sr_{aq}$ mole ratios, ionic strength and solution composition. Adjustments to ionic strength and aqueous Ca concentrations in both distilled and groundwater suspensions were made with Na and Ca perchlorate (Figure 5.47). In the groundwater suspensions the starting ionic strength and $Ca_{aq}:Sr_{aq}$ mole ratio were 16.75 and 1.36 mM, respectively, with the largest contribution to ionic strength coming from Ca ions. All suspensions contained 0.378 g/L apatite to which stable Sr (as $SrCl_2$) and a Sr-90 tracer were added to obtain an initial Sr_{aq} concentration of 0.35 mM. Suspensions were adjusted to an initial pH of 8.4 and were maintained at 82°C during the 9.5-month sampling period. Loss of Sr from solution was determined by Sr-90 measurements. Although the aqueous $Ca_{aq}:Sr_{aq}$ mole ratios were varied from 0 to 220, the mole ratio of Ca in the apatite lattice to the Sr in solution ($Ca_{(s)}:Sr_{(aq)}$) was identical in all suspensions ($Ca_{(s)}/Sr_{(aq)} = 10$).

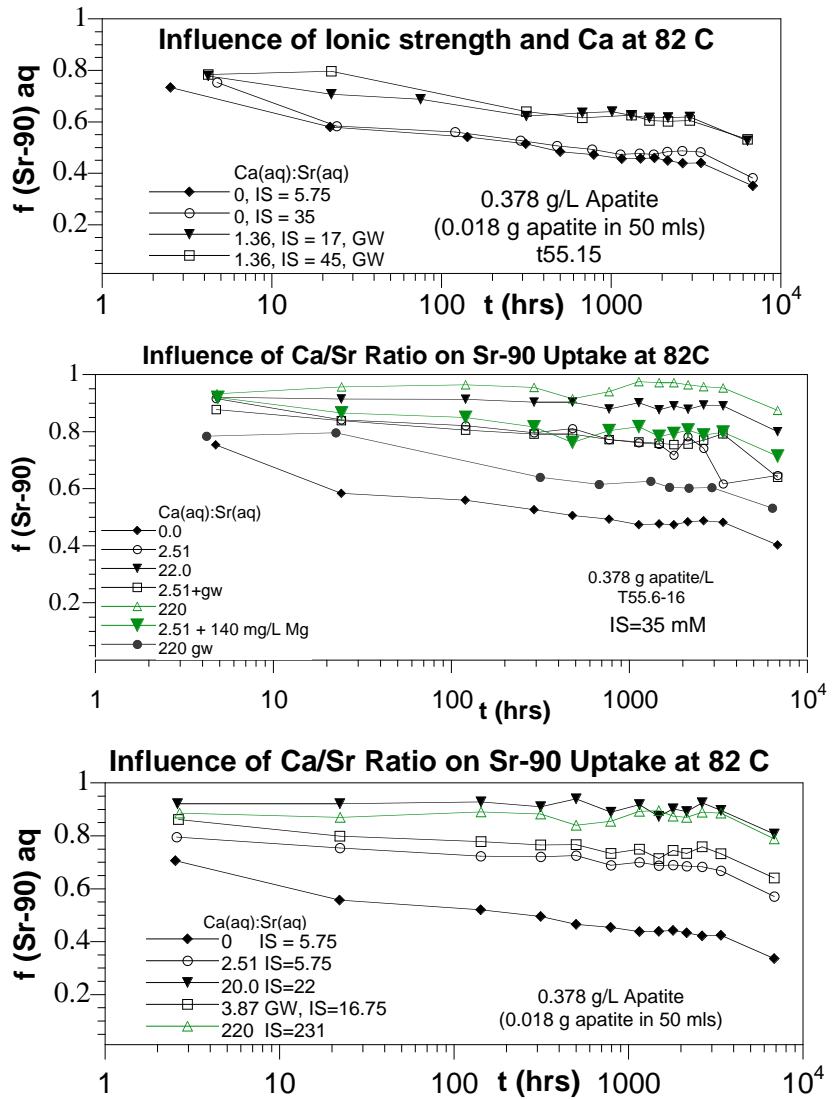


Figure 5.47. Influence of Ca, groundwater and ionic strength at 82°C on Sr uptake by apatite.

The initial rapid Sr uptake by apatite, due to sorption, was followed by the much slower uptake out to 7000 h, due to Sr incorporation by apatite (Figure 5.47). The extent of Sr uptake was greatest for $NaClO_4$ suspensions containing no aqueous Ca ($Ca_{aq}/Sr_{aq} = 0$) for which Sr removal reached 57% after

1000 h in both the 5.75 and 35 mM ionic strength suspensions (Figure 5.47a). Thus, Na ions and the contribution of Na ions to ionic strength had negligible effect on Sr uptake. In groundwater suspensions with $Ca_{aq}:Sr_{aq} = 1.36$ and ionic strengths of 16.75 and 45 mM the uptake of Sr was identical, but uptake had dropped to 37% after 1000 h (Figure 5.47a). The difference in ionic strength (IS) between these two suspensions, due to $NaCl_2$ addition, made no difference in uptake, consistent with uptake in the Ca-free suspensions. The decrease in Sr uptake was due to the presence of di-valent Ca ions and their competitive influence on Sr ion exchange by apatite. This is further demonstrated in distilled water suspensions as the $Ca_{aq}:Sr_{aq}$ ratio was increased to 2.5 (IS=5.75 mM) and 20 (IS=22 mM) and uptake dropped to 30 and 10% , respectively after 1000 h (Figure 5.47b). As the $Ca_{aq}:Sr_{aq}$ ratio was further increased to 220 (IS=231), no further decrease in Sr uptake was observed relative to that at a ratio of 20.

From Sr uptake after 9.5 months (Table 5.20) we can conclude that: 1) the mono-valent background electrolyte $NaClO_4$ has no effect on Sr uptake by apatite and thus Na salts are the preferred choice for injection chemicals, 2) groundwater concentrations of divalent Ca reduces Sr uptake from 62 to 35, 3) at a $Ca_{aq}:Sr_{aq}$ ratio of 220, typical of field injection solutions, Sr uptake by apatite had reached 17%, and 4) Sr uptake from solution by apatite, although slow, has not ceased to occur after 9.5 months and may continue well into the future. In addition, if all of the Sr removed from solution in these experiments was incorporated into the apatite structure by Sr substitution for a structural Ca, the percentage of the total Ca sites occupied by Sr would be small (1% to 7%) for conditions examined here (Table 5.20). For the $Ca_{(s)}/Sr_{(aq)}$ mole ratio (=10) used here suggests that there should be ample capacity for additional Sr incorporation for contact times in excess of the 9.5 mounts.

The rates of Sr/Sr-90 sorption and the subsequent incorporation into the citrate precipitated apatite structure were determined as a function of temperature (22°C, 42°C, 62°C, and 82° C) in aqueous suspensions of apatite. These batch experiments were performed using apatite suspensions made up in 50 ml of two different solutions (Table 5.21). The first suspension was made up in distilled water and contained 2.62 mM $NaClO_4$ as a background electrolyte, no Ca ions and 1.04 mM stable

Table 5.20. Sr uptake by citrate precipitated apatite in Figure 5.38 after 9.5 months versus aqueous Ca to Sr mole ratio.

Ca_{aq}/Sr_{aq} Mole ratio	0 (Na)	1.36(GW)	3.87(Ca+GW)	20(Ca)	220(Ca)
Ionic Strength	5.75	16.75	16.75	22	231
% Sr_{aq} uptake	62.4	35.1	31.9	16.3	17.1
% of Ca_s sites occupied by Sr	7.0	4.4	3.1	1.7	1.0

Symbols in parentheses indicates major electrolyte cation; GW indicates groundwater. Percent Ca_s sites in apatite occupied by Sr is based on measured Ca:P mole ratio = 1.27.

Table 5.21. Conditions of Sr sorption-incorporation versus temperature experiments; units in mM.

	$NaClO_4$	Groundwater
Ionic Strength	5.75	11
Sr_{aq}	1.04	0.0012
Ca_{aq}	0	0.48
Apatite (g/L)	0.38	0.34
$Ca_{aq} : Sr_{aq}$	0	392
$Ca_s : Sr_{aq}$	3.60	2938
Initial pH	8.0	7.6

Sr added as SrCl₂ (Figure 5.48). The second suspension was made up in 100-N groundwater containing 19 mg/L Ca ions and 0.11 mg/L (1.2 μM) Sr (Figure 5.49). Sr-90 was added to each suspension. The total Sr_{aq} in the NaClO₄ suspension was a factor of 867 times greater than the Sr_{aq} present in the groundwater suspensions. This accounts for the difference in the Ca_s : Sr_{aq} ratio between the NaClO₄ and groundwater suspensions. Sr-90 loss from solution was measured periodically over the 9.6-month course of the experiments.

For both suspensions and at all temperatures examined the initial fast sorption/ion exchange phase (0 to 50 hrs) was followed by a slower gradual uptake (50 h to 1300 h) and has continued out to 9.6 (Figures 5.48 and 5.49). The extent of uptake increased approximately 10% with increasing temperature in both solutions (Table 5.21). The percentage of Sr uptake from the groundwater suspension (lower Sr_{aq} concentration with Ca ions) was 14% to 22 % greater than from the NaClO₄ suspension with no apparent temperature dependence (Table 5.22). The reason for greater percentage uptake from the groundwater suspension, despite the presence of Ca ions, was the much higher concentration of Sr_{aq} (x 867) in the NaClO₄ suspension and thus the much higher occupancy of the Ca sites by Sr (Table 5.22). This estimation of Sr occupancy of apatite Ca sites assumes (as above) that all of the Sr_{aq} removed from solution after 9.6 months was substituted into the apatite by replacing a structural Ca. This estimated percent of Ca sites occupied by Sr was typically 580 times higher in the NaClO₄ suspension than in the groundwater suspension. This suggests that Sr incorporation at a low Ca site occupancy (low Sr loading of apatite) may be more ‘effective’ than at a much higher occupancy (or Sr loading) because of differences in Ca site accessibility to the sorbed Sr. This would lead to a saturation effect as aqueous and thus sorbed Sr increased. It should be noted that the assumption made in calculating the percent of Ca sites occupied by Sr, i.e., that all the

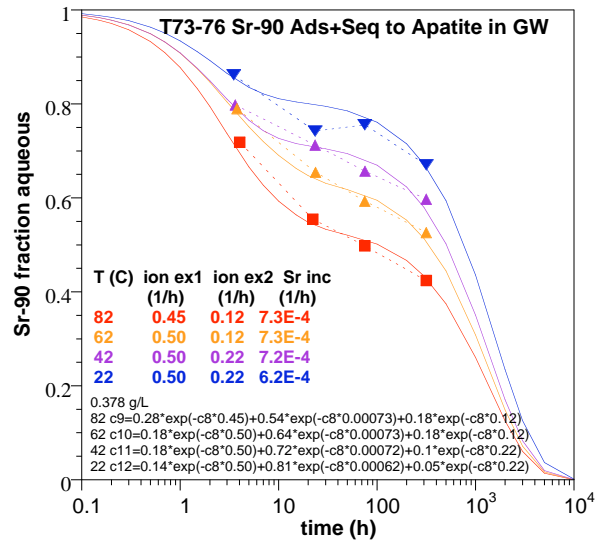


Figure 5.48. Sr-90 uptake by hydroxyapatite at 22°C to 82°C in groundwater with model fit of sorption and incorporation rate.

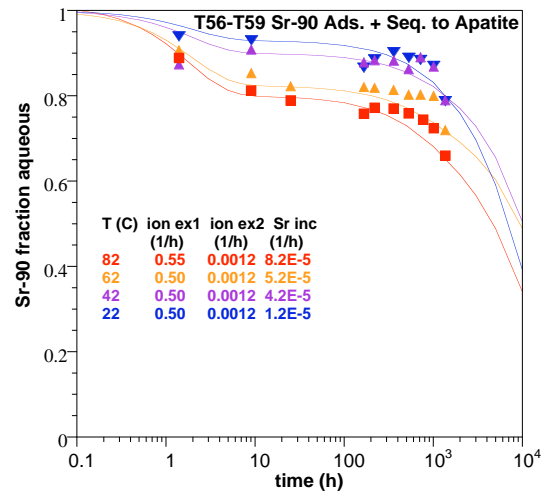


Figure 5.49. Sr-90 uptake by hydroxyapatite at 22°C to 82°C in deionized water with model fit of sorption and incorporation rate.

sorbed Sr is incorporated into apatite, is consistent with the interpretation of data from the solid phase HNO₃ digestion and ICP-MS analysis of apatite suspensions after 6 months of contact with Sr (see below).

Table 5.22. Sr uptake mass fraction and rate by apatite versus temperature after 9.6, 8.6 months; GW indicates 100-N groundwater. Percent Ca_s sites in apatite occupied by Sr is based on measured Ca:P mole ratio = 1.27.

Suspensions		22° C	42° C	62° C	82° C
Apatite only in NaClO₄ (Sr=1 mM, 9.6 mo.) [exp. T56, Fig. 5-48]	% uptake	41.6	47.4	47.3	50.4
	% Ca sites occupied by Sr	13.5	15.3	15.3	16.3
	Sr ion exch. rate (1/h)	1.2E-3	1.2E-3	1.2E-3	1.2E-3
	Sr uptake rate (1/h)	8.2E-5	5.2E-5	4.2E-5	1.2E-5
Apatite only in groundwater (Sr=2.3uM, 8.6 mo.) [exp. T73, Fig. 5-49]	% uptake	61.4	61.2	69.4	72.3
	% Ca sites occupied by Sr	0.023	0.024	0.026	0.028
	Sr ion exch. rate (1/h)	0.12	0.12	0.22	0.22
	Sr uptake rate (1/h)	6.2E-4	7.2E-4	7.3E-4	7.3E-4
apatite + sediment in groundwater (Sr= 2.3 uM, 8.6 mo.) [exp. T69, Fig 5-55]	% uptake	63.5	69.7	66.4	72.6
	% Ca sites occupied by Sr	0.030	0.026	0.028	0.031
	Sr ion exch. rate (1/h)	0.45	0.45	0.45	0.50
	Sr uptake rate (1/h)	6.5E-5	6.5E-5	3.5E-5	2.9eE5

(1) Experiment described is Section 5.5.5.

A first order model was used to derive sorption (two steps) and incorporation rate constants from uptake data from Figures 5.48 and 5.49. The fits to the data are shown by solid curves at each temperature in those figures along with the derived rate constants. Incorporation rate constants in the groundwater suspensions at the low Sr concentration were 8 times and 60 times greater than those in the NaClO₄ suspension at 22°C and 82°C, respectively. This further suggests a difference in the effectiveness or energetics of the Sr incorporation reaction as a function of Sr loading of available Ca sites.

The calculated activation energy of the rate of Sr-90 incorporation into apatite is 11.3 kJ/mol (Figure 5.50), using data of Sr-90 uptake from groundwater (Figure 5.49). This relatively low activation energy suggests the rate-controlling step is diffusion of Sr-90 into the apatite structure (i.e., activation energies <10 kJ/mol). Large activation energies (30 to 50 kJ/mol) suggest chemical control. The rate of diffusion can be altered with a different apatite precipitate particle size, where smaller precipitations with greater surface area will have a more rapid uptake. The amount and location of Sr in the surface apatite has been characterized by several different methods, as described in the following

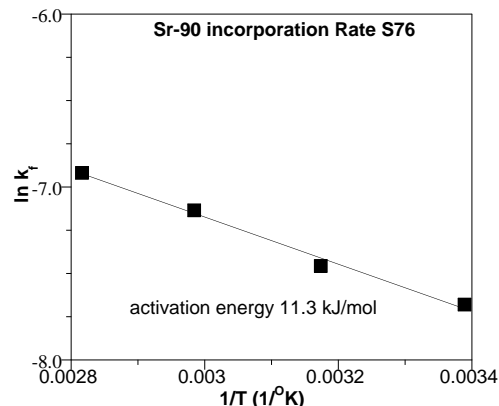


Figure 5.50. Change in Sr-90 incorporate with temperature and calculated activation energy.

section. Additional electron microprobe work is in progress in order to characterize the mass of Sr with depth within the apatite precipitate in order to determine if Sr is diffusing throughout the apatite volume, or is limited to near surface substitution.

5.6.5 Sr Uptake by Apatite: Solid Phase Characterization

In this series of experiments Sr incorporation into apatite was examined by ICP-MS analysis of the HNO₃ digested apatite phase after liquid-solid phase separation and removal of exchangeable and carbonate Sr phases from the apatite by sequential KNO₃ and EDTA extractions. Experimental conditions differed from those described in the preceding paragraphs of this section in that 1) no NaClO₄ was used to maintain the ionic strength, 2) no aqueous Ca was added to suspensions, and 3) both the apatite mass and aqueous Sr concentrations were increased (Table 5.23). In addition, two parallel experimental series were conducted, one using stable Sr plus a Sr-90 tracer and the second using only stable Sr. The stable Sr series was conducted to facilitate SEM, XRD, and FTIR analyses of non-radioactive apatite. In each experimental series aqueous suspensions of both a commercial (Sigma) and citrate precipitated apatite (no sediment) were made up in distilled water to which SrCl₂ was added to obtain the same ratio of solid phase Ca to aqueous Sr ratio (i.e., Ca_s:Sr_{aq} = 3.33 in both series). All suspensions were adjusted to an initial pH of 8 and maintained at 22°C and 82°C until individual suspensions in each series were sacrificed for analysis. The pH of all remaining suspensions were monitored periodically and returned to their original pH of 8 with NaOH. The differences in experimental conditions between the Sr-90 and stable Sr series are summarized in Table 5.23.

Table 5.23. Conditions of Sr sorption-incorporation experiments at 22°C and 82°C.

	Sr-90 Series	Stable Sr Series
Ionic strength (mM)	6.67	14.9
Apatite mass (g)	0.15	0.2
SrCl ₂ (mM)	2.21	5.0
Volume (ml)	203	120
Measurements	Aqueous Sr-90, solid phase incorporated Sr90	Aqueous-ICP, SEM, XRD, FTIR, incorporated-ICP

(Table 5.23). In addition, two parallel experimental series were conducted, one using stable Sr plus a Sr-90 tracer and the second using only stable Sr. The stable Sr series was conducted to facilitate SEM, XRD, and FTIR analyses of non-radioactive apatite. In each experimental series aqueous

suspensions of both a commercial (Sigma) and citrate precipitated apatite (no sediment) were made up in distilled water to which SrCl₂ was added to obtain the same ratio of solid phase Ca to aqueous Sr ratio (i.e., Ca_s:Sr_{aq} = 3.33 in both series). All suspensions were adjusted to an initial pH of 8 and maintained at 22°C and 82°C until individual suspensions in each series were sacrificed for analysis. The pH of all remaining suspensions were monitored periodically and returned to their original pH of 8 with NaOH. The differences in experimental conditions between the Sr-90 and stable Sr series are summarized in Table 5.23.

For the Sr-90 series, five suspensions from each of the 22°C and 82°C experiments were sacrificed at regular intervals. Suspensions were characterized by analyzing for aqueous Sr-90 and performing the sequential KNO₃, EDTA and HNO₃ extractions on the recovered apatite. After aging for 4.9 months the majority of the starting Sr remained in the aqueous phase, however, 11% and 14% of the starting Sr had been incorporated (HNO₃ extraction) into the apatite structure at 22°C and 82°C, respectively (Table 5.24). A small increase

Table 5.24. Percent distribution of Sr in apatite suspension for Sr-90 series (a) and mole percent of apatite Ca sites occupied by incorporated Sr (b) (aged 4.9 months).

	22° C	82° C
a) % of Total Sr in each phase		
Aqueous	86.8	82.9
Exchangeable (0.5 M KNO ₃)	1.19	0.86
Carbonate (0.05 M EDTA)	0.85	1.9
Incorporated (4 M HNO ₃)	11.1	14.3
b) % of apatite Ca sites occupied by Sr	3.14	3.73

in incorporation occurred at the higher temperature. Only a small percentage of the Sr associated with the apatite remained in the exchangeable phase after 4.9 months. The mole percent of apatite Ca sites occupied by incorporated Sr after 4.9 months increased slightly with temperature. Suspensions sacrificed at 7 and 11 months at each temperature are currently being characterized.

For the stable Sr series fifteen apatite suspensions have been sacrificed to date, after ageing between 0.86 and 6.15 months. Following centrifugation the aqueous phase was saved for future Sr and Ca analysis. The apatite pellet was washed with 0.5 M KNO₃ overnight to remove ion exchangeable Sr and then washed several times in DI prior to solid phase analysis. A portion of the apatite was digested in HNO₃ and analyzed for Sr and Ca by ICP-MS with the remainder of

Table 5.25. Percent of total aqueous Sr incorporation into citrate precipitated and Sigma apatites for stable Sr series.

	aged(m)	% aqueous Sr uptake	% Ca sites occupied by Sr
apatite			
22°C	0.86	16.3	4.90
	1.36	19.3	5.79
	2.68	21.9	6.59
	3.89	25.1	7.54
	4.93	21.1	6.33
	5.99	20.0	6.00
82°C	0.86	33.3	10.0
	1.36	33.3	10.0
	2.68	37.3	11.2
	3.89	42.4	12.7
	6.15	38.3	11.5
Sigma			
22°C	5.99	10.6	3.18
82°C	2.68	17.1	5.10
	5.99	19.0	5.69

the apatite used for SEM, XRD and FTIR characterization. No EDTA extraction carried out on these samples because the Sr carbonate phase was typically 1% or less of the total Sr in suspensions after 5 months (Table 5.25). The ICP-MS analysis of the HNO₃ digested citrate precipitated apatite showed that Sr incorporation was 16% and 33 % of the total Sr in the system after 0.86 months at 22°C and 82°C, respectively (Table 5.25). This factor of two difference persisted during the course of these experiments. Comparison of the percent of incorporation that occurred at 0.86 months with that occurring between 2.68 and 3.89 months indicates that the rate of incorporation was decreasing. The Sr incorporation in these stable Sr suspensions at 22°C and 82°C was a factor of 1.9 and 2.7 greater, respectively (Table 5.25), than that found in the Sr-90 series (Table 5.24). The calculation

of the percent of total Ca sites occupied by the observed incorporation of Sr in these HNO₃ extraction experiments after 6 months differed by a factor of two for suspensions at 22°C and 82°C (Table 5.25). This is not consistent with the calculated percent of Ca sites occupied by Sr for uptake experiments (Table 5.22) where the difference between 22°C and 82°C was typically 10%. The reason for these discrepancies is currently being investigated. Incorporation in the commercial Sigma apatite was approximately half of that achieved with the citrate-precipitated apatite. This was most likely due to differences in their morphology, although their BET surface areas are similar (Sigma, 61 m²/g; citrate-precipitated, 55 m²/g).

The stable Sr suspensions aged for 0.86 and 1.36 months at each temperature have been characterized by SEM/EDS. The SEM image of the citrate precipitated apatite used in the stable Sr incorporation series and aged for 1.36 months at 82°C (Figure 5.51) showed discrete aggregated crystalline clusters ranging from 75 to 600 nm in diameter and significant porosity. The presence of Sr associated with the citrate precipitated apatite was examined by EDS in samples aged for 0.86 and 1.36 months at 22°C and 82°C. EDS spectrum obtained at 62 distinct sites on apatite particles in these 4 samples confirmed the presence of Sr at all sites. A typical EDS spectrum for apatite aged at 82°C for 0.86 months shows a clearly resolved Sr peak (Figure 5.52). As noted above, ion exchangeable Sr had been removed by an overnight wash with 0.5 M KNO₃, so the Sr detected by EDS was either a discrete Sr phase on the apatite surface or incorporated into the apatite structure. Although qualitative, the EDS estimation of Sr incorporation into the citrate precipitated apatite was consistent with ICP-MS measurements of Sr incorporation in these same samples (Table 5.25).

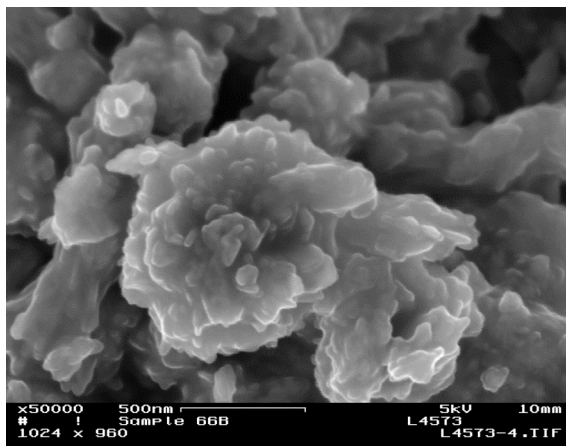
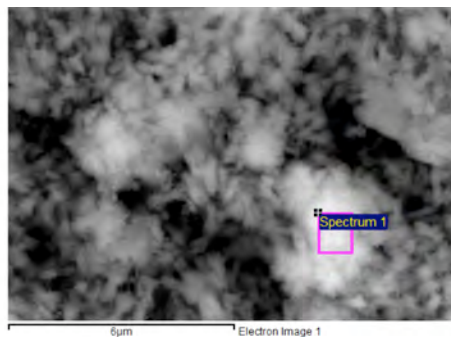
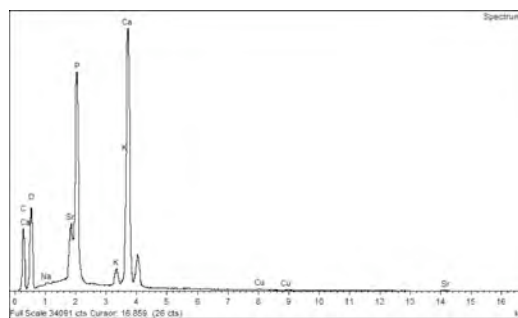


Figure 5.51. SEM image of citrate precipitated apatite used in Sr incorporation studies at 82°C.



a)



b)

Figure 5.52. Image of apatite grain (a) showing square region for which EDS spectrum was obtained (b) for apatite aged at 82°C for 0.86 months.

Fast XRD scans have been carried out on the citrate precipitated and Sigma apatites and confirmed the presence crystalline apatite as the major phase in these starting materials. Fast XRD scans on selected samples of the Sr substituted apatites yield the same result. Currently slower more precise XRD scans are being performed in order to detect trace phases within the major phase and any changes in crystallinity due to Sr substitution. This should confirm Sr incorporation within the apatite structure.

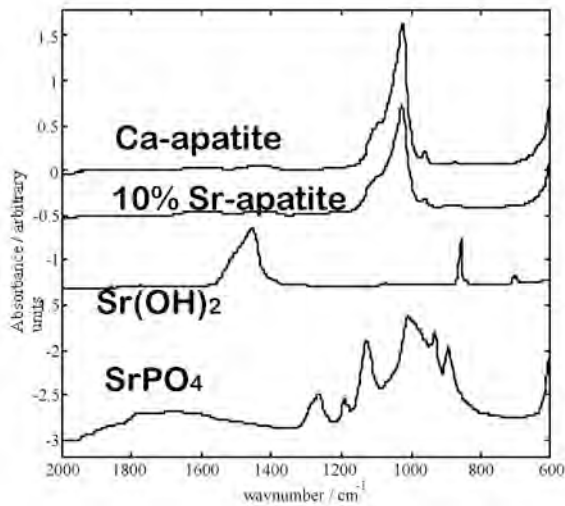


Figure 5.53. SEM image of citrate precipitated apatite used 82°C.

of Sr incorporation are attempting to observe this difference and thus definitively confirm that the Sr is replacing the Ca within the apatite structure.

Control FTIR spectra have been run on both the Sigma and citrate apatite starting materials. FTIR scans of the 82°C citrate precipitated apatite aged for 5.99 months demonstrated that no secondary phases, e.g. SrPO₄ or SrOH precipitate, have formed within the apatite structure, as shown in Figure 5.53 in which peaks for the Ca-apatite (Sigma standard) and Sr-substituted apatite are similar, but do not show characteristic peaks of the Sr(OH)₂ or Sr(PO₄). Although the presence of Sr has been confirmed by ICP-MS and EDS which strongly suggests that Sr has been incorporated, the FTIR analysis has not detected a difference between the Sr incorporated apatite samples and the control samples. Additional FTIR analysis of samples aged for longer periods with a higher percentage

5.6.6 Sr Uptake by Apatite in Groundwater with Sediment

To quantify the influence of a) the presence of sediment, and b) aging of the Sr-90 on sediment, solid phase extractions were conducted on these sediments. As previously described in Section 5.1.1, in untreated sediment (i.e., no apatite added), at the sediment/water ratio of this batch experiment, 5.6% of the Sr-90 was aqueous (Figure 5.5a). In addition, the ion exchangeable fraction was 85%, giving the total “mobile” (= aqueous + ion exchangeable) fraction of 90%, which remained constant over time, since there was no apatite addition. In contrast, the addition of the Ca-citrate-PO₄ solution (4, 10, 2.4 mM) caused several changes in Sr-90 proportions over time, as shown in Figure 5.5b. Between 100 and 300 h, the aqueous + ion exchangeable Sr-90 (mobile) fraction decreased from 90% to 43% (red squares, Figure 5.5b), which is consistent with previous experiments reported, in which a fraction of the Sr-90 (not all) is incorporated into apatite as it precipitates in 100s of hours. The sequential extractions of the solid phase (carbonate and residual together = solid-associated) show that the remaining Sr-90 fraction (41%) cannot be mobilized with a high ionic strength solution as it is incorporated into apatite. By 11,000 h (15 months) 99.4% of the Sr-90 was associated with apatite in the experiment using field contaminated Sr-90 (containing 80 pCi/g Sr-90, no additional Sr-90 was added, Figure 5.54). The experiment in which Sr-90 was added showed essentially no difference in behavior throughout most of the experiment (to 4000 h), but the last data point indicated less Sr-90 incorporation in apatite. Therefore, there appears to be no effect of aging (i.e., decades of Sr-90 contact time with sediment) on the use of this process to incorporate Sr-90 into apatite. These results are consistent with a previous study (Serne and LeGore 1996), in which ion exchange experiments showed Sr-90 was readily desorbed after decades of contact with sediment. Because these experiments contained the spent Ca-citrate-PO₄ solution (i.e., high ionic strength relative to groundwater) for the entire experiment, additional long-term experiments were conducted to characterize the uptake rate and mass under conditions more likely to be encountered in the field, namely a groundwater aqueous phase.

Additional experiments were conducted as a function of temperature to determine the Sr uptake rate from groundwater suspensions of 100-N sediment containing citrate precipitated apatite. The objective was to compare uptake in these suspensions with suspensions containing only apatite (Section 5.6.3). For that reason, experimental conditions were identical to those used in the groundwater suspensions containing only apatite (Table 5.22), except here 1 g of sediment was added. Individual suspensions were adjusted to an initial pH = 7.6 and maintained at 22°C, 42°C, 62°C, and 82°C for 8.6 months, during which time they were periodically samples to determine Sr-90 loss from solution.

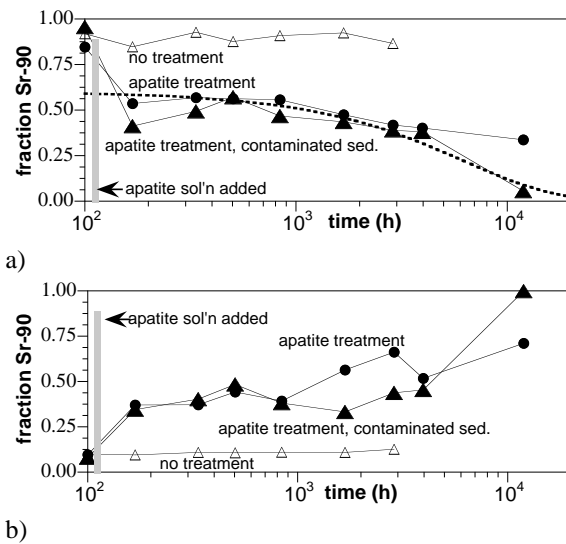


Figure 5.54. Sr-90 extractions of treated sediments originally containing Sr-90 or with Sr-90 added: a) aqueous + ion exchangeable (i.e., mobile), and b) solid phase associated (i.e., incorporated)

At all temperatures the initial uptake of Sr due to sorption was very rapid, as previously observed for suspensions containing only 100-N sediment or apatite. This Sr ion exchange was simulated as a two step sorption process, with a rapid uptake <1 h (assumed to be ion exchange) and a somewhat slower uptake to 100 h (also ion exchange, but rate limited by diffusion to ion exchange sites (likes, Figure 5.55).

After ion exchange equilibrium was reached (100 h), there was a period of much slower uptake out to 6200 h (8.6 months, Figure 5.55). After 8.6 months 63.5% of the Sr had been removed from solution at 22°C compared to 72.6% at 82°C (Table 5.21). This extent of uptake and the difference in uptake with temperature were virtually identical to that observed in suspensions containing only apatite performed under identical conditions (compare results in Table 5.22). It is clearly evident that the sediment was playing a negligible role in the uptake of Sr. Thus, we can conclude that apatite was responsible for the continued uptake after the initial rapid sorption of Sr and that this continuation in uptake was most likely due to Sr substitution for structural Ca.

An additional simulation effort was conducted using the Sr-90 uptake data in the system with groundwater and sediment at 82°C (i.e., Figure 5.55a, experiment T69). The purpose of this EM-22 funded simulation was to accurately simulate ion exchange and incorporation processes from laboratory data, and project the time scales of the same processes at the field scale with a much higher sediment/water ratio. A series of five reactions were used for this modeling effort: a) Ca-Na-Sr ion exchange on the sediment surface (2 reactions), b) Ca-Na-Sr ion exchange on the

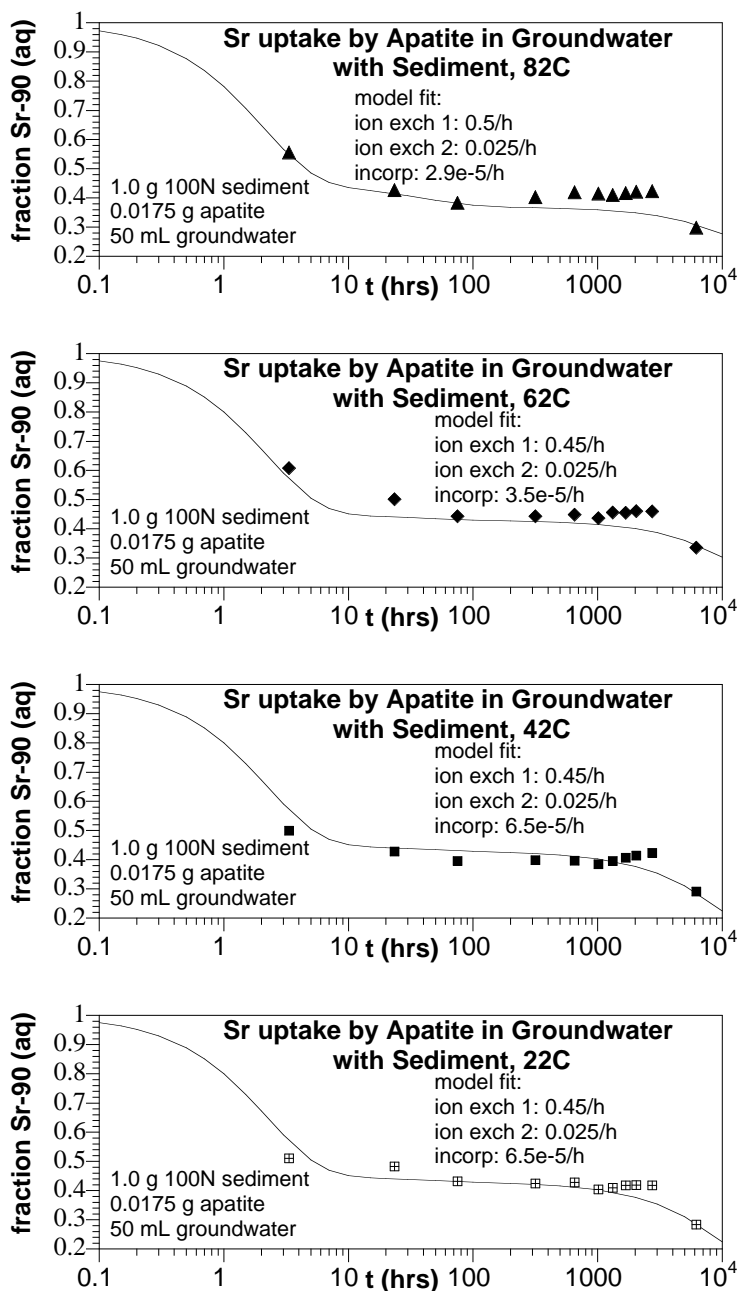


Figure 5.55. Sr uptake from groundwater suspension of 0.34 g/L apatite and 20 g/L sediment at 22°C to 82°C. Model fit of a two-step adsorption reaction and uptake from solution.

apatite surface (2 reactions), and c) Sr incorporation from Sr sorbed to apatite (1 reaction). The partial differential equations describing the time rate of change of 8 species were initially numerically integrated within Mathcad, but later incorporated into a reactive transport code (RAFT) for future reactive transport simulations. The simulation fit (lines, Figure 5.56) have initial conditions of 100% of the Sr in solution and Na-Ca ion exchange equilibrium between aqueous solution, sediment ion exchange sites, and apatite ion exchange sites. The simulation fit to data between 0.1 and 30 h, ion exchange reactions shows Sr (aqueous) decreasing to 0.45 (red), with an increase in ion exchange on the sediment (purple) and on apatite (blue). The Sr ion exchange rate onto sediment was set slightly faster than onto apatite, so there is initially somewhat more Sr on the sediment (1 to 3 h), which decreases by 30 h as equilibrium is reached. Sr incorporation from Sr sorbed on the apatite occurs in 1000s of hours, which is generally simulated. One interesting aspect of the simulation is that the incorporation data (red triangles) show an 11% drop in aqueous Sr, the actual incorporation is 32% (i.e., 1000 h to 7000 h), as Sr mass is also removed from ion exchange sites on the sediment (5% decrease) and on apatite (11% decrease).

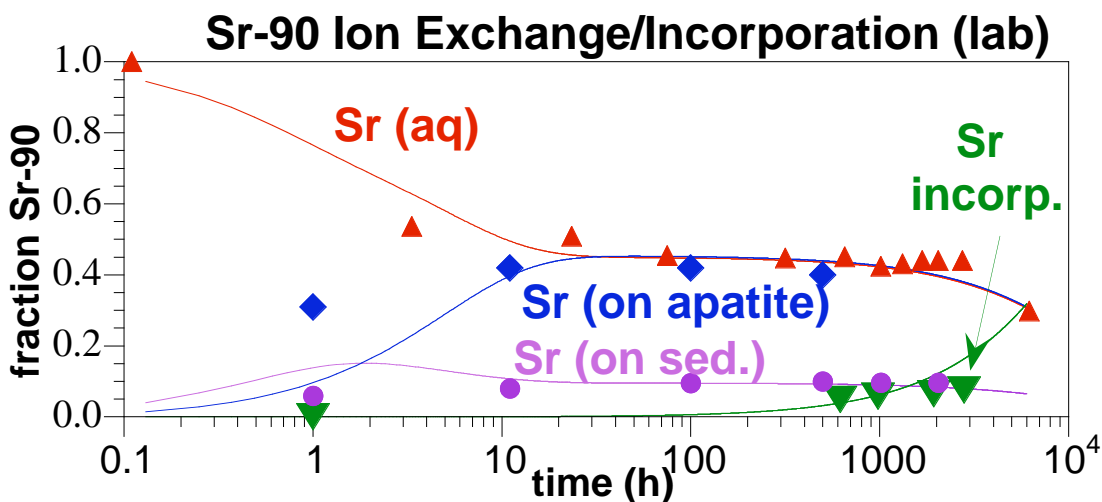


Figure 5.56. Sr uptake from groundwater suspension of 0.34 g/L apatite and 20 g/L sediment at 82°C. Model fit consists of Ca-Na-Sr ion exchange on sediment, Ca-Na-Sr ion exchange on apatite, and Sr incorporation within the apatite structure.

One fundamental question driving many experiments was whether the incorporation rate differs if the amount of Sr sorption on the apatite is different. At very high sediment/water ratios in the field, there is a significant amount of sorption to sediment, so there is proportionally less sorption to apatite. In addition, experiments described in Section 5.6 start with a simple system of aqueous Sr (no Ca or groundwater) and apatite only, and build in complexity with the addition of increasing amounts of Ca (which competes for ion exchange sites on the apatite surface), and sediment (which sorbs both Ca and Sr). The mass fraction of Sr-90 sorbed in different apatite/sediment/water systems (lab and field) can be illustrated to describe Sr-90 sorbed mass differences between lab and field systems (Table 5.26). First, comparison of Sr/apatite and Sr/sediment laboratory systems (lines 1 to 4, Table 5.26) show the 55x stronger Sr affinity for apatite results in a higher fraction sorbed. More specifically, for the system with 1.0 mL of water and 0.0038 g apatite (line 2), 84% of the Sr-90 is sorbed on the apatite. In contrast, for the

system with 1.0 mL of water and 0.0038 g of sediment (line 4), only 9% of the Sr-90 is sorbed. When the system contains both sediment and apatite (line 6, 0.0038 g apatite, 0.0038 g sediment), sorption on apatite drops slightly (82%), but sorption on the sediment drops significantly (1.5%).

Table 5.26. Sr-90 fraction sorbed in different sediment/apatite/water systems.

system	#	Kd, apa. (cm ³ /g)	Kd, sed. (cm ³ /g)	apatite mass (g)	sediment mass (g)	volume (mL)	ion exchange equilibrium			
							fraction aqueous	fraction sorbed on apatite	fraction sorbed on sediment	fraction sorbed total
laboratory systems										
Sr/apatite only	1	1350		0.0038		50	0.9069	0.0931	0	0.0931
	2	1350		0.0038		1.0	0.1631	0.8369	0	0.8369
Sr/sediment only	3		25		0.0038	50	0.9981	0	0.0019	0.0019
	4		25		0.0038	1.0	0.9132	0	0.0868	0.0868
Sr/apatite/sed.	5	1350	25	0.0038	0.0038	50	0.9054	0.0929	0.0017	0.0946
	6	1350	25	0.0038	0.0038	1.0	0.1606	0.8241	0.0153	0.8394
	7	1350	25	0.0038	1.0	50	0.6240	0.0640	0.3120	0.3760
	8	1350	25	0	1.0	50	0.6667	0.0000	0.3333	0.3333
field systems										
Sr/sediment only	9	1350	25	0	1.0	0.2	0.0079	0.0000	0.9921	0.9921
Sr/sed./apatite	10	1350	25	0.00038	1.0	0.2	0.0078	0.0200	0.9723	0.9922
Sr/sed./apatite	11	1350	25	0.0038	1.0	0.2	0.0066	0.1691	0.8243	0.9934

While laboratory systems can contain significant quantities of apatite and only a little sediment, the field system has a very high sediment/water ratio. Assuming 20% porosity, 1.0 g of sediment is in contact with 0.2 mL of water, so Sr is 99.2% sorbed (line 9), leaving 0.8% in solution. If 3.8E-4 g of apatite per gram of sediment is added (i.e., Table 2.1, amount injected in field injections #3 to #18), Sr-90 total sorption is essentially the same (line 10, last column), but 2% of the sorbed mass is now on apatite. If the final design mass fraction of apatite is added (3.8E-3 g apatite/g sediment, line 11), the total Sr-90 sorption fraction increases very slightly, but now 17% of the Sr-90 mass is sorbed on apatite.

To test whether Sr-90 incorporation into apatite is dependent on the mass fraction of Sr-90 sorbed onto the apatite, reaction parameters derived from a laboratory experiment (Figure 5.56), which includes Ca-Na-Sr ion exchange on apatite and sediment, and Sr incorporation into apatite, was used in a simulation of the same system with the only changing being the increased sediment/water ratio of the field (20% porosity assumed). Comparison of the laboratory simulation (Figure 5.56) to field simulation (Figure 5.57) shows the obvious much

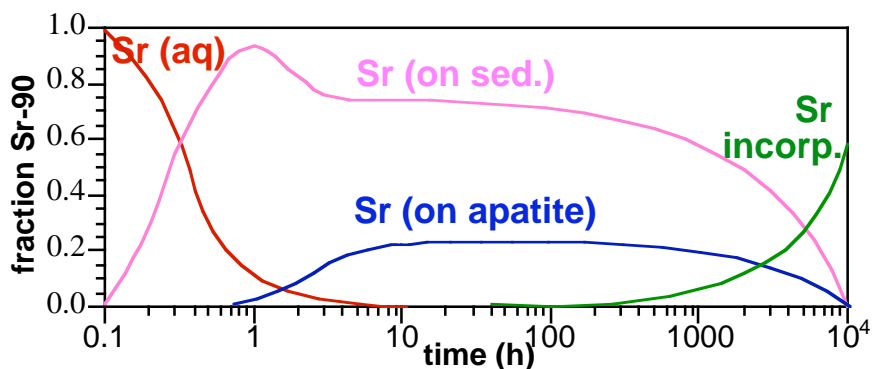


Figure 5.57. Simulation of Sr-90 mass changes under field conditions of 20% porosity and 0.0038 g apatite/g sediment. Simulation includes Ca-Na-Sr ion exchange on sediment, Ca-Na-Sr ion exchange on apatite, and Sr incorporation into apatite.

greater proportion of Sr mass sorbed on the sediment in the field system (1 h to 1000 h), as compared to the laboratory system. The proportion of Sr mass sorbed on apatite, therefore decreased from 45% (laboratory system) to 17% (field simulation, Figure 5.57). This decrease in Sr mass sorbed to apatite did not change the Sr incorporation rate (green line in Figures 5.56 and 5.57), which has a half-life of 15 months in both cases. The reason for this lack of change is the relative time scales of ion exchange reactions versus the incorporation reaction being 5 to 6 orders of magnitude different. Any small amount of Sr sorbed on apatite is slowly incorporated and additional Sr mass sorbs onto the apatite. Ion exchange equilibrium is quickly reached, so has no influence on slowing down the incorporation reaction. In contrast, if the ion exchange and incorporation reaction rates were only an order of magnitude different, then there the ion exchange reaction would slow the apparent incorporation rate.

5.7 Alternate Injection Strategy: Injection of PO₄ Only

Injection of Na-PO₄ only and various sequential injections of Na-PO₄ and Ca-citrate-PO₄ solutions were investigated as alternate injection strategies of Ca-citrate-PO₄ injection only.

5.7.1 PO₄ Sorption/Precipitation in Sediments

Batch and 1-D column experiments were initially conducted to quantify PO₄ sorption and precipitation time scales. It was hypothesized that PO₄ sorption would be relatively rapid (minutes), and Ca-PO₄ precipitation would occur over much longer time scales (10s to 100s of hours).

Adsorption appeared to reach equilibrium within 5 minutes at all soil water ratios (Figure 5.58a), although observed over 100 to 600 h (Figure 5.58b and c), it is not clear what is an appropriate time scale for adsorption equilibrium and for Ca-PO₄ precipitation.

Adsorption isotherms were then conducted at 1 h and 24 h contact time to characterize whether sorption was occurring or there was some precipitation. If Ca-PO₄ precipitation was a significant component of the PO₄ mass loss from solution, the isotherm line would be closer to vertical and not exhibit a 1:1 slope at low concentration indicative of sorption. Adsorption isotherms for 1 h and 24 h contact time, pH 8, 50 mM PO₄ and r_{sw} (Figure 5.59) implies that the PO₄ removal from solution is due primarily to sorption. If it was precipitation, there would be no regular partitioning with change in concentration (pure precipitation would show as a vertical line, where there would be a finite amount in aqueous solution (no matter how much PO₄ is added)). Each isotherm was fit to a Langmuir equation with identical sorption maxima ($M = 1500 \text{ mg sites/Kg sediment}$).

The linear region of the isotherms at both 1 h and 24 h (low concentration) and same adsorption maxima (high concentration) appear to be indicative of adsorption in the short time scale.

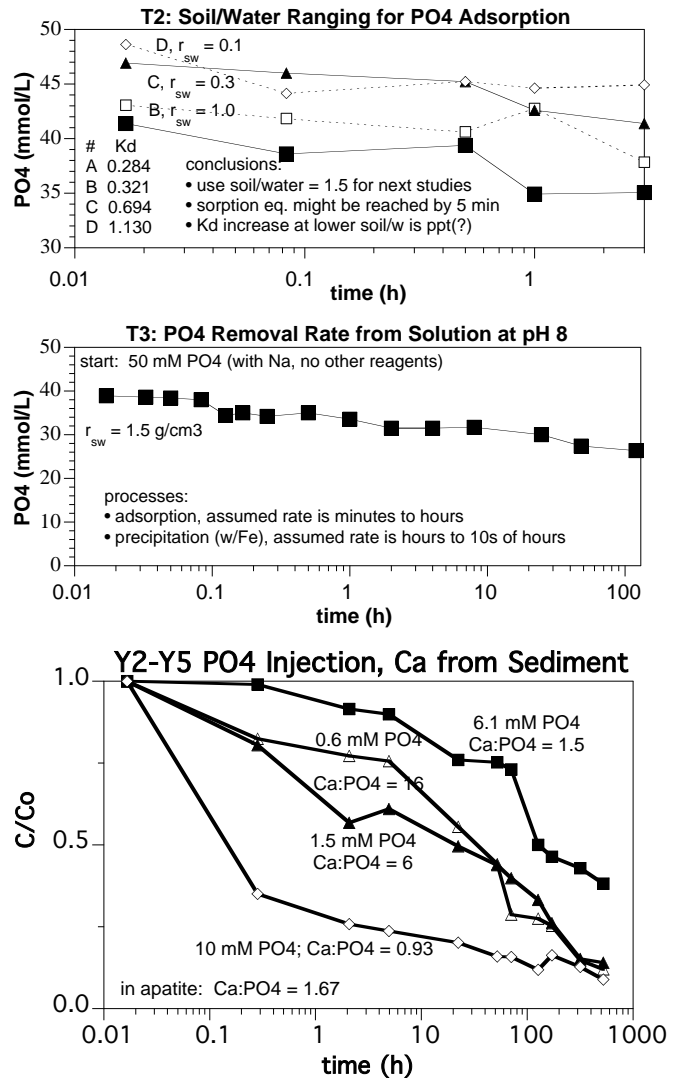


Figure 5.58. Time scale of PO₄ removal rate from solution at differing sediment/water ratio (a), at a high PO₄ concentration (b), and at different Ca/PO₄ ratios (c)

5.7.2 PO₄ Injection into Sediments

Phosphate solutions were injected into 1-D sediment columns at different PO₄ concentration and flow rates to separate sorption from precipitation. In a flow through system, sorption results in a lag in breakthrough, whereas precipitation (mass loss from solution) results in mass loss, which is observed in the breakthrough concentration leveling out at a lower concentration than the injected concentration, and a final mass balance of PO₄ (area under the breakthrough curve) being less than the injected mass.

Sodium phosphate injection at a low 0.4 mM or 50 mg/L concentration (Figure 5.60a) and fast flow rate (i.e., 20-minute contact time) exhibited only

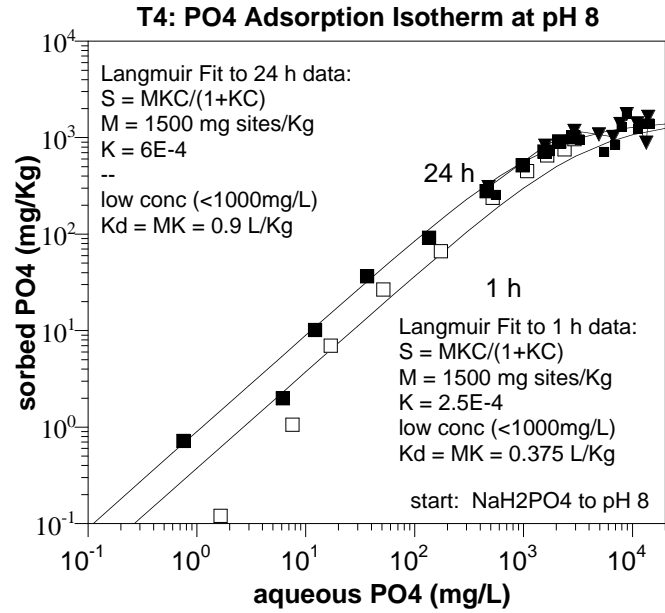


Figure 5.59. Adsorption isotherm for Na-PO₄ at 1 h and 24 h.

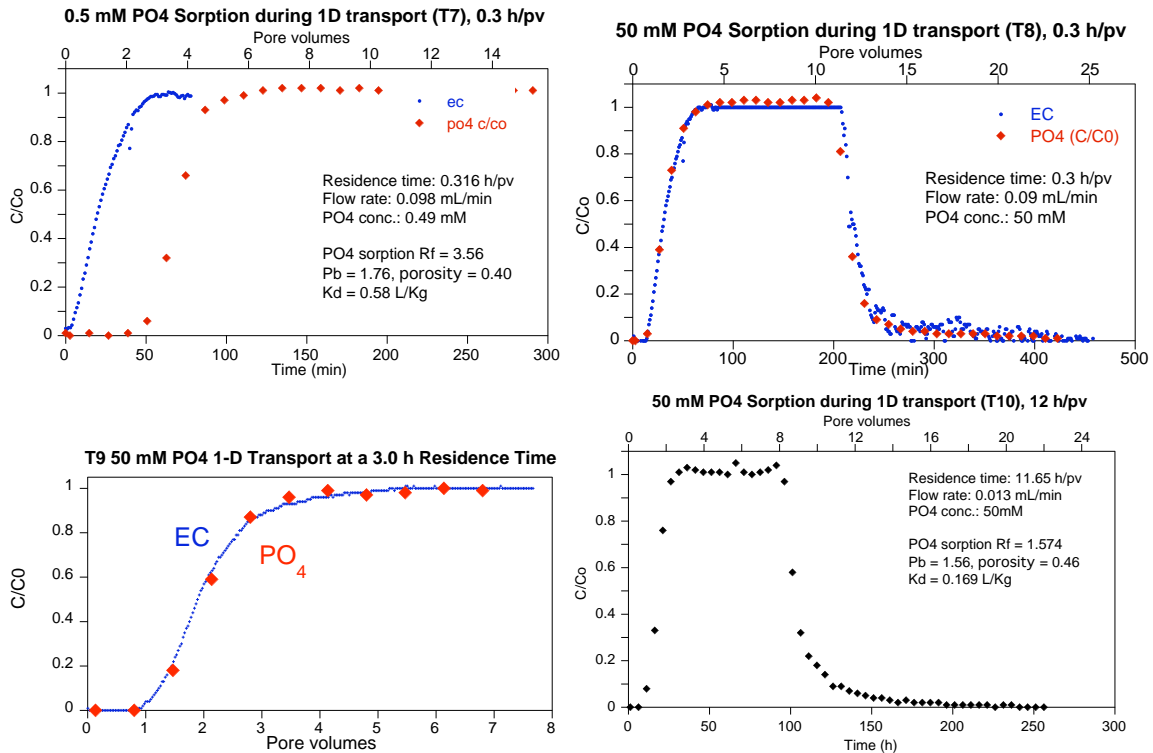


Figure 5.60. Na-PO₄ injection at different contact times: a) 0.5 mM PO₄, 19 minutes residence time, b) 50 mM PO₄ at 18-minute residence time, c) 50 mM PO₄ at a 3-h residence time, and d) 50 mM PO₄ at a 12-h residence time.

sorption, as PO_4 lagged a tracer, and the breakthrough concentration was equal to the injection concentration. At a vastly greater PO_4 concentration (50 mM or 5000 mg/L), which will eventually exceed the number of sorption sites (Figure 5.61b) showed no sorption lag. These results are predictable from the sorption isotherm. At a longer residence time, the 50 mM PO_4 injection at 3-h and 12-h residence time still showed no lag and no precipitation (Figure 5.60c and d), although it may be difficult to measure small amounts of precipitate at these high concentrations.

Injection of Na-PO_4 at field-relevant concentrations (0.6 mM, 2.6 mM, and 10 mM, Figures 5.61 and 5.62) at field-relevant flow rates to achieve 3- to 7-h residence times was conducted in 1-meter long sediment columns. For these experiments, breakthrough of PO_4 , Ca, and Sr was measured. For the injection of Na-PO_4 at 0.63 mM and 2.6 mM concentration, the monovalent injection solution resulted in stronger Ca and Sr exchange to the sediment, so these concentrations actually decreased during initial solution breakthrough. Phosphate breakthrough exhibited an initial lag (sorption) and a final breakthrough concentration less than the injected concentration (precipitation), although the experiments were terminated at 15 h and 37 h, so a steady-state concentration was not reached. These results indicated that both sorption and precipitation of PO_4 would be observed in field injections (which was the case).

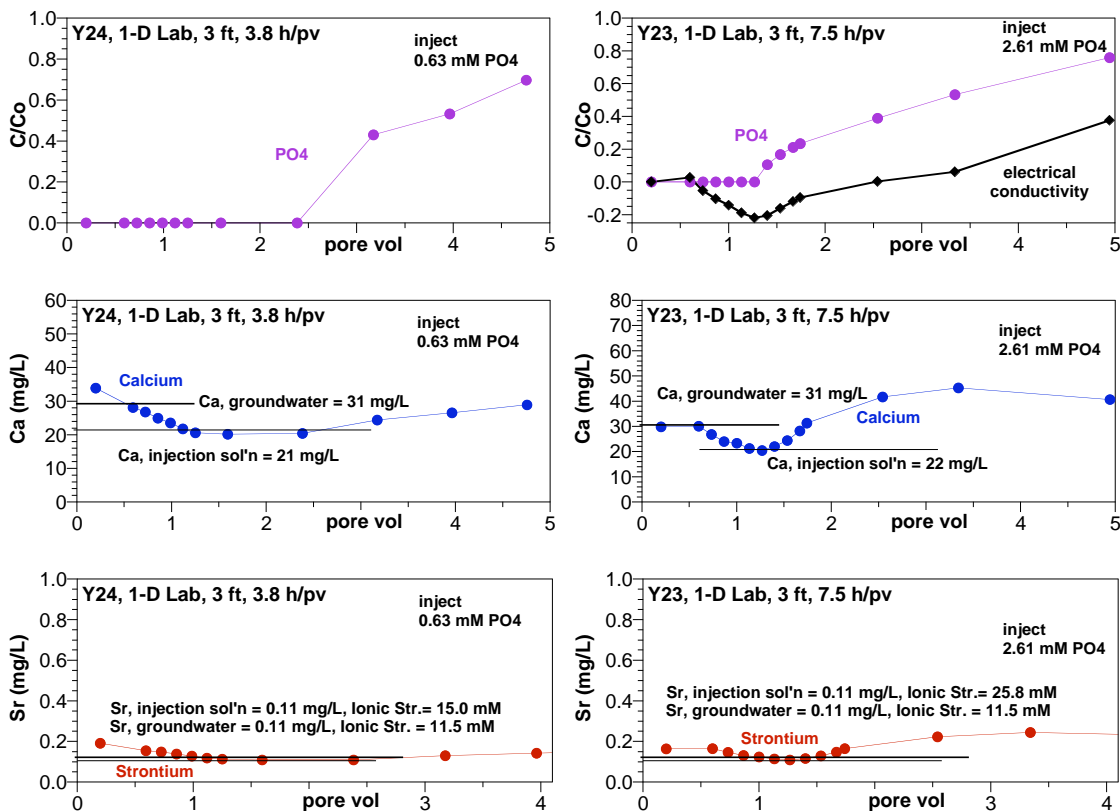


Figure 5.61. Injection of a) 0.63 mM Na-PO_4 and b) 2.61 mM Na-PO_4 with PO_4 , Ca, and Sr behavior shown.

In a final Na-PO₄ injection experiment, 10 mM was injected (Figure 5.62). In this case, the ionic strength of the injected solution (66 mM) was sufficiently greater than the groundwater that was in equilibrium with the sediment (11 mM), and even though the injection solution did not contain divalent cations, some Na exchange onto the sediment occurred. The result of the ion exchange was that Ca and Sr breakthrough peaked at ~3x the initial value, as Na⁺ replaced some Ca²⁺ and Sr²⁺ on the sediment ion exchange sites. Phosphate breakthrough at this relatively rapid residence time (3.4 h) showed somewhat less sorption (Rf ~ 1.5), which is consistent with the sorption isotherm with less sorption nearer the sorption maxima. Simulation of the ion exchange, precipitation, and solution speciation reactions that occurred in this experiment were simulated (Section 5.9.5).

In conclusion, the injection of Na-PO₄ results in a time-dependent PO₄ sorption and time-dependent PO₄ precipitation. The apparent sorption results in retardation factors ranging from 1.0 to 2.4 (average PO₄ Rf = 2.0 ± 1.1). This is an apparent K_d = 0.433 ± 0.248 cm³/g (apparent as it may include sorption and precipitation mass removal from solution).

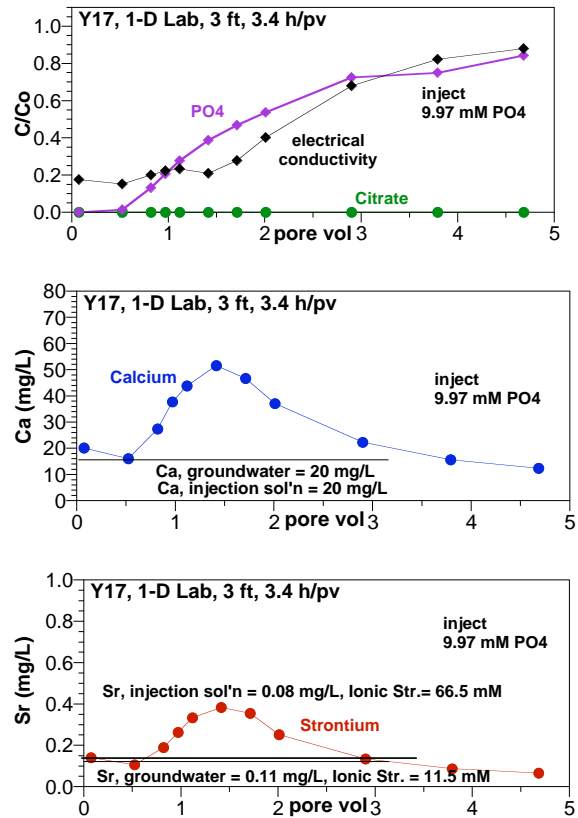


Figure 5.62. Injection of 10 mM Na-PO₄ with PO₄, Ca, and Sr behavior shown.

5.8 Alternate Injection Strategy: Sequential Injection of PO₄ and Ca-Citrate-PO₄

Alternate injection strategies have been explored to determine if a change in the injection sequence of apatite forming chemicals or changes in the concentration of individual components could improve the remediation of Sr by in-situ precipitation of apatite. All wells in the 100-N Area have had one complete injection of either Ca-Citrate-Phosphate (4-10-2.4 mM) or (1-2.5-10 mM). The sequence of chemical addition controls the reactions that take place and hence the phase and solubility of the resulting precipitates formed. Batch experiments using Hanford groundwater (0.10 mg/L Sr, 19.03 mg/L Ca) and 100-N sediment with a solid/water ratio of 2.5-5.1 were used to determine the fate of Ca and Sr using two isotopic tracers (Sr-90 and Ca-45).

5.8.1 PO₄ Addition Then Ca-Citrate-PO₄

The possibility of adding a PO₄ only solution first followed by a Ca-Cit-PO₄ mix was investigated since this would allow for a higher concentration of PO₄ addition with a much lower increase in ionic strength (the effects of which have previously been discussed in Section 5.6). The sequential addition of solutions was broken up into two individual batch experiments whereby the first step, PO₄ addition, was left in contact with the sediment for one week then sacrificed for analysis. The second batch experiment underwent the same treatment as the first but at the end of one week a Ca-Cit-PO₄ solution was added and left for four weeks then analyzed. The aqueous residual fraction of Ca and Sr were determined by liquid scintillation and then the sediment was extracted three times with 0.5 M KNO₃ and finally with 4 M HNO₃ to determine the fraction of permanently incorporated Ca and Sr. The permanently incorporated fraction of the Sr and Ca is a result of the co-precipitation of Sr and Ca during apatite formation and incorporation of Sr into the crystal structure once the apatite has formed. The amount of Sr permanently removed by incorporation being less significant due to the duration and scale of the batch experiments. The fraction of Sr and Ca remaining in solution after one week contact with an 8.38 mM phosphate solution was very low and compares well with the results obtained for the solution mix used for field injection #3 (line 1, Table 5.27). The ion-exchangeable, which is not permanently sequestered, and the acid extraction (permanently sequestered) fraction of this system were the same as field injection #3 to #18. Based on these results there does not appear to be any benefit of adding either calcium or citrate to the low ionic strength injection solution, by omitting these species the ionic strength of the injection solution would be lower and more phosphate could be added. The amount of phosphate that could be added would depend on the amount and how fast precipitates form, given that these experiments were batch experiments effects on pore volume are not considered. The addition of 10 mM citrate with only 2.4 mM of phosphate gave similar results to both the phosphate (8.38 mM) only and field injection #3 (1-2.5-10 mM) systems (line 6, Table 5.27). The residual Ca concentration after the 100-N field injections was observed to be 4 mM, by adding 10 mM with 2.4 mM phosphate the formation of apatite should be favored over other phosphate species. With the addition of citrate, the potential of pore space plugging would be reduced allowing the formation of apatite over a larger area. The objective of using sequential injections is to increase the amount of apatite emplaced in the sediment while minimizing the transportation of contaminants due to desorption/ion-exchange resulting from the addition of higher ionic strength solutions. The addition of the second

solution, Ca-Cit-PO₄ (14-35-8.38 mM; line 2, Table 5.27), left to react 4 weeks to allow the citrate to degrade and the apatite to form resulted in an 8% increase in the permanently sequestered Sr with only 5% aqueous Sr present.

While the PO₄ only injection did result in some Sr-90 incorporation, it appeared to be half as efficient as injecting Ca-citrate-PO₄. After injecting 8 mM PO₄ (line 1, Table 5.27), 14% of the Sr-90 was incorporated in apatite. In contrast, injecting a Ca-citrate-PO₄ solution containing only 4 mM PO₄ (line 4, Table 5.27), 13.7% of the Sr-90 was incorporated. Injection of Citrate-PO₄ alone (line 3, Table 5.27) appeared most efficient, as 2.4 mM PO₄ sequestered 16% of the Sr-90.

Table 5.27. Distribution of calcium and strontium from alternate injection strategies in 100-N sediment.

PO ₄ Application Description	total PO ₄	Aqueous		Sorbed (ion exch.)		Incorporated in Apatite		Sr-90 incorporated per mM PO ₄
		Ca-45 (fraction)	Sr-90 (fraction)	Ca-45 (fraction)	Sr-90 (fraction)	Ca-45 (fraction)	Sr-90 (fraction)	
Sequential PO ₄ , then Ca-citrate-PO ₄								
1) 8.34 mM PO ₄ , 1 week	8.34	0.015	0.011	0.851	0.848	0.134	0.141	0.0169
2) Ca-Cit-PO ₄ (14-35-8.38 mM) 4 weeks	16.7	0.15	0.09	0.63	0.70	0.22	0.21	0.0126
Citrate-PO ₄ only (no Ca addition)								
Cit-PO ₄ (10-2.4 mM) 3 weeks	2.4	0.051	0.068	0.815	0.769	0.134	0.163	0.0679
Sequential Ca-citrate-PO ₄ , then PO ₄								
1) Ca-Cit-PO ₄ (7-17.5-4.19) 2 weeks	4.2	0.076	0.056	0.736	0.807	0.189	0.137	0.0326
2) 8.38 mM PO ₄ 3 weeks	12.6	0.061	0.045	0.728	0.778	0.211	0.178	0.0141
Sequential low conc., high conc. Ca-citrate-PO ₄								
1)*Ca-Cit-PO ₄ (1-2.5-10 mM) 2weeks	10	0.016	0.019	0.892	0.839	0.092	0.142	0.0142
2) Ca-Cit-PO ₄ (28-70-16.8 mM) 2 weeks	26.8	0.187	0.186	0.643	0.52	0.17	0.293	0.0109
Ca-citrate-PO ₄ only (high conc.)								
Ca-Cit-PO ₄ (28-70-16.75) 5 weeks	16.8	0.111	0.086	0.508	0.657	0.381	0.256	0.0152

* Injection #3 solution

5.8.2 Ca-Citrate-PO₄ Addition Then PO₄

The possibility of adding phosphate second in the sequential injection series was also investigated. Again the batch experiments were broken up into two steps with the first solution left in contact with the sediment for 2 weeks to allow for citrate degradation and apatite formation. Due to ionic strength constraints a Ca-Cit-PO₄ (7-17.5-4.19 mM; lines 4 and 5, Table 5.27) mix was chosen. If we compare this addition to field injection #3 both systems resulted in the same amount of permanently sequestered Sr with a slight higher residual Sr²⁺ concentration. The addition of 8.38 mM phosphate, left in contact with the sediment for 3 weeks, increased the permanently sequestered Sr by 4%. Given that the objective is to increase the amount of apatite emplaced in the sediment this injection order is less effective than the addition of phosphate followed by a Ca-Cit-PO₄ mix. Principally due to the fact that the second solution added can be of higher concentration resulting in the formation of more apatite.

A final comparison of these sequential injections was to injecting only a high concentration Ca-citrate-PO₄ solution (line 8, Table 5.27) or sequential low, then high concentration Ca-citrate-PO₄ solutions (lines 6 and 7, Table 5.27). In general, use of PO₄ only results in a lower Sr-90 fraction incorporation per mM of PO₄ used (last column, Table 5.27), whereas low concentrations of Ca-citrate-PO₄ solutions result in twice the incorporation fraction (line 4 versus line 1). The solution used in field injections #3 to #18 (1 mM Ca, 2.5 mM citrate, 10 mM PO₄) has little citrate, so has an incorporation efficiency (line 6) roughly that of PO₄ only. However, high concentration Ca-citrate-PO₄ solutions (as a single high concentration or sequential low, then

high concentration) resulted in a low fraction incorporation (lines 7 and 8, Table 5.27). This may be caused by the limited 4- to 5-week time of the experiments (i.e., the citrate was not entirely degraded, keeping the PO₄ in solution) or the high ionic strength could maintain Sr-90 in solution. The greatest incorporation efficiency was actually a citrate-PO₄ solution that contained no Ca (line 3, Table 5.27). Further studies are needed to determine the cause(s) of the differences in the Sr-90 incorporation.

5.9 Vadose Zone Application: Infiltration of Ca-Citrate-PO₄

A number of experiments were conducted with Ca-citrate-PO₄ solutions to determine applicability of this technology to an infiltration application, on a DOE/EM-22 funded project.

5.9.1 Citrate Biodegradation and Water Content

Because the observed anaerobic citrate degradation products (acetate and formate) could possibly interfere or hinder the formation of apatite the extent of citrate mineralization in 100-N sediments was investigated over a range of conditions, including initial citrate concentrations, percent of sediment water saturation, sediment depth and biomass. All experiments were performed under initially aerobic conditions.

Mineralization of ¹⁴C-labeled citrate was examined over a range of initial citrate concentrations (5, 25 and 125 mM) and percent water saturation of the composite 100-N sediment (35 to 100%) at 20°C to 22°C. These Ca-citrate-PO₄ solutions contained the exact proportions of constituents to form citrate (i.e., Table 3.1, solutions similar to field injection #1).

A 5-mM citrate solution (i.e., 2 mM Ca, 5 mM citrate, 1.2 mM PO₄) in contact with the 100-N sediment at differing water content showed a weak trend of increasing water content and mineralization rate and extent. The very lowest water content (35%) had the slowest citrate mineralization rate (Figure 5.63a), whereas most of the higher water saturations showed greater mineralization extent with a slightly faster rate. Comparison of the actual citrate mineralization rate (as a half-life) and extent as a function of water saturation (Figure 5.64) for this low Ca-citrate-PO₄ concentration data does show the trend indicated in the raw experimental data: a) slower citrate mineralization rates at lower water saturation, and b) lower mineralization extent at lower water saturation. This low Ca-citrate-PO₄

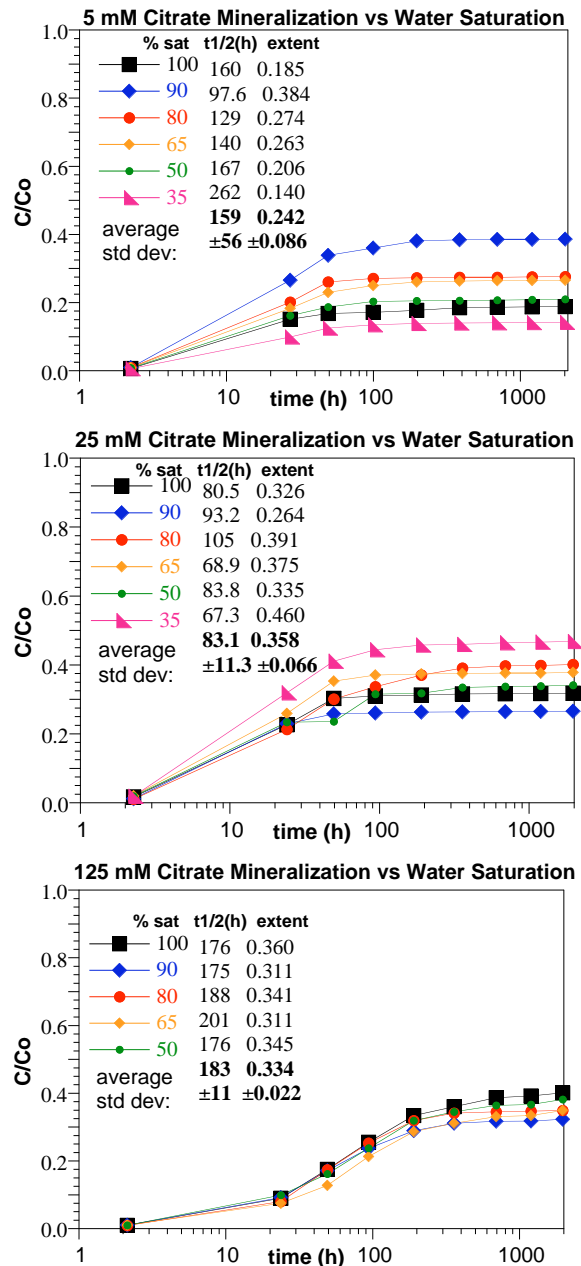


Figure 5.63. Citrate mineralization at different water saturations with: a) 5 mM, b) 25 mM, and c) 125 mM citrate in Ca-citrate-PO₄ solutions.

concentration solution is more likely the first solution that would be infiltrated at the field scale. The experimental data suggests that higher water saturations would produce better results (i.e., greater and more rapid citrate mineralization, so greater and more rapid apatite precipitation). Higher (nearly saturated) water conditions may also be required to drive the system anaerobic, which may be needed for the most rapid apatite formation. Infiltration simulations (Section 5.9.5) certainly show that more rapid infiltration rates achieve higher water saturations, even at steady state.

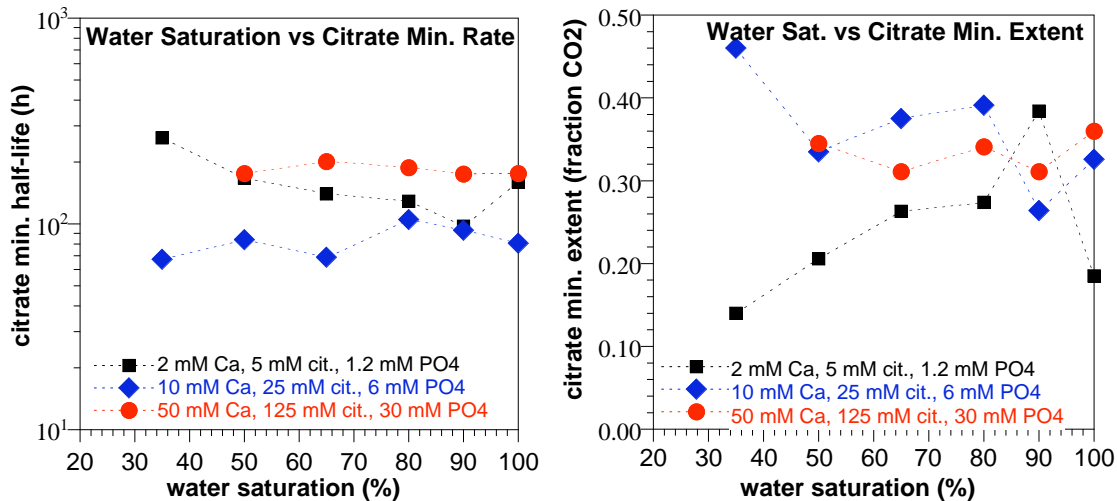


Figure 5.64. Correlation between water saturation and citrate mineralization half-life (a) and extent (b).

Infiltration of a higher concentration Ca-citrate-PO₄ solution (10 mM Ca, 25 mM citrate, 6 mM PO₄) actually shows a rough inverse trend compared with the low concentration solution. Citrate mineralization was slightly more rapid at lower water saturation (Figure 5.64a) and the mineralization extent was greater at lower water saturation (Figure 5.64b). Infiltration of a very high concentration Ca-citrate-PO₄ solution (50 mM Ca, 125 mM citrate, 30 mM PO₄) showed essentially the same mineralization rate and extent at different water saturation.

In conclusion, citrate mineralization studies at water saturations from 35% to 100% showed that the mineralization rate (expressed as a half-life) only varied by a factor of 4 (i.e., 80 h to 300 h) for all experiments at citrate concentrations ranging from 5 mM to 125 mM. Citrate mineralization rates generally did not show a consistent trend with water saturation. Citrate mineralization extent, however, was significantly greater for higher citrate concentrations (30% to 50%) and lower for 5 mM citrate (extent 15% to 26%). The most rapid mineralization rates were at the intermediate citrate concentration (25 mM) with an average mineralization half-life of 83 h, as opposed to 159 h (5 mM citrate) and 183 h (125 mM citrate). High citrate concentrations may be causing some toxic effects (and lower rates). Mineralization extent also did not show a consistent trend with water saturation, although there was generally a trend of higher mineralization extent with lower water saturation. Mineralization extent averaged 33% to 36% for 25 mM and 125 mM citrate concentrations (all water contents), with lower extent for the 5 mM citrate (24%). Water saturated systems generally drive the system anaerobic, resulting in citrate degradation to formate and acetate (incomplete degradation) with the lack of oxygen. It is possible that low water saturation experiments maintain sufficient oxygen for mineralization.

Application of these studies to the field scale need to consider that the infiltrating water will likely contain a significant microbial population, as at the field scale, injection water is typically composed of concentrated solutions diluted with river water. In all, the laboratory studies showed that citrate is degraded and mineralized under greatly differing conditions of citrate concentration and water saturation with less variability than expected.

5.9.2 Citrate Mineralization and Biomass in Sediments

The spatial variations in microbial population and citrate mineralization at the 100-N site was investigated as a function of depth and location in sediments from monitoring and injection wells along the Columbia River shoreline at the 100-N remediation site. The microbial population in sediment samples from three wells decreased with increasing depth (Figure 5.65). Populations per gram of sediment, reported as cell equivalents or colony forming units (cfu), decreased by 5 orders of magnitude in these wells and were higher in the Hanford formation than in the deeper Ringold formation.

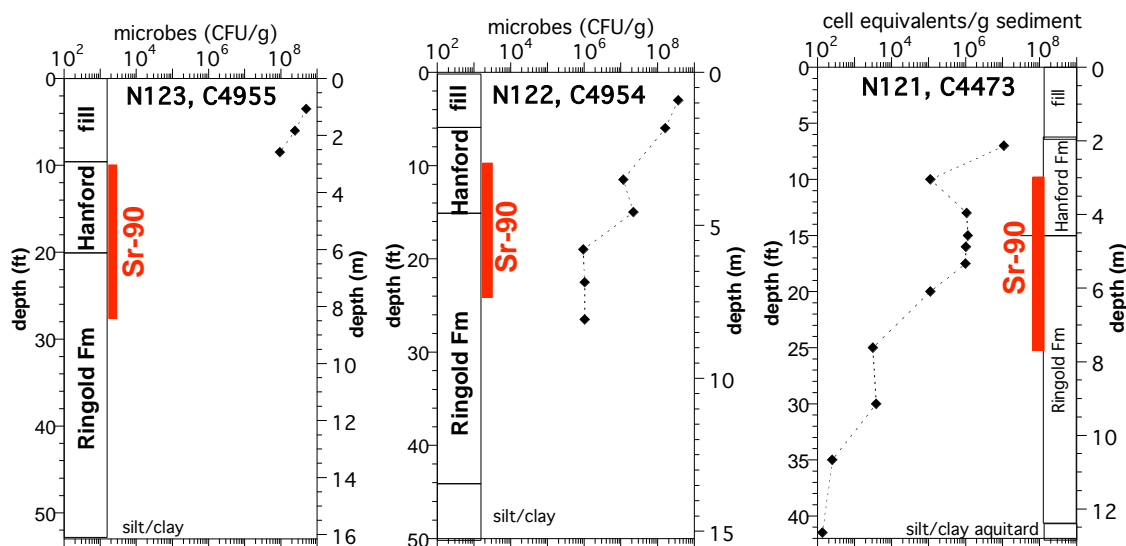


Figure 5.65. Microbial distribution with depth in 100-N wells.

Citrate mineralization was measured in suspensions of sediments taken from different depth intervals from these wells. Experiments were conducted with a Ca-citrate- PO_4 solution (2 mM, 5 mM, 2.4 mM) solution (Figure 5.66). The citrate mineralization rate showed a modest correlation ($R=0.52$) with the microbial density (cfu/ml) measured in the sediment suspensions used in these experiments (Figure 5.66), with generally slower rates (to 733 h half-life) at very low populations and the highest rates (46 h half-life) with higher microbial populations. The correlation of the mineralization half-life versus biomass (Figure 5.67a) shows that while biomass in sediments changed five orders of magnitude, the mineralization half-life only changed about one order of magnitude.

The extent of mineralization varied from 3% to 80% with an average of 23%. The important point to note here is that the half-life is a slowly varying function of microbial density. That is, with almost a 10^5 difference in microbial density in these 100-N sediments the resultant citrate

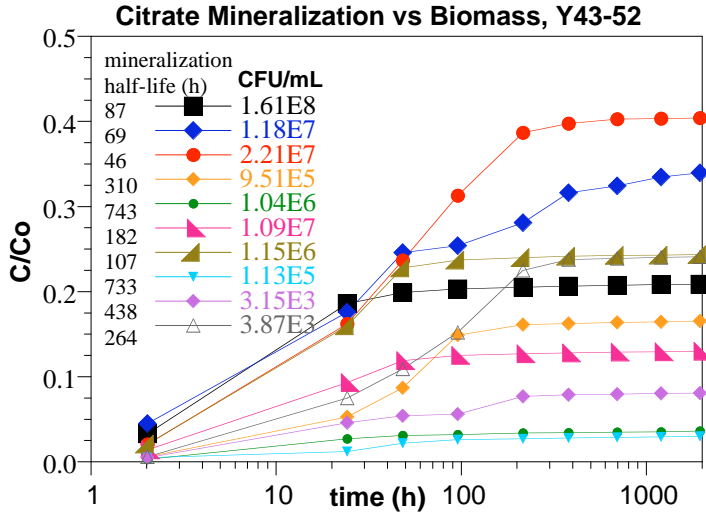


Figure 5.66. Citrate mineralization and biomass.

mineralization half-life only varied from 69 to 743 h, a little over a factor of 10, with very little correlation with microbial population (Figure 5.67b).

The spatial variability in the extent and half-life of citrate mineralization was examined in depth composites (6 to 16 ft) of Hanford formation sediments from 10 injection wells (C5042 – C5051) and two monitoring well (C4955 and C5116) along the shoreline of the 100-N remediation site. The extent and half-lives were also measured as a function of depth in two additional wells in this area. The

extent of mineralization ranged from 8% to 17% with an average of 15% (Figure 5.66a) and the half-lives varied between 97 and 473 h with an average of 263 h (Figure 5.66b). Although the microbial densities in these experiments were not determined, the average extent and half-lives were within the range of those where microbial densities had been determined. Thus, for a wide range of depths and locations at the 100-N site the extent and rate of mineralization is not strongly dependent on microbial density. Degradation and mineralization of citrate injected into the shallow Hanford formation with higher microbial densities will not be so great as to preclude citrate migration to the deeper and/or far distant regions of the proposed treatment zone. As a result a larger, more uniform spatial distribution of apatite formation will occur along the groundwater flow path than if degradation was strongly dependent on microbial population density.

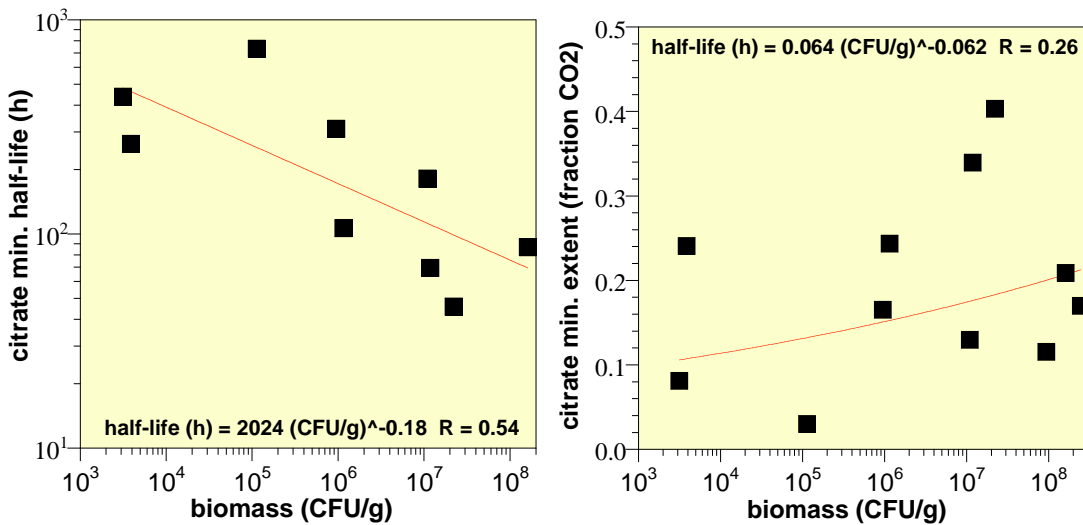


Figure 5.67. Sediment biomass relationship to citrate mineralization rate (a) and mineralization extent (b).

The likely cause of the relative uniformity of the citrate biodegradation rate in sediments that varied 5 orders of magnitude in biomass may be due to the biomass of microbes injected. In field injection experiments, 5% concentrated Ca-citrate-PO₄ chemicals (by volume, see Sections 5.2, 5.3, and 5.4) are injected with 95% river water (by volume), and the 10⁷ cfu/mL (in sediment equivalent to 2 x 10⁶ cfu/g) in the river water varies from an insignificant amount of mass relative to the 10⁸ cfu/g (shallow sediment) to a significant amount of mass for deep sediment (with 10⁴ cfu/g). Microbes attach by multiple and dynamic mechanisms, so when injected are not evenly distributed in the subsurface (or during infiltration). For these simple batch laboratory experiments, the biomass in the infiltration water is evenly distributed throughout the sediment.

5.9.3 1-D Infiltration of Ca-citrate-PO₄ Solutions

Numerous 1-D water-saturated experiments have been conducted in which a Ca-citrate-PO₄ solution has been injected into Hanford sediment. This section describes EM-22-funded experiments in which the Ca-citrate-PO₄ solution is vertically infiltrating into a 1-D sediment column at low water saturation. The purpose of these experiments is: a) determine if the citrate biodegradation/apatite precipitation reaction rates can be predicted from previous batch studies (i.e., scale up of batch results to high sediment/water ratios in columns with advective flow), b) quantify the resulting spatial distribution of apatite and determine if changes in the infiltration strategy (i.e., infiltration rate, chemical composition) can be used to change the apatite spatial distribution, and c) quantify the short- and long-term effect on Sr mobility from the infiltration solution and subsequent incorporation into apatite. All of these processes were previously investigated in water saturated batch and 1-D column systems, but the vadose zone transport may create differences. In water-saturated systems after dissolved oxygen is consumed, the anaerobic microbial system degrades citrate to formate and acetate (Section 5.1.2), whereas in a system with excess oxygen, citrate degradation proceeds more quickly to CO₂. The high excess of CO₂ in the oxic systems may result in the formation of some CaCO₃ along with Ca-phosphates, whereas in anaerobic systems with significantly less carbonate present, fairly high purity apatite is formed (inorganic carbon content 0.02%). In addition, the physical transport of the Ca-citrate-PO₄ solution is more challenging to control in the vadose zone compared with hydraulic head controlled transport in the saturated zone.

Several different 1-D column systems were used for infiltration experiments. Some 1-D column experimental systems used in these experiments consisted of both simple 1-D columns (50-cm length, 1.5-cm diameter) with no sampling along the length of the column (Figure 5.68a). In these columns, the apatite precipitate mass was quantified by two methods: a) a 10-pore-volume flush of groundwater after the infiltration experiment was used to elude PO₄ that did not precipitate, and b) PO₄ extractions on sediment samples taken along the length of the column after the infiltration experiment. For some 1-D experiments, a more sophisticated column apparatus was used (Figure 5.68b) which enabled additional characterization: a) nonintrusive water content measurement of the moisture front during the experiment by gamma attenuation, and b) sampling ports along the length of the column. This 1-D and a 2-D experimental apparatus (described in the following section) were designed by M. Oostrom in the Subsurface Environmental Research Laboratory in EMSL with funding from both the EM-22 project and an EMSL-funded project.

The phosphate breakthrough curves showed that varying the infiltration rate by only an order of magnitude (0.4 to 4 cm/h) did not change the amount of PO₄ precipitate (76%, Figure 5.69 and 5.70). In each case 8-10 mM of PO₄ was injected into the column and 2 to 2.4 mM of PO₄ was eluted. These results are not surprising, given that the infiltration time scale did not significantly change between experiments. The PO₄ extraction from the 10 samples for each sediment column showed a possible trend of increasing precipitate with depth (Figure 5.70), but with considerable variability. This PO₄ extraction consisted of a 3.0 g sediment sample extracted for 15 minutes with 0.5M HNO₃. The method is currently still under development (Section 5.5). The amount of PO₄ extracted from the sediment is much higher than the detection limits, but the amount of apatite added results in a very low PO₄ extraction concentration. There are some mineral phases that dissolved in the HNO₃ and elude PO₄, so the background PO₄ from the sediment with no added PO₄ is high.

The phosphate profiles might indicate an increase in precipitated PO₄ with depth, but there is too much variability in the data to draw

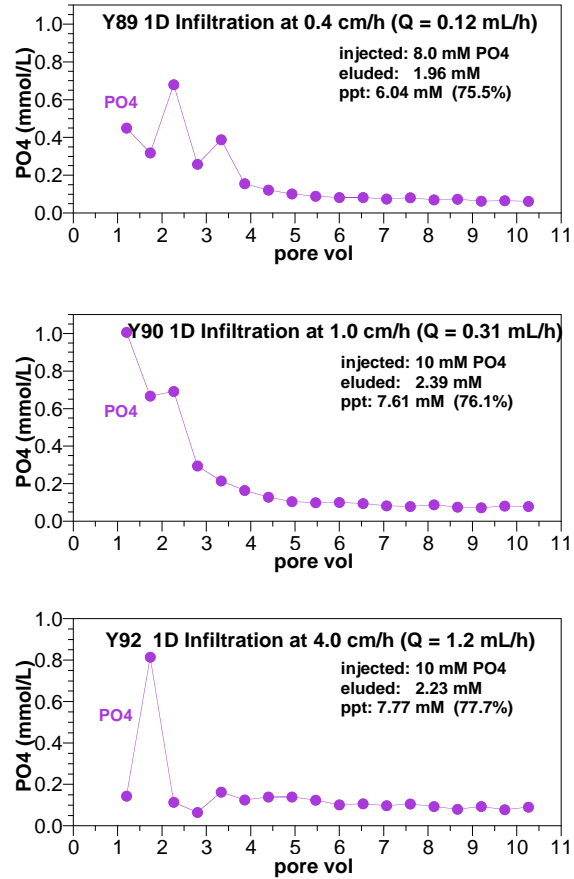


Figure 5.69. 1-D unsaturated column experiments varying the infiltration rate with PO₄ breakthrough mass shown.

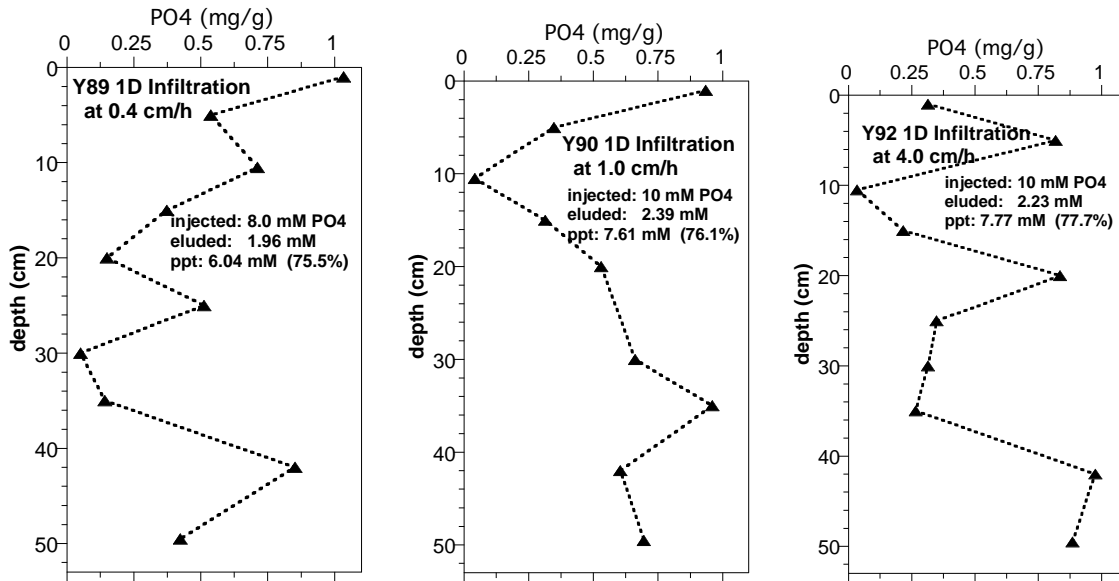


Figure 5.70. 1-D unsaturated column experiments varying the infiltration rate with PO₄ profile in the column after the experiment shown.

conclusions. At the high sediment/water ratio in the columns, the 10 mM PO₄ precipitating in the pore space should theoretically result in 0.38 mg apatite/g of sediment, or about 0.21 mg PO₄/g apatite. The background PO₄ from the sediment is about 1 mg PO₄/g sediment, so this amount represents about 20% of the background (i.e., a small signal with large background). This technique is being refined, and while it may work for cases with a much greater mass of apatite precipitated, it may not provide accurate numbers for these low amounts of PO₄ precipitate.

One additional 1-D infiltration experiment was conducted with a higher solution concentration (2 mM Ca, 5 mM citrate, and 20 mM PO₄, experiment Y91, Figure 5.71) at the same infiltration rate as experiment Y90 (Figure 5.69 and 5.70). The PO₄ breakthrough curve showed that 90% of the PO₄ injected precipitated (i.e., only 10% was eluted, Figure 5.71). In this case, the amount of PO₄ precipitated per gram of sediment was about 40% of the background PO₄ from the sediment, and the vertical profile in the 50-cm long column (Figure 5.71b) did show increasing PO₄ with increasing depth. Uniform apatite precipitate would result in 0.42 mg PO₄/g of sediment. The profile shows that PO₄ varies from a relatively uniform 0.25 mg PO₄/g sediment for the upper 30 cm, then increases to 1.0 mg PO₄/g sediment for the last 10 cm. Currently, the cause of this apparent PO₄ increase with depth is not known. It is hypothesized that more of the solution could have been present in the lower portion of the column. Moisture content measurements of the sediment column, however, does not support this hypothesis. This column showed a relatively high uniform water content for the upper 45 cm of the column (14.6% water content), with the lowest 5 cm at a slightly lower water content (11.2%), so the moisture levels do not correspond to the PO₄ mass change (which occurs from 35 cm to 50 cm depth). An alternate hypothesis is that microbes are transported with the infiltration front (i.e., higher ionic strength solution will desorb microbes off surfaces), so there could be a higher microbial population in the lower portion of the sediment column. Subsequent experiments will investigate this hypothesis.

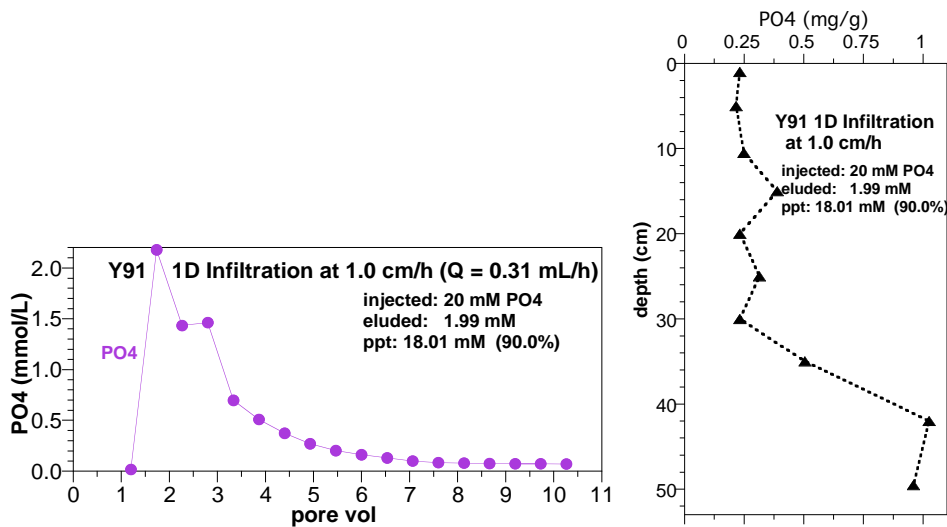


Figure 5.71. 1-D unsaturated column experiments of high PO₄ injection concentration showing a) PO₄ breakthrough, and b) PO₄ precipitate profile with depth.

5.9.4 2-D Infiltration Experiments of Ca-Citrate-PO₄ Solutions

2-D experiments were initiated to quantify Ca-citrate-PO₄ solution infiltration and spatial variability of apatite precipitate vertically (as in 1-D studies) and also laterally. The overall goal of the infiltration studies is to develop an infiltration strategy (i.e., constant or varying flow rate, concentration, etc.) to effectively precipitate apatite in desired locations. In general, an even apatite precipitate distribution is desired. However, vertical profiles of the apatite distribution (Figure 1.3) show 50% to 70% of the Sr-90 located in the more permeable Hanford formation, which overlies the remaining Sr-90 mass in the upper 10 to 15 ft of the Ringold Formation. During most of the year, the groundwater level is roughly at the Ringold/Hanford contact, although during spring runoff (high river stage), the water table is a few feet into the Hanford formation. Therefore, the zone of expected Ca-citrate-PO₄ treatment by infiltration is essentially the lower half of the vadose zone, as illustrated in Figure 5.72.

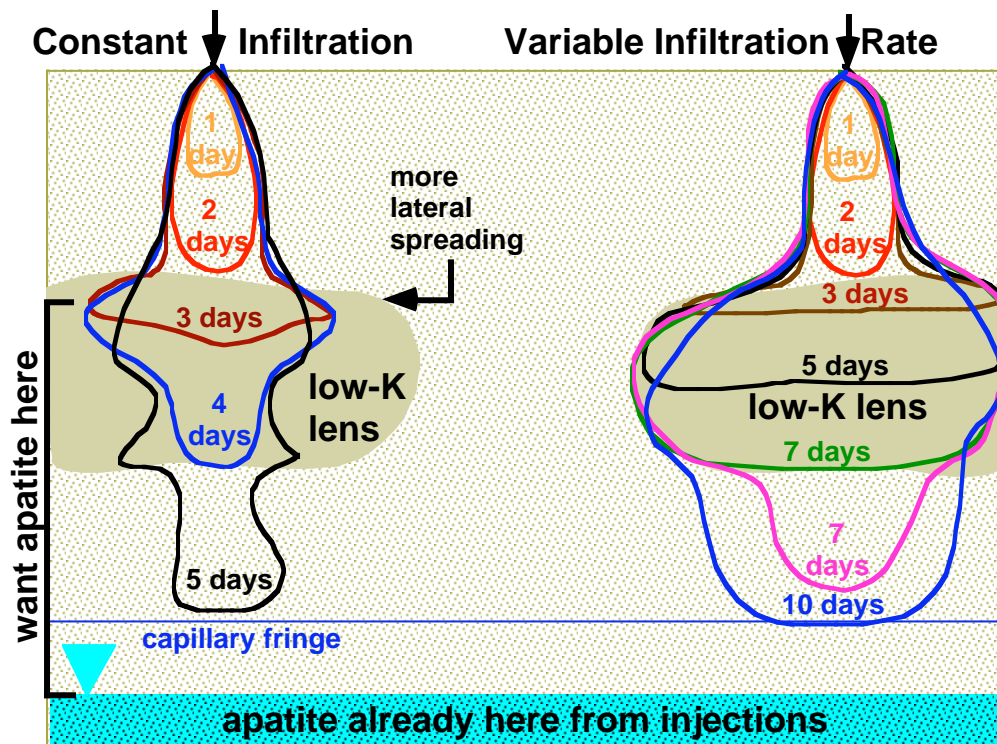


Figure 5.72. Conceptual profiles for 2-D infiltration into an area with a low hydraulic conductivity zone.

As the river (and aquifer) water level rises, additional Sr-90 mass enters the aquifer in some wells, as shown in Figure 1.4, likely due to Sr-90 entrapped in pore water in the vadose zone. Over the decades of these water level change cycles, some Sr-90 mass in the vadose zone has leached away, although it is hypothesized that there is a higher proportion of Sr-90 mass in low hydraulic conductivity layers in the vadose zone, due simply to lower leaching rates. Therefore, 2-D experiments are focused on delivering a relatively even Ca-citrate-PO₄ solution in low-K layers, and underneath low-K layers.

A concept (Figure 5.71) illustrates that variation in the infiltration rate can be used to vary the amount of lateral spread of the Ca-citrate-PO₄ solution, thereby changing the spatial distribution of the precipitate.

A 2-D visualization experiment was conducted to demonstrate the process of varying the infiltration rate of a solution to achieve solution coverage in desired areas (Figure 5.73). Constant infiltration rate into homogeneous and heterogeneous (low-K lens) are shown in the left panel. Infiltration at a constant rate results in some lateral spreading and slower infiltration through the low-K layer. By the last time picture (bottom left), the solution has infiltrated through the low-K unit, but not all the low-K unit was saturated with the solution. In addition, the area underneath the low-K unit did not receive uniform solution coverage (red arrows). In contrast, by varying the infiltration rate (Figure 5.73, right panels), all of the low-K unit was saturated with the infiltrating solution and nearly all the area under the low-K unit was also saturated (blue arrows, bottom right panel). To achieve this spatial solution coverage, the rate of infiltration of the solution was actually slowed during the time period when the solution was infiltrating within the low-K unit (second and third right panels) to allow sufficient time for lateral transport at lower water saturation. Once the solution had nearly saturated the low-K lens with some solution, the infiltration rate was now increased significantly to exceed the infiltration rate of the low-K unit, thereby forcing lateral transport of water at high saturation across the top of the low-K unit and down the sides (fourth down, right panel). This resulted in multiple locations that were infiltrating into the sediment under the low-K lens.

The most significant challenge to implementing a field infiltration strategy is overcoming or compensating for the effects of heterogeneities, which will influence the resulting spatial distribution of precipitated apatite. While beyond the scope of the funded EM-22 project, field infiltration rate (and solution concentration) can be varied to minimize the impact of high-K and low-K bedding that occurs in the Hanford 100-N Area sediments by using surface geophysical methods to monitor the infiltration front in real time. Because heterogeneities in the 100-N Area sediments have length scales ranging from feet to 10s of feet (e.g., buried braided stream channels), the first step would be to conduct a relatively large-scale line-source infiltration experiment (50 to 75 ft long). Infiltration should be monitored using both neutron probes and surface electrical resistivity tomography (ERT), which will enable us to map the 3-D infiltration front during the experiments. A surface ground-penetrating radar survey should also be conducted prior to field experiments to help guide the selection of locations for sampling and neutron probe placement. During the experiments, the infiltration rate would then be altered, as needed, to minimize the impacts of subsurface heterogeneities (e.g., lateral diversion due to capillary barrier effects). The overall goal is to have continuous and relatively uniform apatite precipitation in the lower half of the vadose zone (i.e., where the Sr-90 is).

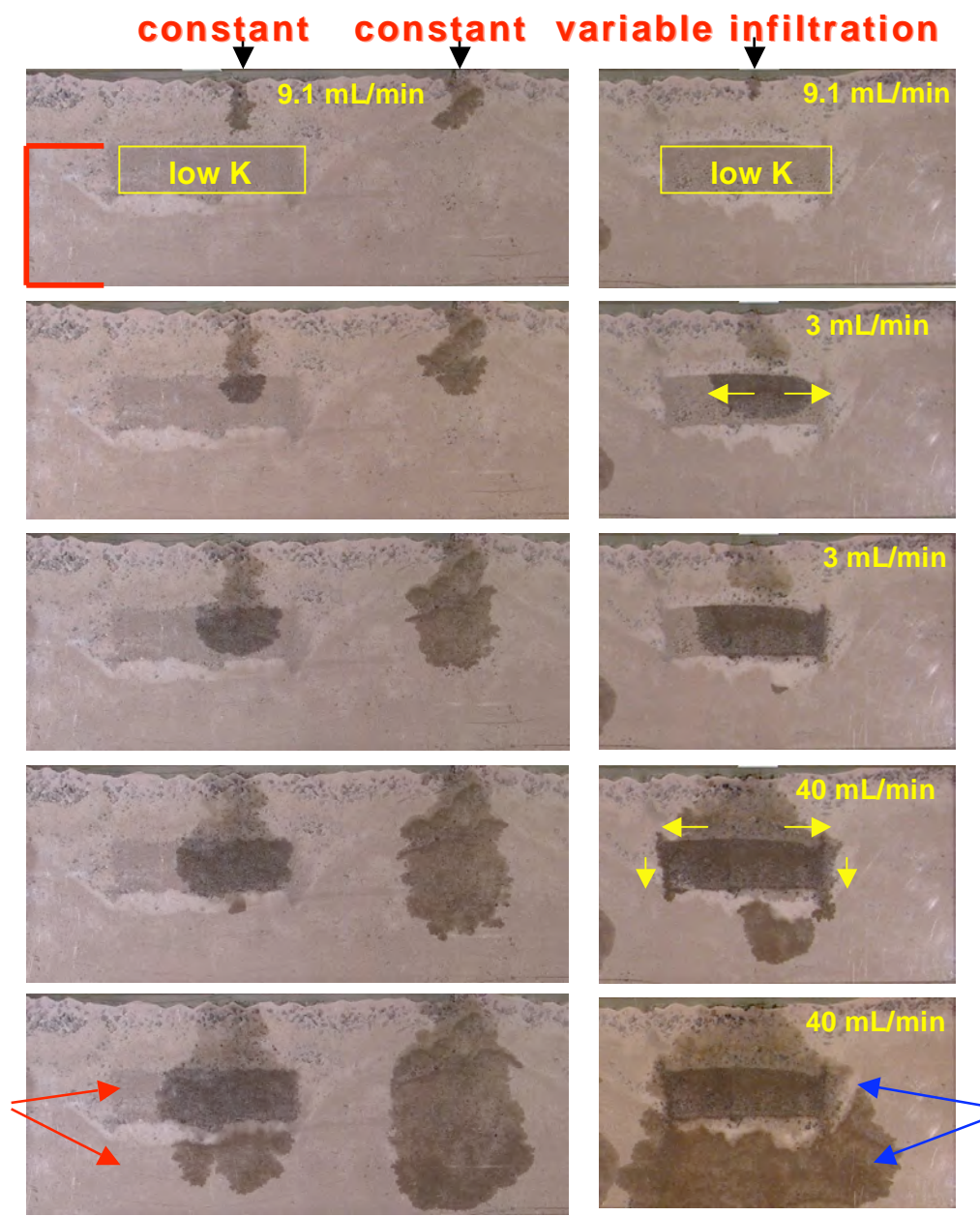


Figure 5.73. Conceptual profiles for 2-D infiltration into an area with a low hydraulic conductivity zone.

To date, four quantitative 2-D experiments have been conducted with infiltration of the Ca-citrate- PO_4 solution into a system containing a low-K lens. Simulation of the initial conditions of the system and the final steady-state water content (Figure 5.74) show higher water content within the low-K lens developing as well as some lateral spreading. The lower portion of the 2-D system at high water saturation represents the water table with a few centimeters of a capillary fringe.

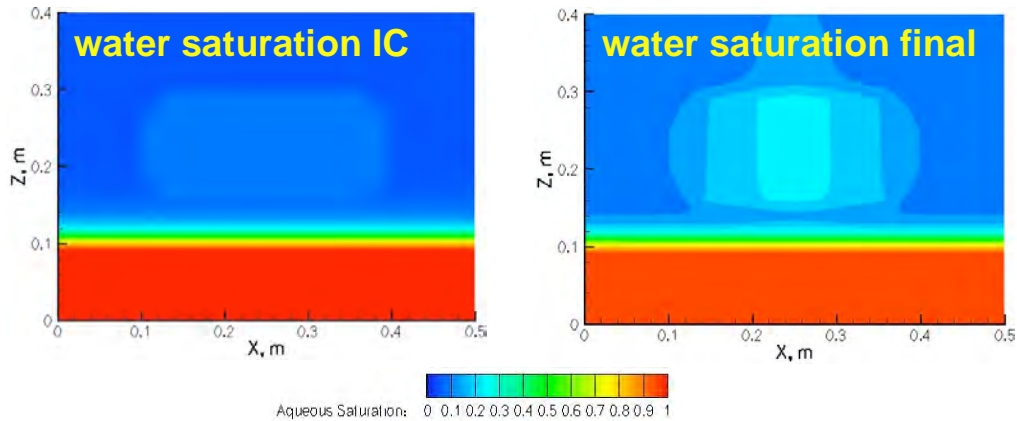


Figure 5.74. Presimulation of 2-D solution infiltration into a heterogeneous system.

A picture of dye injection into the 2-D system after experiment #3 was completed (Figure 5.75) clearly shows the lateral spreading that occurs in the finer sediments of the low-K zone, then necked down infiltration below the low-K zone.



Figure 5.75. Dye injection into a 2-D system illustrating water infiltration patterns.

The movement of the blue dye toward the left in the water saturated zone is caused by the slow groundwater movement toward the left. Water transport in the 2-D experiment was quantified nonintrusively using an automated gamma attenuation system (shown in Figure 5.68b) in the EMSL subsurface transport laboratory. A comparison of the data obtained in a vertical transect down the center of the low-K unit (Figure 5.76) to simulations conducted for the initial and steady state condition show fairly good agreement for this transect. Some fingering was observed in the natural sediment, which resulted in more irregular lateral movement within the low-K lens.

The presence of the Ca-citrate- PO_4 solution in specific subsurface zones does not directly translate to an even distribution of apatite precipitate forming. Additional processes of the citrate biodegradation rate and apatite precipitation rate understood in smaller scale experiments will be incorporated into future 2-D experiments.

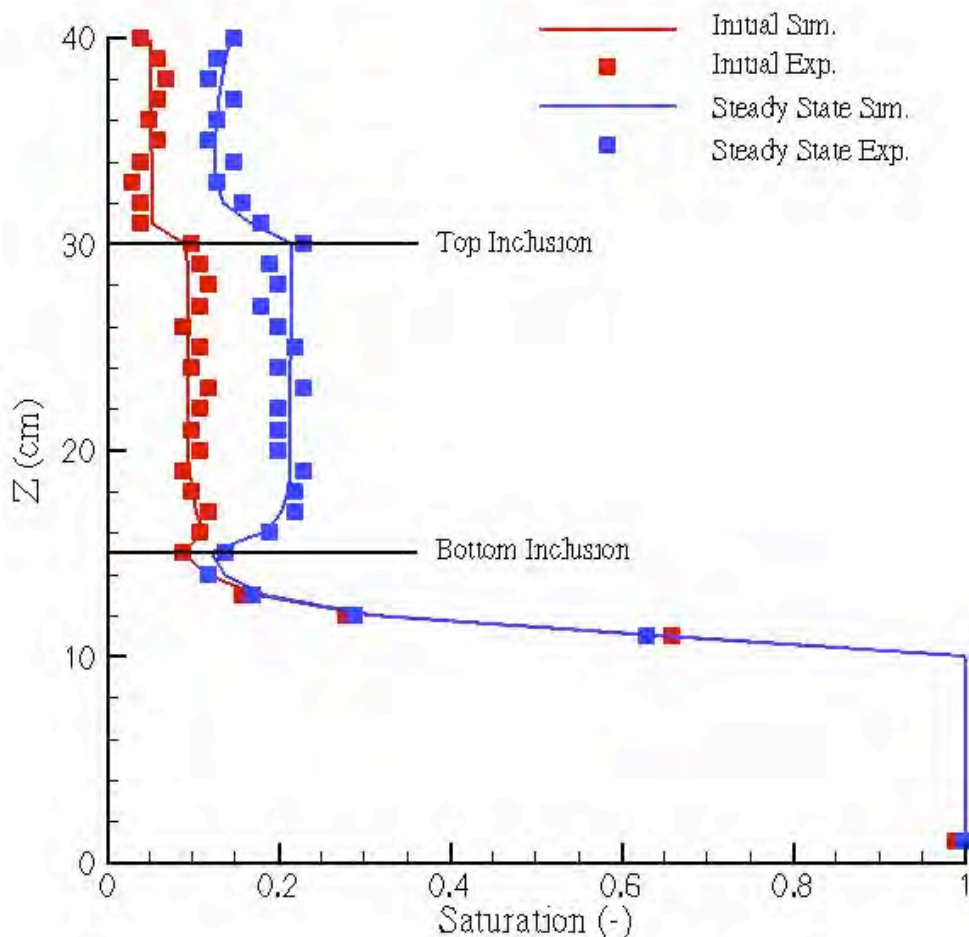


Figure 5.76. Comparison of water content data from 2-D experiment #3 (red and blue squares) to simulation (lines) for vertical transect down the center of the low-K zone.

A series of 2-D simulations were conducted to illustrate the relationship between the timing of apatite precipitate formation and the residence time in specific areas during infiltration of the Ca-citrate-PO₄ solution. The most spatially uniform apatite precipitate distribution will form when the residence time in a zone of sediment is roughly equal to the precipitation half-life. With significantly slower residence time, precipitate will form near the infiltration point, and with significantly more rapid infiltration, the solution will be advected out of the vadose zone into the saturated zone before precipitation occurs. The 2-D simulations were conducted with the Columbia River on the left (Figure 5.77, constant head boundary). As the solution infiltrates, some calcium desorbs and aqueous Ca²⁺ is pushed away from the PO₄, which infiltrates more slowly due to some sorption (Section 5.7.1). As the Ca-citrate complex biodegrades, Ca²⁺ is available, and zones with available Ca²⁺ and PO₄ for apatite precipitate (only laterally near the infiltration trench in this case). It should be noted that the series of reactions used for these infiltration simulations do not correctly account for ion exchange (Ca²⁺ assumed to be sorbed). In reality, the solution injection results in about 1.5% of the Ca²⁺ mass being advected out of the system (i.e., the majority of the Ca²⁺ remains on sediment ion exchange sites, as described in simulations in the following section. These simulations do, however, illustrate the concept of controlling the time scale of infiltration to match the time scale of precipitation to have a relatively even apatite precipitate distribution. Given the 48-h half-life for citrate biodegradation, setting the infiltration rate to achieve a few day residence time in the vadose zone (Figure 5.78, left panels) resulted in a relatively even spatial distribution of apatite. In contrast, a 10x greater infiltration rate (Figure 5.77, right panels) resulted in very rapid transport of the solution through the vadose zone with apatite precipitate forming only at the edges where there was sufficient residence time. In addition, much of the solution was flushed into the river.

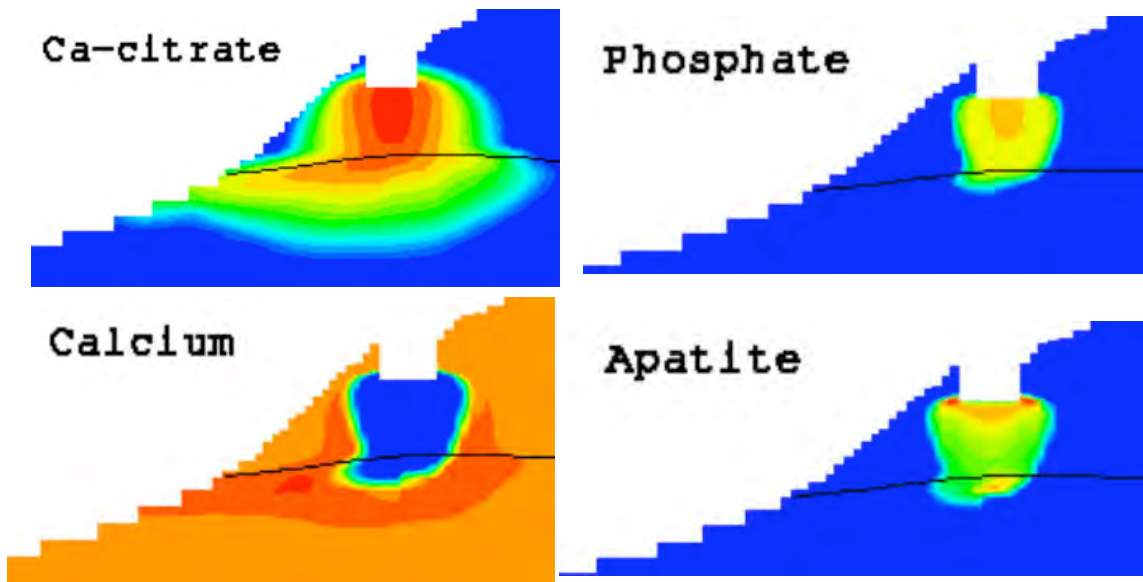


Figure 5.77. 2-D infiltration experiment showing infiltration of chemicals and eventual formation of apatite precipitate.

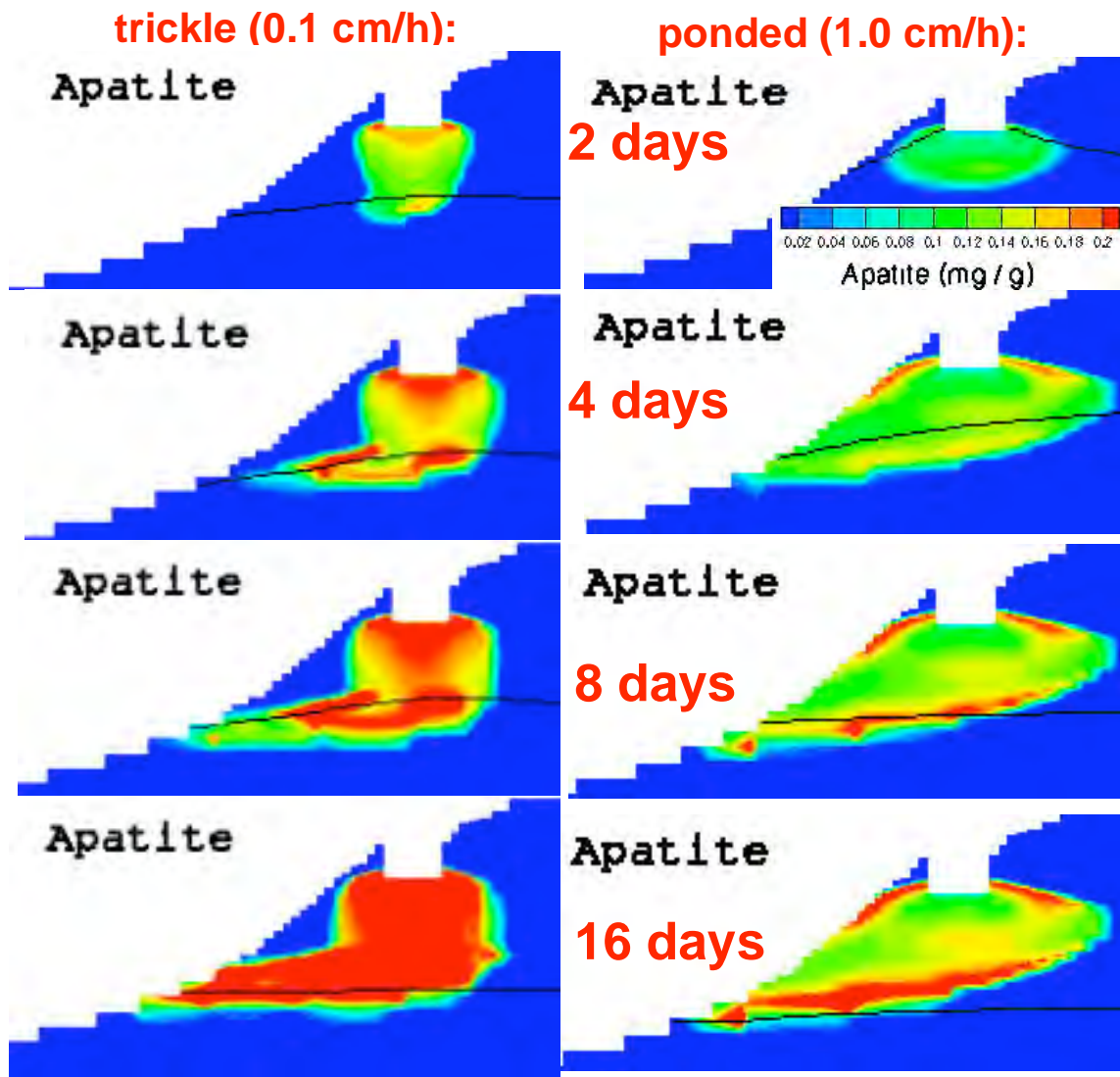


Figure 5.78. 2-D infiltration simulation effect of varying the infiltration rate on the apatite precipitate.

5.9.5 Simulation of Ca-Citrate-PO₄ or PO₄ Reactive Transport Experiments

A reactive transport model (STOMP) capable of 3-D unsaturated and saturated zone transport was modified with the series of reactions to account for metal-CO₃, -OH, -citrate and PO₄ aqueous speciation, cation exchange (Sr, Ca, Mg, Na, K, NH₄), citrate biodegradation, and solids precipitation/dissolution (apatite, CaCO₃, SrCO₃). This was ~42 reactions with 51 species. Simulation of 1-D injection of ammonium phosphate into a 1-meter long column (experiment Y17, Figure 5.79) with this highly complex model well fit the experimental data. Calcium and strontium peaks (~3x) by solution injection due to ion exchange, while appear large, actually account for an insignificant amount of Ca and Sr mass desorbing from the sediment ion exchange sites. Integration of the Sr mass desorbing (Figure 5.79b) relative to the mass on ion exchange sites (Figure 5.79d) shows that 3.1% of the Sr was removed by the injection process. The dip in Na sorbed to sediment (X-Na) resulted from the NH₄ replacing about 30% of the Na (NH₄ has a stronger affinity for the surface compared with Na).

Field simulations of field injections or hypothetical field infiltrations have not yet been conducted, but a similar mass balance of Sr-90 would be highly useful in projecting just how much Sr-90 is removed from the sediment during initial breakthrough of the injecting solution.

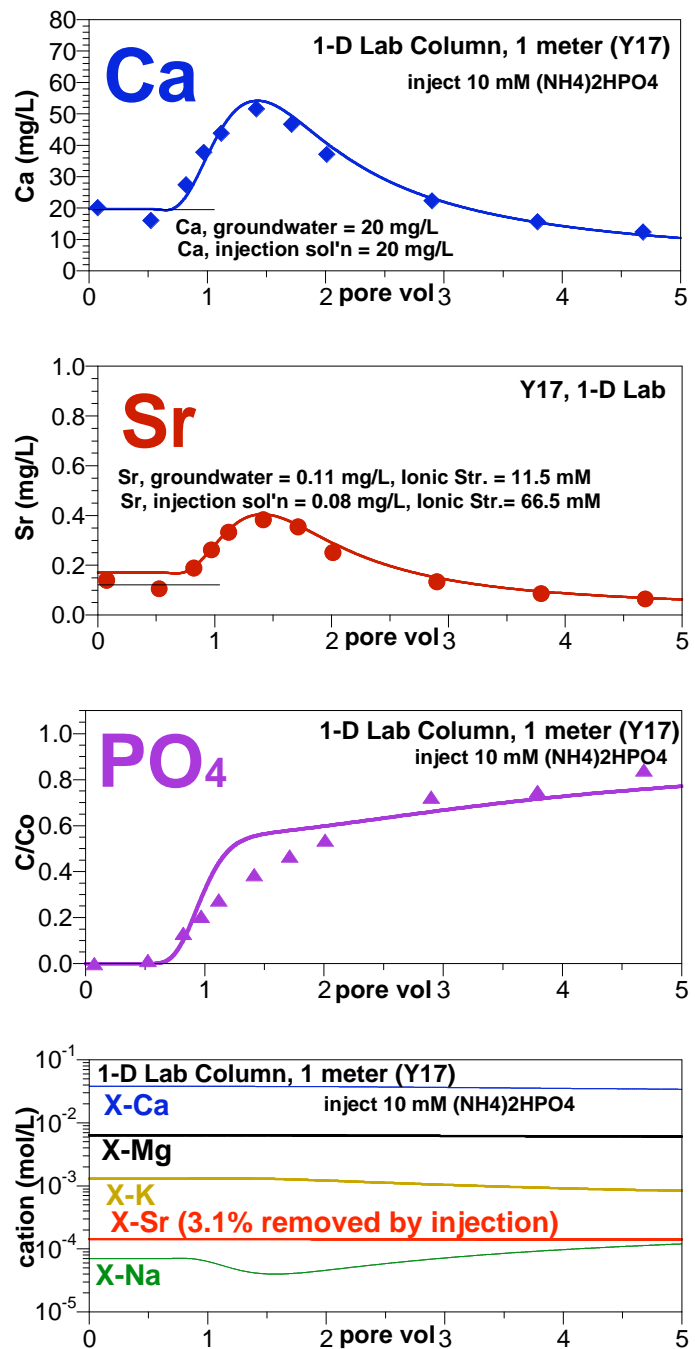


Figure 5.79. 1-D reactive transport simulation of a 1-meter sediment column injection of a PO₄ solution (experiment Y17).

Simulation of the injection of a Ca-citrate- PO_4 solution (1, 2.5, 10 mM) over a 31-day period (Figure 5.80, experiment Y88) also shows general agreement between the data and simulation of the multiple breakthrough species. In this experiment, the Ca-citrate- PO_4 solution was injected at a rapid rate to achieve a 6.9-h residence time for a total of 24 h or 3.5 pore volumes (similar to a field injection), followed by a 30-day slow flow rate injection of groundwater with a 453-h residence time (details in Section 5.4.1). This solution is similar in major component concentrations to field injections #3 to #18, but differs in the fact that this laboratory experiment used 20 mM NH_4^+ , whereas the field injection used 17.6 mM Na^+ and 1.0 mM NH_4^+ , to limit both N for microbes and also limit Ca^{2+} and Sr^{2+} ion exchange.

The experimental data shows Ca^{2+} (third panel, Figure 5.80) and Sr^{2+} (first panel) concentration during initial solution breakthrough at 5 to 10 h peaking at $\sim 6\times$ the equilibrium groundwater concentration. Phosphate breakthrough lags (green line, second panel), but apatite precipitation starts to occur in the 10 h to 100 h time frame, then decreases in extent. The final change that occurs in the system is at 800 h, when the large Na^+ pulse is eluded out of the system due to the slow groundwater injection, and Sr^{2+} and Ca^{2+} decrease, largely (in this case) due to ion exchange onto the sediment (not precipitation).

Simulation of 1-D and 2-D infiltration experiments with this reactive transport code are in progress. It is expected that these simulations will be used to plan some aspects of the 2-D experiments described in the previous section.

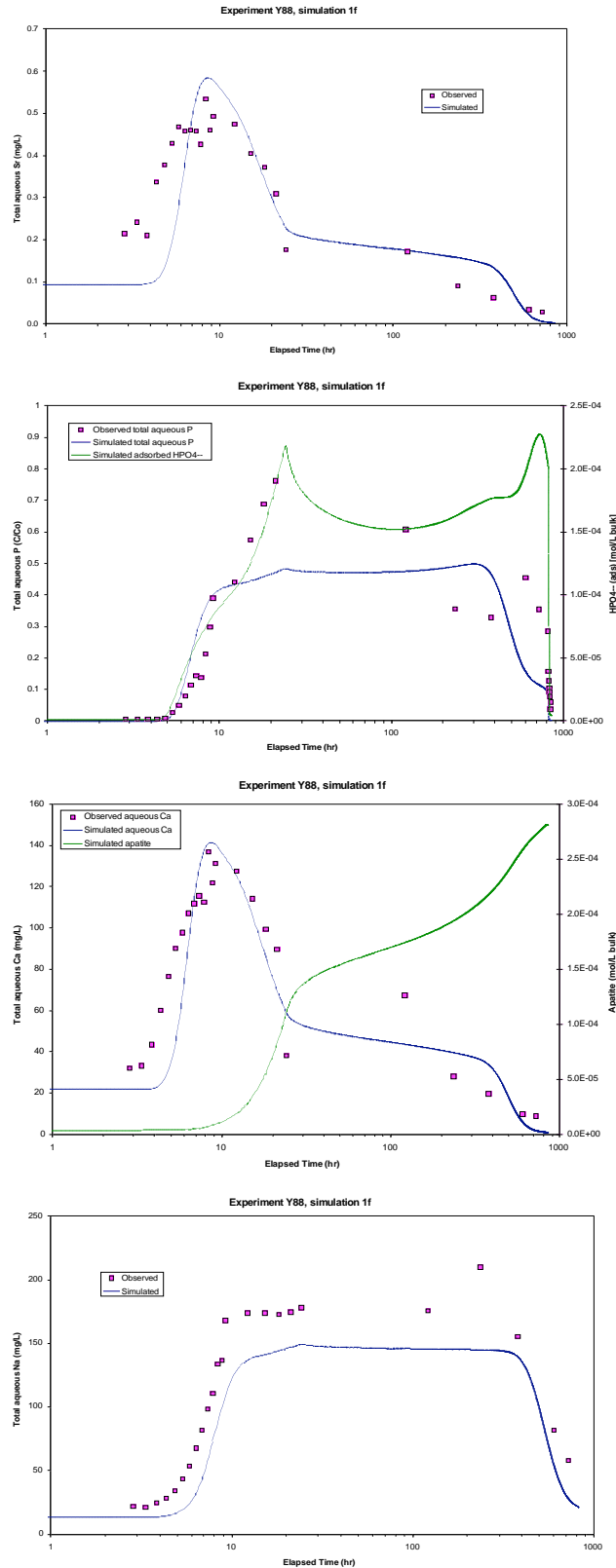


Figure 5.80. Simulation of 1-D injection of a Ca-citrate- PO_4 solution (experiment Y88, similar to field #3 to 18).

6.0 Summary

This report summarizes laboratory-scale studies investigating the remediation of Sr-90 in Hanford 100-N sediments by the use of a Ca-citrate-PO₄ solution to form apatite precipitate, which incorporates the Sr-90 in its structure. Although Sr-90 is retained strongly on subsurface sediments by ion exchange (99% sorbed, <1% in groundwater), this sorbed mass is slowly migrating into the Columbia River so is still considered mobile. In addition, physical and chemical processes occurring in the 100-N Area create conditions of varying Sr-90 concentration in groundwater. First, seasonal increases in the river (and groundwater) water level mobilize some Sr-90 in vadose zone sediments. Second, plumes of higher ionic strength water migrating through the 100-N Area easily mobilize some Sr-90 off sediments (by ion exchange). Emplacement of apatite in the 100-N subsurface results in strong sorption of Sr-90 (and Sr) onto the apatite surface, then slow apatite recrystallization of Sr-90 substitution for Ca in the apatite. This substitution occurs because Sr-apatite is thermodynamically more stable than Ca-apatite. Once the Sr-90 is in the apatite structure, Sr-90 will decay to Y-90 then Zr-90 without the potential for migration into the Columbia River. The use of the injection (or infiltration) of a Ca-citrate-PO₄ solution into subsurface sediments to form apatite is currently being used at field scale because it is a more economic means of delivering apatite precipitate to near-river shore subsurface sediments and involves less Sr-90 mobilization risk compared with trench-and-fill with solid phase apatite. The results of this study are summarized into two main sections of formation of apatite precipitate and incorporation of Sr-90 in apatite.

In situ apatite formation by this technology occurs by: 1) injection of Ca-PO₄-citrate solution (with a Ca-citrate solution complex), 2) in situ biodegradation of citrate which slowly releases the Ca required for apatite [Ca₆(PO₄)₁₀(OH)₂] precipitation (amorphous, then crystalline). Because the injection solution has a higher ionic strength compared to groundwater, some Sr and Sr-90 desorption from sediment occurs (i.e., Sr-90 in groundwater increases during injections). Therefore, a primary objective of the apatite formation studies is to come up with a method to deliver sufficient apatite into subsurface sediments, but minimize Sr-90 initial mobility. This can be accomplished by sequential injections of low, then high concentration Ca-citrate-PO₄ solutions. Injection of a low concentration Ca-citrate-PO₄ solution results in minimal Sr-90 mobilization (i.e., groundwater Sr-90 concentration increases <6 times relative to preinjection concentration), but results in a small amount of precipitate that over the course of a year will incorporate Sr-90 in the immediate injection area. Once most of the Sr-90 is incorporated, then one or more high concentration Ca-citrate-PO₄ solution injections are then used to increase the apatite mass in the subsurface but have minimal Sr-90 groundwater concentration increase.

6.1 Citrate Biodegradation Rate

Within a few days of Ca-citrate-PO₄ solution contact with sediment, biodegradation of the citrate occurs in both oxic and anoxic environments (Figure 6.1). Upon citrate biodegradation in aerobic systems (Figure 6.1a) and anaerobic systems (Figure 6.1b), the aqueous Ca²⁺ and PO₄ decrease, forming apatite and other Ca-PO₄ precipitates, which over several weeks recrystallize into apatite. In aerobic systems, citrate is mineralized (i.e., forms CO₂, Figure 6.1b), whereas in an anaerobic environment, citrate degrades to some lower molecular weight organic acids (acetate, formate; degradation pathway in Figure 5.7).

Citrate biodegradation is more rapid in an anaerobic environment, which is expected to occur in most groundwater injections, but both aerobic and anaerobic citrate biodegradation is expected to occur during solution infiltration. Citrate biodegradation rates determined from experiments conducted at different temperature and citrate concentration indicate that initial field injections (10 mM citrate, 15°C) should have a half-life of ~50 h. At higher concentration, the citrate biodegradation rate slows.

Citrate biodegradation depends on subsurface microbial activity, and there should be a direct correlation between the microbial biomass and the citrate biodegradation rate. As expected, microbial biomass decreased significantly with depth from 10⁸ cells/g at 6 ft depth to 10⁵ cells/g at a 25 ft depth to <10³ cells/g at a 40 ft depth (Figure 5.64). However, the citrate mineralization rate decreased only one order of magnitude for a five order of magnitude decrease in biomass (Figure 5.66), indicating likely significant control by another process. The likely cause of the relative uniformity of the citrate biodegradation rate in sediments that varied 5 orders of magnitude in biomass may be due to the biomass of microbes injected. In field injection experiments, 5% concentrated Ca-citrate-PO₄ chemicals (by volume, see Sections 5.2, 5.3, and 5.4) are injected with 95% river water (by volume), and the 10⁷ cfu/mL (in sediment equivalent to 2 x 10⁶ cfu/g) in the river water varies from an insignificant amount of mass relative to the 10⁸ cfu/g (shallow sediment) to a significant amount of mass for deep sediment (with 10⁴ cfu/g). Microbes attach by multiple and dynamic mechanisms, so when injected are not evenly distributed in the subsurface (or during infiltration). For these simple batch laboratory experiments, the biomass in the infiltration water is evenly distributed throughout the sediment. The net result is the citrate mineralization rate and extent (i.e., fraction CO₂ produced) decreased only slightly with depth, as shown by rates observed for sediments at specific depth intervals in five different boreholes (Figure 5.13 and 5.14). The citrate mineralization rate was also investigated in depth composites from ten different 100-N Area wells (Figure 5.12), which did not show significant variation (citrate mineralization half-life average 250 ± 114 h, range 133 h to 472 h), indicating there should be no significant trends with lateral distance along the injection barrier. The conclusion of

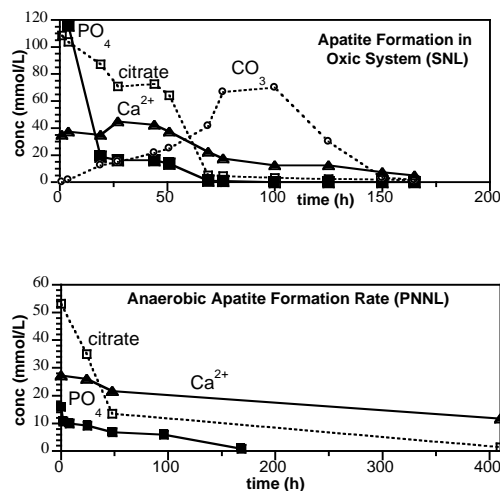


Figure 6.1. Citrate biodegradation in a) aerobic system and b) anaerobic system.

the citrate mineralization studies is there will be relatively uniform citrate degradation observed in field-scale injection at different locations and at different depth.

6.2 Injection of Ca-Citrate-PO₄ Solution: Apatite Precipitation and Sr-90 Mobility

Injection of different Ca-citrate-PO₄ solutions into sediment columns have shown differing apatite precipitation and Sr mobilization behavior depending on ion exchange reactions occurring and citrate degradation rates. The injection solution used in the latest field injections (#3 to #18) consisted of 10 mM PO₄ with 1 mM Ca and 2.5 mM citrate, is significantly deficient in Ca (a total of 16.7 mM needed to form apatite with 10 mM of PO₄). This 1-meter long laboratory column experiment was conducted to approximate field injected with initial Ca-citrate-PO₄ solution injection for 24 h followed by much slower groundwater injection for 30 days. Solution injection in this experiment resulted in the Sr peak (24 h) at 4.7x groundwater and Ca peak (24 h) at 4.5x groundwater (Figure 6.2). By 30 days, the aqueous Sr concentration was 0.28x groundwater and Ca 0.43x groundwater, as both Sr and Ca are used to form initial precipitates.

Simulation of the injection of a Ca-citrate-PO₄ solution (1, 2.5, 10 mM) over a 31-day period (Figure 5.79) also shows general agreement between the data and simulation of the multiple breakthrough species. This solution is similar in major component concentrations to field injections #3 to #18, but differs in the fact that this laboratory experiment used 20 mM NH₄⁺, whereas the field injection used 17.6 mM Na⁺ and 1.0 mM NH₄⁺, to limit both N for microbes and also limit Ca²⁺ and Sr²⁺ ion exchange.

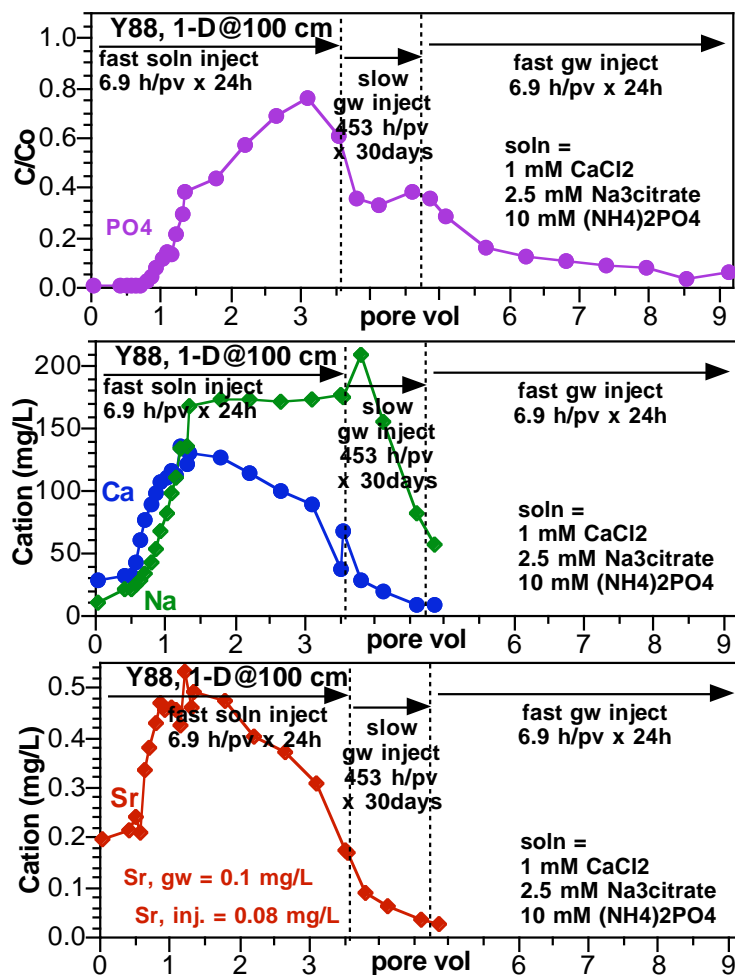


Figure 6.2. 1-meter long 1-D column experiment (Y88) with the injection of 1 mM Ca, 2.5 mM citrate, and 10 mM PO₄ with results of: a) PO₄ breakthrough, b) Ca, Na breakthrough, and c) Sr breakthrough.

6.3 Apatite Precipitate Characterization: Properties and Mass in Sediment

Different experimental techniques were used to identify the small amount of apatite precipitate that results from Ca-citrate- PO_4 injection into sediments. Field injections #1 and #2 (2.4 mM PO_4) should have ~0.1 mg apatite/g of sediment, whereas field injections #3 to #18 (10 mM PO_4) should have 0.4 mg apatite/g of sediment (Table 2.1). The final 300-year design capacity should have 3.4 mg apatite/g of sediment. Techniques have been used and are being developed on this project include: a) x-ray diffraction, b) scanning electron microscope with EDS and elemental detectors (Figure 6.3), c) acid dissolution of the sediment and phosphate measurement (i.e., aqueous PO_4 extraction, Figure 6.4), and d) fluorescence of substituted apatites. Results of these techniques are described below. Additional characterization techniques were used on the apatite precipitate to determine specific properties that included: a) BET surface area, b) FTIR scan to determine apatite crystallinity and change in crystallinity upon Sr substitution, and c) organic and inorganic carbon analysis. Some of these techniques overlap in application to determine the amount of Sr substitution in the apatite.

While the use of the electron microprobe shows that very small concentrations of apatite can be quantitatively identified, the cost of the process is significant, as is the time to process the samples. An example (Figure 6.3) shows 0.016 mg apatite/g of sediment with an EDS detector clearly identifying apatite precipitate outside mineral grains. One method involves the aqueous measurement of phosphate, after the apatite was dissolved in acidic solution, which does not

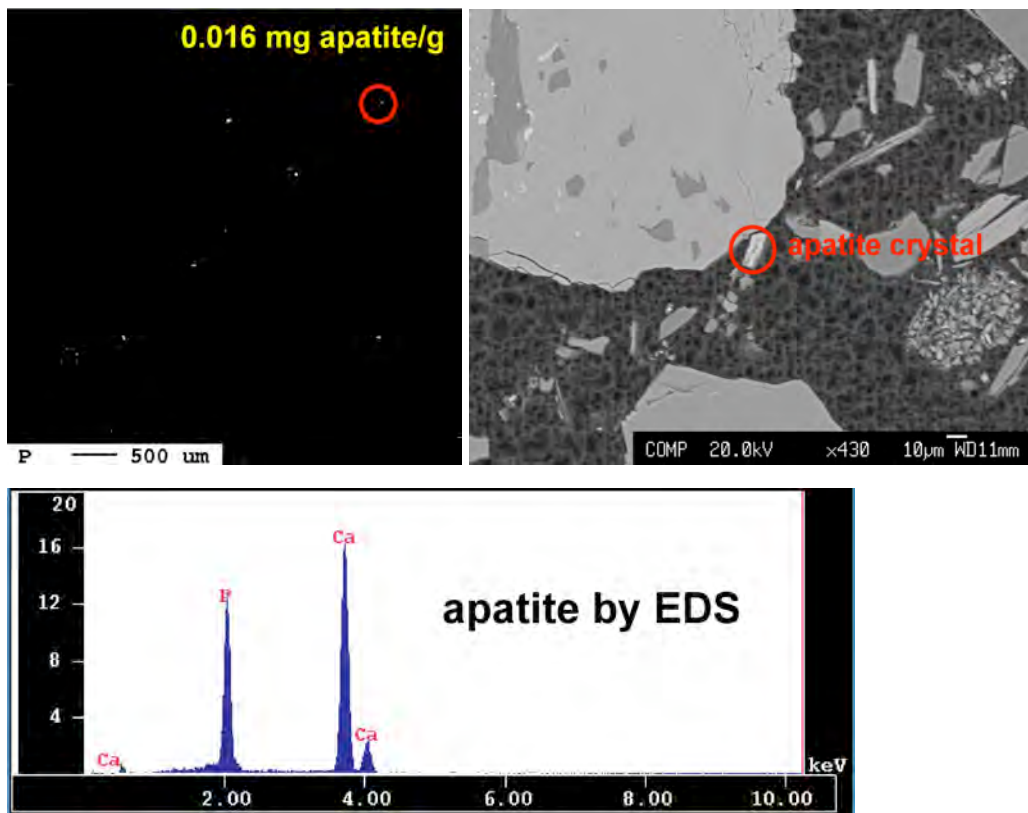


Figure 6.3. Scanning electron microscope images of a single apatite crystal.

have the low detection limits of the electron microprobe (Figure 6.4). Field injections #1 and #2, which resulted in a calculated 0.1 mg apatite/g of sediment are likely not detectable, but field injections #3 to #18 (calculated 0.4 mg apatite/g sediment) are likely detectable. A third method of measuring added apatite in sediment investigated was the use of fluorescence scans. While pure hydroxyapatite does not fluoresce, apatites with F or carbonate substitution do fluoresce. Apatite precipitated in groundwater (Figure 5.38, black line) does fluoresce, and the sediment sample (no apatite added, green line) does not. This method is still in development, and how low a concentration of substituted apatite cannot be measured as yet.

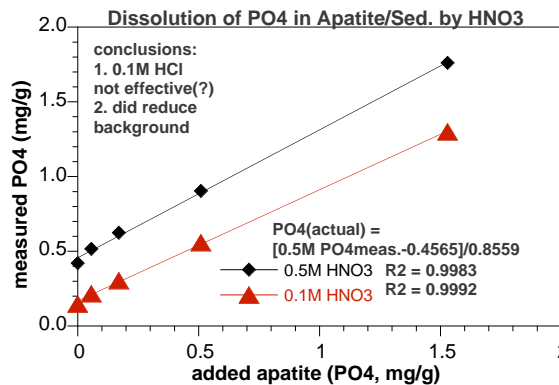


Figure 6.4. Aqueous phosphate measurement after 15-minute acid dissolution of apatite sediment mixtures using 0.1M or 0.5M HNO₃.

6.4 Sr-90 Incorporation Mass and Rate Into Apatite

Two factors control the amount of apatite needed to sequester Sr-90 in the Hanford 100-N Area. First, from a mass balance perspective, a specific amount of apatite is needed to remove all Sr and Sr-90 from groundwater over the next 300 years (i.e., 10 half lives of Sr-90 decay, half-life 29.1 years). This calculation is dependent on the crystal substitution of Sr for Ca in apatite. If 10% substitution is assumed, then 1.7 mg of apatite (per gram of sediment) is sufficient to sequester Sr and Sr-90 from the estimated 3300 pore volumes of water that will flow through an apatite-laden zone. Various experiments in this study have measured Sr substitution (for Ca in apatite) values of <1% to 16.3% after 9 months. There is a slower Sr substitution rate in more crystalline apatite, as shown by the 5.7% Sr in crystalline Sigma apatite versus 12.7% in the precipitated apatite under the same conditions. Apatite precipitated in sediment is less crystalline, which may lead to more rapid solid phase substitution.

The second factor that controls the amount of apatite needed to sequester Sr-90 is the rate of Sr-90 incorporation into apatite. This permeable reactive barrier concept of apatite solids in the aquifer works if the flux rate of Sr and Sr-90 is slower than the removal rate of Sr and Sr-90 by apatite. If the groundwater flow rate is too high, even highly sorbed Sr and Sr-90 could advect through the apatite-laden zone more quickly than it is removed. The way to circumvent this issue is to have additional apatite in the groundwater system to remove Sr-90 at the increased flux rate. Based on the experience in the 100-D Area where partially reduced sediment is slowly removing chromate (and nitrate), seasonal fluctuations in the river level lead to specific times of year when flow in the aquifer exceeded the chromate removal rate of the reduced sediment. Therefore, numerous experiments have been conducted in this study to clearly define the rate at which Sr and Sr-90 is incorporated into the crystal structure of apatite.

Sr-90 is incorporated into apatite by two mechanisms: a) during initial precipitation of apatite (time scale of days), and b) slow recrystallization of Sr-laden apatite (time scale of months to

years). Sr-90 incorporation in apatite is somewhat difficult to measure, as it needs to be separated from Sr-90 adsorption on sediment and Sr-90 adsorption onto apatite surfaces (both of which can be ion exchanged off the surfaces). The initial incorporation (Figure 6.5b, black triangles and circles) occurs within days and typically incorporates a fraction of the Sr-90 mass equal to the fraction Ca uptake in apatite (i.e., Ca and Sr and Sr-90 behave similarly). The Sr-90 incorporation rate into solid phase apatite is observed at times scales of months by: a) additional decrease in aqueous Sr-90 (Figure 6.5a, red triangles), b) decrease in adsorbed Sr-90 on sediment (Figure 6.5a, purple circles), c) decrease in Sr-90 sorbed on apatite (Figure 6.5a, blue diamonds), and d) increased Sr-90 in apatite (Figure 6.5a, green triangles and Figure 6.5b, black triangles and circles).

Simulation of Ca-Sr-Na ion exchange in sediment, Ca-Sr-Na ion exchange on apatite, and Sr incorporation in apatite was conducted to quantify the incorporation rate in this specific laboratory system (Figure 6.5a), then simulate the field system with a much higher sediment/water ratio (Figure 6.5b). Because Sr-90 incorporation is dependent on Sr-90 being sorbed to the apatite surface, it was hypothesized that the Sr-90 incorporation rate would slow with less Sr-90 sorbed on apatite. At high sediment/water ratios in field sediments, there is proportionally greater Sr-90 sorption on sediment relative to apatite (Table 5.22). For example, the laboratory experiment in Figure 6.5a (50 mL, 1 g sediment, 0.38 mg apatite, Table 5.22, line 7) shows 31% Sr-90 sorption on sediment, 6.4% sorption on apatite, and 61% aqueous Sr-90. In contrast, a comparable field system (1 g sediment 0.2 mL water [20% porosity, saturated], 0.38 mg apatite, Table 5.22, line 10) shows 97.2% Sr-90 mass sorbed on sediment, 2.0% sorbed on apatite, and 0.8% aqueous. This amount of apatite is equivalent to field injections #3 to #18. With the total amount of apatite estimated needed in the field (3.8 mg apatite per g of sediment), the Sr-90 sorption on apatite increases to 17%. A field scenario simulation (Figure 5.57) using the total apatite needed in the field showed the same time scale for Sr-90 incorporation into apatite as the laboratory experiment (Figure 6.5a). The reason for this lack of change is the relative time scales of ion exchange reactions versus the incorporation reaction being 5 to 6 orders of magnitude different. Any small amount of Sr sorbed on apatite is slowly

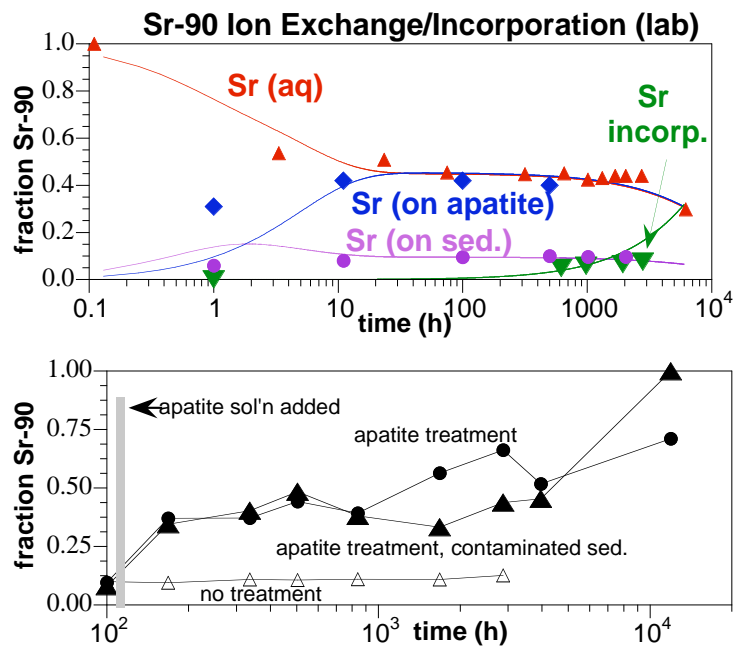


Figure 6.5. Sr uptake from groundwater suspension of 0.34 g/L apatite and 20 g/L sediment at 82°C with a) solid phase apatite added, and b) Ca-citrate-PO₄ solution added. Model fit consists of Ca-Na-Sr ion exchange on sediment, Ca-Na-Sr ion exchange on apatite, and Sr incorporation within the apatite structure.

incorporated and additional Sr mass sorbs onto the apatite. Ion exchange equilibrium is quickly reached, so has no influence on slowing down the incorporation reaction. In contrast, if the ion exchange and incorporation reaction rates were only an order of magnitude different (i.e., coupled), then there the ion exchange reaction would slow the apparent incorporation rate.

The amount of Sr-90 uptake during the initial apatite precipitation phase varies with the type of solution (Figure 6.6a). For the Ca-citrate-PO₄ (1, 2.5, 10 mM) solution used in injections #3 to #18, several laboratory experiments show this uptake should be ~60% of the Sr-90 mass by 30 days (Figure 6.2), which includes both Sr-90 sorbed and incorporated in apatite. Over the long term (months), the amount of Sr-90 uptake resulting from apatite recrystallization with Sr-90 incorporation varies with the Ca/Sr ratio (Figure 6.6a and b). Uptake mass in long-term studies consisted of a specific mass of sediment/apatite exposed to the equivalent of 350 pore volumes of a Sr-90 laden solution (diamonds, Figure 6.6). In contrast, uptake mass in short-term studies consisted of the sediment/apatite exposed to the equivalent of 3 pore volumes of Sr-90 laden solution (triangles, Figure 6.6 and Table 6.1).

By one month, Sr-90 total uptake was 95 to 99% (Figure 6.6a, triangles), with 18% to 25% incorporation into apatite (i.e., during initial precipitation, Figure 6.6b, triangles). The remaining fraction of Sr-90 uptake was held on apatite/sediment surfaces by ion exchange. These batch studies were conducted at near field sediment/water ratios, so represent what should occur to the Sr-90 in the Ca-citrate-PO₄ injection zone.

Experiments conducted at very low sediment/water ratios (diamonds, Figure 6.6)

represent uptake of 350 pore volumes of Sr-90 laden water by apatite. The total Sr-90 uptake (Figure 6.6a) decreased with increasing Ca/Sr, which was mainly caused simply by less sorbed Sr-90 on the surface. The Sr-90 fraction incorporated into apatite (by 9 months) varied from 3% to 18% (of the 350 pore volumes of Sr-90 laden water). It is unclear if there was a relationship between increasing Ca/Sr ratio and decreasing Sr-90 uptake. The ionic strength had less effect on Sr incorporation, as Sr adsorption on apatite was more highly correlated with divalent cation

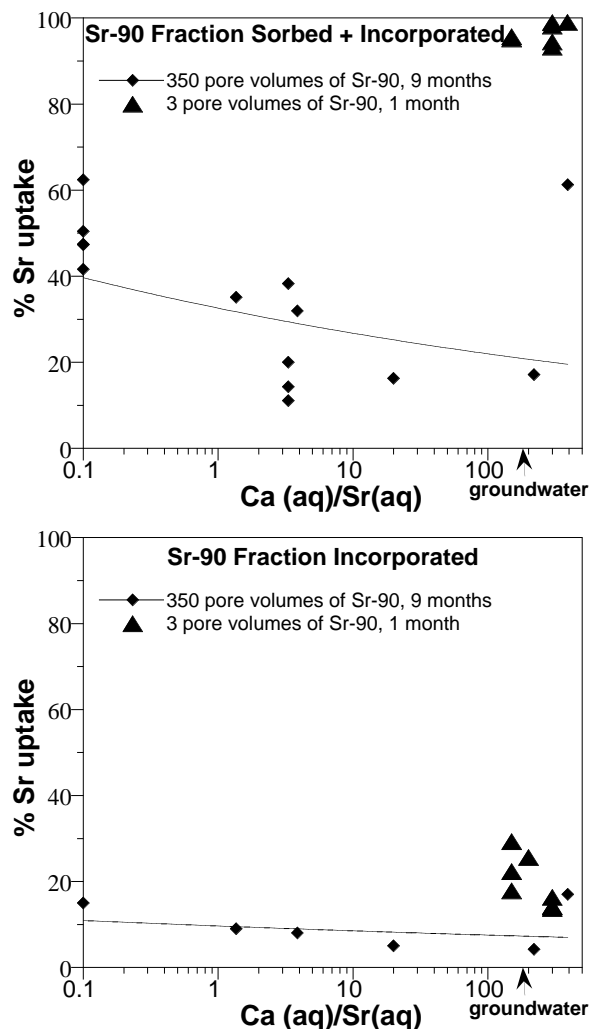


Figure 6.6. Sr uptake from groundwater suspension of 0.34 g/L apatite and 20 g/L sediment at 82°C. Model fit consists of Ca-Na-Sr ion exchange on sediment, Ca-Na-Sr ion exchange on apatite, and Sr incorporation within the apatite structure.

concentration. Temperature had only a small effect on the Sr-90 incorporation rate, but temperature studies indicated the activation energy is low (11.3 kJ/mol), which suggests the rate-controlling step is diffusion of Sr-90 into the apatite structure. Experiments are in progress to measure the Sr profile with depth using an electron microprobe to prove if diffusion is the rate-limiting step.

The rate of Sr-90 incorporation in experiments calculated from experiments with varying Ca/Sr conditions (Figure 6.7) showed a slight decrease in rate with increasing Ca/Sr ratio. The Sr-90 incorporation rate into apatite during initial precipitation (by 1 month, triangles, Figure 6.7) averaged $4.64 \pm 1.9 \times 10^{-4} \text{ h}^{-1}$ (half-life $1500 \pm 430 \text{ h}$, $8.85 \times 10^{-7} \text{ mg Sr/day/mg apatite}$). The Sr-90 incorporation rate into apatite already in solid phase averaged $2.7 \pm 2.6 \times 10^{-5} \text{ h}^{-1}$ (half-life 1080 days, $1.42 \times 10^{-8} \text{ mg Sr/day/mg apatite}$) for the 350 pore volumes of Sr-90 laden water. There did not appear to be a reliable trend of the incorporation rate changing with increasing Ca/Sr (r^2 for trend line was 0.07, Figure 6.7). Experiments did show that more highly crystalline apatite had a slower Sr-90 solid phase uptake rate. Apatite precipitated at high sediment/water ratio in laboratory and field experiments are considered low crystallinity, so should exhibit somewhat higher rates than shown in these 9-month long studies, which used more highly crystalline apatite.

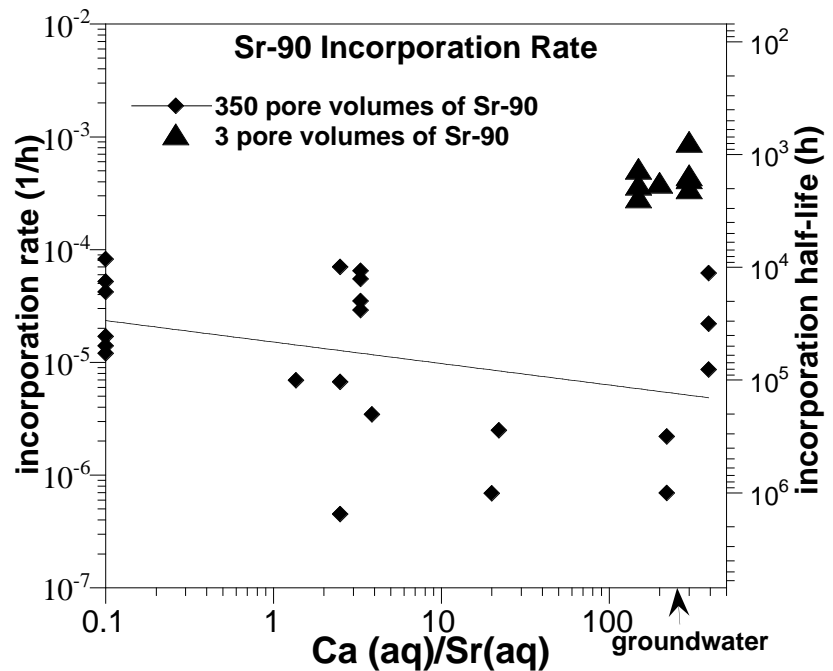


Figure 6.7. Sr uptake from groundwater suspension of 0.34 g/L apatite and 20 g/L sediment at 82°C. Model fit consists of Ca-Na-Sr ion exchange on sediment, Ca-Na-Sr ion exchange on apatite, and Sr incorporation within the apatite structure.

To be able to assess whether Sr-90 incorporation rates into apatite can be an effective field-scale reactive barrier in the Hanford 100-N Area, the natural Sr groundwater flux rate toward the river needs to be compared to calculated Sr uptake rates based on experimental results. For these calculations, the total Sr in each was considered. Sr incorporation rates were calculated for both initial uptake during apatite precipitation (more rapid uptake rate, Figure 6.7), and for solid phase incorporation. Two different amounts of apatite were considered in the sediment that included the 0.38 mg apatite/g sediment produced from field injections #3 to #18, and the 3.4 mg apatite/g sediment final design (Table 2.1), which is based on 10% Sr substitution for Ca in apatite. The Sr uptake (incorporation) rate was calculated in mmol Sr per day per cm² cross sectional area of sediment within a 30-ft wide barrier (Table 6.1). These calculated uptake rates were initially fairly rapid during the initial apatite precipitation phase, then decreased about two orders of magnitude during solid phase incorporation. For the field scenario of current injections (i.e., 10 mM PO₄ injected in wells, or 0.34 mg apatite/g sediment), the Sr uptake rate was 8.8 x 10⁻⁶ mmol Sr/day/cm², or 6.5 x the average Sr groundwater flux rate in groundwater (1.36 x 10⁻⁶ mmol Sr/day/cm²). Therefore, on a rate basis, all of the Sr (and Sr-90) would be consumed by the apatite in the barrier. It should be noted that zones of higher groundwater flux (10x to 100x) would exceed the barrier uptake rate for this low apatite loading (0.38 mg apatite/g sediment). This low apatite loading would also not be able to incorporate Sr and Sr-90 for 300 years, so additional apatite is needed to increase the loading to 3.4 mg apatite/g sediment. At this high loading, the Sr uptake rate during initial precipitation is 3600x more rapid than the average Sr groundwater flux rate and the Sr uptake rate during solid phase incorporation is 57x more rapid than the average Sr groundwater flux rate, so the barrier will effectively remove all Sr except in extreme high groundwater flow conditions.

Table 6.1. Calculated Sr uptake rates in apatite-laden sediment for a 30-ft wide barrier.

scenario	barrier dia. (ft)	apatite mass (mg apatite/g sed)	apatite total mass (g/cm2 cross sect.)	Sr uptake rate (mmol Sr/day/cm2)
during initial ppt (1 month), inj. #3-18 apatite	30	0.38	0.619	5.5E-04
during initial ppt (1 month), final apatite	30	3.4	5.53	4.9E-03
solid phase incorp. (9 months), inj. #3-18 apatite	30	0.38	0.619	8.8E-06
solid phase incorp. (9 months), final apatite	30	3.4	5.53	7.8E-05
natural Sr flux rate toward river*				1.36E-06

*assumes 0.1 mg/L Sr, Kd = 14 cm³/g, porosity 0.20, bulk density 1.78 g/cm³, 1 ft/day groundwater flow rate

6.5 Sequential Injection Scenarios

Experiments were conducted to test the efficiency of Sr-90 uptake by sequential injections of different phosphate solutions to increase the amount of apatite in the sediment. These experiments were conducted for a relatively short time period (2-5 weeks) so Sr-90 incorporation represents only the initial incorporation during apatite precipitation. The baseline case is sequential low, then high concentration injection of Ca-citrate-PO₄ solutions (lines 6 and 7, Table 6.2), which showed 14.2% Sr-90 incorporated by 2 weeks (after just the low concentration injection, line 6) and 29.3% incorporation after two weeks of the subsequent high concentration injection. Over this relatively short time period, not all of the high concentration solution had precipitated, so the efficiency of Sr-90 uptake (i.e., mmol Sr uptake per mmol of PO₄ injected) did not increase. Alternate single injection scenarios considered included injection of PO₄ alone, citrate-PO₄ alone (no Ca), and a high concentration Ca-citrate-PO₄ solution.

Of these single injection scenarios, there was little difference in Sr-90 uptake fraction and incorporation efficiency, except the incorporation efficiency of the citrate-PO₄ solution (no Ca) was much higher. Sequential injection schemes considered included injecting PO₄ first, then Ca-citrate-PO₄ and Ca-citrate-PO₄ first, then PO₄. Of these sequential injection scenarios, the amount of Sr-90 incorporation was nearly the same, but the incorporation efficiency was greater for solutions containing citrate. In general, injection solutions containing citrate and PO₄ appeared somewhat more efficient at Sr-90 uptake over these 5-week long experiments compared with PO₄ only injection solutions. Additional experiments are needed to quantify the long-term Sr-90 uptake rates for these different sequential solution applications.

Table 6.2. Sequential treatments of Sr-90 laden sediment with fraction Sr-90 uptake and efficiency.

PO ₄ Application Description	Sr-90 incorporation in apatite				
	PO ₄ total (mM)	mass fraction	half-life (h)	incorp. efficiency Sr/PO ₄ (mM/mM)	Sr/Ca incorp.
Sequential PO ₄ , then Ca-citrate-PO ₄				(by time indicated)	
1) 8.34 mM PO ₄ , 1 week	8.34	0.141	770	0.0017	1.052
2) Ca-Cit-PO ₄ (14-35-8.38 mM) 4 weeks	16.7	0.21	1850	0.0013	0.955
Citrate-PO ₄ only (no Ca addition)					
Cit-PO ₄ (10-2.4 mM) 3 weeks	2.4	0.163	1980	0.0068	1.216
Sequential Ca-citrate-PO ₄ , then PO ₄					
1) Ca-Cit-PO ₄ (7-17.5-4.19) 2 weeks	4.2	0.137	1610	0.0033	0.725
2) 8.38 mM PO ₄ 3 weeks	12.6	0.178	2390	0.0014	0.844
Sequential low conc., high conc. Ca-citrate-PO ₄					
1)*Ca-Cit-PO ₄ (1-2.5-10 mM) 2weeks	10	0.142	1520	0.0014	1.543
2) Ca-Cit-PO ₄ (28-70-16.8 mM) 2 weeks	26.8	0.293	1330	0.0011	1.724
Ca-citrate-PO ₄ only (high conc.)					
Ca-Cit-PO ₄ (28-70-16.75) 5 weeks	16.8	0.256	1780	0.0015	0.672

In summary, laboratory-scale experiments have demonstrated that injection of different Ca-citrate-PO₄ solutions into Hanford 100-N subsurface sediments results in citrate biodegradation and subsequent formation of microcrystalline apatite. Both Sr-90 uptake mass and uptake rate were quantified to assess the viability of a long-term permeable reactive barrier. Some Sr-90 uptake occurs during the initial apatite precipitation phase (i.e., 20% to 60%), especially if divalent-poor Ca-citrate-PO₄ solutions are injected. Solid phase substitution of Sr (and Sr-90) for Ca in the apatite structure occurs due to higher thermodynamic stability of Sr-laden apatite. This solid phase Sr-90 incorporation is slow (months to years), but more rapid than the natural groundwater migration of rate of Sr, so from a rate perspective should for an effective permeable reactive barrier. From an Sr-90 mass perspective, there is sufficient apatite mass to uptake Sr (and Sr-90) for 300 years (10 half-lives of Sr-90 decay) assuming 10% Sr substitution for Ca in apatite. The measured Sr substitution for Ca in apatite varied from 1.0% to 16.3% (at 9 months), with less (or slower) uptake in more crystalline apatite. Precipitated apatite in sediments at the field scale is expected to exhibit higher rates of substitution, due to the less crystalline structure (i.e., more impurities, smaller crystal precipitate size). Because most laboratory experiments were focused on relatively low concentration Ca-citrate-PO₄ solutions, additional experiments are needed to determine the most efficient method of sequential injections to increase the amount of apatite precipitation needed to prevent migration of Sr-90 in the 100-N aquifer toward the Columbia River.

7.0 References

- Andronescu E, E Stefan, E Dinu, and C Ghitulica. 2002. "Hydroxyapatite Synthesis." *Key Engineering Materials* 206-213:1595-1598.
- Arey JS, JC Seaman, and PM Bertsch. 1999. "Immobilization of Uranium in Contaminated Sediments by Hydroxyapatite Addition." *Environmental Science & Technology* 33:337-342.
- Amrhein C and DL Suarez. 1990. "Procedure for Determining Sodium-Calcium Selectivity in Calcareous and Gypsiferous Soils." *Soil Science Society of America Journal* 54:999-1007.
- Bailey JE and DF Ollis. 1986. *Biochemical Engineering Fundamentals*. McGraw-Hill Publishing Co., New York.
- Bailliez S, A Nzihou, E Beche, and G Flamant. 2004. "Removal of Lead by Hydroxyapatite Sorbent." *Process Safety and Environmental Protection* 82:175-180.
- Belousova EA, WL Griffin, SY O'Reilly, and NI Fisher. 2002. "Apatite as an Indicator Mineral for Mineral Exploration: Trace-Element Compositions and Their Relationship to Host Rock Type." *Journal of Geochemical Exploration* 76:45-69.
- Bynhildsen L and T Rosswall. 1997. "Effects of Metals on the Microbial Mineralization of Organic Acids." *Water, Air, and Soil Pollution* 94(1-2):45-57.
- Chairat C, EH Oelkers, S Kohler, N Harouiya, and JE Lartique. 2004. "An Experimental Study of the Dissolution Rates of Apatite and Britholite as a Function of Solution Composition and pH from 1-12," In W S II (ed.), p. 671-674, *Water-Rock Interaction*. Taylor & Francis Group, London.
- Department of Energy, Richland (DOE-RL). 1994. *Limited Field Investigation Report for the 100-NR-2 Operable Unit*. DOE/RL-93-81, U.S. Department of Energy, Richland Operations Office, Richland, Washington.
- DOE-RL. 1997. *Corrective Measures Study for the 100-NR-1 and 100-NR-2 Operable Units*. DOE/RL-95-111, U.S. Department of Energy, Richland Operations Office, Richland, Washington.
- DOE-RL. 2004. *Calendar Year 2003 Annual Summary Report for the 100-HR-3, 100-KR-4, and 100-NR-2 Operable Unit (OU) Pump & Treat Operations*. DOE/RL-2004-21, U.S. Department of Energy, Richland Operations Office, Richland, Washington.
- DOE-RL. 2005. *Aquatic and Riparian Receptor Impact Information for the 100-NR-2 Groundwater Operable Unit*. Available at http://www.washingtonclosure.com/projects/endstate/risk_library.html#narea.

Edrington RS. 2005. Unpublished Columbia River stage data. Fluor Hanford, Inc., Richland, Washington.

Elliot JC, PE Mackie, and RA Young. 1973. "Monoclinic Hydroxyapatite." *Science*, 180:1055-1057.

Fluor/CH2M HILL. 2004. *Evaluation of Strontium-90 Treatment Technologies for the 100-NR-2 Groundwater Operable Unit*. Letter Report. Available at http://www.washingtonclosure.com/projects/endstate/risk_library.html#narea.

Fuller CC, JR Bargar, and JA Davis. 2003. "Molecular-Scale Characterization of Uranium Sorption by Bone Apatite Materials for a Permeable Reactive Barrier Demonstration." *Environmental Science & Technology* 37:4642-4649.

Fuller CC, JR Bargar, JA Davis, and MJ Piana. 2002. "Mechanisms of Uranium Interactions with Hydroxyapatite: Implications for Groundwater Remediation." *Environmental Science & Technology* 36:158-165.

Geochem Software, Inc. 1994. *Mac MINTEQ-A2: Aqueous Geochemistry for the Macintosh*. Published by Geochem Software, Inc., Reston, Virginia.

Heslop DD, Y Bi, AA Baig, M Otsuka, and WI Higuchi. 2005. "A Comparative Study of the Metastable Equilibrium Solubility Behavior of High-Crystallinity and Low-Crystallinity Carbonated Apatites Using Ph and Solution Strontium as Independent Variables." *Journal of Colloid and Interface Science* 289:14-25.

Hill RG, A Stamboulis, RV Law, A Clifford, MR Towler, and C Crowley. 2004. The Influence of Strontium Substitution in Fluorapatite Glasses and Glass-Ceramics. *Journal of Non-Crystalline Solids* 336:223-229.

Hughes JM, M Cameron, and KD Crowley. 1989. "Structural Variations in Natural F, OH and Cl Apatites." *Amer Mineral* 74:870-876.

Hughes JM and J Rakovan. 2002. "The Crystal Structure of Apatite, $\text{Ca}_5(\text{PO}_4)_3(\text{F},\text{OH},\text{Cl})$." In *Phosphates: Geochemical, Geobiological and Materials Importance*, Reviews in Mineralogy and Geochemistry, vol 48, Mineralogical Society of America, Washington, D.C., p. 1-12.

Jeanjean J, JC Rouchaud, L Tran, and M Fedoroff. 1995. "Sorption of Uranium and Other Heavy Metals on Hydroxyapatite." *J. Radioanal. Nucl. Chem. Letters* 201:529-539.

Koutsoukos PG and GH Nancollas. 1981. "Influence of Strontium Ion on the Crystallization of Hydroxylapatite from Aqueous-Solution." *Journal of Physical Chemistry* 85:2403-2408.

Lazic S and Z Vukovic. 1991. "Ion-Exchange of Strontium on Synthetic Hydroxyapatite." *Journal of Radioanalytical and Nuclear Chemistry-Articles* 149:161-168.

Legeros RZ, G Quirolgico, and JP Legeros. 1979. "Incorporation of Strontium in Apatite - Effect of pH." *Journal of Dental Research* 58:169-169.

Lindsay WL, PLG Vlek, and SH Chien. 1989. "Phosphate Minerals." *Minerals in Soil Environments*, 2 ed. Soil Science Society of America, Madison, Wisconsin, p. 1089-1131.

Lower SK, PA Maurice, SJ Traina, and EH Carlson. 1998. "Aqueous Pb Sorption by Hydroxylapatite: Application of Atomic Force Microscopy to Dissolution, Nucleation, and Growth Studies." *American Mineralogist* 83:147-158.

Ma QY, SJ Traina, and TJ Logan. 1995. "In Situ Lead Immobilization by Apatite." *Environmental Science and Technology* 27:1803-1810.

Mavropoulos E, AM Rossi, AM Costa, CAC Perez, JC Moreira, and M Saldanha. 2002. "Studies on the Mechanisms of Lead Immobilization by Hydroxyapatite." *Environmental Science & Technology* 36:1625-1629.

Misra DN. 1998. "Interaction of Some Alkali Metal Citrates with Hydroxyapatite - Ion-Exchange Adsorption and Role of Charge Balance." *Colloids and Surfaces a-Physicochemical and Engineering Aspects* 141:173-179.

Moelo Y, B Lasnier, P Palvadeau, P Leone, and F Fontan. 2000. "Lulzacite, $\text{Sr}_2\text{Fe}_{2+}(\text{Fe}_{2+},\text{Mg})_2\text{Al}_4(\text{PO}_4)_4(\text{OH})_{10}$, a New Strontium Phosphate (Saint-Aubin-des-Chateaux, Loire-Atlantique, France)." *Comptes Rendus De L Academie Des Sciences Serie Ii Fascicule a-Sciences De La Terre Et Des Planetes* 330:317-324.

Moore RC, J Szecsody, MJ Truex, K Helean, R Bontchev, and C Ainsworth. 2006. "Formation of Nanosize Apatite Crystals in Sediments for Containment and Stabilization of Contaminants." *Environmental Applications of Nanomaterials*, CRC Press, in press.

Moore RC, M Gasser, N Awwad, KC Holt, FM Salas, A Hasan, MA Hasan, H Zhao, and CA Sanchez. 2005. "Sorption of Plutonium(VI) by Hydroxyapatite." *Journal of Radioanalytical and Nuclear Chemistry* 263:97-101.

Moore RC, C Sanchez, K Holt, P Zhang, H Xu, and GR Choppin. 2004. "Formation of Hydroxyapatite in Soils Using Calcium Citrate and Sodium Phosphate for Control of Strontium Migration." *Radiochimica Acta* 92(9-11/2004):719-723.

Moore RC, K Holt, HT Zhao, A Hasan, N Awwad, M Gasser, and C Sanchez. 2003. "Sorption of Np(V) by Synthetic Hydroxyapatite." *Radiochimica Acta* 91:721-727.

Nancollas GH and MS Mohan. 1970. "The Growth of Hydroxyapatite Crystals." *Archives of Oral Biology* 15(8):731-745.

Papargyris A, A Botis, Papargyri. 2002. "Synthetic Routs for Hydroxyapatite Powder Production." *Key Engineering Materials* 206-213:83-86.

- Raicevic S, Z Vukovic, TL Lizunova, and VF Komarov. 1996. "The Uptake of Strontium by Calcium Phosphate Phase Formed at an Elevated pH." *Journal of Radioanalytical and Nuclear Chemistry-Articles* 204:363-370.
- Rendon-Angeles JC, K Yanagisawa, N Ishizawa, and S Oishi. 2000. "Effect of Metal Ions of Chlorapatites on the Topotaxial Replacement by Hydroxyapatite under Hydrothermal Conditions." *Journal of Solid State Chemistry* 154:569-578.
- Routson RC, G Barney, R Smith, C Delegard, and L Jensen. 1981. *Fission Product Sorption Parameters for Hanford 200 Area Sediment Types*. RHO-ST-35, Rockwell Hanford Operations, Richland, Washington.
- Serne RJ and VL LeGore. 1996. *Strontium-90 Adsorption-Desorption Properties and Sediment Characterization at the 100-N Area*. Pacific Northwest Laboratory, Richland, Washington.
- Smiciklas I, A Onjia, and S Raicevic. 2005. "Experimental Design Approach in the Synthesis of Hydroxyapatite by Neutralization Method." *Separation and Purification Technology* 44:97-102.
- Spence RD and C Shi. 2005. *Stabilization and Solidification of Hazardous, Radioactive, and Mixed Wastes*. CRC Press, Boca Raton, Florida.
- Sposito G. 1982. Flow Diagram for Sequential Extraction I of 100-N Sediments - Sr and ⁹⁰Sr Determination.
- Sposito G, LJ Lund, and AC Chang. 1982. "Trace-Metal Chemistry in Arid-Zone Field Soils Amended with Sewage-Sludge. 1. Fractionation of Ni, Cu, Zn, Cd, and Pb in Solid-Phases." *Soil Science Society of America Journal* 46:260-264.
- Sposito G, KM Holtzclaw, C Jouany, and L Charlet. 1983a. "Cation Selectivity in Sodium - Calcium, Sodium - Magnesium, and Calcium - Magnesium Exchange on Wyoming Bentonite at 298-K." *Soil Science Society of America Journal* 47:917-921.
- Sposito G, CS Levesque, JP Leclaire, and AC Chang. 1983b. Trace-Metal Chemistry in Arid-Zone Field Soils Amended with Sewage-Sludge. 3. Effect of Time on the Extraction of Trace-Metals." *Soil Science Society of America Journal* 47:898-902.
- Steeffel CI. 2004. "Evaluation of the Field-Scale Cation Exchange Capacity of Hanford Sediments." In W. S. II (ed.), *Water-Rock Interaction*, p. 999-1002, Taylor & Francis Group, London.
- Syers J and D Curtin. 1989. "Inorganic Reactions Controlling Phosphorus Cycling." In H Tiessen (ed.), *Phosphorus Cycles in Terrestrial and Aquatic Ecosystems*, p. 17-29, Saskatchewan Institute of Pedology, Saskatoon, Canada.
- Technical Advisory Group (TAG). 2001. *Hanford 100-N Area Remediation Options Evaluation Summary Report*. November 2001.

Tofe AJ. 1998. "Chemical Decontamination Using Natural or Artificial Bone." US Patent 5,711,015.

Van der Houwen JAM and AE Valsami-Jones. 2001. "The Application of Calcium Phosphate Precipitation Chemistry to Phosphorus Recovery: The Influence of Organic Ligands." *Environmental Technology* 22:1325-1335.

Verbeek RMH, M Hauben, HP Thun, and F Verbeek. 1977. "Solubility and Solution Behavior of Strontium hydroxyapatite." *Z. Phys. Chem. (Wiesbaden)* 108(2):203-215.

Vukovic Z, S Lazic, I Tutunovic, and S Raicevic. 1998. "On the Mechanism of Strontium Incorporation into Calcium Phosphates." *J. Serbian Chem. Soc.* 63.5:387-393.

Waychunas G. 1989. "Luminescence, X-ray Emission and New Spectroscopies." *Rev Mineral.* 18:638-698.

White MD and M Oostrom. 2004. *Subsurface Transport Over Multiple Phases (STOMP): User's Guide*. Version 3.1. PNNL (UC-14478), Pacific Northwest National Laboratory, Richland, Washington.

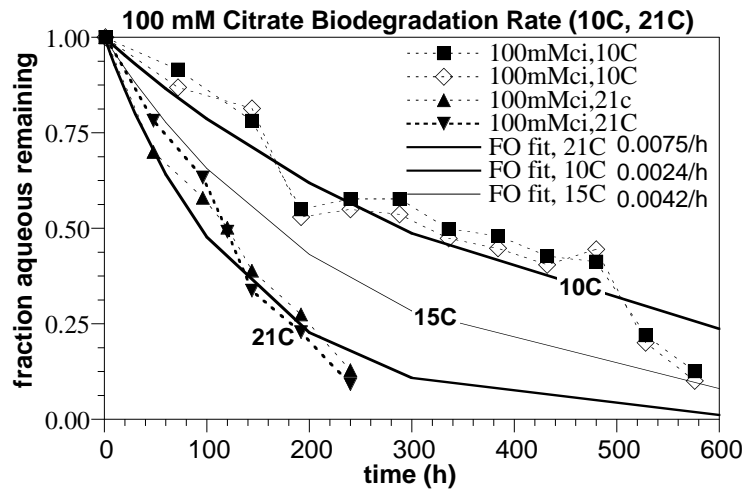
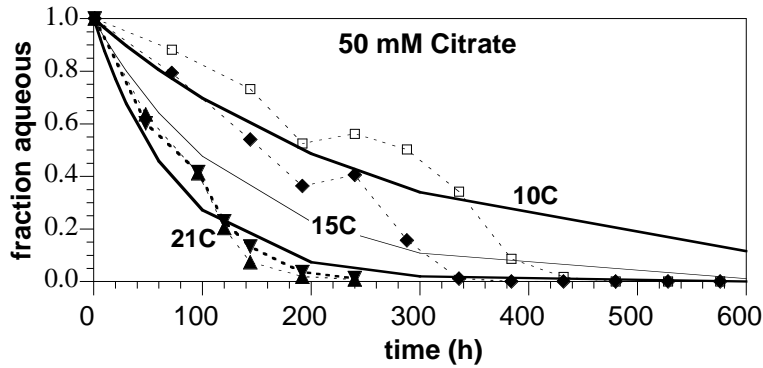
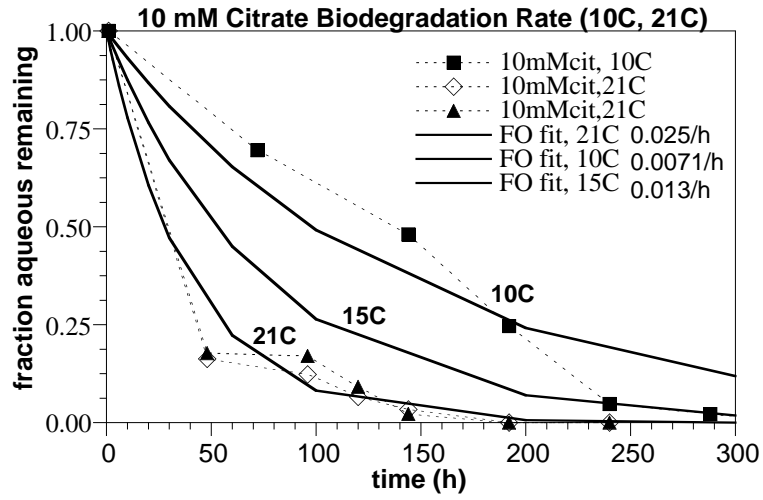
Wright J. 1990. "Conodont Apatite: Structure and Geochemistry." *Biomineralization: Patterns, Processes and Evolutionary Trends*. J Carter (ed.), Van Nostrand Reinhold, New York.

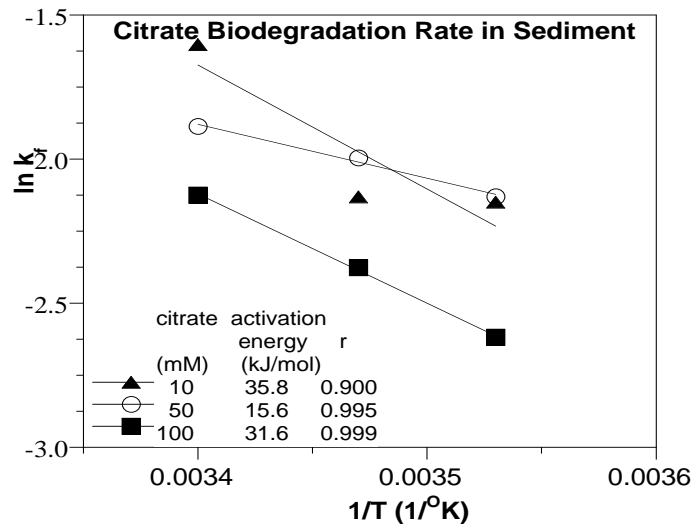
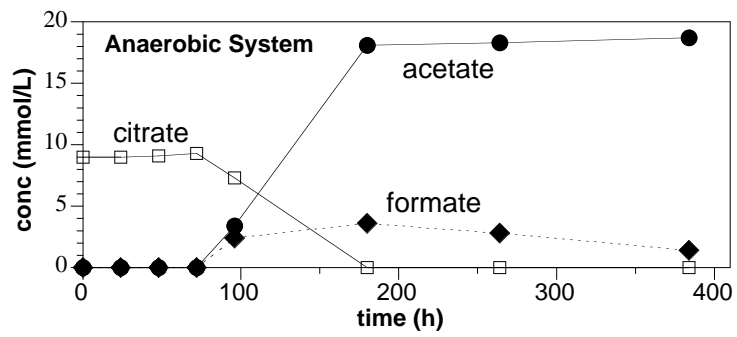
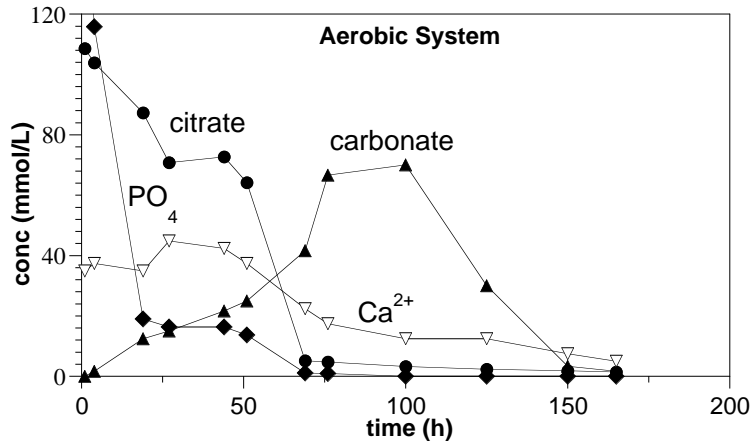
Wright J, KR Rice, B Murphy, and J Conca. 2004. "PIMS Using Apatite II™: How It Works To Remediate Soil and Water." *Sustainable Range Management*, RE Hinchee and B Alleman (eds.), Battelle Press, Columbus, Ohio. www.battelle.org/bookstore, ISBN 1-57477-144-2, B4-05.

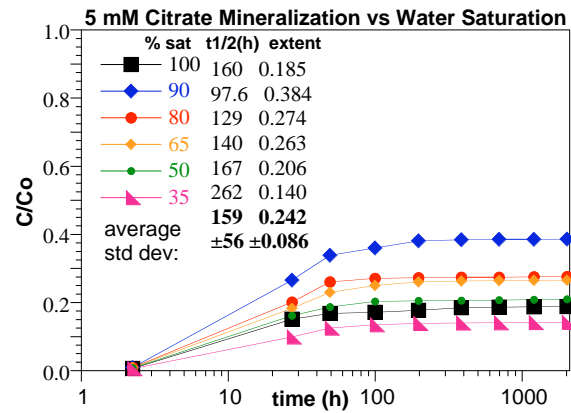
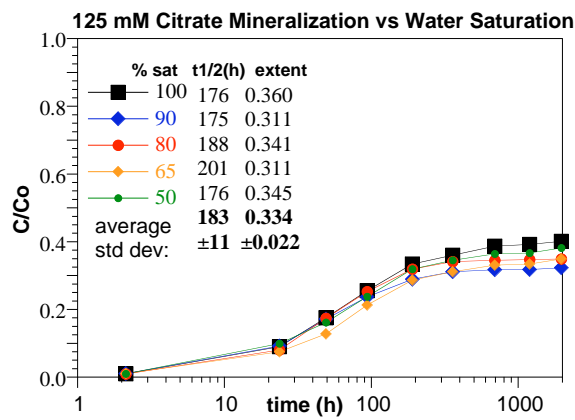
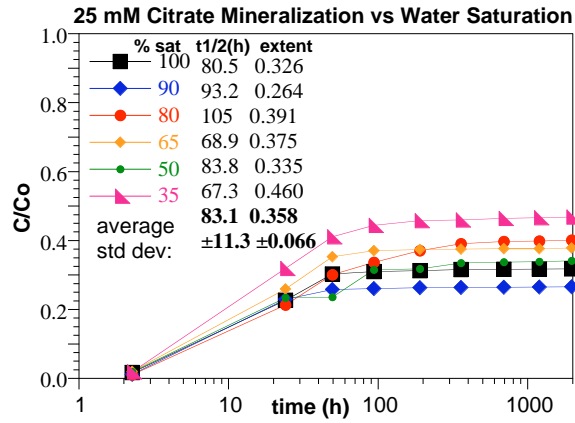
Appendix

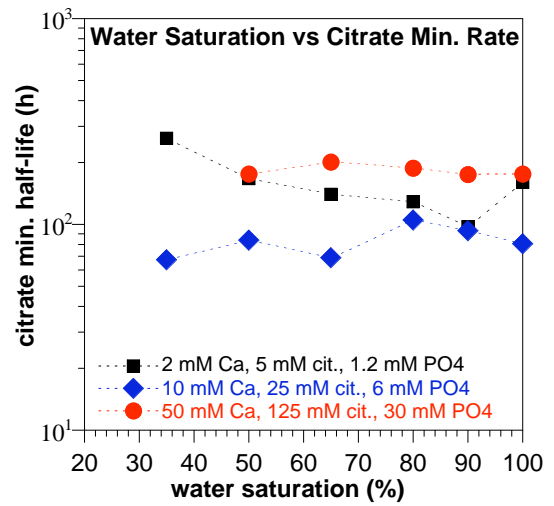
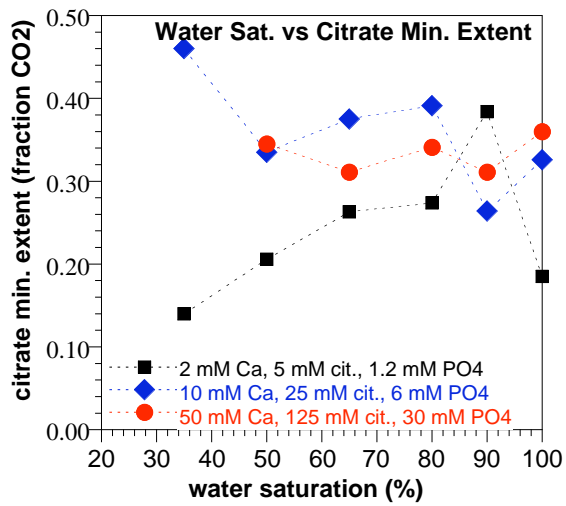
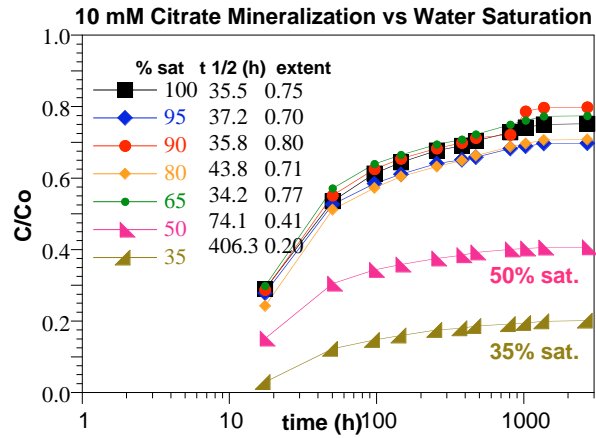
Experimental Data Characterizing Injection Solution – Sr - Sediment Reactions

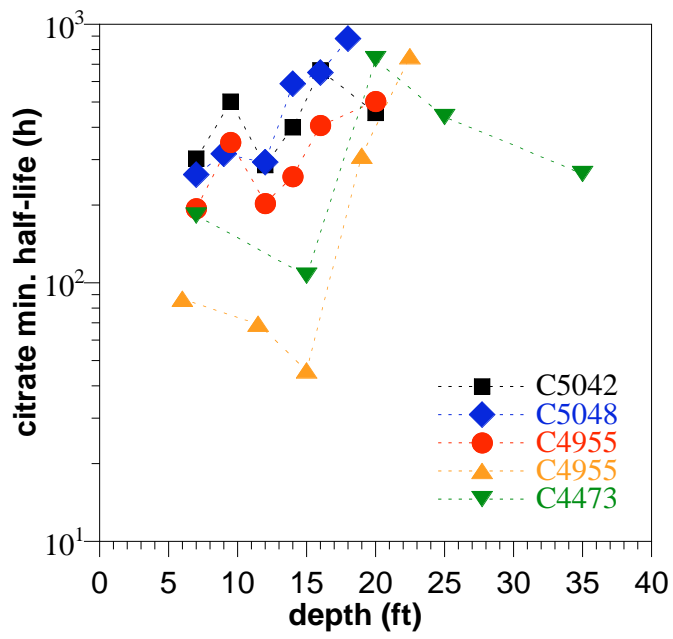
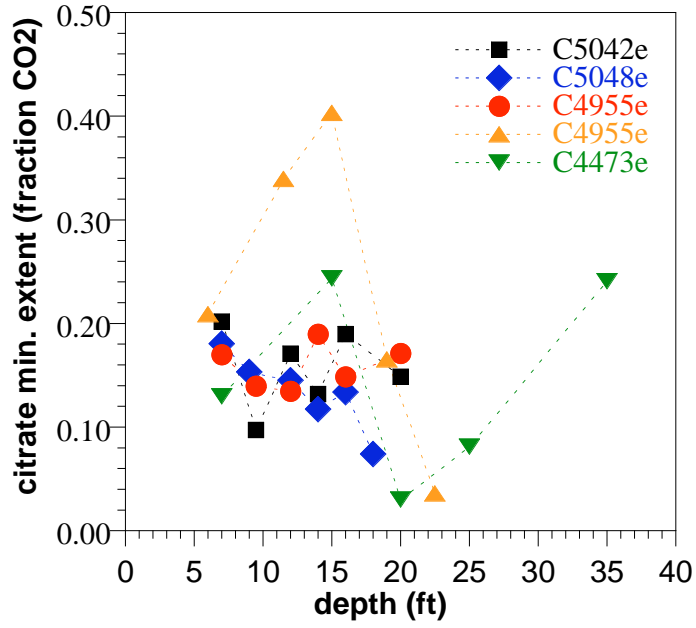
A.1 Citrate Biodegradation and Mineralization

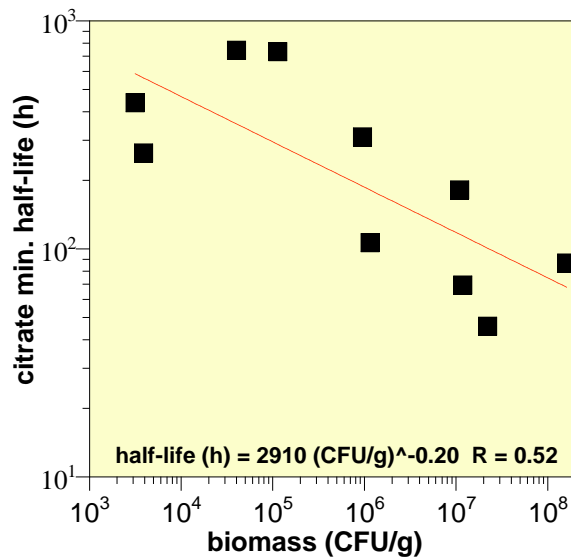
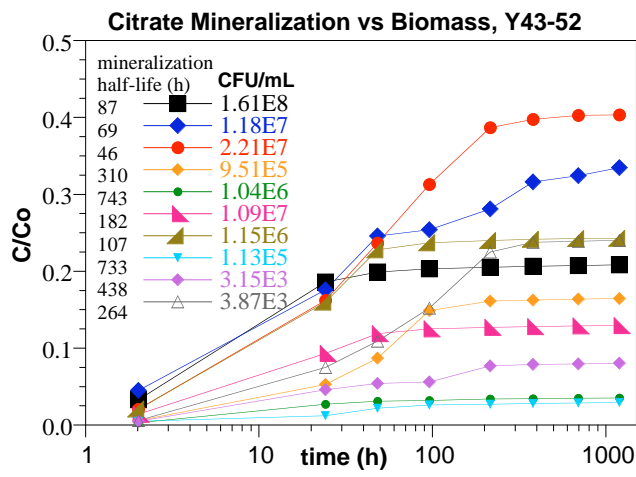
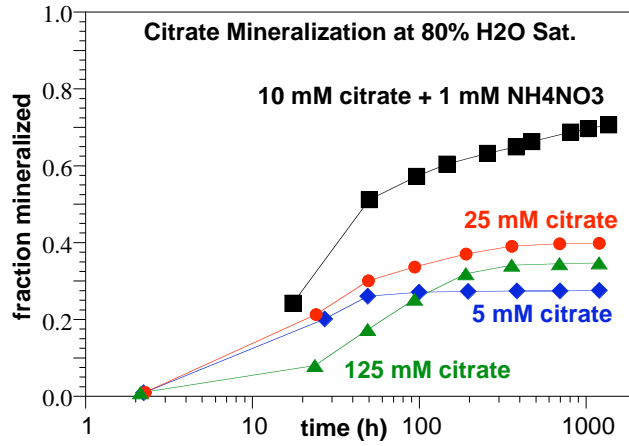


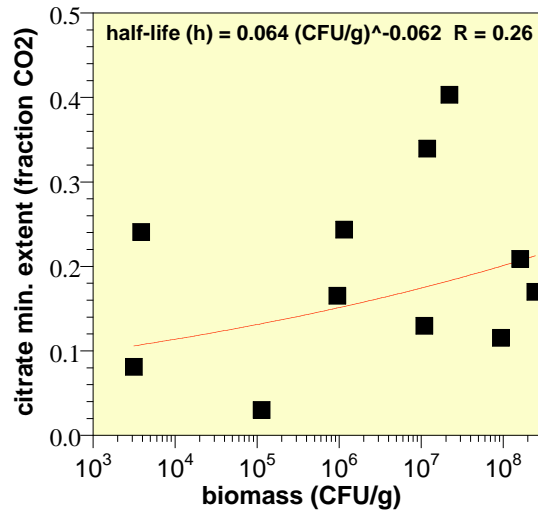
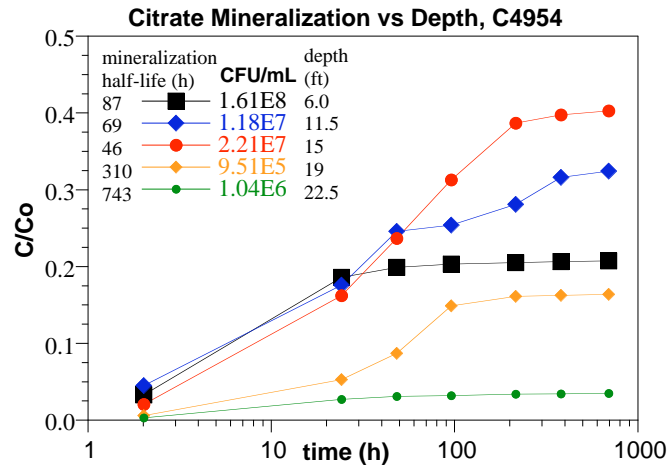
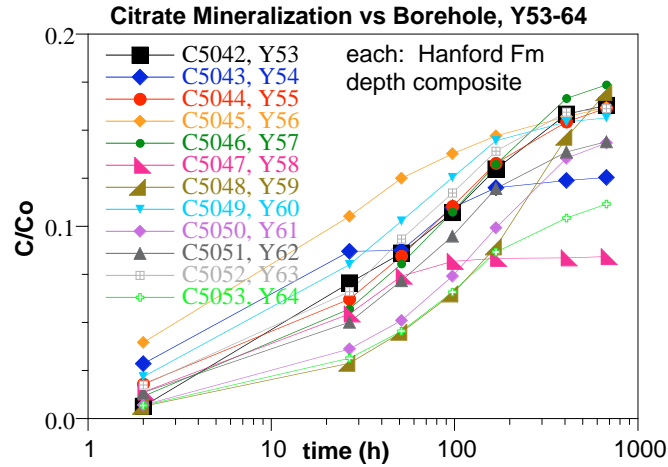


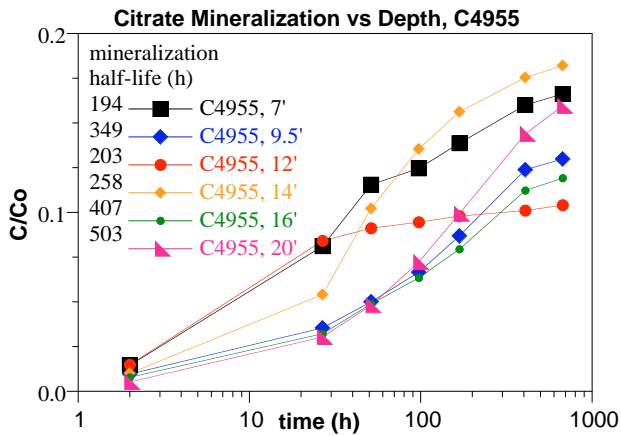
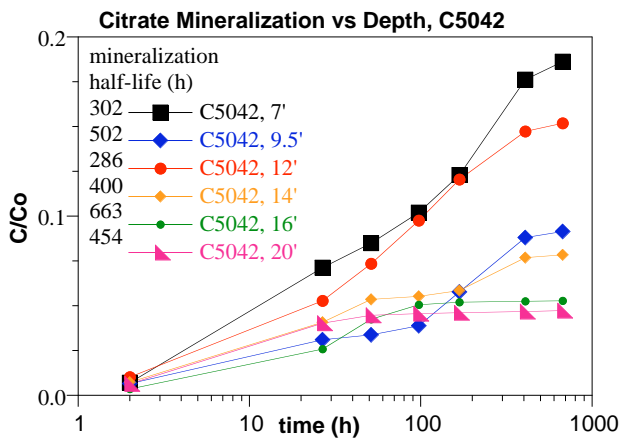
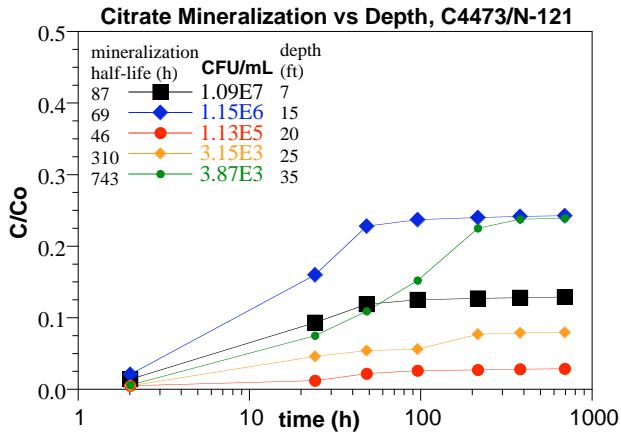


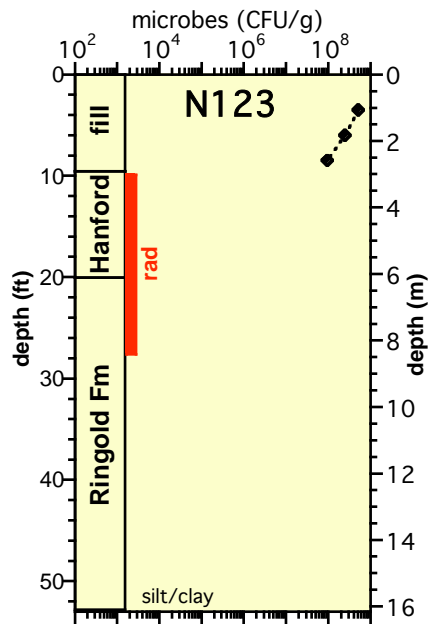
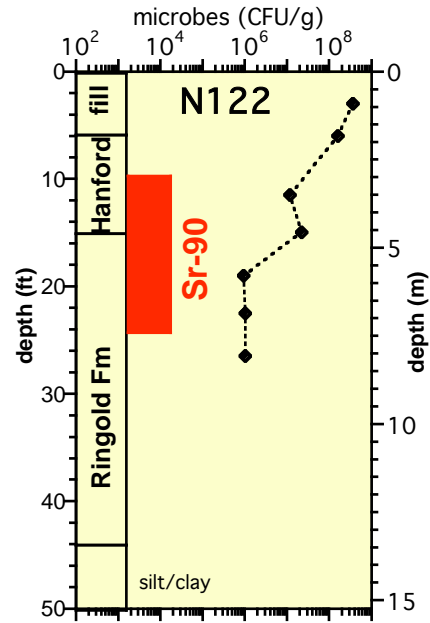
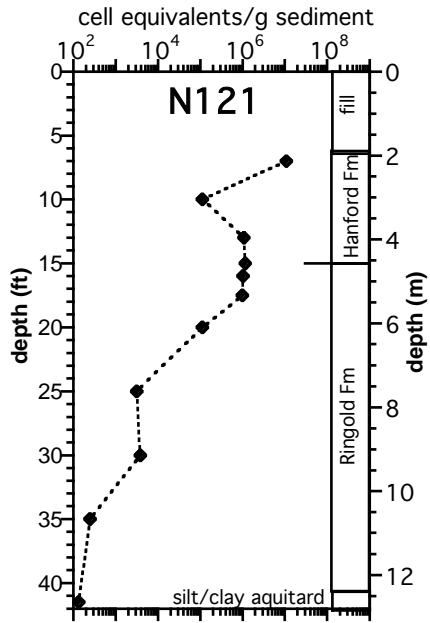




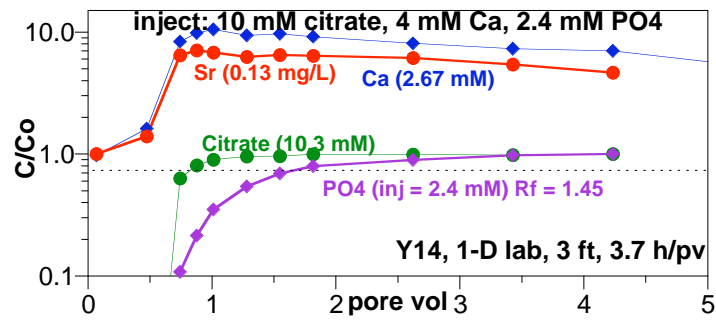
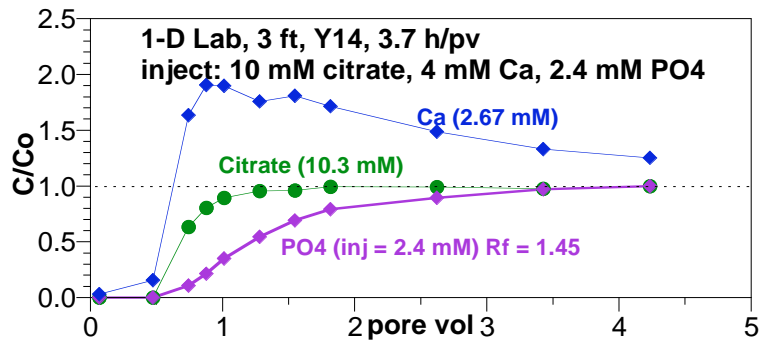
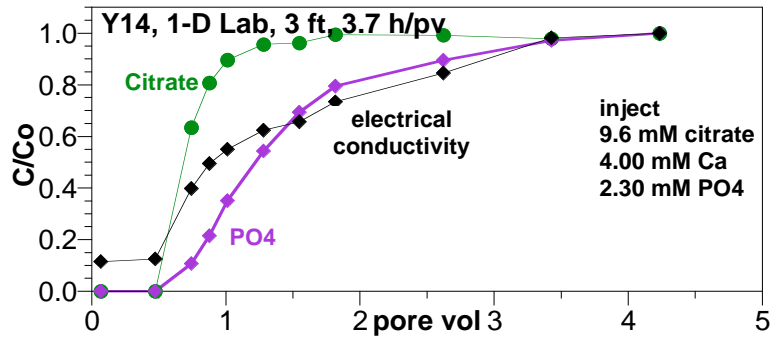
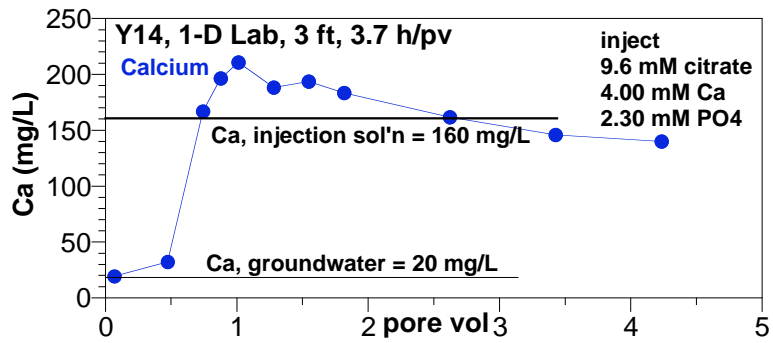


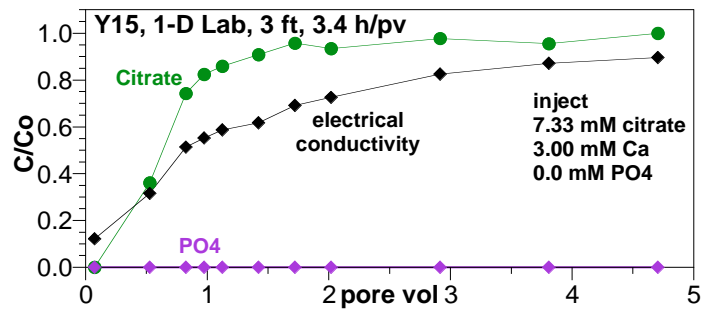
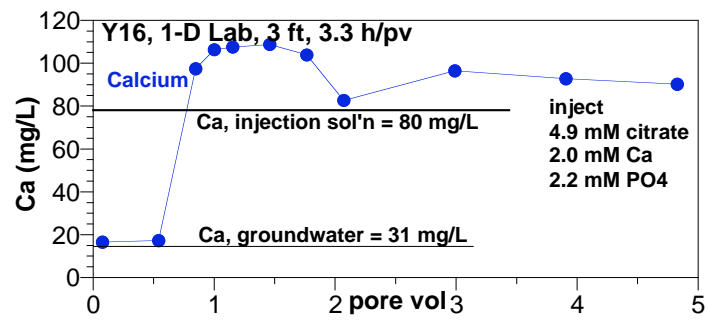
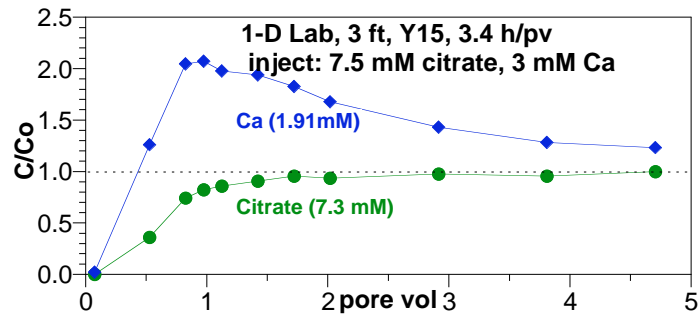
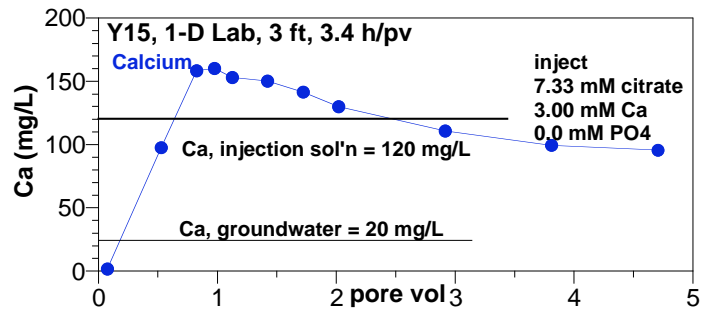


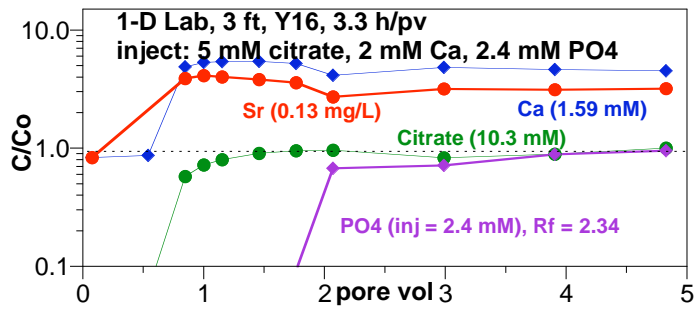
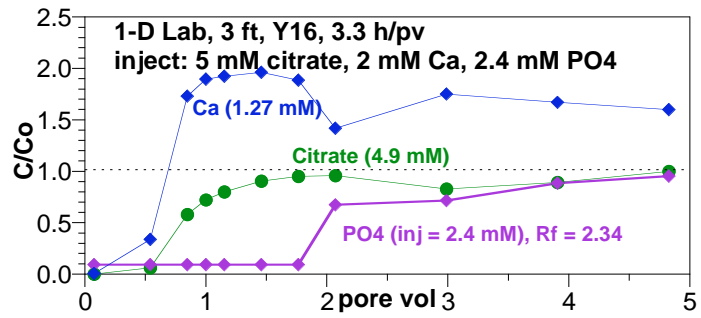
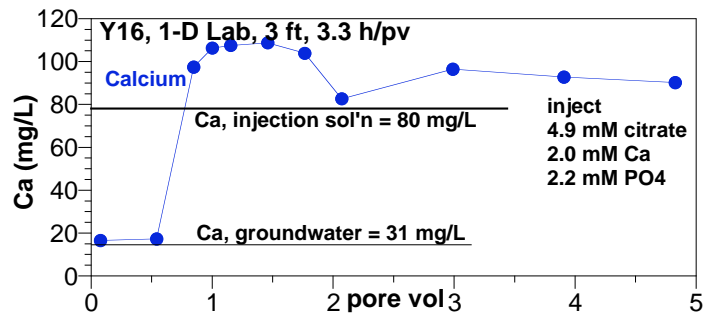


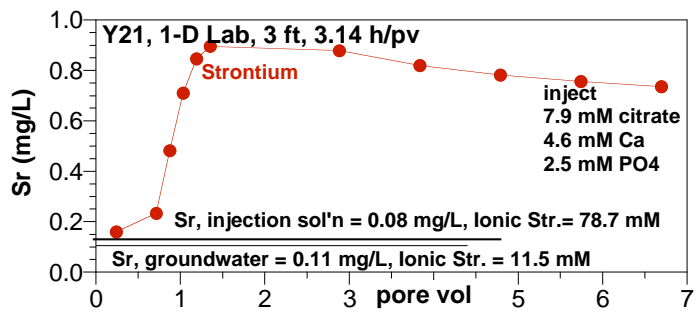
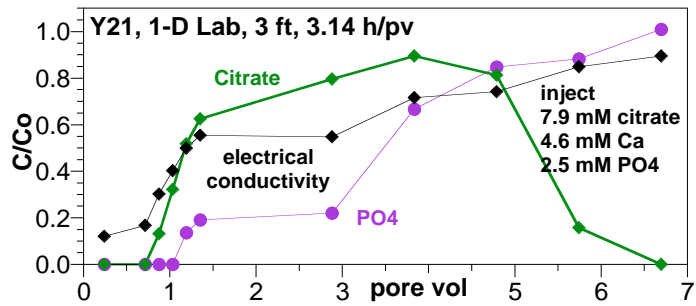
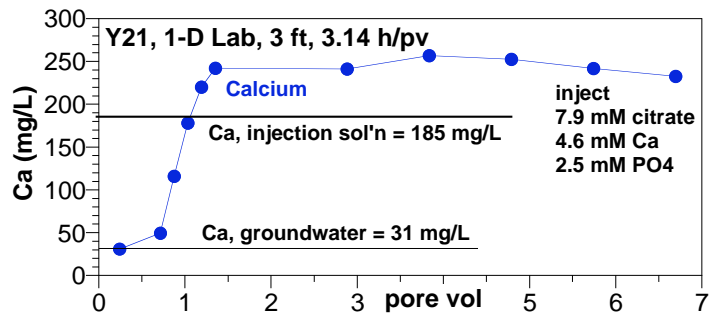


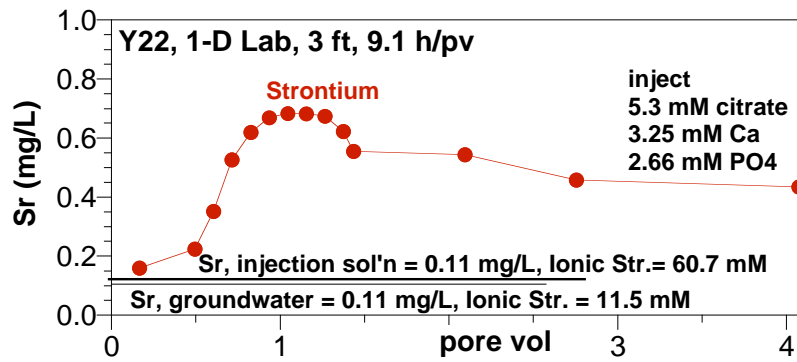
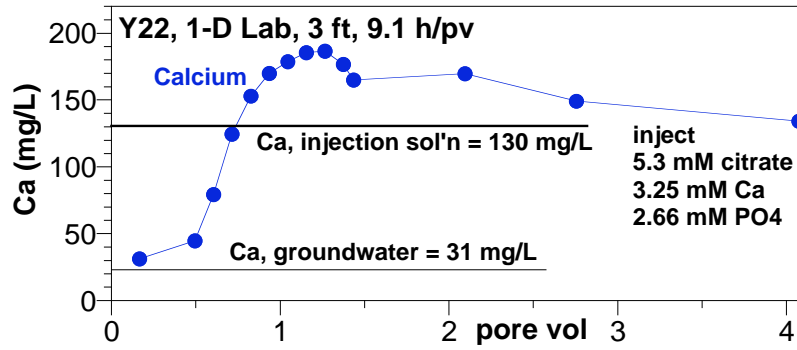
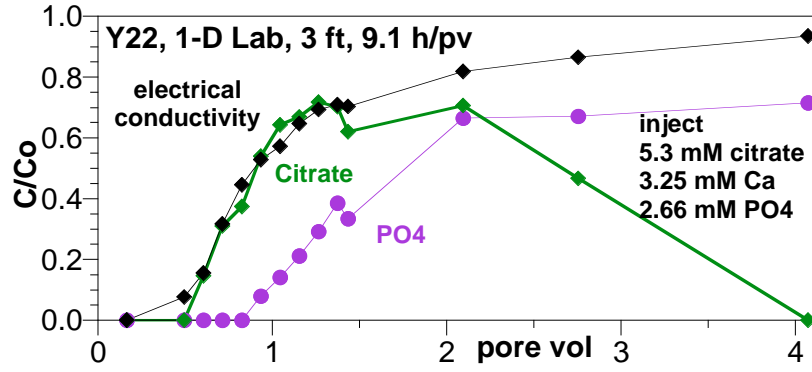
A.2 Ca-Citrate-PO₄ Injection into 1-D Sediment Columns

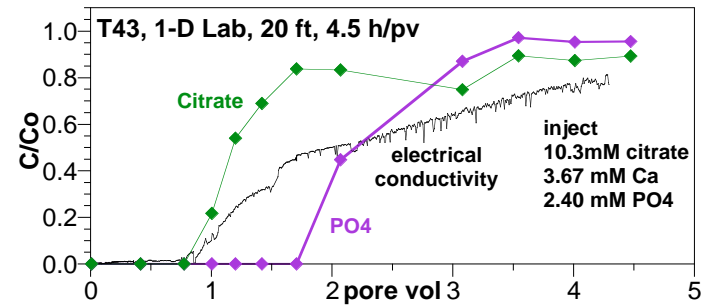
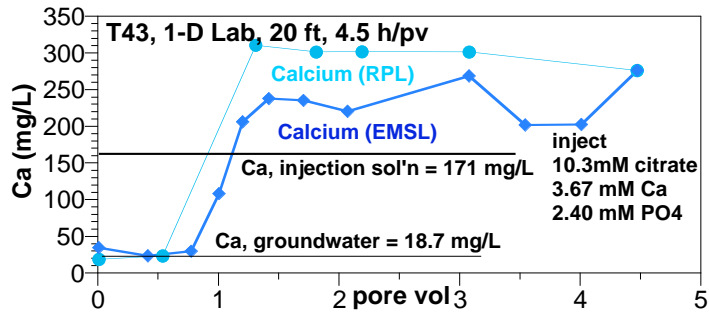
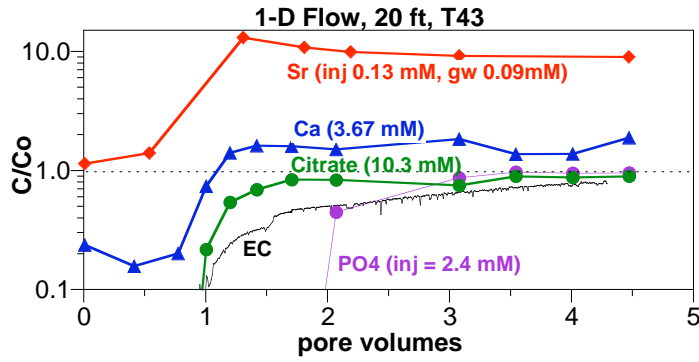
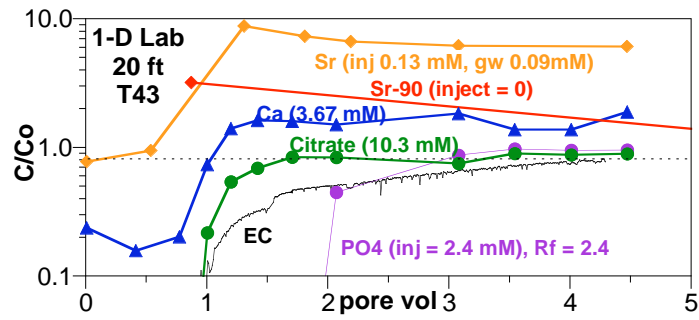


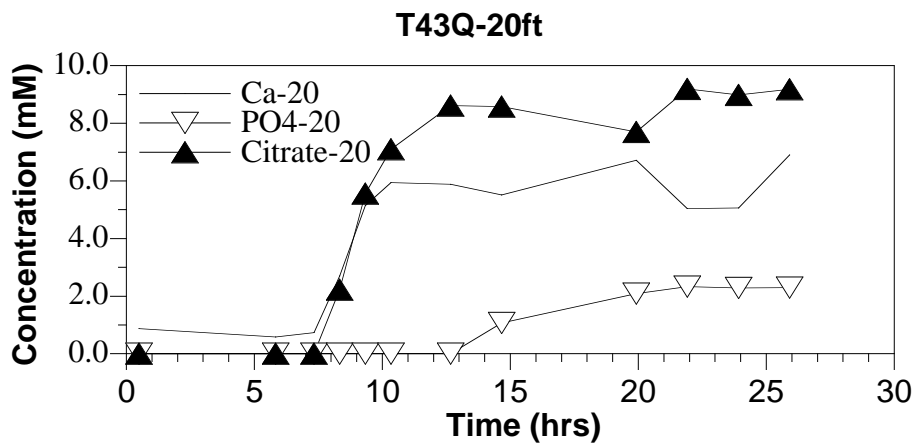
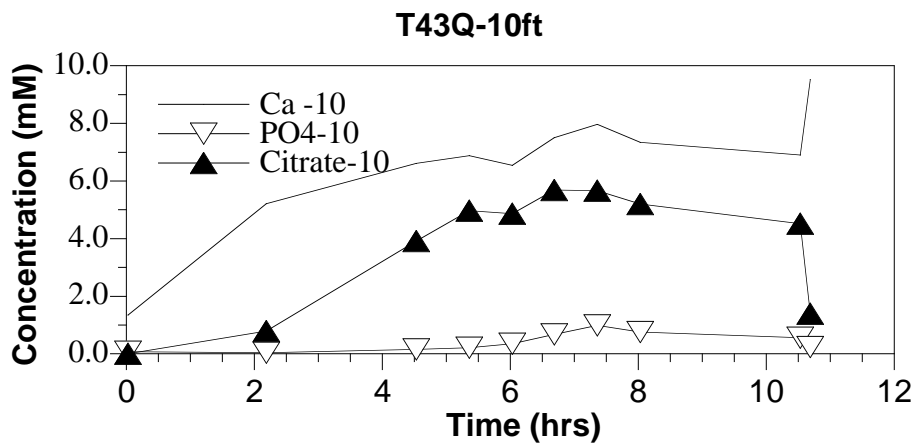
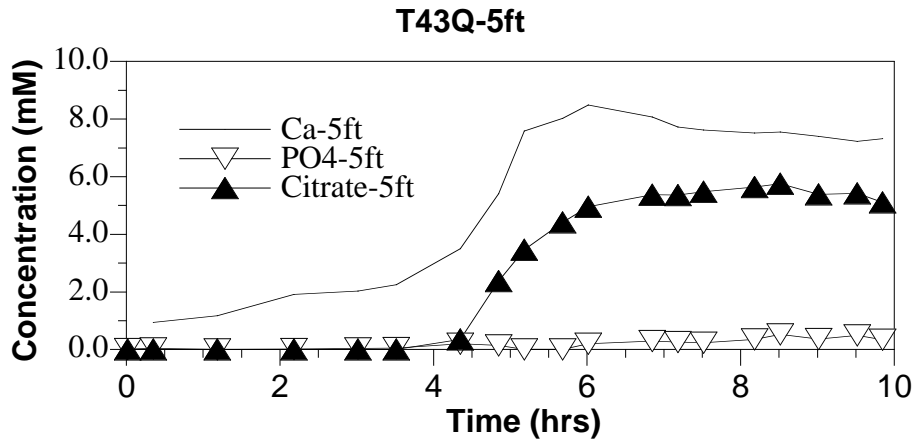


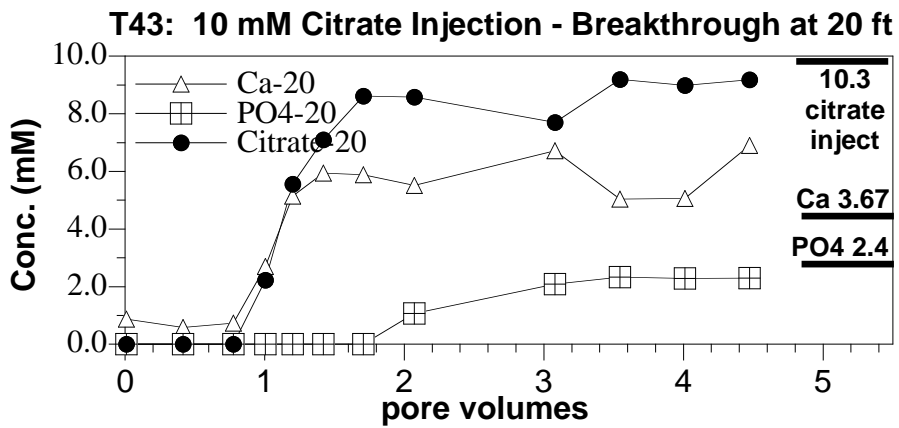
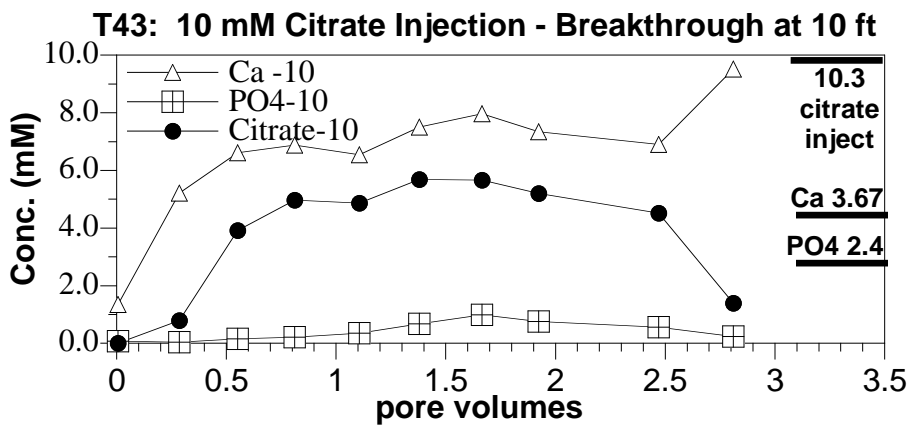
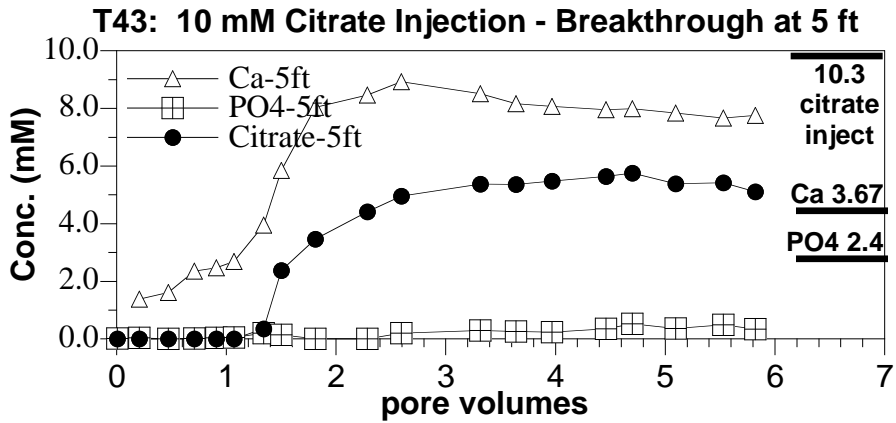


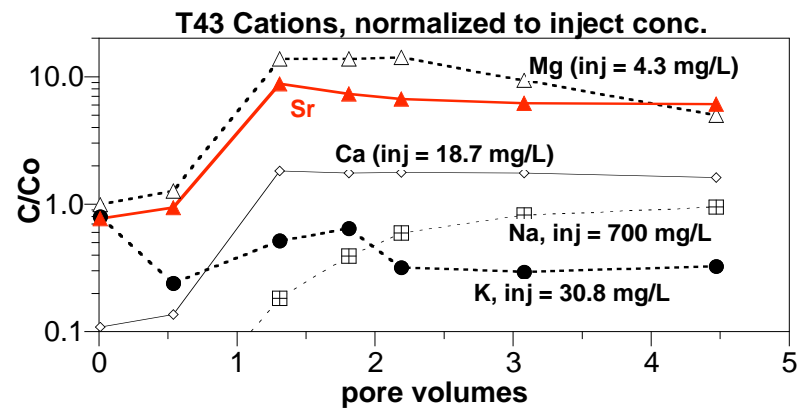
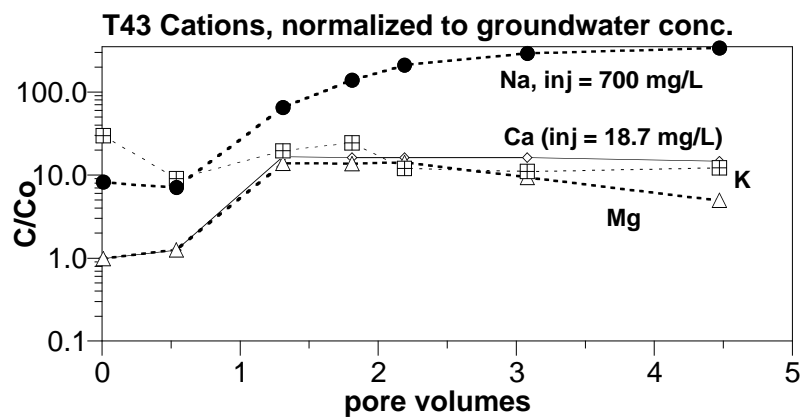
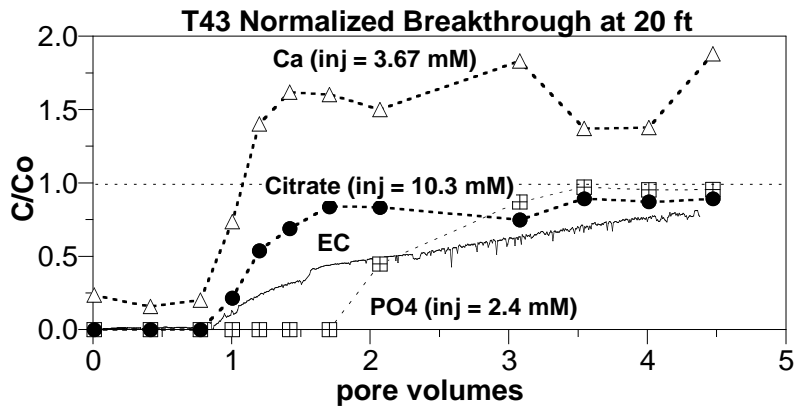


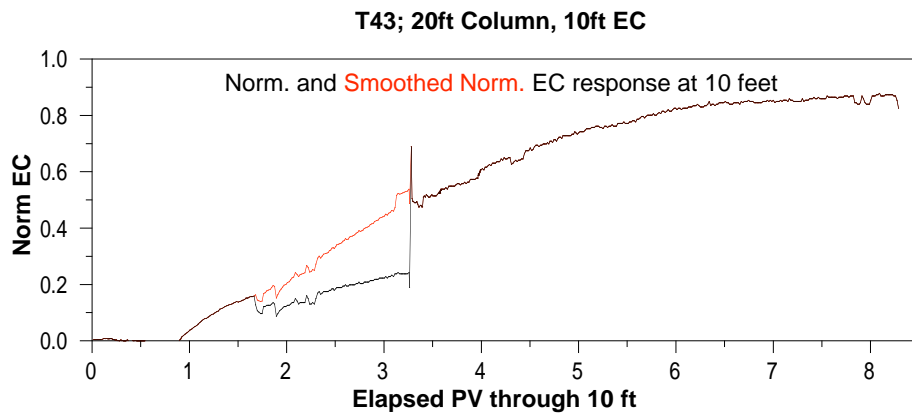
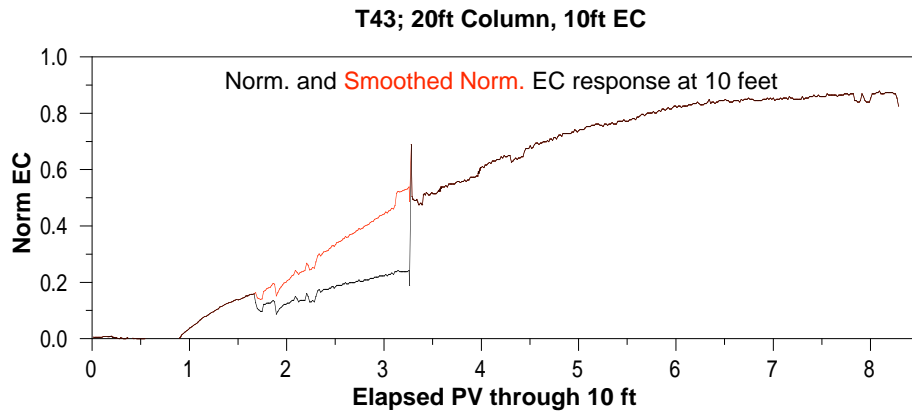
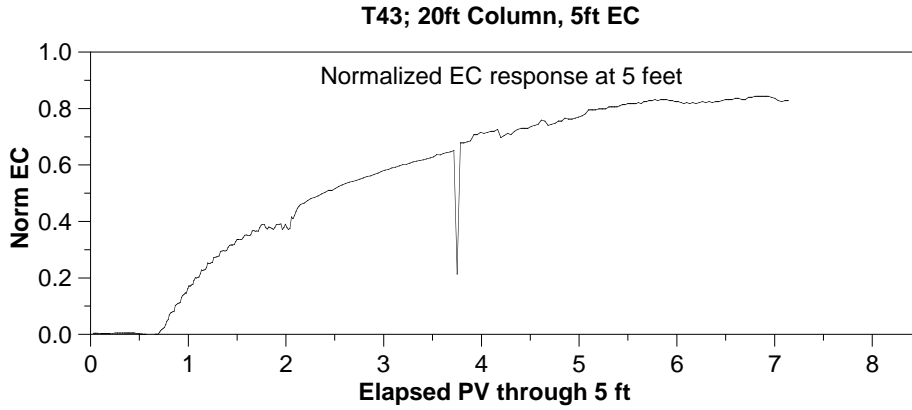




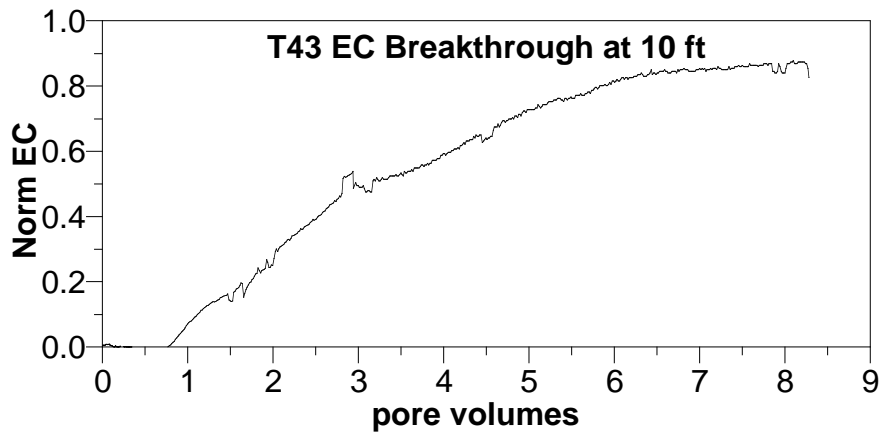
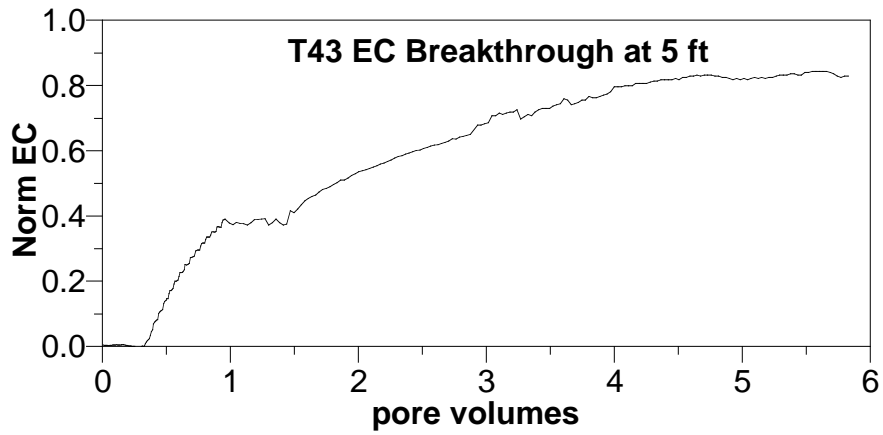
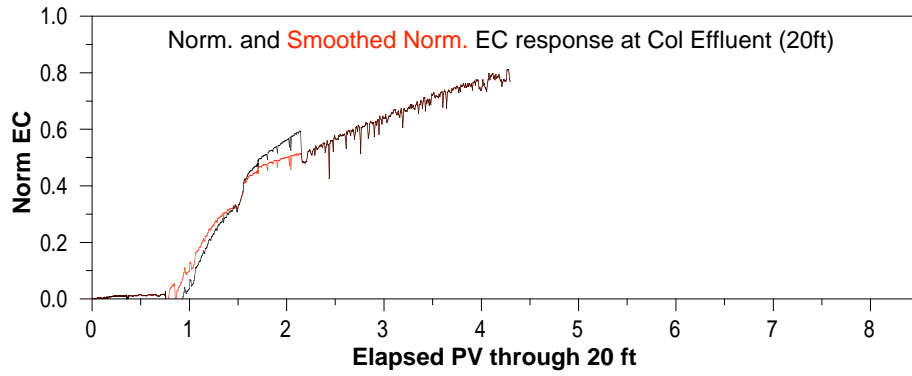


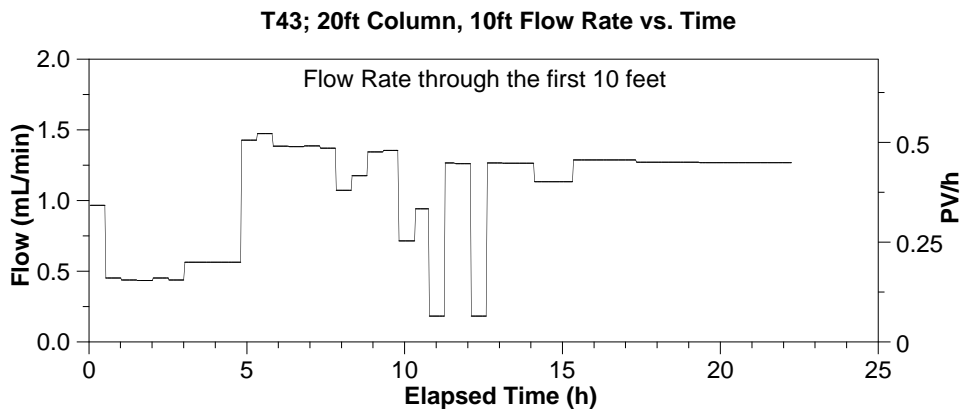
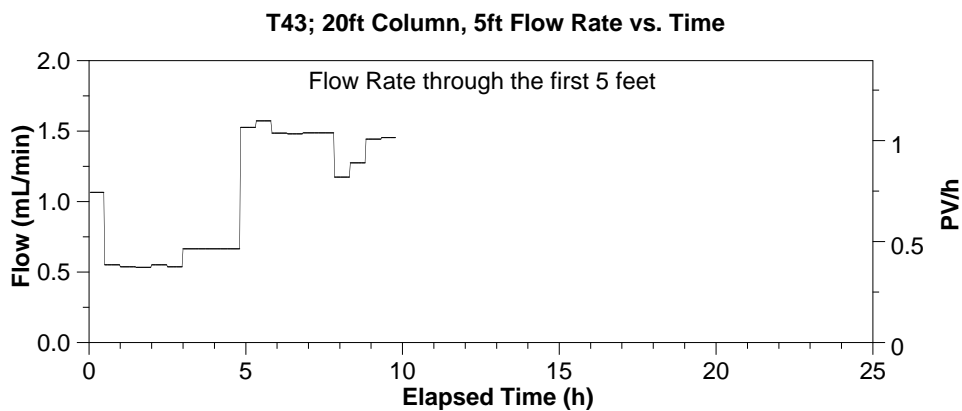
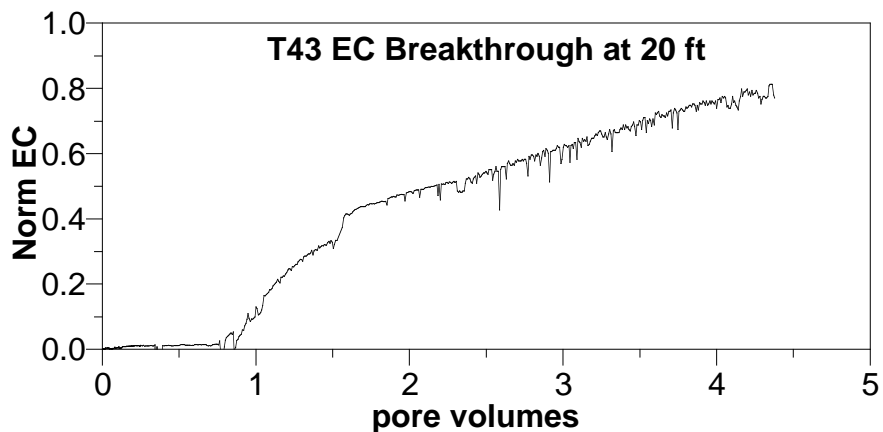


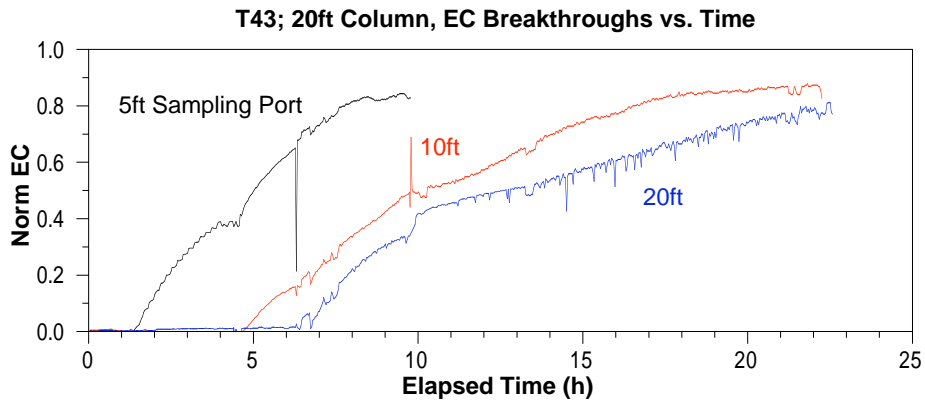
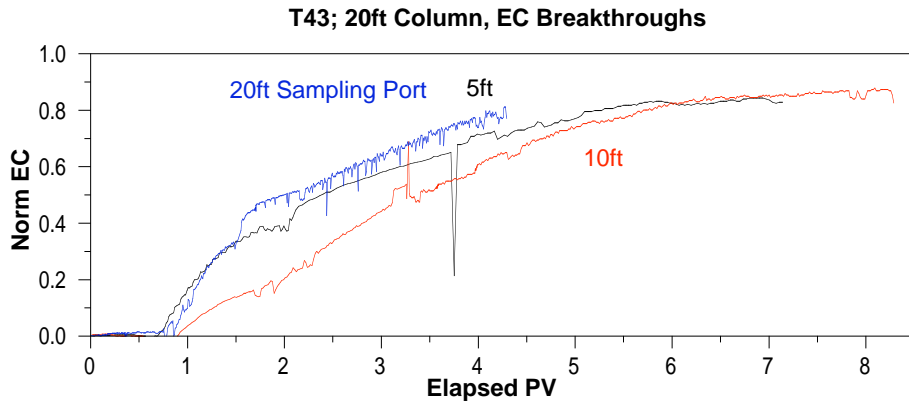
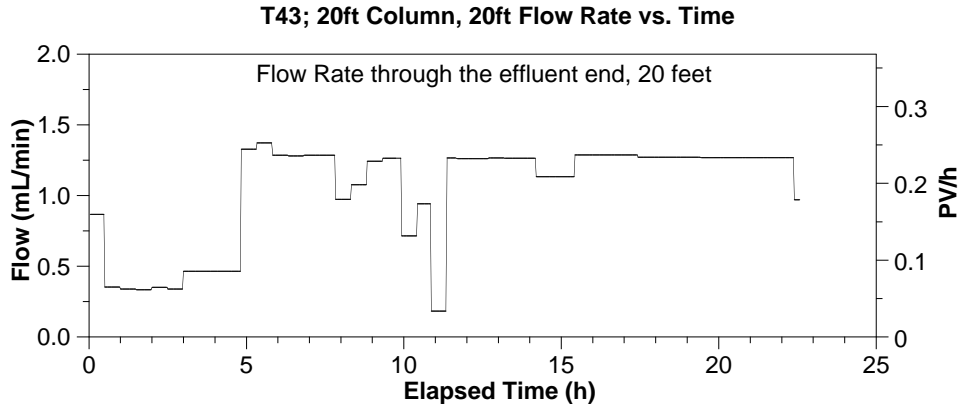




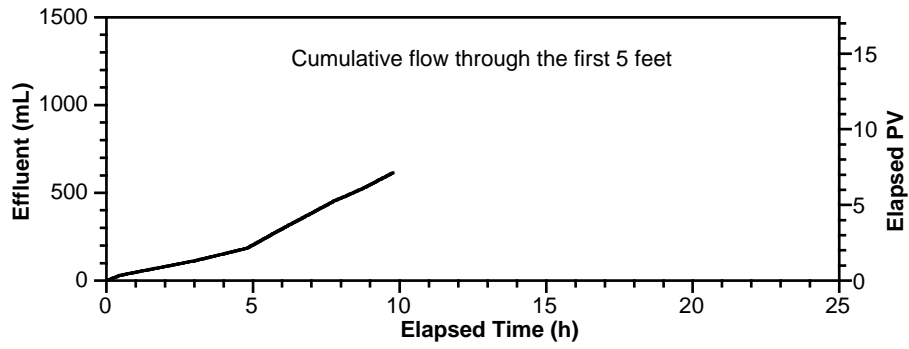
T43; 20ft Column, Effluent (20ft) EC



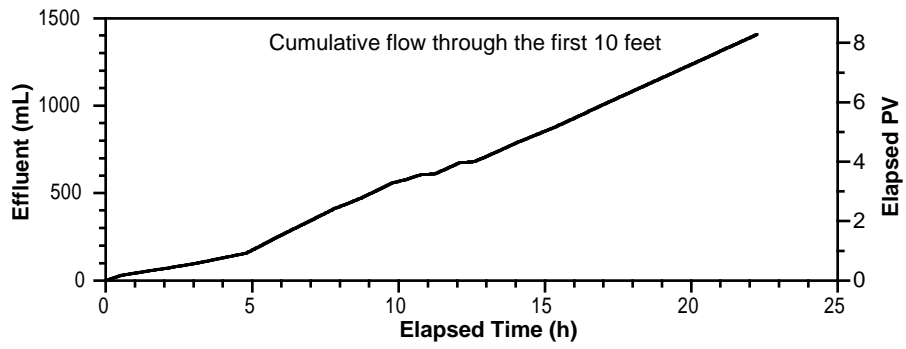




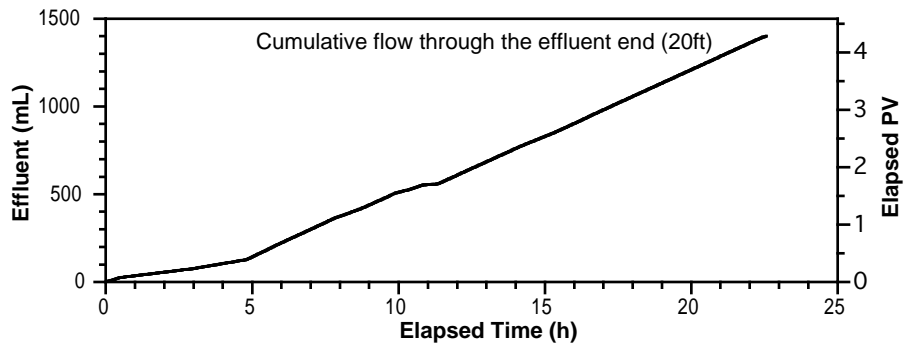
T43; 20ft Column, 5ft Flow vs. Time

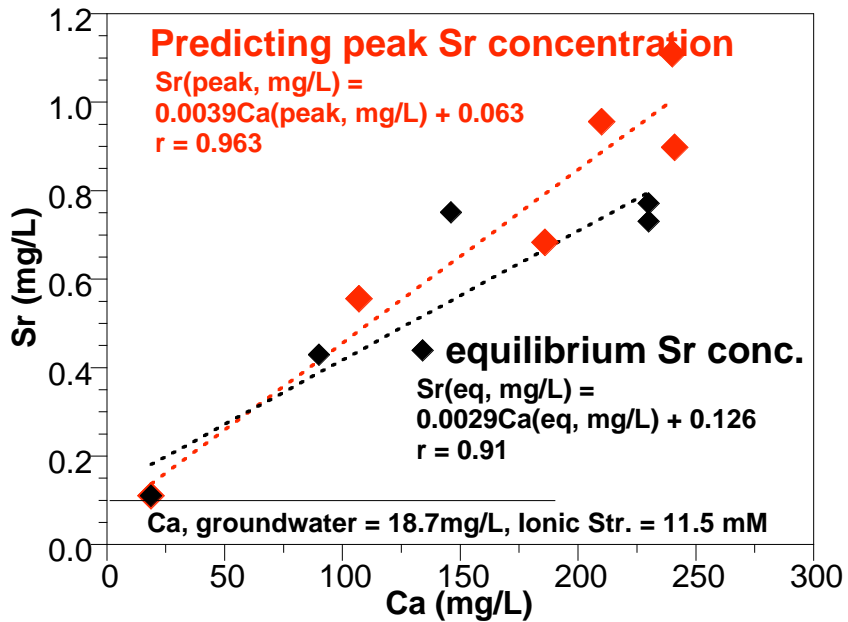
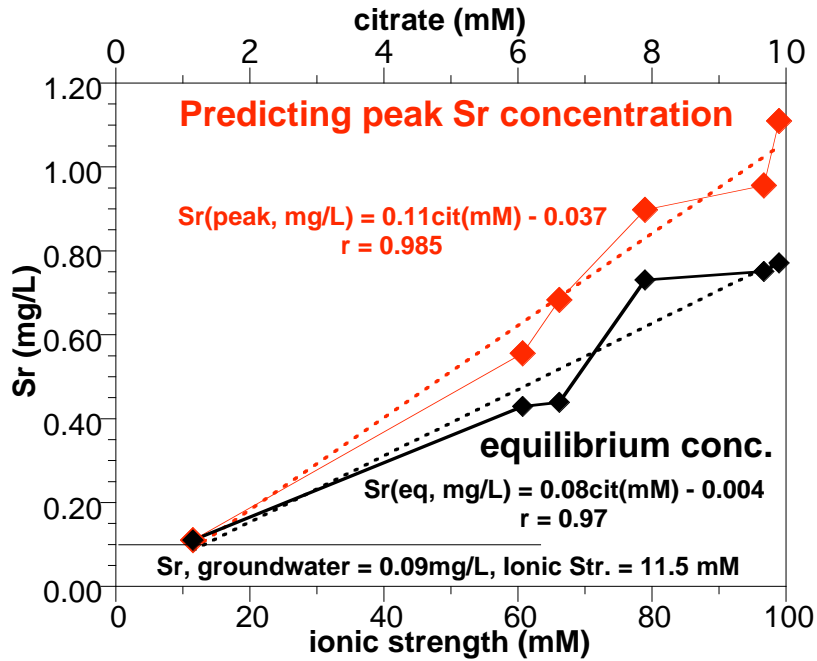


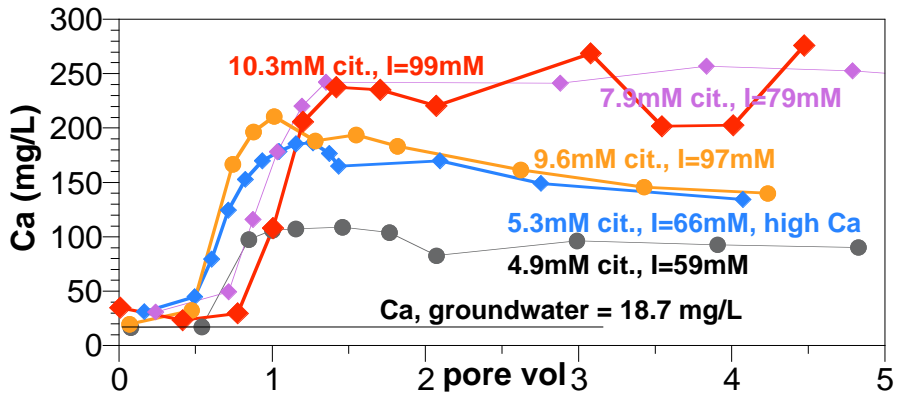
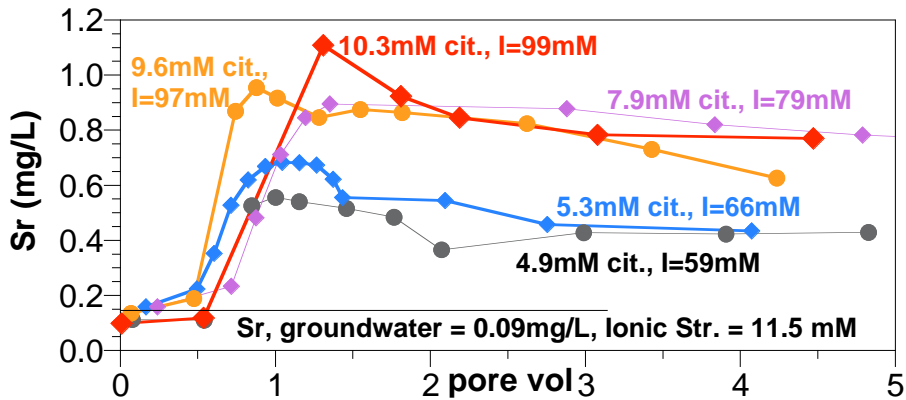
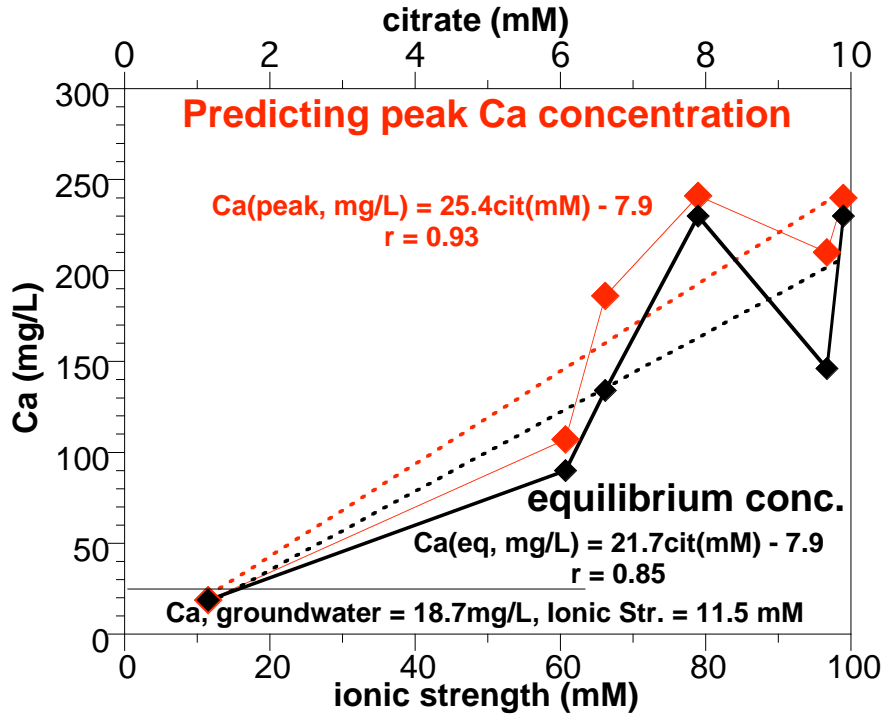
T43; 20ft Column, 10ft Flow vs. Time

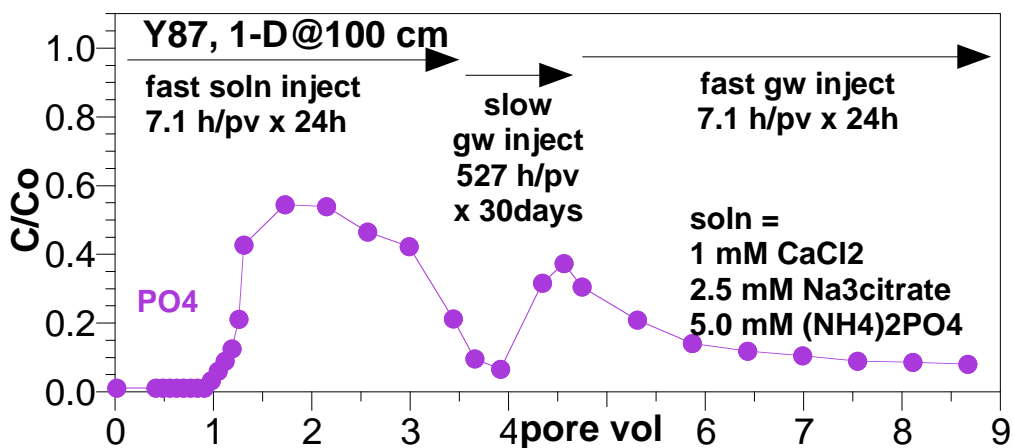
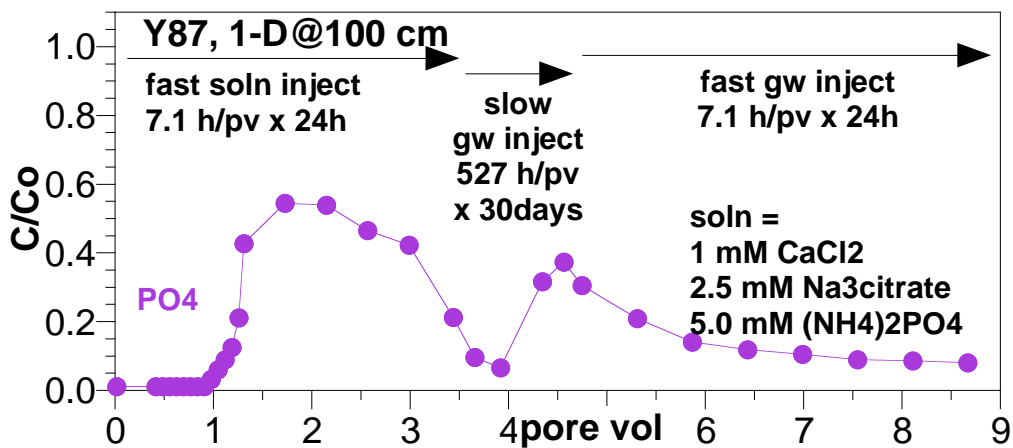
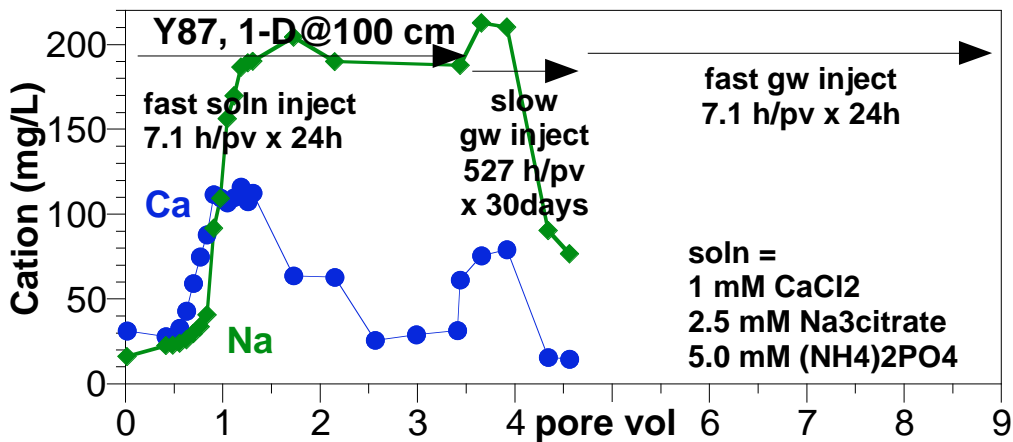


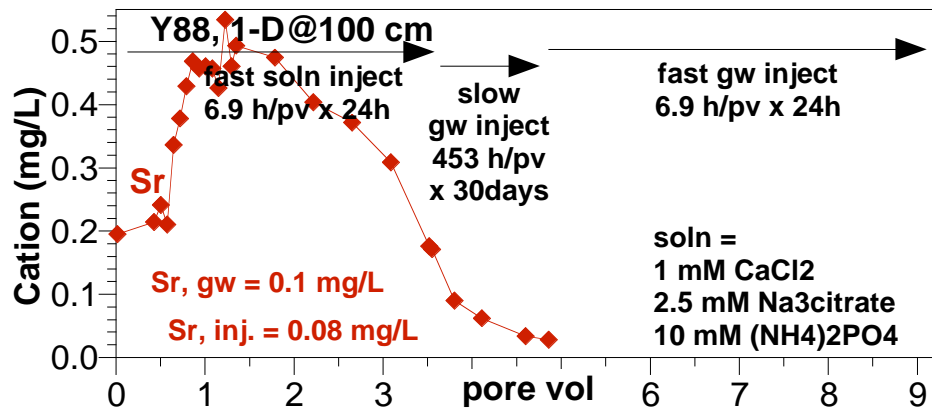
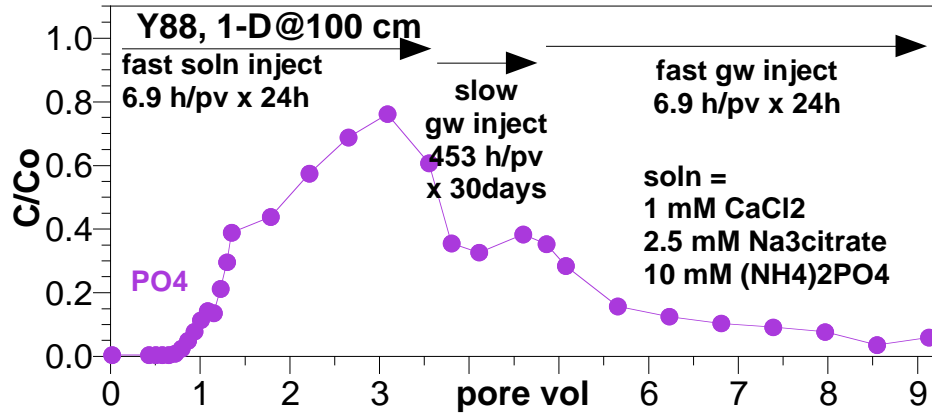
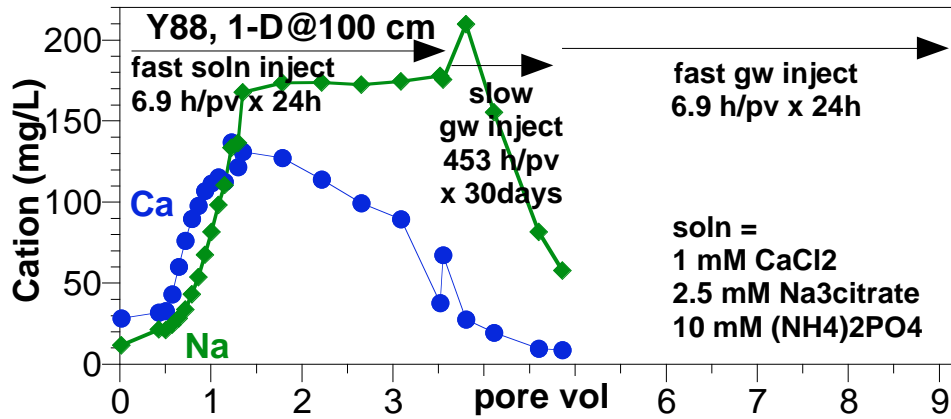
T43; 20ft Column, Effluent (20ft) Flow vs. Time



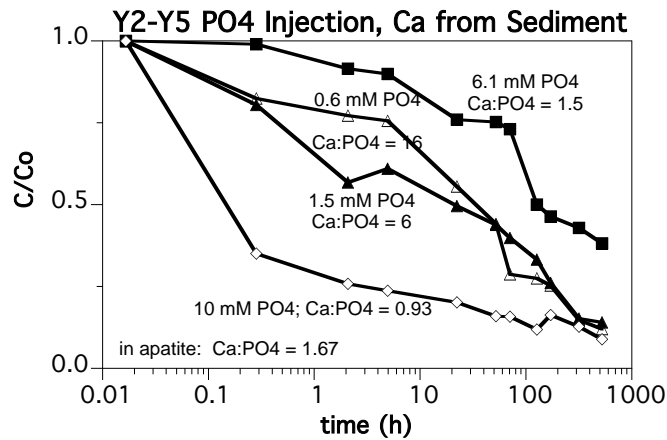
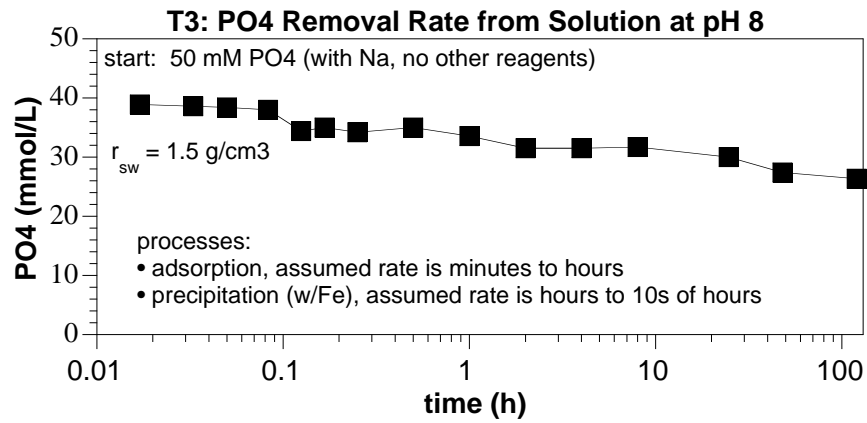
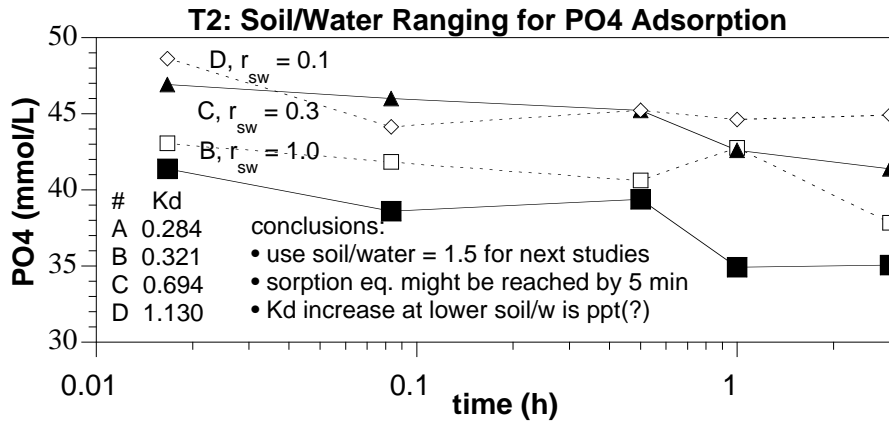




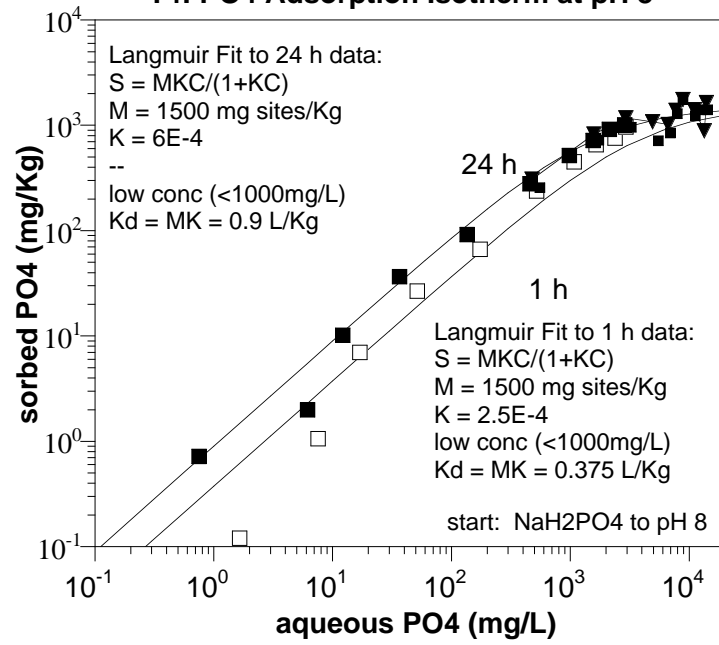




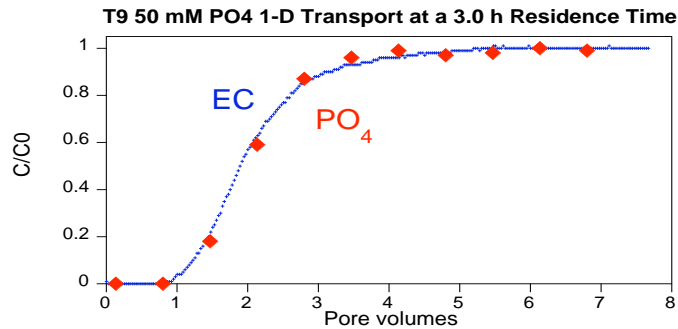
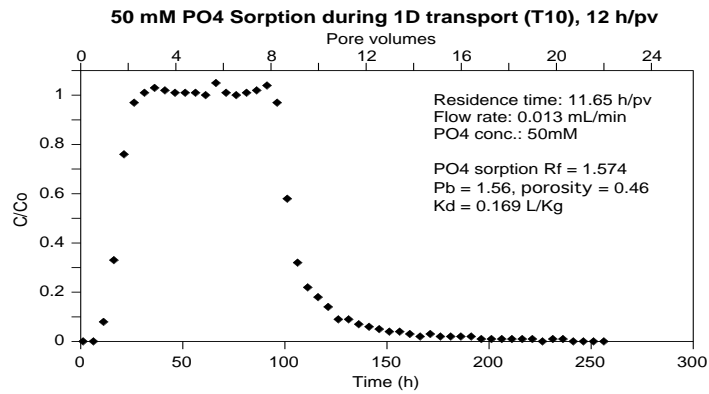
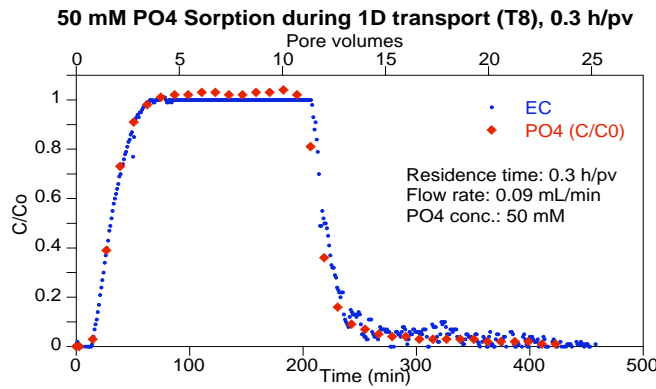
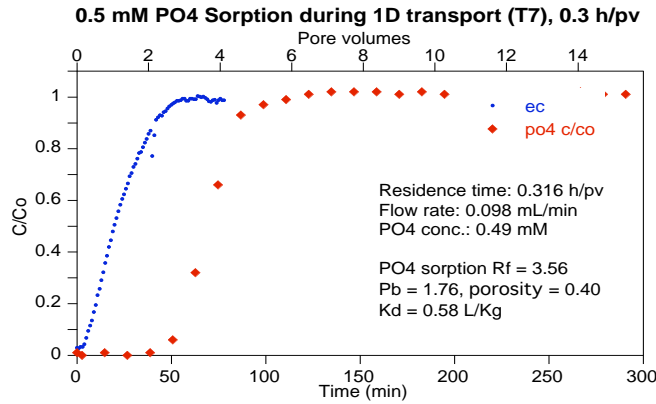
A.3 PO₄ Sorption to Sediment

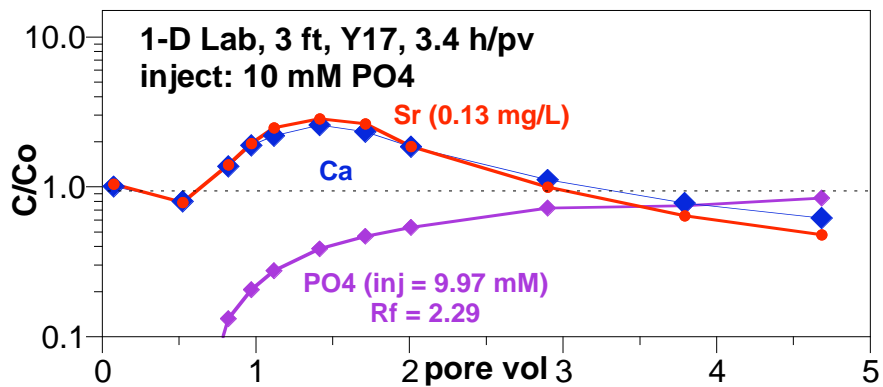
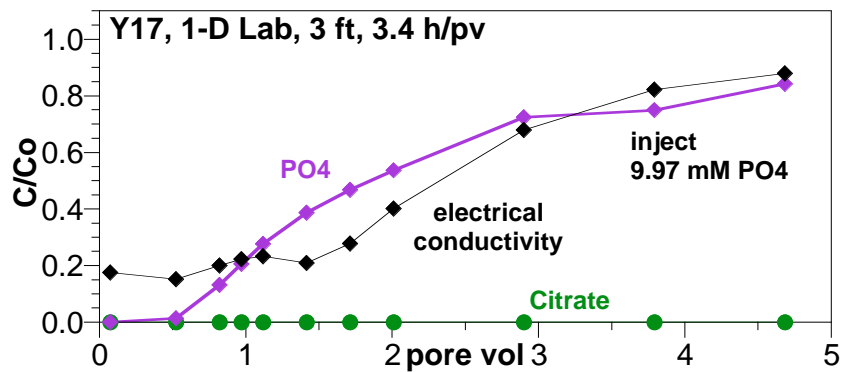
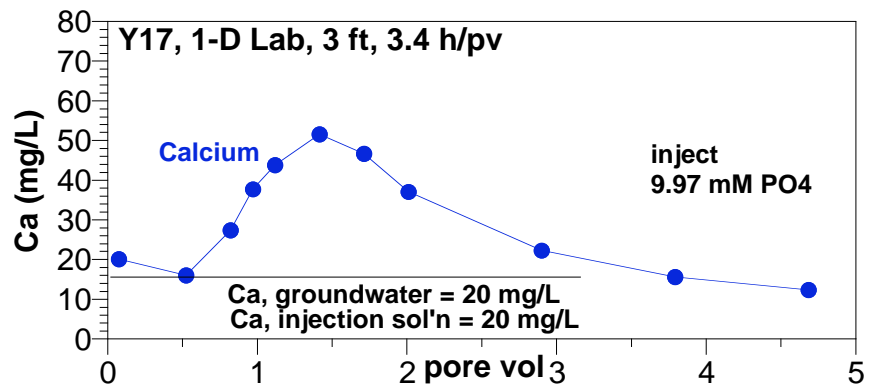


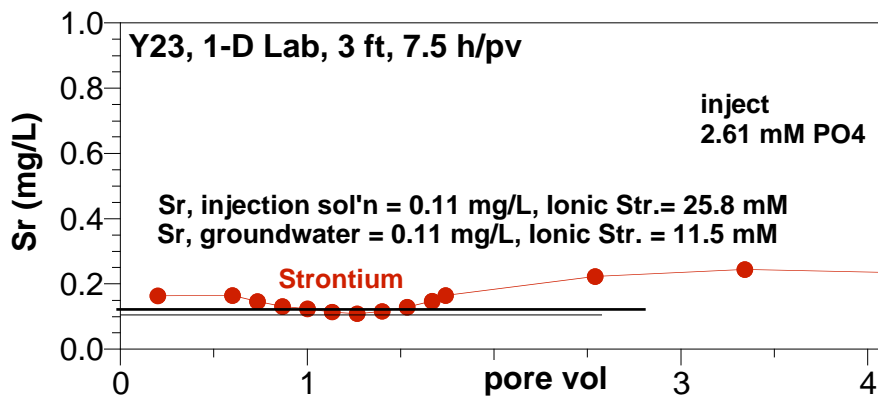
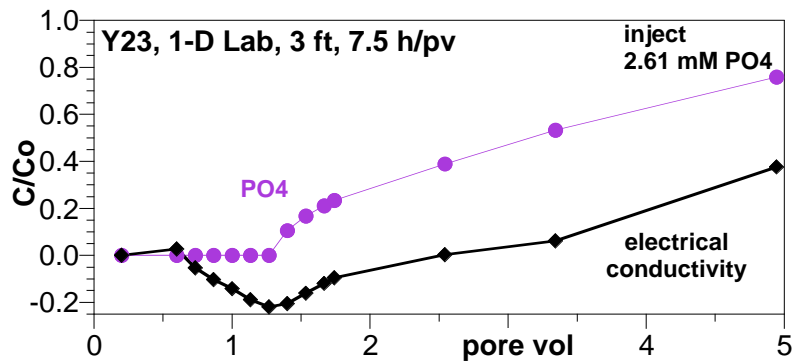
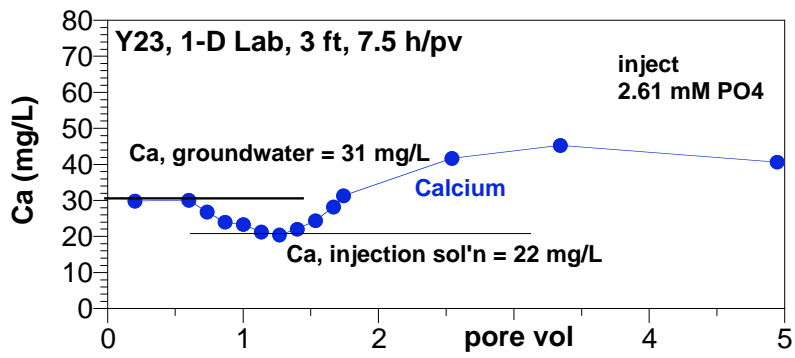
T4: PO4 Adsorption Isotherm at pH 8

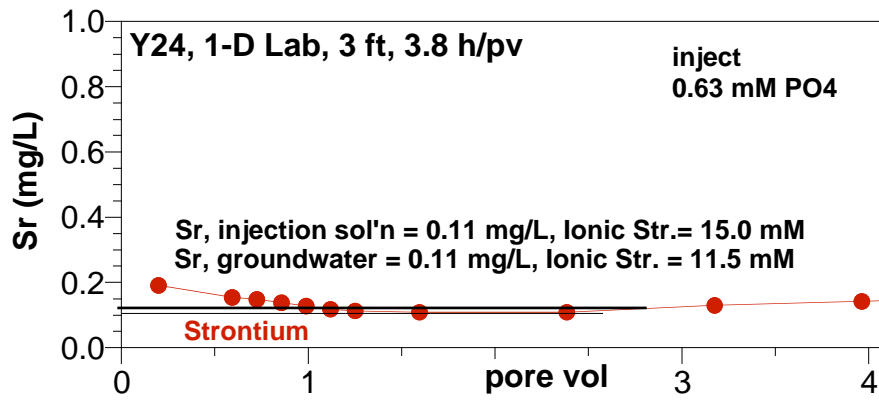
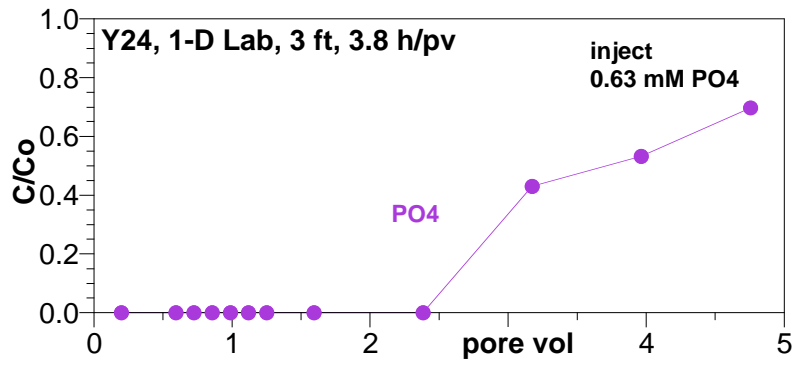
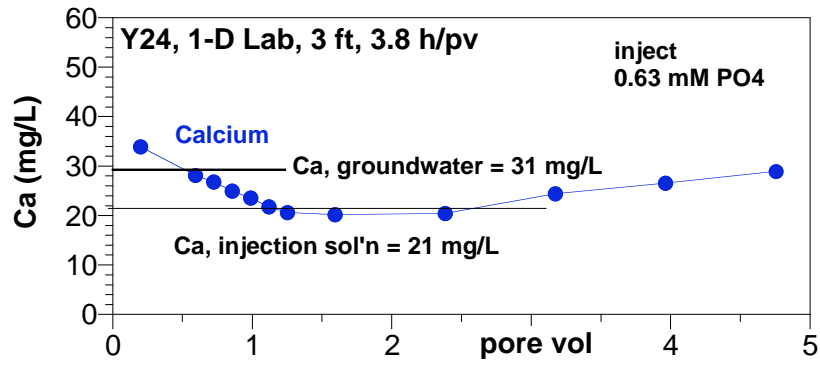


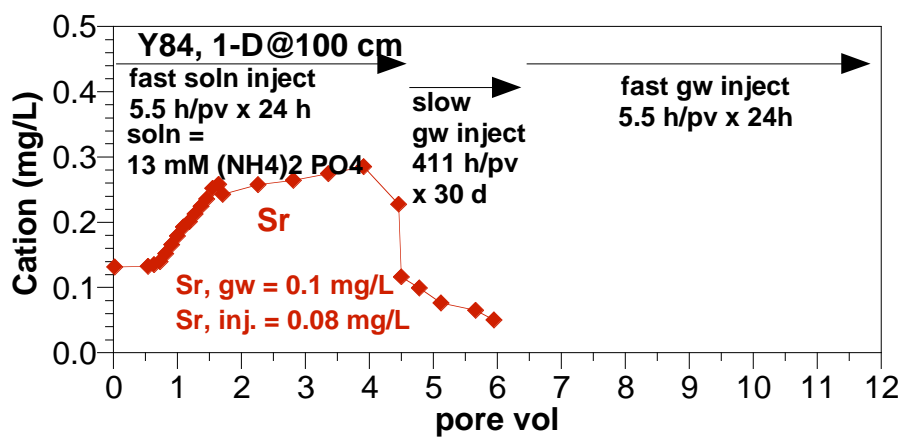
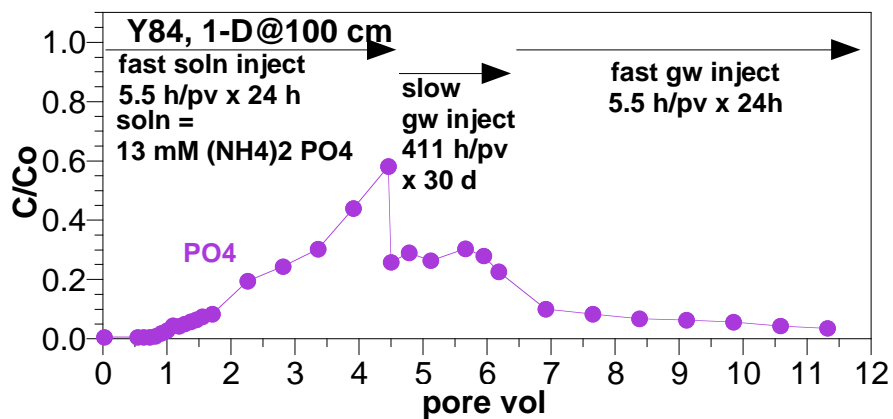
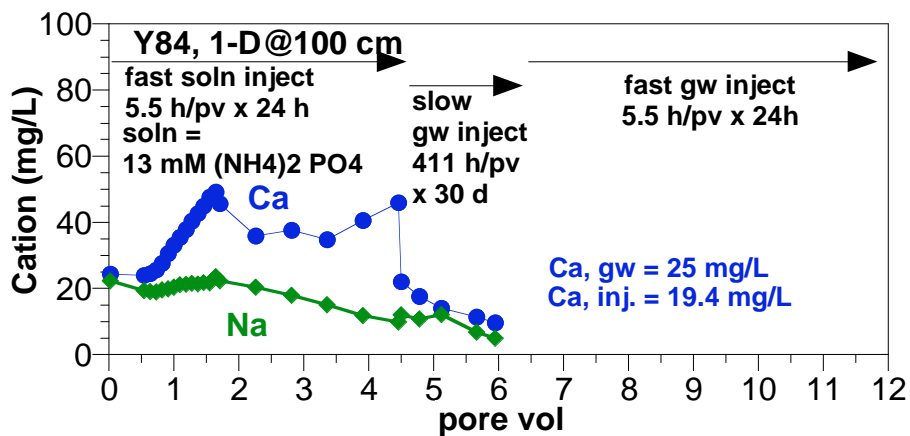
A.4 PO₄ Injection into 1-D Sediment Columns

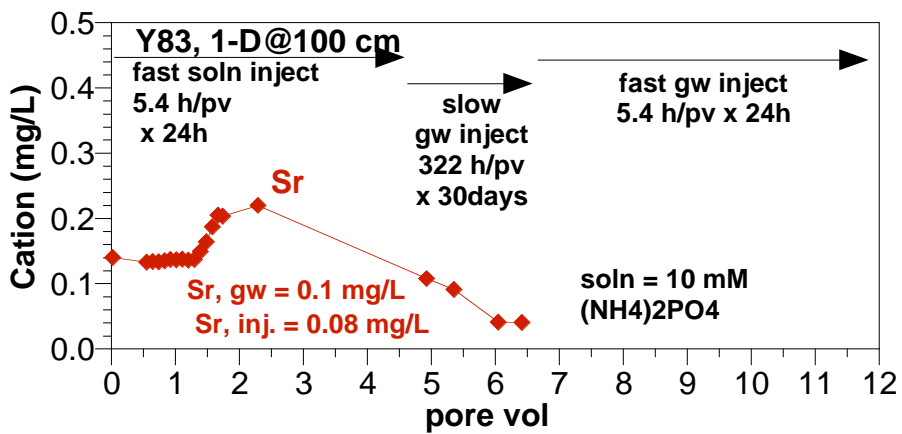
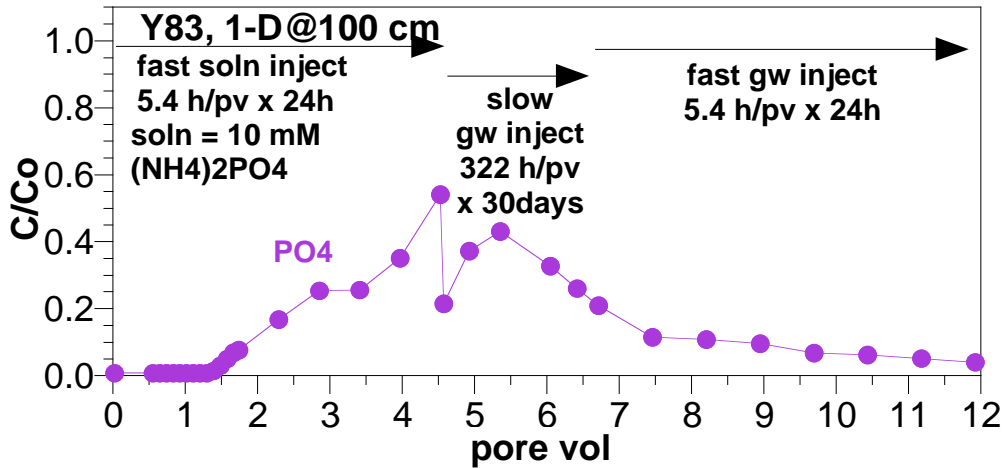
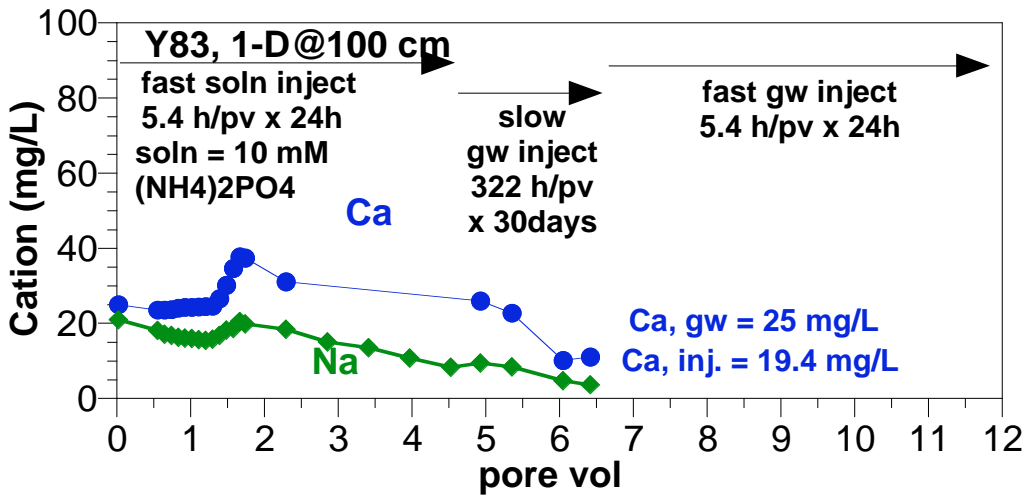


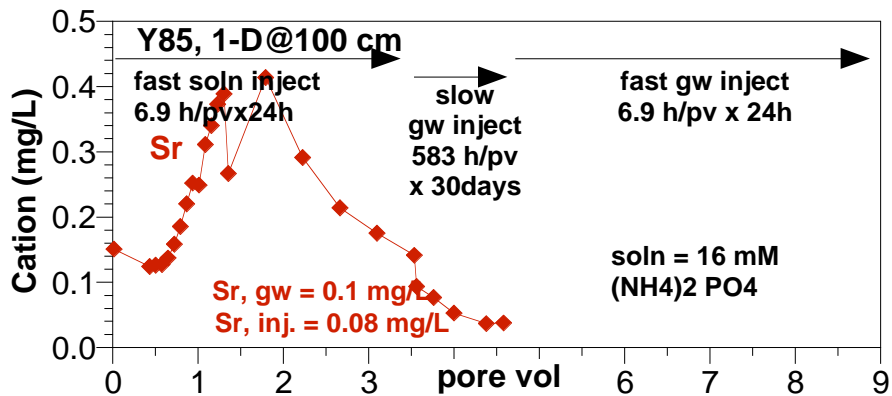
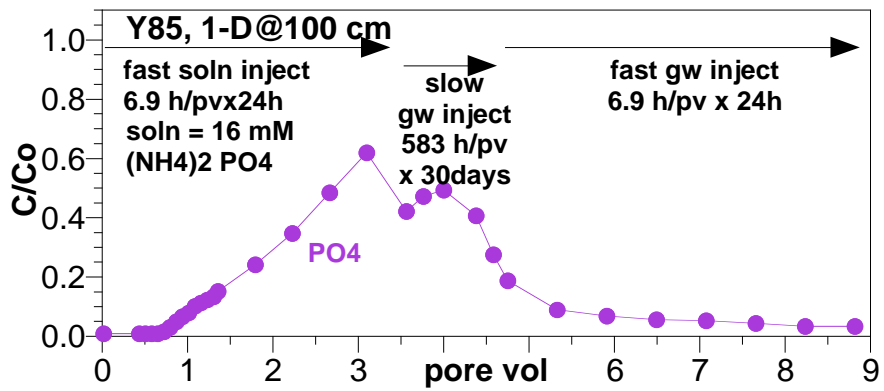
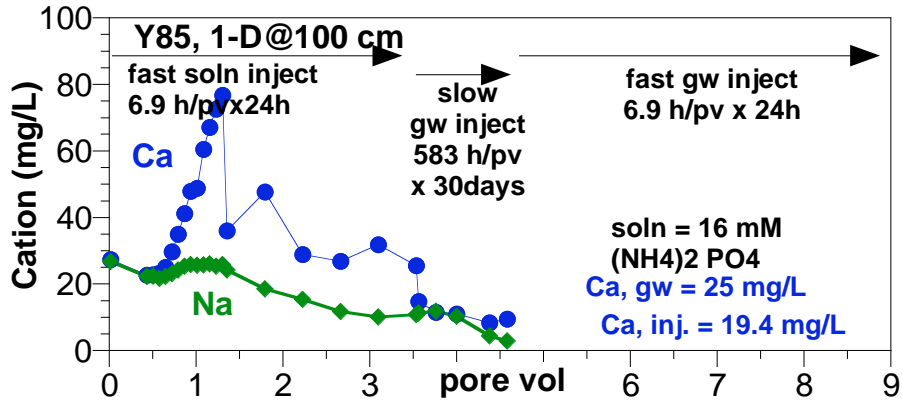


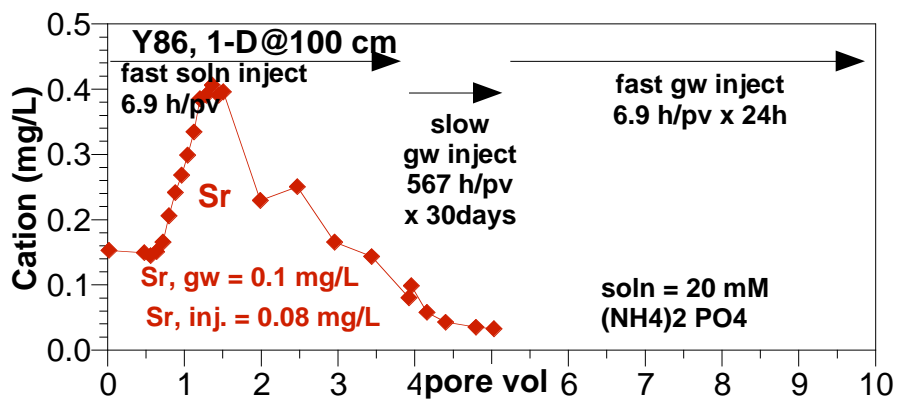
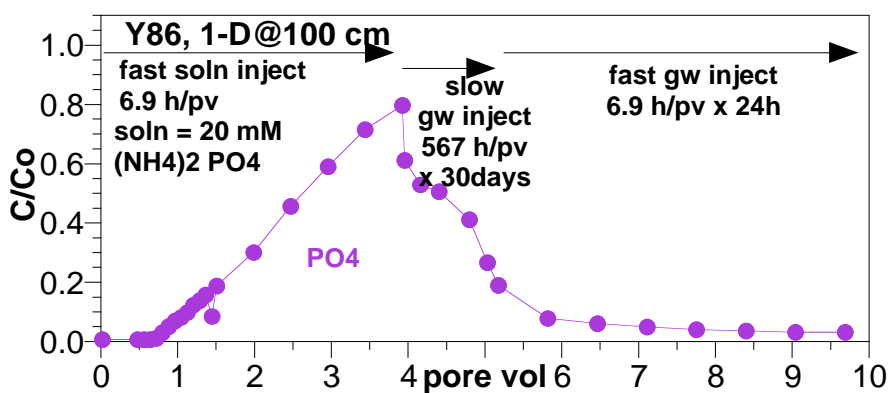
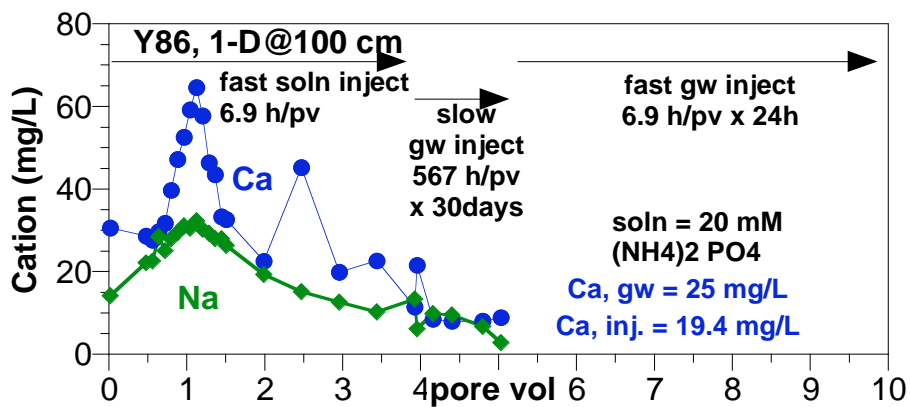


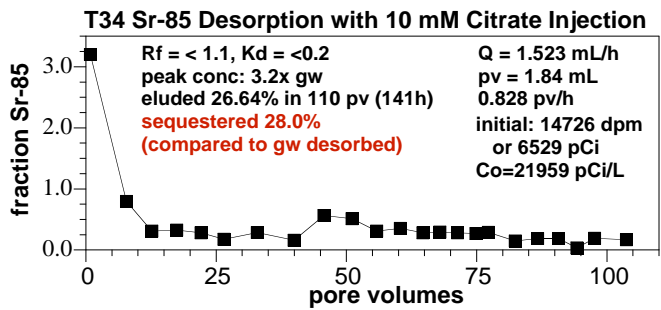
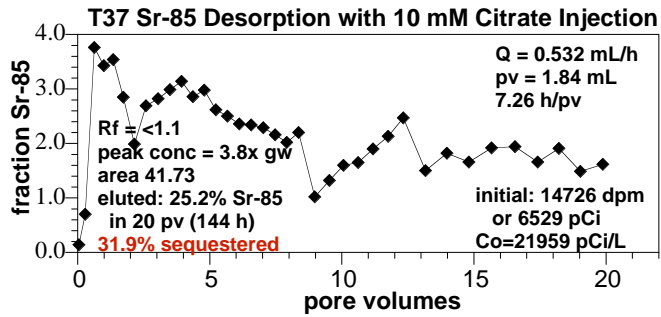
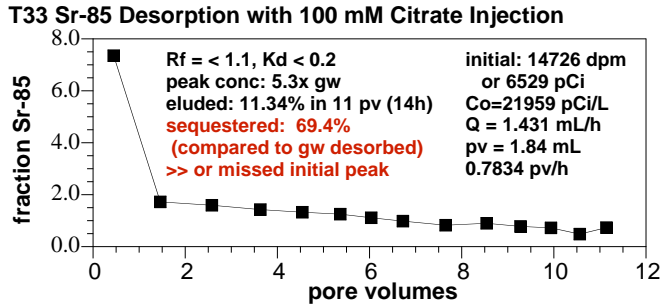
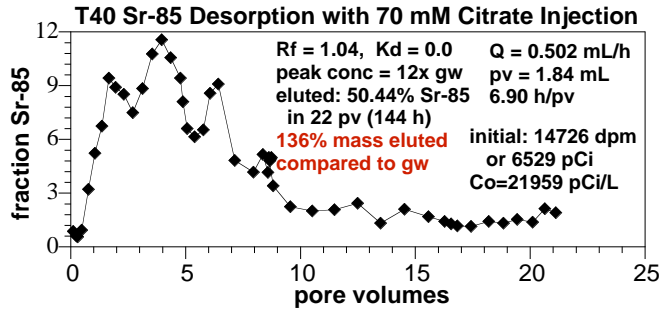




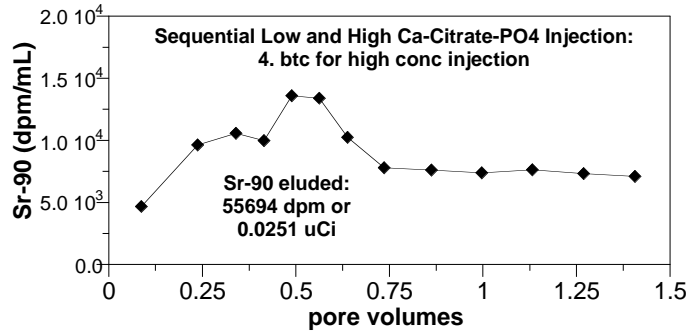
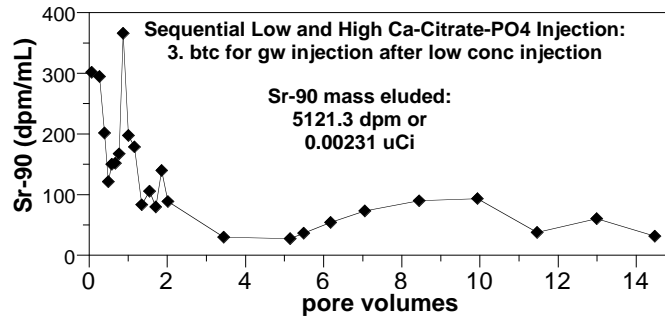
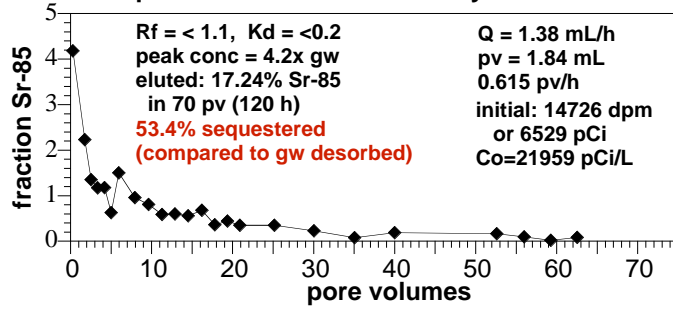




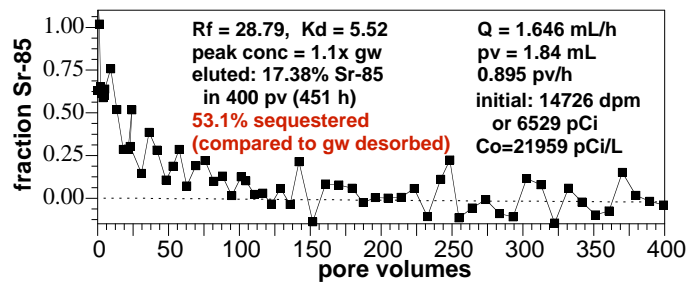




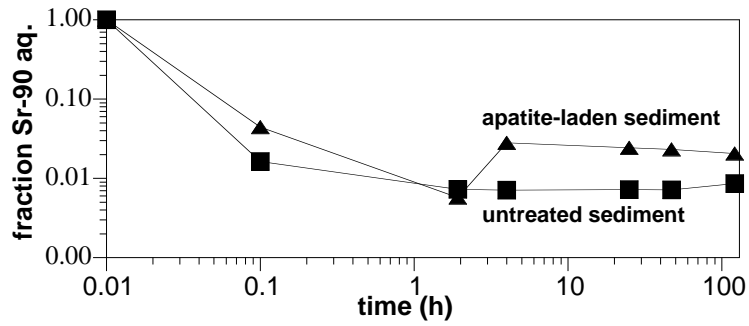
T36 Sequential: 10 mM cit -> 125 days -> 70 mM cit inj



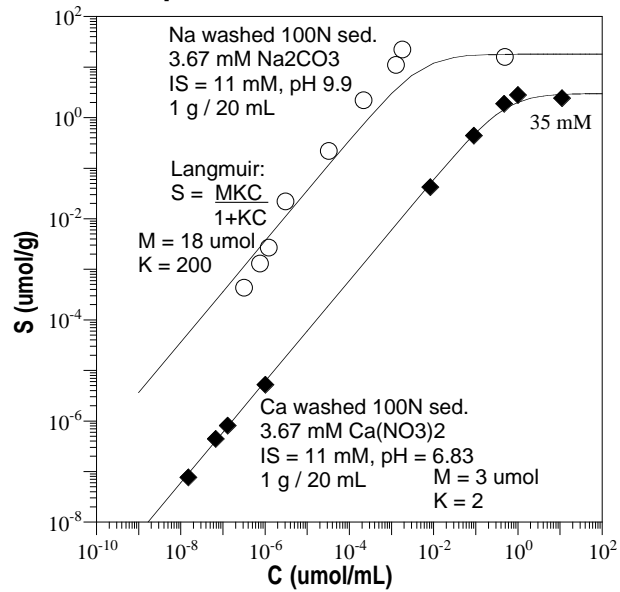
T35 Sr-85 Mobility after 90 day Treatment of 10 mM Citrate

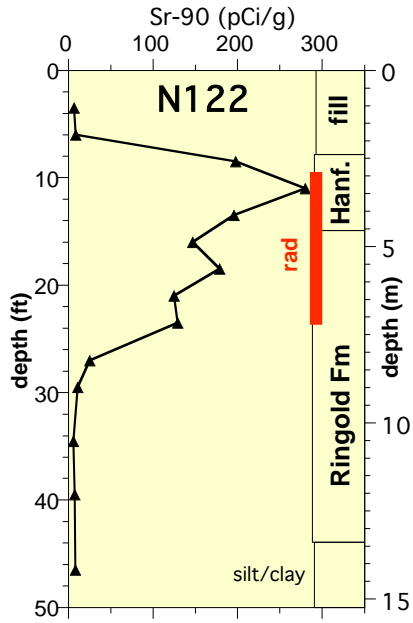


A.5 Sr, Sr-90 Ion Exchange on Untreated Sediment

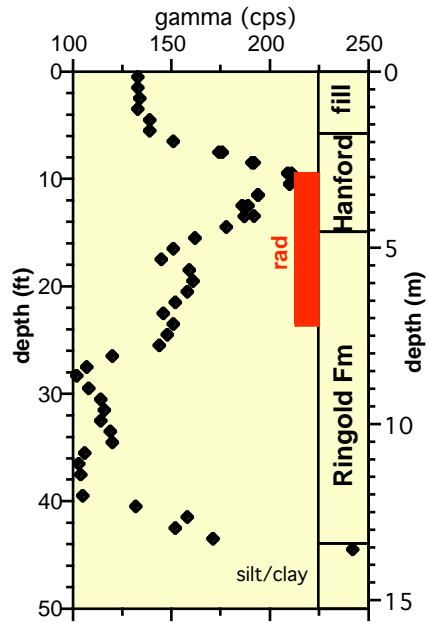


Sr-85 Sorption Isotherm on 100N Sediment

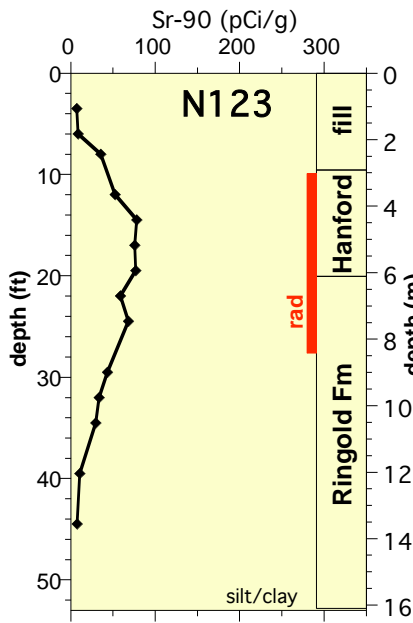




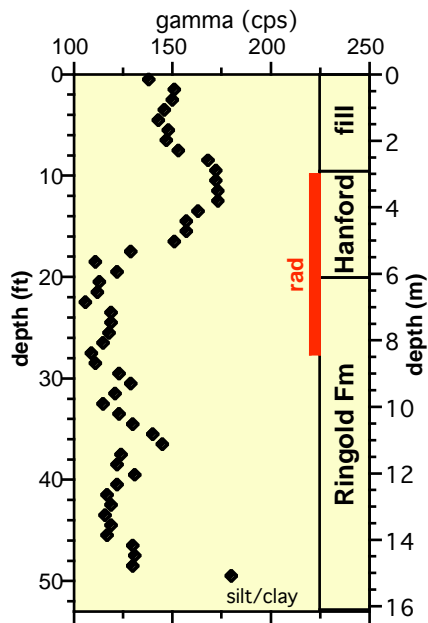
C4954Sr-90



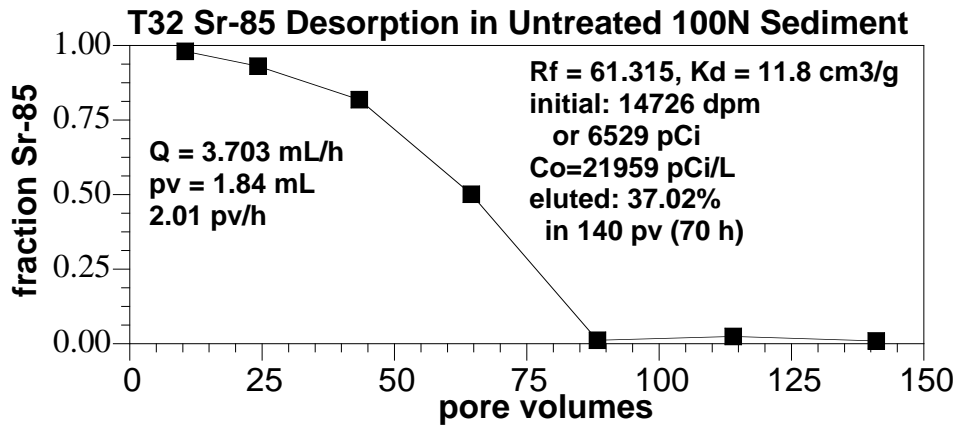
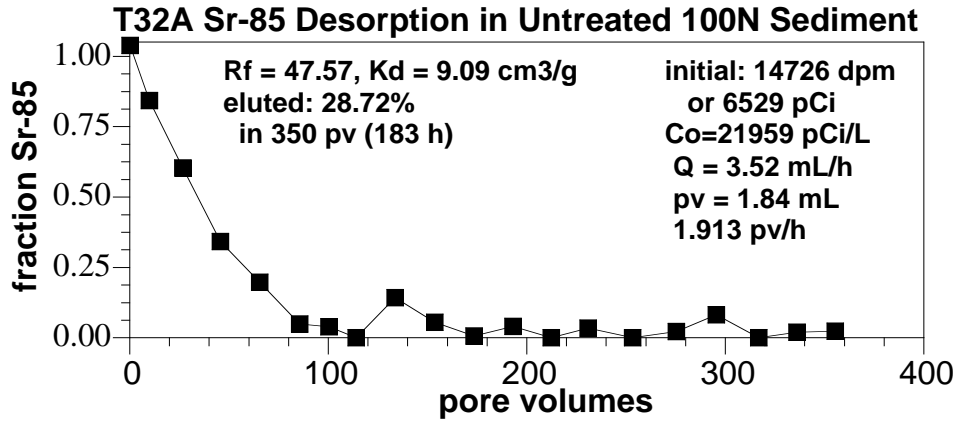
C4954gamma



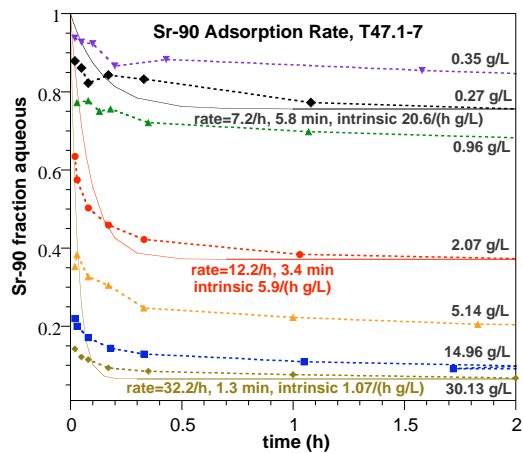
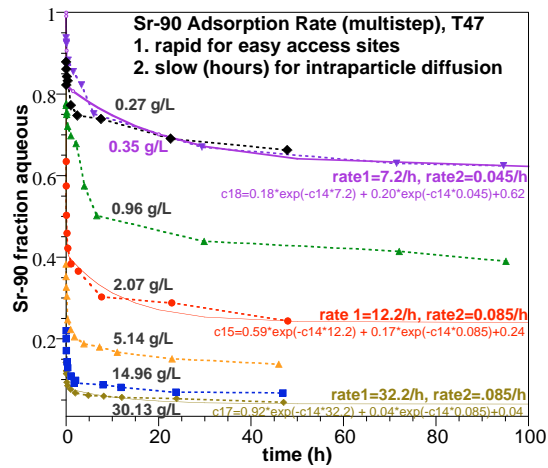
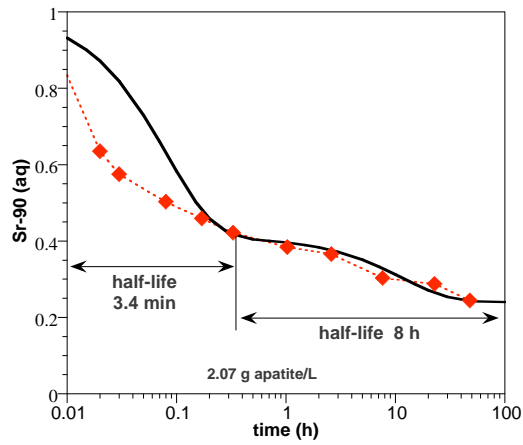
C4955Sr-90



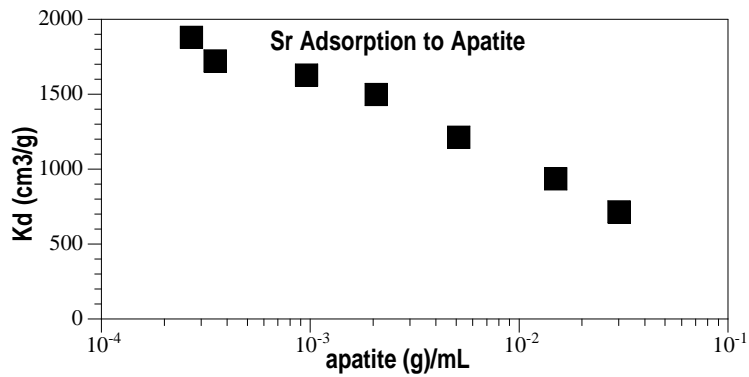
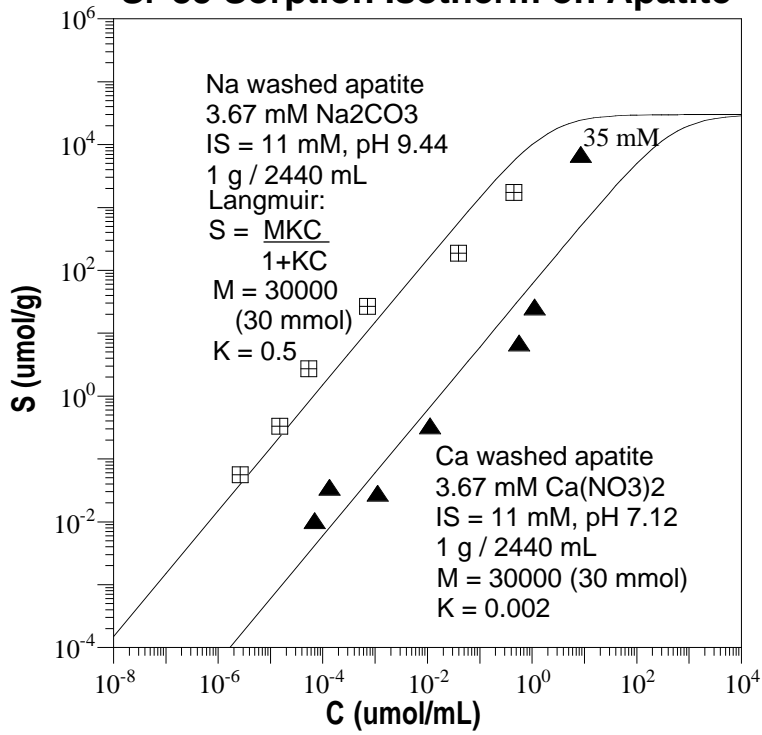
C4955gamma

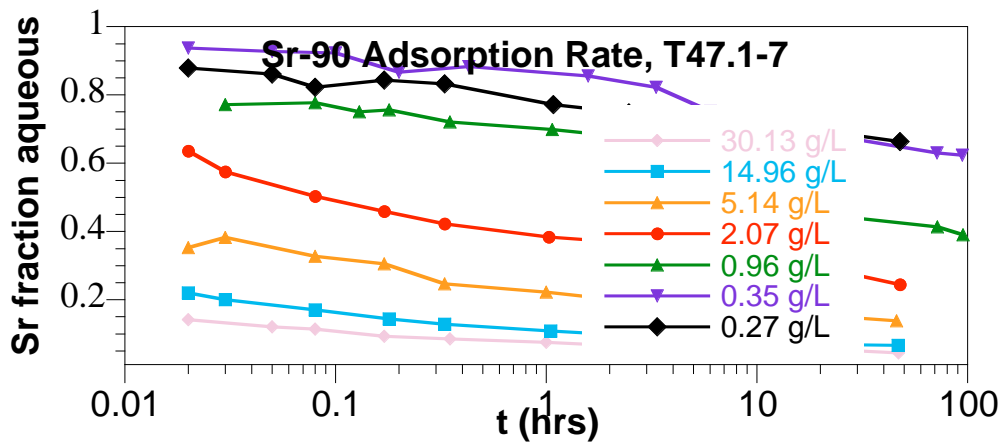
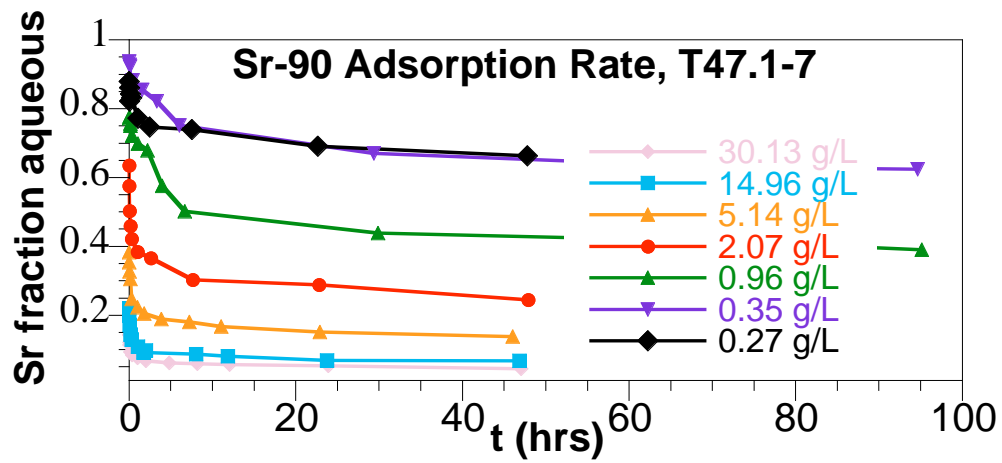


A.6 Sr, Sr-90 Ion Exchange on Apatite (<100 h)

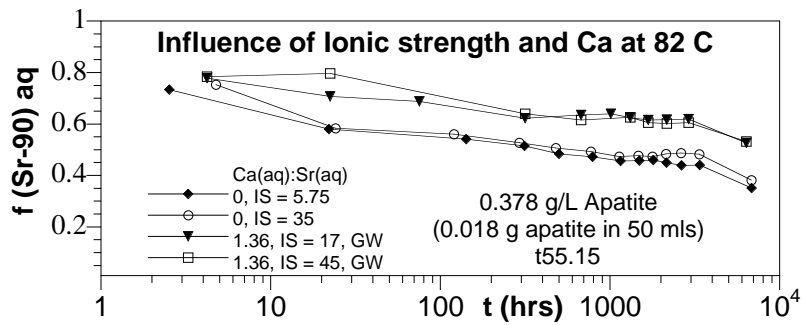
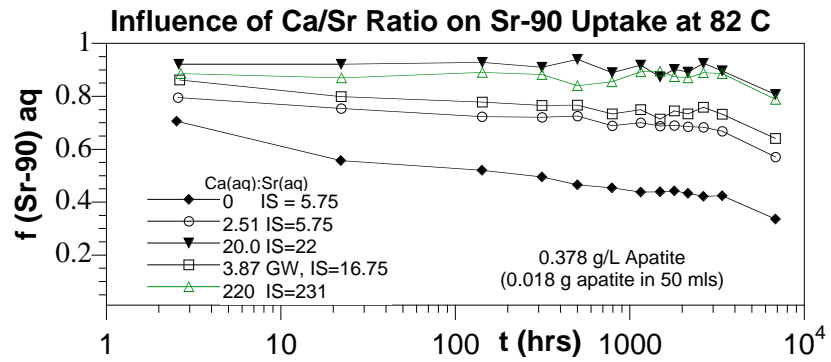
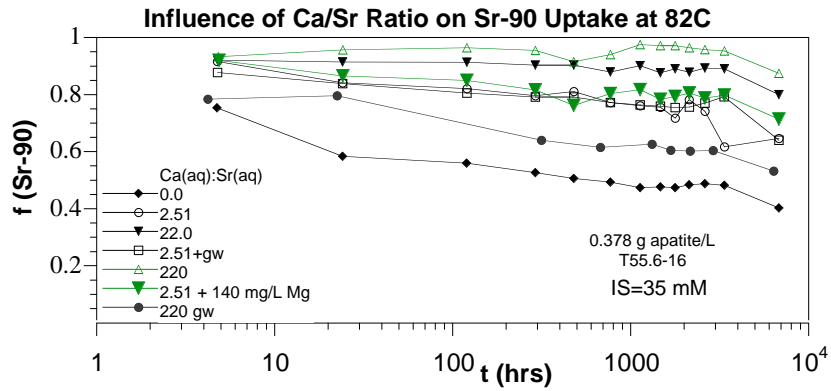


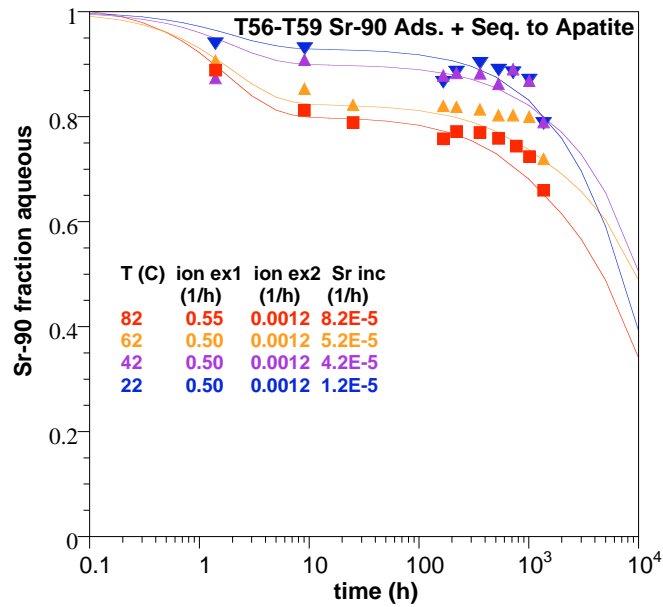
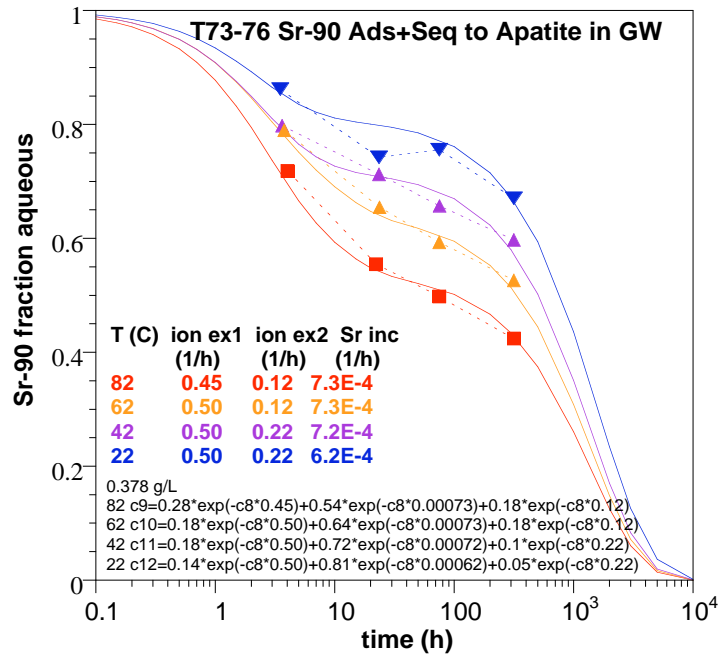
Sr-85 Sorption Isotherm on Apatite





A.7 Sr, Sr-90 Ion Exchange on and Incorporation in Apatite





A.8 Sr, Sr-90 Ion Exchange on Apatite and Sediment with Incorporation in Apatite

